

**Charles University**

**Faculty of Science**

Study programme: Developmental and Cell Biology



**Mgr. Filip Knop**

Non-enzymatic roles of kinases and phosphatases – the case of MTMR9 and AAK1  
Neenzymatické role kináz a fosfatáz na příkladu MTMR9 a AAK1

Doctoral thesis

Supervisor: Mgr. Marie Macůrková, PhD.

Prague, 2024

**Prohlášení:**

Prohlašuji, že jsem závěrečnou práci zpracoval samostatně a že jsem uvedl všechny použité informační zdroje a literaturu. Tato práce ani její podstatná část nebyla předložena k získání jiného nebo stejného akademického titulu.

V Praze, 10.03.2024

Mgr. Filip Knop

## **Poděkování**

Tímto bych rád poděkoval především své školitelce Mgr. Marii Macůrkové, PhD. pod jejímž vedením byla tato práce vytvořena. Dále bych chtěl poděkovat všem současným i minulým členům Laboratoře molekulární genetiky vývoje jejichž odborné rady a pomoc byly nezbytné v různých fázích tohoto projektu. V neposlední řadě bych rád vyjádřil vděk všem institucím Přírodovědecké fakulty Univerzity Karlovy za finanční, administrativní a organizační podporu.

## Abbreviations

AAK1	AP2-associated kinase
ALS	Amyotrophic lateral sclerosis
AP2	Adaptor protein complex 2
ATP	Adenosine triphosphate
BMP2K	BMP2-inducible kinase
CCP	Clathrin-coated pit
CCV	Clathrin-coated vesicle
CK1 $\alpha$	Casein kinase 1 $\alpha$
CME	Clathrin-mediated endocytosis
DENN	Differentially expressed in normal and neoplastic cells (domain)
Dvl	Disheveled
EGF	Epidermal growth factor
EGFR	EGF receptor
ER	Endosomal reticulum
ERGIC	ER-GA intermediate compartment
GA	Golgi apparatus
GAK	Cyclin G-associated kinase
GSK3 $\beta$	Glycogen synthase kinase 3 $\beta$
GTP	Guanosine triphosphate
HCV	Hepatitis C virus
INSR	Insulin receptor kinase
LDLR	Low-density lipoprotein receptor
LRP5/6	Low-density lipoprotein receptor-related protein 5/6
MPSK1	Myristoylated and palmitoylated serine/threonine kinase
MTMR	Myotubularin-related protein
NAK	Numb-associated kinase
NECAP	Adaptin ear-binding coat-associated proteins
NSID	Non-syndromic intellectual disability
OAC	Oesophageal adenocarcinoma
PH	Pleckstrin homology (domain)
PH-GRAM	PH, Glucosyltransferase, Rab-like GTPase Activator and MTMR (domain)
PI3K	PI3P-generating kinase
PI3P	Phosphatidylinositol 3-monophosphate
PI(3,5)P2	Phosphatidylinositol 3,5-bisphosphate



PIP	Phosphatidylinositol phosphates
PIP2	Phosphatidylinositol 4,5-bisphosphate
PKB	Protein kinase B
PM	Plasma membrane
PORC	Membrane-associated O-acyl transferase
PP1	Protein phosphatase 1
PSTP	Protein serine/threonine phosphatase
PTEN	Phosphatase and tensin homologs
PTK	Protein tyrosine kinase
PTM	Post-translational modification
PTP	Protein tyrosine phosphatase
RPTP $\alpha$	Receptor protein tyrosine phosphatase $\alpha$
RTK	Receptor tyrosine kinase
SAC	Sac domain-containing proteins
Sars-CoV2	Severe acute respiratory syndrome coronavirus 2
SNP	Single nucleotide polymorphism
SOD1	Superoxide dismutase 1
SPR	Surface plasmon resonance
STK	Serine/threonine kinase
TCF/LEF	T-cell factor/lymphoid enhancer factor
Tfn	Transferrin
TfnR	Tfn receptor
TGN	<i>trans</i> -GA
TRN	Touch receptor neuron
VSV-G	Vesicular stomatitis virus protein G
WASP	Wiscott-Aldrich syndrome protein
Y2H	Yeast two-hybrid system

## Abstract

Enzymatic roles of kinases and phosphatases in almost every aspect of cellular life are well described in a wide variety of examples. Lately the role of the same proteins independent of their catalytic activity is being increasingly appreciated. In this work, we focus on two proteins, mammalian MTMR9, and *Caenorhabditis elegans* SEL-5/AAK1. MTMR9 belongs to the myotubularin-related family of lipid phosphatases (MTMR) and is known to be a pseudophosphatase, a catalytically inactive member of the MTMR group. SEL-5/AAK1, on the other hand, is characterized by its kinase activity with at least two putative substrates identified so far. We described the localization of MTMR9 to early secretory pathway and its colocalization with known ER-to-GA compartment (ERGIC) markers. We also identified several possible MTMR9-interacting partners, such as RAB1 and MTMR6, whose localization and/or activity could be potentially regulated by MTMR9 binding. Disruption of proper MTMR9 levels led to an alteration in WNT3A secretion and subsequently to a reduced activity of the Wnt signaling pathway. Similarly, we identified SEL-5/AAK1 role in two separate Wnt-regulated developmental processes in *C. elegans*. Firstly, SEL-5 along with other members of the retromer complex regulate a proper QL.d migration. Secondly, excretory cell canals depended on SEL-5 for their ability to grow to their full length. Interestingly, whereas SEL-5 does seem to phosphorylate the AP2 complex  $\mu$ 2 subunit, we found that its kinase activity is dispensable for both QL.d and excretory canals regulation.

## **Abstrakt**

Enzymatické role kináz a fosfatáz v regulaci buněčných procesů byly popsány na mnoha příkladech. V posledních letech se objevuje rostoucí počet případů postradatelnosti katalytické aktivity těchto enzymů. Tato práce se soustředí na dva konkrétní proteiny, savčí MTMR9 a SEL-5/AAK1 v hád'átku obecném. MTMR9 z rodiny lipidových fosfatáz příbuzných myotubularinu (MTMR) patří do skupiny pseudofosfatáz, které jsou charakteristické nepřítomností enzymatické aktivity. Na druhou stranu, SEL-5/AAK1 je typickou aktivní kinázou s nejméně dvěma známými substráty. Podařilo se nám zjistit důležitost MTMR9 v časné sekretorní dráze buňky, kde kolokalizuje s markery intermediálního kompartmentu mezi endosomálním retikulem a Golgiho aparátem (ERGIC). Dále jsme identifikovali několik možných interakčních partnerů, například RAB1 a MTMR6, jejichž lokalizaci a/nebo aktivitu by mohla vazba na MTMR9 regulovat. Změna úrovně MTMR9 způsobila narušení WNT3A sekrece a následně vedla k redukci aktivity Wntové signální dráhy. Pro SEL-5/AAK1 se nám podařilo identifikovat dva procesy, oba taktéž regulované Wntovou signální dráhou, které jsou důležité ve vývoji hád'átka obecného. Jednak je SEL-5 společně s několika členy retromerového komplexu zodpovědný za regulaci správné QL.d migrace, a jednak SEL-5 reguluje růst exkretorních kanálů do řádné délky. Ačkoliv jsme potvrdili schopnost SEL-5 fosforylovat  $\mu 2$  podjednotku AP2 komplexu, tato kinázová aktivita není nezbytná pro regulaci procesů QL.d migrace a růstu exkretorních kanálů.

## Table of contents

1. Introduction .....	9
1.1. Kinases and phosphatases in posttranslational modifications .....	9
1.1.1. Kinase function and regulation .....	9
1.1.2. Phosphatase function and regulation .....	11
1.2. Non-enzymatic functions of kinases and phosphatases.....	13
1.2.1. Pseudokinases and pseudophosphatases .....	13
1.3. Myotubularin-related proteins (MTMRs).....	14
1.3.1. MTMRs structure and function.....	15
1.3.2. Myotubularin-related protein 9 (MTMR9) .....	15
1.4. AP2-associated kinase (AAK1) .....	17
1.4.1. Clathrin-mediated endocytosis (CME) .....	17
1.4.2. AAK1 function in CME .....	19
1.5. MTMR9 and AAK1 in Wnt signaling .....	22
1.5.1. Wnt signaling .....	23
1.5.2. Known roles of MTMR9 and AAK1 in Wnt signaling.....	24
2. Publications .....	26
3. Unpublished results .....	83
3.1. Effects of <i>sel-5</i> on touch receptor neurons (TRNs) migration, position, and polarity ..	83
3.2. Effects of <i>sel-5</i> on excretory cell canals morphology .....	87
4. Discussion .....	91
4.1. MTMR9 regulation of autophagy and early secretory pathway .....	91
4.2. MTMR9 regulation of secretory pathway .....	94
4.3. SEL-5/AAK1 regulation of QL.d migration in <i>C. elegans</i> .....	96
4.4. SEL-5/AAK1 regulation of <i>C. elegans</i> excretory system .....	98
5. Conclusions .....	102
6. Publications and author contributions .....	103
7. References .....	104

# 1. Introduction

## 1.1. Kinases and phosphatases in posttranslational modifications

Posttranslational modifications (PTM) are vital for the proper function, localization, and stability of both enzymatic and non-enzymatic proteins. While there are various kinds of PTM, this work will focus on the addition and removal of phosphate groups to/from proteins. The removal of phosphate groups from lipid molecules will also be discussed. Strictly speaking, lipid phosphorylation and dephosphorylation are not classified as PTM. However, the common evolutionary origin and similarity in their mechanism allow for inclusion of both under this thesis' topic. The processes of protein (and lipid) phosphorylation and dephosphorylation are accomplished by two types of enzymes, kinases, and phosphatases, respectively. The reversibility of protein phosphorylation is the main point where opposing roles of kinases and phosphatases come together in the regulation of a wide range of cellular processes. At least two-thirds of proteins encoded in the human genome are regulated by phosphorylation (reviewed in Ardito et al., 2017). Such a high number of different protein phosphorylations requires a substantial amount of protein kinases. Indeed, there are over 500 identified genes coding for kinases in the human genome (Manning et al., 2002). Correspondingly, approximately 180 protein phosphatases counteracting kinase activity are also identified in the human genome (Chen et al., 2017). An imbalance between the actions of kinases and phosphatases caused by their mutations is associated with a large variety of diseases (reviewed in Lahiry et al., 2010).

### 1.1.1. Kinase function and regulation

Protein kinases are enzymes that selectively bind their substrates and use ATP or very rarely GTP molecule to covalently attach one phosphoryl group ( $\text{PO}_3^{2-}$ ) to a targeted amino acid (Liu & West, 2017). Most protein kinases phosphorylate -OH groups on side chains of amino acids serine, threonine, or tyrosine. Phosphorylation on serine or threonine represents the vast majority of all such modifications by protein kinases, accounting for 98% of all protein phosphorylations (Olsen et al., 2006). Tyrosine phosphorylations by protein tyrosine kinases (PTK) are extremely important despite them representing only the remaining 2% of the overall amount (Olsen et al., 2006). The function of receptor tyrosine kinases (RTKs) for effective signal transduction and other aspects of cellular life is indispensable (reviewed in Saraon et al., 2021; Schlessinger, 2000).

Despite a high number of identified kinases and a variety of their substrates, there are sequential and structural similarities that enable the formation of one protein superfamily of kinases (Figure 1). Based on the structure, function, and regulation mode the protein kinase superfamily can be divided into 10 groups of "typical" kinases (AGC, CAMK, CK1, CMGC, NEK, RGC, STE, TKL, TYR, and OTHER) and six groups of "atypical" kinases (ADCK, Alpha-type, PI3-PI4-related, RIO, PDK/ BCKDK, and FASTK) (Modi & Dunbrack, 2019a). Some kinase regions within the superfamily are highly homologous among all its members. The vital catalytic domain is one such region (Hanks & Hunter, 1995). Roles of this domain are very similar in all kinases. It binds ATP as a source of the phosphate group, selects and binds the substrate to be phosphorylated, and finally, it executes the process of phosphorylation

(Knighton et al., 1991). A kinase domain usually consists of up to 300 amino acids and can be divided into two spatially distinguishable subunits an N-terminal lobe, predominantly made of  $\beta$ -sheets, and mostly  $\alpha$ -helical C-terminal lobe (Figure 2).

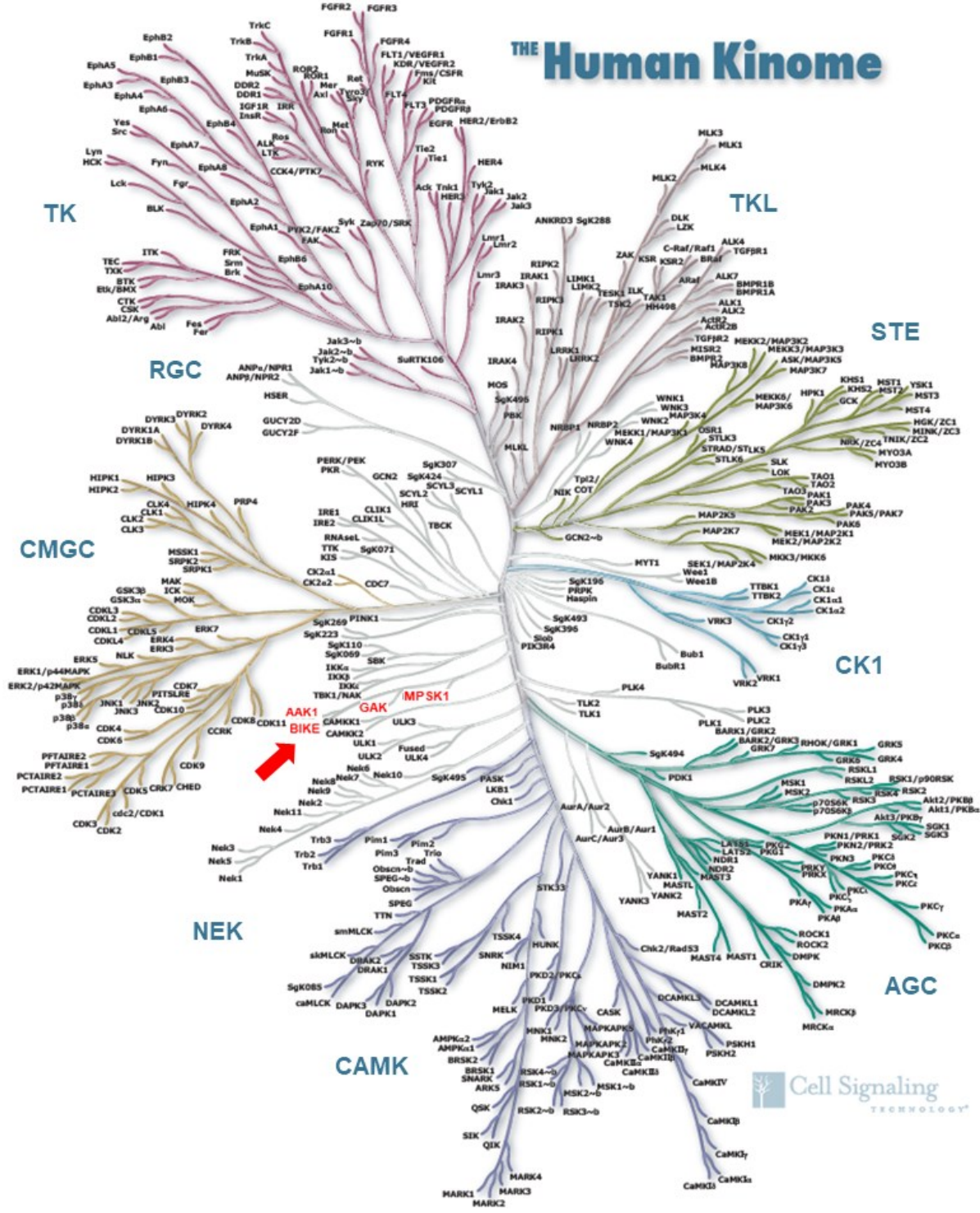


**Figure 1. The human kinome dendrogram.** Depiction of the kinase superfamily of proteins in the form of a dendrogram. The red arrow points to a group of Numb-associated kinases (NAK). The dendrogram was adjusted and reproduced with the consent of Cell Signalling Technology company.

The catalytic site of a kinase domain is located at the intersection of these two lobes and apart from catalysis itself it is also chiefly responsible for substrate selection (Knighton et al., 1991). The activation segment, a part of the C-terminal lobe, contains the DFG motif that chelates  $Mg^{2+}$  cation and facilitates a proper interaction with ATP and its positioning towards a substrate (Hanks et al., 1988). The activation segment is often disordered in inactive kinases and needs to be phosphorylated itself to change conformation and switch the kinase “on” (Levin & Zoller, 1990). Alternatively, allosteric activation or a combination of phosphorylation and allosteric activation may also be necessary in some cases (Groenen et al., 1997).

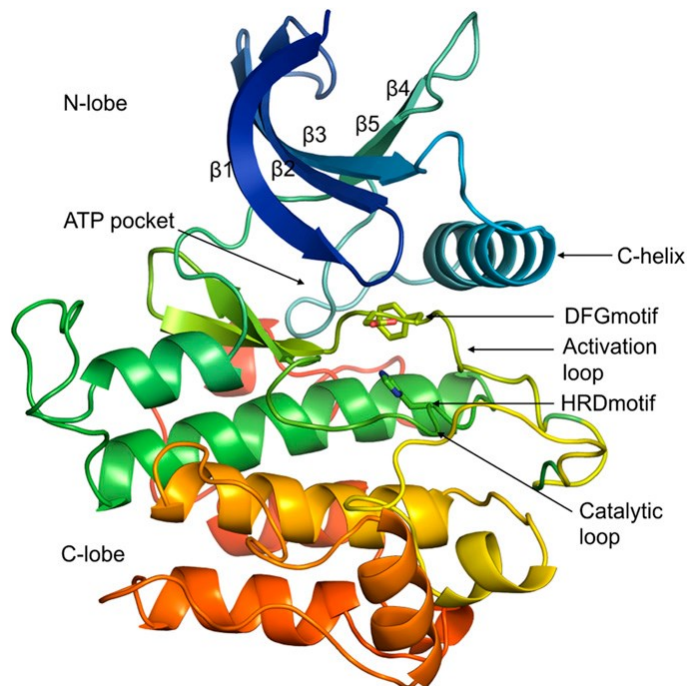


**Figure 2. A typical bilobate kinase domain structure on the example of INSR kinase.** Depiction of INSR containing typical features of kinase domain. Two separate lobes are mapped out. N-lobe at the top predominantly consists of  $\beta$ -sheets while C-lobe is mostly  $\alpha$ -helical. Catalytic activity is located to the interface of the two lobes. ATP binding pocket, HRD motif and other segments and loops vital for kinase enzymatic function are all found here. Adapted from (Modi & Dunbrack, 2019b) (PDB ID code 1GAG).

Proper substrate recognition is necessary for the specific protein kinase interaction and phosphorylation. Phosphorylation site sequence (P-site), a potentially phosphorylated serine/threonine or tyrosine on the substrate and its immediate neighboring amino acids, form a consensus sequence recognized by its corresponding kinase (Pearson & Kemp, 1991). To accomplish sufficient substrate specificity, it is necessary for kinases and their substrates to interact with other, sometimes more distal substrate docking sites (Bardwell & Thorner, 1996). Once a substrate,  $Mg^{2+}$ , and ATP are properly bound by a kinase, the N- and C-terminal lobes conformation changes by rotation and closing of the catalytic cleft (Olah et al., 1993). This causes the catalytic loop, containing the HRD motif, direct interaction with a hydroxyl group of serine/threonine or tyrosine in the substrate P-site and phosphorylation can take place. Regulation of protein kinase location and activity is done either by kinase regulatory domains or by separated regulatory proteins (regulatory subunits).

### 1.1.2. Phosphatase function and regulation

As already mentioned, the main role of protein phosphatases is the removal of phosphoryl groups from amino acids modified by kinases. Catalytic domains of protein kinases are fairly conserved throughout the protein kinase superfamily. Contrary to this, protein phosphatases



seem to be more diverse in their catalytic site folds and activity mechanisms (Chen et al., 2017). The numbers of PTKs and protein tyrosine phosphatases (PTPs) in the human genome are very similar (Alonso et al., 2004). This is not the case for protein serine/threonine kinases (STK) and protein serine/threonine phosphatases (PSTP) (Shi, 2009). PSTPs account for roughly 30 of 180 known phosphatases while there are well over 300 STKs (Chen et al., 2017). This means that there are at least 10-fold as many STKs compared to PSTPs. PSTPs thus need to be more versatile in their substrates to properly counter the activity of STKs. It is indeed the case of Protein phosphatase 1 (PP1) that interacts with more than 50 individual regulatory subunits which greatly expands the spectrum of its substrates (reviewed in Cohen, 2002).

Chen et al. classified protein phosphatases into 10 groups (AP, CC1, CC2, CC3, HAD, HP, PHP, PPPL, PPM, and RTR1) depending on their phosphatase fold structure (Figure 3.) (Chen et al., 2017). CC1, CC2, and CC3 groups, which collectively account for more than half of the human phosphatome, share a common cysteine-based catalytic motif C(X)<sub>5</sub>R (Alonso, et al., 2004). Interestingly, the CC1 group also contains families of non-protein phosphatases which predominantly use phosphatidylinositol phosphates (PIPs) as their substrate. This category includes myotubularin-related proteins (MTMRs), phosphatase and tensin homologs (PTENs), and Sac domain-containing proteins (SACs) (Blondeau et al., 2000; Hughes et al., 2000; Maehama & Dixon, 1998; Taylor et al., 2000). These PIP-specific phosphatases represent an important counterbalance to PIP-specific kinases (reviewed in Sasaki et al., 2009). Given the nature of their substrate, PIP phosphatases should not be classified as protein phosphatases. However, the conservation of their catalytic domains points towards a common origin and they are usually included in protein phosphatases dendrograms. The involvement of PIPs in various cellular processes and their regulation by MTMRs will be described later in chapter 1.3.

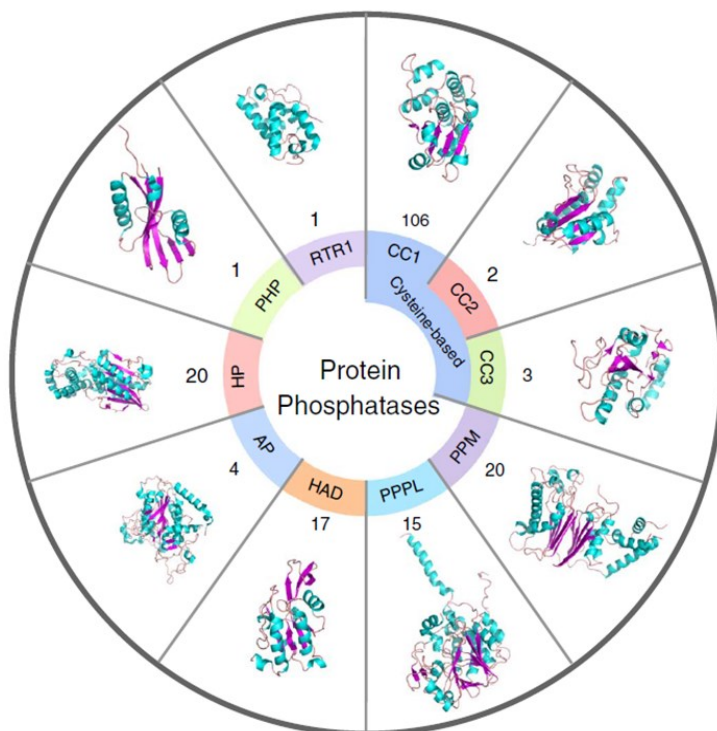


**Figure 3. Human phosphatases divided according to their phosphatase fold structures.** Using structures of phosphatase folds, human phosphatases can be divided into ten different groups (AP, CC1, CC2, CC3, HAD, HP, PHP, PPPL, PPM, and RTR1). Most phosphatases (including lipid-specific phosphatases MTMRs) belong to the first of cysteine-based phosphatase groups. Adapted from (Chen et al., 2017).



## 1.2. Non-enzymatic functions of kinases and phosphatases

Apart from the standard roles associated with kinases and phosphatases, these enzymes also exhibit functions independent of their “canonical” enzymatic mode of action. A subset of genes for both kinases and phosphatases encodes enzymes with amino acid variations in their key regions that alter the original enzymatic activity. In extreme cases, their catalytic activity can be abolished completely giving rise to kinase/phosphatase dead (catalytically inactive) proteins. Of the 500 identified human kinases up to 50 are classified as pseudokinases (reviewed in Eyers & Murphy, 2013). Similarly, of the 180 identified human phosphatases 28 are classified as pseudophosphatases (reviewed in Reiterer et al., 2020). Despite the inactivity (or near inactivity) of these pseudoenzymes, they are still important regulators of catalytically intact enzymes, signaling pathways, cell cycle, intracellular trafficking, and other cellular processes (reviewed in Boudeau et al., 2006 and in Eyers & Murphy, 2013).

### 1.2.1. Pseudokinases and pseudophosphatases

Pseudokinases have been classified into different groups based on deviations from the established catalytic motif sequences (Manning et al., 2002). Alternatively, they can be divided in accordance with their ability to bind nucleotides and/or bivalent metal cations, both of which are necessary for full enzymatic activity. Regarding these binding abilities, pseudokinase domains can be categorized into four groups as follows: class I pseudokinase domains are unable to bind nucleotides or cations, class II pseudokinase domains are able to bind nucleotides only, class III pseudokinase domains are able to bind cations only, and class IV pseudokinase domains are nucleotide- and cation-binding (Murphy et al., 2014). More than half of tested pseudokinase domains were unable to bind nucleotides, suggesting that these are truly catalytically inactive domains. Only six human pseudokinase domains (of 21 tested) were detected to interact with both ATP and metal cations and thus fit class IV (Murphy et al., 2014). This gives at least a hypothetical chance for these pseudokinase domains to retain some of their enzymatic activity. Despite invariantly having their HRD motif disrupted, a partial enzymatic activity was indeed reported for at least some of them (Shi et al., 2010; Ungureanu et al., 2011).

Similarly to pseudokinases, pseudophosphatases have usually retained the 3D structure of functional enzymes. In most cases, it is substitutions in their catalytic motifs that render them inactive. The most active phosphatases belong to the CC1 group based on the Chen et al. categorization and accordingly, this group also contains the most known pseudophosphatases (Chen et al., 2017). Several pseudophosphatases were identified in the PIPs-specific enzyme category. Among these are some members of the MTMR family as well as Tensin 1 and 2 from the PTEN family of phosphatases (reviewed in Alonso, et al., 2004 and in Mattei et al., 2021). Both active and inactive MTMRs are discussed later in chapter 1.3. Protein-specific pseudophosphatase domains are frequently present in otherwise active PTPs. RPTP $\alpha$  is a receptor tyrosine-phosphatase containing two active phosphatase domains (Wang & Pallen, 1991). D2 phosphatase domain activity is lower compared to D1 (Wu et al., 1997). However, other RPTPs with two phosphatase domains may also consist of one membrane proximal active phosphatase domain D1 and one distal inactive pseudophosphatase domain D2 (Chen et al., 2017).

### 1.3. Myotubularin-related proteins (MTMRs)

Myotubularin 1 (MTM1) and related MTMRs are a family of lipid-specific phosphatases (Laporte et al., 1997). MTMRs are enzymatically active in removing phosphate groups from some of the PIPs (Blondeau et al., 2000; Taylor et al., 2000). PIPs belong to a category of amphiphilic phospholipids with a polar inositol head group (Figure 4). This inositol can be modified with one, two, or three phosphorylations forming seven different PIPs with a variety of functions in cells (reviewed in Vicinanza et al., 2008). The conversion of one PIP type into another is mediated by several groups of phosphoinositide kinases and phosphatases (reviewed in Sasaki et al., 2009). MTMRs are able to remove a phosphate group from the D3 inositol position of phosphatidylinositol 3-monophosphate (PI3P) (Blondeau et al., 2000; Taylor et al., 2000) and phosphatidylinositol 3,5-bisphosphate (PI(3,5)P2) (Walker et al., 2001) (Figure 4). Different PIPs are distributed throughout cell membranes in diverse spatial and temporal patterns. For example, phosphatidylinositol 4,5-bisphosphate (PIP2) is typically present in the inner leaflet of the PM, whereas PI3P and later PI(3,5)P2 are usually associated with early and late endosomes, respectively (reviewed in Vicinanza et al., 2008). While these specific PIPs localizations are not exclusive, they are nevertheless important for the recruitment of effector proteins to their intended destinations. Disruption of tight PIPs regulation by mutations in their kinases and/or phosphatases potentially causes various diseases including myopathies, neuropathies, and cancers (reviewed in Hnia et al., 2012).

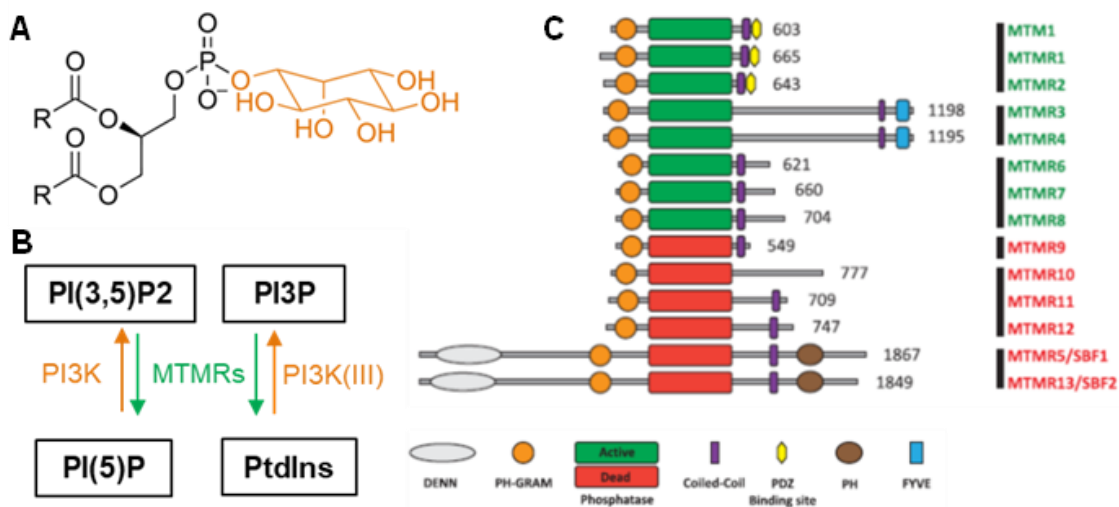


**Figure 4. A lipid-specific phosphatases of MTMRs family and their domain structure.** Myotubularins are PIP-specific phosphatases that are able to exclusively remove phosphates from positions 3' of the inositol group (A). PI(3,5)P2 and PI3P are targets of MTMRs activity giving rise to PI(5)P and PtdIns, respectively. MTMRs counterbalance activity of PIP-specific group of kinases PI3K (B). MTMR phosphatase family can be further divided into several subgroups depending on their domain content, sequence, and binding partners. Several members of these subgroups carry a mutation in their active site that renders them enzymatically inactive. These MTMRs can therefore be classified as pseudophosphatases and function as important regulators of their active partners (C). Adapted from (Raess et al., 2017).

### 1.3.1. MTMRs structure and function

MTMRs in humans consist of 16 conserved proteins (reviewed in Alonso et al., 2004). All members of the MTMR family contain a catalytic motif C(X)<sub>5</sub>R typical for the CC1 group of PTPs despite their non-protein PIPs substrates. Sequence and domain composition are highly conserved within the MTMR family (Figure 4). One noticeable exception is MTMR5 and MTMR13 with an extra N-terminal DENN domain which is not found in other MTMRs (reviewed in Laporte et al., 2003). DENN domains typically stimulate the GTPase activity of the small G protein Rab family (Yoshimura et al., 2010). MTMR5 and MTMR13 were each shown to form a complex with MTMR2 and to coordinate the turnover of PI3P as well as the activity of Rab GTPases in different stages of neural development (Jean et al., 2012; Mammel et al., 2022). Interestingly, both MTMR5 and MTMR13 have their catalytic C(X)<sub>5</sub>R motif mutated abolishing their phosphatase activity. This is also the case with several other MTMRs namely, MTMR9, MTMR10, MTMR11, MTMR12, and MTMR15. Despite their inability to directly dephosphorylate PIPs, they are still important in this process. Inactive MTMRs were shown to form heterodimers with their active homologs and thus regulate this complex activity and/or recruitment to a specific membrane (Lorenzo et al., 2006). C-termini of nearly all MTMRs contain coiled-coil domains that play a role in their homo- and heterodimerization (Kim et al., 2003; Mochizuki & Majerus, 2003). The interaction of MTMRs with membranes is mediated by their PH-GRAM domain. However, PH-GRAM affinity to PIPs in membranes is relatively low, suggesting a necessity for other MTMR regions in membrane recruitment (Berger et al., 2003).

The main substrates of MTMRs, PI3P and PI(3,5)P<sub>2</sub>, are important in endocytic vesicle maturation. Nevertheless, these two PIPs and concomitantly MTMRs' roles are not limited to this phenomenon exclusively. Different MTMRs were reported as regulators of many other cellular processes. Autophagy is a mechanism of damaged macromolecules and organelles degradation that takes place in the cytosol (reviewed in Levine & Deretic, 2007). Metabolic stress is one of the possible triggers that cause upregulation of autophagocytosis. Its initiation is mediated by PI3P-generating kinase (PI3K) activation which leads to PI3P accumulation. PI3P then serves as a docking site for autophagosome-generating protein complexes. PI3K action needs to be countered by MTMRs phosphatase activity to tightly regulate the level of PI3P production. MTMR14 and to a lesser degree MTMR6 were identified as phosphatases specifically regulating autophagy in various mice-derived cells (Liu et al., 2014; Vergne et al., 2009). Knock-down of MTMR2 or MTMR5 also caused the upregulation of autophagy activity in human neuronal cells (Chua et al., 2022). Moreover, decreased ability to clear damaged organelles caused by age-associated defects in autophagy was shown to occur along with the accumulation of MTMR14 in *Drosophila melanogaster* neurons. A similar observation was made in post-mortem human brains as well (Kovács et al., 2022).

### 1.3.2. Myotubularin-related protein 9 (MTMR9)

MTMR9 is the sole member of one MTMR subfamily and similarly to several other MTMRs, it has its active site mutated. Inactive MTMRs tend to form heterodimers with active MTMR family members regulating their functions (Lorenzo et al., 2006). MTMR9 was indeed identified as a binding partner for active phosphatases MTMR6 and MTMR7. These interactions are mainly mediated by the C-terminal coiled-coiled domains. The SID domain of

MTMR9 also binds to MTMR7, however, this interaction is extremely weak. Interestingly, apart from heterodimers with MTMR6 and MTMR7, MTMR9 is also capable of homodimerization (Mochizuki & Majerus, 2003). The potential role of this inactive phosphatase complex is yet to be elucidated. While inactive MTMR5 was shown to regulate the subcellular localization of its binding partner MTMR2, this was not the case of MTMR9 dimerization with MTMR7 (Kim et al., 2003). Coexpression of MTMR9 with MTMR7 in COS-7 cells does not change the ratio of cytosolic and membranous MTMR7 pools. However, *in vitro* MTMR7 activity towards its substrate increases substantially when complexed with MTMR9 (Mochizuki & Majerus, 2003). Similarly, coexpression of MTMR9 with MTMR6 greatly increases MTMR6 activity. At the same time, higher protein levels of both MTMR6 and MTMR9 were measured, suggesting that dimerization also prevents degradation of these MTMRs (Zou et al., 2009). MTMR6 and MTMR7 belong to the MTMR subfamily that includes MTMR8 as well. Likewise, MTMR9 interaction with MTMR8 was also detected. Results of the initial yeast two-hybrid system (Y2H) screen were confirmed by coimmunoprecipitation experiments in transfected HeLa cells. Apart from effects on MTMR activity and protein stability, dimerization of MTMR6 or MTMR8 with MTMR9 also shifts their substrate specificity. MTMR9-MTMR6 complex prefers PI(3,5)P2 as a substrate and regulates apoptosis, while the MTMR9-MTMR8 complex preferentially uses PI3P in the regulation of autophagy (Zou et al., 2009, 2012).

The complex of MTMR6-MTMR9 was additionally identified as a possible regulator of macropinocytosis. EGF stimulation of serum-starved A431 cells leads to dextran internalization via macropinocytosis. Treatment of these cells with a macropinocytosis inhibitor predictably causes a significant decrease in dextran uptake. Interestingly, a knock-down of either MTMR6 or MTMR9 has the same effect on macropinocytosis. Tfn internalization via the CME was on the other hand, not perturbed neither by MTMR6 nor MTMR9 knock-down in A431 cells (Maekawa et al., 2014). Contrary to this, experiments in *C. elegans* showed that *mtm-6* or *mtm-9* genes mutation cause a significant reduction of coelomocytes endocytosis (Dang et al., 2004). MTMR9 was also described as a regulator of CD4<sup>+</sup> T-cell differentiation. Knock-down of MTMR9 leads to a preferential differentiation into T-helper subtype Th1 whereas knock-down of MTMR7 causes differentiation into T-cell subtypes Th2 and Th17. Both of these knock-downs exhibit increased protein kinase B (PKB)-mediated phosphorylation in their respective T-helper cells. This PKB activity regulation by various MTMRs probably works through PIPs content changes in relevant membranes (Guo et al., 2013).

The physiological importance of MTMR9 is underscored by its identification as a cause or a contributor of several human diseases. Single nucleotide polymorphisms (SNPs) in the *MTMR9* gene were associated with an increased risk of obesity and high blood pressure (Yanagiya et al., 2007). Although the exact role of MTMR9 is not known, a higher level of its mRNA was measured in the murine hypothalamus as a result of fasting. Contrary to that, mice fed with a high-fat diet exhibited lower MTMR9 mRNA levels in their hypothalamus (Yanagiya et al., 2007). The same SNPs in the *MTMR9* gene were shown to be associated with the development of a condition called metabolic syndrome which encompasses previously described risk of obesity and hypertension as well as other metabolic abnormalities (Hotta et al., 2011). A subset of patient oesophageal adenocarcinoma (OAC) samples showed overexpression of MTMR9 and several other genes. At the same time, a six-fold increase in MTMR9 protein level was detected (Goh et al., 2011). It is, however, not known whether the difference in expression of MTMR9 is a cause or a consequence of OAC. Several MTMR9

SNPs were also associated with non-syndromic intellectual disability (NSID), epilepsy, and even personality traits of neuroticism and extraversion (Baulac et al., 2008; Lo et al., 2017; Shi et al., 2020). The mode of action of MTMR9 in these diseases and traits is completely unknown.

#### **1.4. AP2-associated kinase (AAK1)**

Adaptor protein 2 (AP2) is a tetrameric complex important for the regulation of clathrin-mediated endocytosis (CME). AP2 enables indirect clathrin binding to the plasma membrane (PM) around the selected cargo and supports subsequent membrane invagination and maturation of clathrin-coated pit (CCP) (reviewed in Schmid, 1997). AP2 tetramer consists of two large subunits  $\alpha$ - and  $\beta$ 2-adaptins, one small subunit  $\sigma$ 2 and one medium subunit  $\mu$ 2 (reviewed in Kirchhausen, 1999). Phosphorylations of AP2 subunits were suggested to regulate its activity in proper cargo selection and its ability to recruit clathrin (Wilde & Brodsky, 1996). This notion was supported by the detection of the kinase activity of proteins isolated along with clathrin-coated vesicles (CCV) (Pauloin et al., 1982). AP2-associated kinase 1 (AAK1) was copurified from a pig brain lysate along with the AP2 complex and shown to phosphorylate the AP2 subunit  $\mu$ 2 (Ricotta et al., 2002). Based on its homology with several yeast kinases, AAK1 was classified as a novel member of the Prk/Ark kinase group (Conner & Schmid, 2002). Outside of the yeast research community, Prk/Ark kinase group is mostly referred to as NAK group of kinases. The group name is derived from Numb-associated kinase (NAK), a relatively well-studied member of this group in fly *D. melanogaster*. Throughout this work, the latter classification of AAK1 as a NAK member will be used preferentially.

##### **1.4.1. Clathrin-mediated endocytosis (CME)**

During endocytosis in eukaryotic cells, some transmembrane proteins and receptors are specifically selected for their internalization and further processing in the cell interior. This can be done via several independently regulated ways working in parallel. CME is endocytosis which depends on clathrin for its proper function and is highly selective for its cargo and tightly regulated at every step of this process.

Initiation of CME is triggered by F-BAR domain only proteins (FCHO1/2) binding to the PM (Henne et al., 2010) (Figure 5). Compared to standard BAR domains, BAR domains of FCHOs are suited to bind less curved membranes, making them ideal for interaction with the PM (Henne et al., 2007). Moreover, FCHO1/2 showed a preference for membranes containing PIP2, a PIP typically present in the PM. PIP2 decrease causes FCHO1/2 relocation from the PM to the cytosol (Henne et al., 2010). FCHO1/2 along with their interacting partner, epidermal growth factor receptor substrate 15 (Eps15), appear to be the first markers of nascent CCP at the PM (Henne et al., 2010; Ma et al., 2015). Multiple DPF motifs on Eps15 are able to bind FCHO1/2 and simultaneously AP2 complex in a non-competitive way. The initiator complex FCHO1/2-Eps15 helps to orient AP2 for its efficient interaction with the PM (Ma et al., 2015). AP2 orientation and conformational shift expose its subunits to PIP2 in the PM (Jackson et al., 2010). Several AP2-PIP2 interactions stabilize AP2 in open conformation which is favorable for its search of a potential CME cargo (Höning et al., 2005) (Figure 5). A typical cargo internalization signal recognized by the  $\mu$ 2 subunit is a tyrosine-based sequence Yxx $\Phi$  (Ohno et al., 1995). This canonical motif is present in the transferrin receptor (TfnR), one of the most studied receptors undergoing CME (Jing et al., 1990). Other frequently encountered

internalization motifs are NPxY found on the low-density lipoprotein receptor (LDLR), and dileucine motif LL (Chen et al., 1990; Letourneur & Klausner, 1992). However, these two motifs are recognized either by a different AP2 subunit or different adaptor proteins altogether (Boll et al., 2002). AP2 open conformation bound with its cargo recruits clathrin to the nascent CCP (Kadlecova et al., 2017). Interaction of AP2 with other proteins and PIP2 leads to a gradual displacement of FCHO1/2 from this complex. FCHO1/2 is pushed to the edges of a future CCP, forming a ring-like structure that prevents AP2-clathrin complex lateral diffusion (Figure 5). At the same time, FCHO1/2 in this ring supports further recruitment of AP2 and promotes CCP maturation (Zaccai et al., 2022).

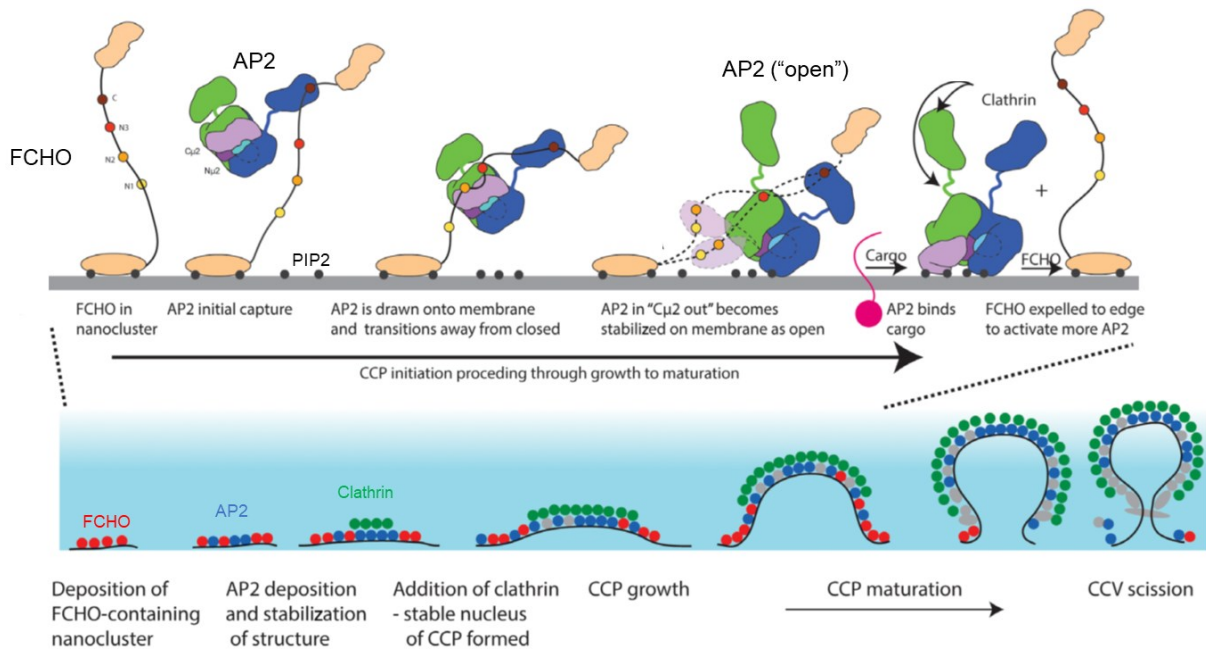


**Figure 5. Detail of initiation and progress of clathrin-mediated endocytosis (CME).** One of the pioneering proteins at the nascent endocytosis site is FCHO. It interacts with PIPs in the plasma membrane (PM) and recruits AP2 complex. The AP2 complex switches into an “open state” once it interacts with both FCHO and PIPs in the PM. In the “open state” AP2 is able to recognize and bind a prospective cargo protein. This leads to a gradual displacement of FCHO from the nascent endocytosis complex. Clathrin accumulates in the complex and together with other endocytosis regulators control formation of the clathrin-coated pit (CCP) and its maturation. After scission of the mature CCP from the PM clathrin-coated vesicle is formed and later its protein coat is removed. Adapted from (Zaccai et al., 2022).

Accumulation of a clathrin lattice on the PM is by itself not sufficient to drive membrane invagination and CCP formation. Other proteins are necessary for clathrin to deform the membrane and give rise to a mature CCV (Bhave et al., 2020). These proteins either help to polymerize clathrin or reshape its interactions to produce enough force for the PM to curve inward (Kroppen et al., 2021). One of the vital components of CME is actin polymerization (Lamaze et al., 1997). Mammalian cells seem to require actin in the later stages of the CME when pinching of CCP from the PM occurs (Merrifield et al., 2002). Similarly to clathrin adaptors, some actin polymerization regulators also interact with phospholipids.

Wiscott-Aldrich syndrome protein (WASP) binds to the PM through its PIP2 binding domains and recruits Arp2/3 which in turn stimulates the branching of new actin filaments (Merrifield et al., 2004; Rohatgi et al., 1999). A host of actin-interacting proteins then accumulate and create an actin meshwork mechanically stabilizing a nascent CCP (Goode et al., 2014). The base of the new CCP is made of a highly curved membrane which is recognized by BAR domain-containing sorting nexin-9 (SNX9) (Lo et al., 2017; Schöneberg et al., 2017). Amphiphysin and endophilin which also recognize highly curved membranes then along with SNX9 recruit dynamin (Meinecke et al., 2013). Dynamin polymerization around a narrow CCP neck causes its fission from the PM and a formation of CCV (Hinshaw & Schmid, 1995).

Immediately after CCV detachment from the PM, its protein coat and clathrin lattice undergo rapid disassembly. This step is important for membranous vesicles' ability to fuse with other endocytic vesicles and to form early endosomes. A complex of auxilin and heat shock cognate 71 kDa protein (HSC70) interacting with a clathrin lattice is thought to be mainly responsible for its dismantling (Schlossman et al., 1984; Ungewickell et al., 1995). HSC70 is recruited to a triskelion in the clathrin network by the J-domain of auxilin (Holstein et al., 1996). This interaction stimulates the ATPase activity of HSC70 and the dynamic assembly-disassembly balance of clathrin cages is pushed towards rapid disassembly effectively peeling clathrin from CCV (Rothnie et al., 2011). During CCP maturation a phospholipid composition of the PM and later of CCV is very important. PIPs especially play a significant role in CME regulation (reviewed in Posor et al., 2015). At the beginning of the process, PIP2 is the prevalent PIP in the inner PM leaflet. CCP budding and its fission from the PM are accommodated by a gradual decrease of PIP2 (Zoncu et al., 2007). Dynamin in the neck region of CCP recruits PIP phosphatase synaptojanin that reduces PIP2 and increases phosphatidylinositol 4-monophosphate (PI4P). This loss of PIP2 destabilizes adaptor proteins' interaction with the membrane and helps the process of uncoating (Cremona et al., 1999).

#### **1.4.2. AAK1 function in CME**

As previously stated, CCV formation depends on tight regulation of phosphorylation on the participating proteins. Pauloin et al. showed in 1982 that coated vesicles isolated from bovine brains contain cyclic nucleotide- and  $\text{Ca}^{2+}$ -independent protein kinase. They also showed this kinase ability to phosphorylate a 50 kDa protein, later identified as the AP2  $\mu 2$  subunit (Pauloin et al., 1982). The same group later discovered that the  $\mu 2$  subunit threonine 156 is a target of the said kinase (Pauloin & Thuriereau, 1993). Overexpression of  $\mu 2$  subunit with a threonine 156 to alanine mutation causes a severe reduction in transferrin internalization (Olusanya et al., 2001). A series of *in vitro* experiments using AP2 subunit  $\alpha$ -adaptin as a bait identified a novel serine/threonine kinase AAK1 and its ability to directly phosphorylate the  $\mu 2$  subunit of AP2 (Conner & Schmid, 2002; Ricotta et al., 2002). It seems likely that AAK1 and the originally discovered cyclic nucleotide- and  $\text{Ca}^{2+}$ -independent protein kinase are identical enzymes. CCVs isolated from pig brains contain two individual kinases, AAK1 and cyclin G-associated kinase (GAK), which are both able to phosphorylate the  $\mu 2$  subunit (Ricotta et al., 2002; Umeda et al., 2000). However, further separation of pig brain isolates showed that GAK is associated with AP1 rather than with AP2 (Ricotta et al., 2002). GAK was also shown to localize to the trans-Golgi network (TGN) instead of the PM (Greener et al., 2000). These experiments suggest that AAK1 might be functionally specific but not necessarily exclusive kinase phosphorylating the AP2 subunit  $\mu 2$ .



Both AAK1 and GAK are classified as members of the NAK kinase family. This kinase family consists of four homologs in mammals (Figure 6). Apart from AAK1 and GAK, there are BMP-2-inducible kinase (BMP2K) and myristoylated and palmitoylated serine/threonine kinase (MPSK1). AAK1 and BMP2K are structurally most related to each other (Sorrell et al., 2016). Their kinase domains with a relatively high sequence homology are located N-terminally. Outside of the kinase domains, the NAK family shows little similarity among its members. GAK, a more distant relative of AAK1 and BMP2K, carries two unique features, one PTEN domain and one DNA-J domain (Kanaoka et al., 1997) (Figure 6). MPSK1, evolutionary even more separated from the other NAK members, has its C-terminal portion substantially shortened leaving only the kinase domain intact. Unlike kinases whose activity is regulated by activation loop phosphorylation, the NAK kinase family activation loop stably interacts with the kinase active site (Sorrell et al., 2016) (Figure 6). This leads to a permanently active conformation of the NAK kinases. Despite the relative similarity of BMP2K, GAK, and AAK1 kinase domains and their proven ability to phosphorylate  $\mu$ 2, it is currently unclear to what extent, if any, are these kinases functionally redundant (Ramesh et al., 2021; Ricotta et al., 2002; Umeda et al., 2000).

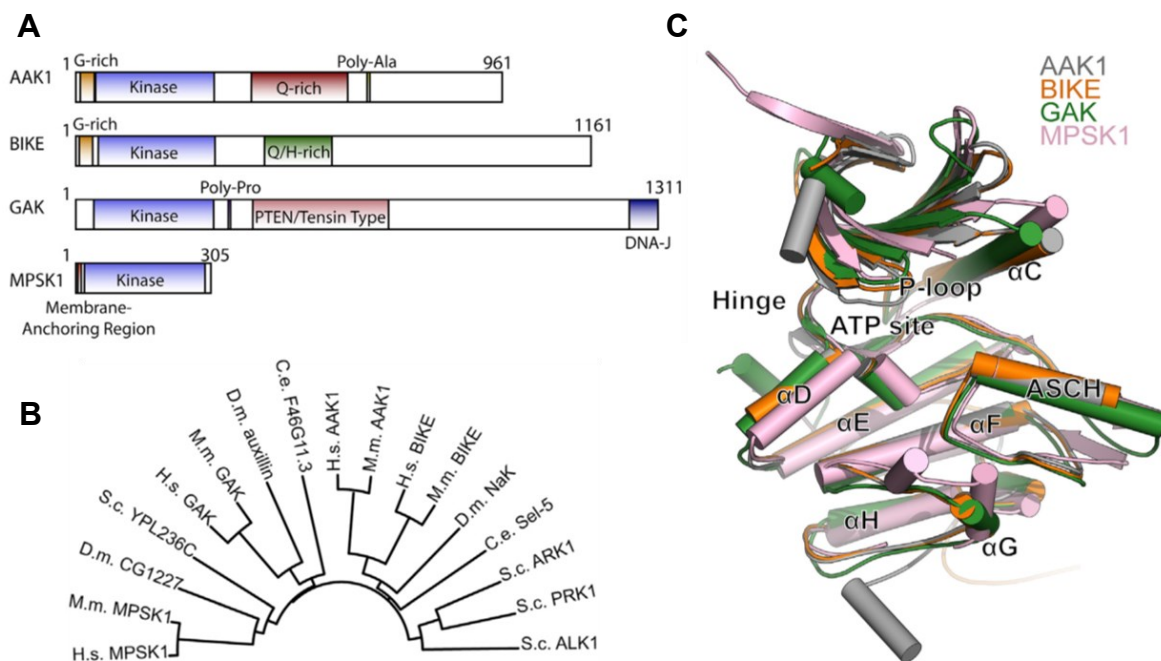


**Figure 6. A family of Numb-associated kinases (NAK) and structure of their active site.** There are four members of NAK family of kinases in mammals. These kinases are highly conserved in their kinase domain. AAK1 and its closest homolog BIKE additionally share a Q-rich region in C-terminal half. GAK contains two unique domains PTEN and DNA-J and MPSK1 consists of kinase domain only (A). NAK homologs are found throughout animal kingdom including *C. elegans* and as early in evolutionary tree as in *Saccharomyces cerevisiae* (B). The activation loop of NAK kinases continually interacts with active site rendering these kinases permanently active (C). Adapted from (Sorrell et al., 2016).

AAK1 carries several motifs and regions enabling protein-protein interactions. DPF and NPF motifs in the C-terminal region seem to be important for AAK1 interaction with AP2 (Jha et al., 2004). Truncated AAK1 with missing C-terminus showed severely limited ability to



phosphorylate the  $\mu 2$  subunit. This could be bypassed by overexpression of the truncated AAK1, suggesting AP2-interacting motifs other than DPF and NPF might be involved (Conner & Schmid, 2003). Additional motifs, DLL, SLL, and LIDL enable AAK1 interaction with clathrin (Morgan et al., 2000). Multiple interactions were detected between AAK1 and assembled clathrin triskelia as well as isolated clathrin light or heavy chains. Sites of these interactions are dispersed throughout all AAK1 regions including its kinase domain. Interestingly, AAK1 interaction with clathrin enhances its phosphorylation activity towards  $\mu 2$  (Conner et al., 2003; Jackson et al., 2003). This would be one conceivable way of physiological regulation of AAK1 function given its inherently active conformation (Sorrell et al., 2016). Apart from the  $\mu 2$  subunit, an endocytic adaptor Numb was identified as another substrate of AAK1. Phosphorylation of Numb leads to its relocalization from the PM to a perinuclear region. Concomitantly, AAK1 depletion causes accumulation of Numb at the PM. Kinase-dead AAK1 mutant does not cause Numb relocalization proving the necessity of AAK1 phosphorylation activity in this process (Sorensen & Conner, 2008). AAK1 interaction with Numb seems to play a role in Notch pathway regulation. After cleavage of the Notch receptor, its membrane-tethered fragment distribution and activity are regulated by AAK1 and Numb in an opposing manner (Gupta-Rossi et al., 2011).

AAK1 generally localizes to places with a high rate of endocytosis, such as presynaptic terminals in neuronal cells or leading edges of migrating cells. At the same time, AAK1 colocalizes with known endocytic machinery regulators AP2, clathrin, and dynamin (Conner & Schmid, 2003). Overexpression of AAK1 reduces the amount of internalized transferrin (Tfn) and low-density lipoprotein receptor-related protein (LRP) in both *in vitro* and *in vivo* experiments. Surprisingly, epidermal growth factor (EGF), which enters cells in the same way as Tfn, was not affected by AAK1 overexpression (Conner & Schmid, 2003). This suggests that rather than a global regulator of CME, AAK1 functions selectively in only a subset of cargo internalizations. It was also shown that AAK1 partially colocalizes with early endosome marker EEA1 hinting at its role in processes downstream of CME. Accordingly, AAK1 knock-down causes an accumulation of TfnR in perinuclear compartments (Henderson & Conner, 2007). Therefore, it seems possible that AAK1 regulates multiple steps of selected receptors' endocytosis and recycling.

Apart from Notch signaling and endocytosis of TfnR and LRP, AAK1 was found to regulate several other important processes. NAK, a *D. melanogaster* homolog of AAK1, was shown to colocalize with clathrin puncta specifically in growing and branching dendrites during their arborization (Yang et al., 2011). Similarly, AAK1 was identified to regulate dendrite growth and branching in mouse neurons (Ultanir et al., 2012). AAK1 interaction with a mutated form of superoxide dismutase 1 (SOD1) was also detected in the Y2H experiment. SOD1 mutation is known to cause amyotrophic lateral sclerosis (ALS). The same mutation that causes SOD1 aggregation also stimulates an accumulation of AAK1 into these aggregates. A possible role of AAK1 in at least a subset of ALS is also supported by lower AAK1 protein levels in ALS patients (Shi et al., 2014). In viral infectious diseases, several enveloped viruses hijack CME for their own entry into a host cell. Hepatitis C virus (HCV) entry and assembly in its host cells are blocked by the inhibition of AAK1 and/or GAK (Neveu et al., 2015). Interestingly the same inhibitors or siRNAs against AAK1 also proved to be effective in blocking the entry of severe acute respiratory syndrome coronavirus 2 (SARS-CoV-2). This blockage affects the entry of pseudo-virus as well as wild-type SARS-CoV-2 into lung epithelial cells *in vitro* (Karim et al., 2022).

The exact role of the AAK1-mediated phosphorylation on AP2 subunit  $\mu 2$  in CME is still not entirely clear. Incubation of AP2 with AAK1 *in vitro* showed up to a 25-fold increase in AP2 affinity towards the sorting motif Yxx $\Phi$  (Ricotta et al., 2002). Whether phosphorylated  $\mu 2$  is necessary for AP2 conformational change, initiation, or for its stabilization is yet to be elucidated. Initial  $\alpha$ -adaptin interaction with PIP2 causes a shift in AP2 conformation so that all its other PIP2 and cargo binding sites are juxtaposed and accessible to the PM (Jackson et al., 2010). This change in shape also exposes the clathrin binding site on  $\beta 2$ -adaptin and thus stimulates clathrin cage assembly (Kadlecova et al., 2017). The amount of  $\mu 2$  phosphorylation was shown to increase as CCP growth progresses (Wrobel et al., 2019). The number of CCP that failed to pinch off from the PM increased dramatically upon AAK1 inhibition. At the same time, a longer lifetime of successfully pinched CCP was observed (Wrobel et al., 2019). Surface plasmon resonance experiment (SPR) suggested that contrary to previously published data,  $\mu 2$  phosphorylation did not play a significant role in AP2 affinity towards its cargo. Instead, this phosphorylation was vital for the recruitment of adaptin ear-binding coat-associated proteins (NECAPs). Loss of NECAPs or  $\mu 2$  phosphorylation significantly reduced the amount of SNX9 (Wrobel et al., 2019). As already mentioned, SNX9 is a BAR-domain-containing protein that recognizes curved membranes and is important for the later stages of CCP maturation (Lo et al., 2017; Schöneberg et al., 2017). Experiments in *C. elegans* also showed accumulation of phosphorylated AP2 in NECAP mutations further supporting the role of AAK1-mediated  $\mu 2$  phosphorylation in later rather than initiation stages of CME (Beacham et al., 2018).

## 1.5. MTMR9 and AAK1 in Wnt signaling

Wnt signaling is necessary in early embryonal development as well as in the homeostasis of adult multicellular organisms. Components of the Wnt signaling pathway are present in protozoans, however, a complete pathway is only found in metazoans (reviewed in Holstein, 2012). Wnt signaling was identified as a developmental regulator in some early-branching animals such as cnidarians and ctenophores (Lee et al., 2007; Pang et al., 2010). Its role in the oral-aboral axis establishment and regeneration in *Hydra vulgaris* is relatively well-described (Hobmayer et al., 2000). This function seems to be conserved throughout the animal kingdom all the way to humans. Asymmetrical cell divisions, differentiation, and organogenesis are all affected by properly functioning Wnt signaling (reviewed in Wang et al., 2012). Tight regulation of stem cell proliferation is another well described Wnt-dependent process (reviewed in Reya & Clevers, 2005). An uncontrolled growth of various tissues can lead to cancerous cell multiplication, especially in fast regenerating parts of organs such as gut epithelium. The vast majority of colorectal cancers are associated with one or more Wnt signaling pathway proteins mutations (reviewed in Kinzler & Vogelstein, 1996). Among other diseases associated with a disruption of Wnt signaling are hepatocellular carcinoma, type II diabetes, and schizophrenia to name just a few (Cotter et al., 1998; Cui et al., 2003; Lee et al., 2008). Wnt signaling is usually divided into canonical and non-canonical branches. In this work, we are mostly dealing with the canonical ( $\beta$ -catenin dependent) arm of the Wnt pathway unless otherwise specified.

### 1.5.1. Wnt signaling

Wnt ligands are cotranslationally transported into the endoplasmic reticulum (ER) of the Wnt-producing cells. Wnts are bound by a membrane-associated O-acyl transferase (PORC) immediately after entering the ER (Tanaka et al., 2000). PORC is active in modifying Wnts with a palmitoleoyl moiety (Coombs et al., 2010). This hydrophobic modification is typical for Wnts and seems to be indispensable for their subsequent transport and signaling activity (Kurayoshi et al., 2007). PORC binds to a conserved hairpin motif of nascent Wnt proteins and uses palmitoleoyl-CoA from cytosol as a substrate for the Wnt acylation (Liu et al., 2022). Wnt is then recognized and bound by a transmembrane protein Wntless (Wls) which is necessary for its efficient transport from the ER to the PM (Bänziger et al., 2006; Bartscherer et al., 2006; Goodman et al., 2006). While in the ER, Wnts are also glycosylated at multiple sites (Smolich et al., 1993). The purpose of these glycosylations is not well described and glycosylation pattern varies in different Wnts. After reaching the PM, Wnt is released from Wls which is then recycled back to the ER through early endosomes and the Golgi apparatus (GA) (Yu et al., 2014). It is the CME that is responsible for Wls internalization from the PM (Pan et al., 2008). The retromer complex together with SNX3 targets Wls in early endosomes and mediates its transport to the GA (Belenkaya et al., 2008; Franch-Marro et al., 2008; Pan et al., 2008; Port et al., 2008; Yang et al., 2008). The GA to ER transport is facilitated by the COPI retrograde transport system (Yu et al., 2014). The ER-targeting sequence of Wls along with ERGIC2 protein and several ARFs were identified to regulate this process (Yu et al., 2014). After its return to the ER, Wls is available for the next round of Wnt secretion.

Owing to their lipid modification, Wnts are highly hydrophobic and thus unable to form a gradient in the hydrophilic extracellular space. This hydrophobicity problem is overcome in various ways in different organisms depending on their developmental stage and tissue. There are enzymes able to remove the palmitoleoyl group from Wnts and thus eliminate their hydrophobic properties. An extracellular protein carboxylesterase Notum can deacylate Wnts, however, as previously mentioned, this acylation is necessary for Wnts to effectively interact with their receptors (Kakugawa et al., 2015; Kurayoshi et al., 2007). Therefore, Notum likely serves rather as a negative Wnt gradient regulator (Petersen & Reddien, 2011). Another protein, secreted wingless-interacting molecule (SWIM) which is a member of the lipocalin protein family, binds *D. melanogaster* Wnt homolog wingless (Wg) in its purified form as well as *in vivo*. A shielding of Wg lipid moiety by SWIM enables long-range Wg signalization (Mulligan et al., 2012). Another way of overcoming Wnt hydrophobicity is its loading into lipoprotein particles or membranous exosomes (Gross et al., 2012; Panáková et al., 2005). Both means of Wnt transport were observed in *Drosophila melanogaster* as well as in cultured human cells (Gross et al., 2012; Neumann et al., 2009). Stanganello et al. showed Wnt delivery via the long PM protrusions (signaling filopodia) during brain development in *Danio rerio* (Stanganello et al., 2015). An extensive interaction of Wnts with proteins of the extracellular matrix could also help in lipid modification shielding (Reichsman et al., 1996). Several members of the glypican family were shown to participate in the Wnt gradient sculpting (Baeg et al., 2001). Whichever manner of Wnt ligand transport between cells is dominant, it is clear that the problem of the Wnt hydrophobicity was solved several times during Wnt pathway evolution.

Wnt-receiving cells carry Wnt receptors and coreceptors on their PM. These receptors and coreceptors do not interact with each other until the Wnt ligand is available. In this “Wnt off” state several proteins form the  $\beta$ -catenin destruction complex (Salic et al., 2000). As the name

suggests, the key role of this complex is to bind  $\beta$ -catenin and mark it for destruction. This is achieved via sequential  $\beta$ -catenin phosphorylation by glycogen synthase kinase (GSK3 $\beta$ ) and casein kinase (CK1 $\alpha$ ) (Liu et al., 2002; Siegfried et al., 1992). Phosphorylated  $\beta$ -catenin then serves as a substrate for ubiquitin-protein ligase complex SCF (Kitagawa et al., 1999). Once ubiquitylated,  $\beta$ -catenin is degraded in the proteasome and its cytoplasmic level is thus kept low (Aberle et al., 1997). To switch Wnt signaling to the “on” state, the Wnt ligand needs to be bound by its receptor Frizzled (Fz) and coreceptor LRP5/6 (Bhanot et al., 1996; Tamai et al., 2000). This leads to the recruitment of Dishevelled scaffold protein (Dvl) from the cytoplasm to the PM (Klingensmith et al., 1994). Dvl in turn recruits Axin and facilitates the formation of the Wnt receptor signalosome (Bilić et al., 2007; Itoh et al., 2000). The signalosome assembly inhibits the  $\beta$ -catenin destruction complex causing a gradual accumulation of  $\beta$ -catenin in the cytoplasm (Papkoff et al., 1996). Upon its nuclear relocation,  $\beta$ -catenin interacts with the T-cell factor/lymphoid enhancer factor family (TCF/LEF) which leads to transcription of the Wnt target genes (Molenaar et al., 1996).

### 1.5.2. Known roles of MTMR9 and AAK1 in Wnt signaling

The role of MTMR9, and MTMRs generally, in the Wnt signaling pathway is not very well understood. Silhankova et al. showed the importance of MTM-6 and MTM-9 in the migration of QL neuroblast descendant cells (QL.d) and other Wnt-dependent processes in *Caenorhabditis elegans* (Silhankova et al., 2010). As described in the previous chapter, Wnt signal production is dependent on the recycling of Wls from the PM back to the ER (Bänziger et al., 2006; Bartscherer et al., 2006; Goodman et al., 2006). A mutation in the *mtm-6* gene causes a reduction of MIG-14/Wls levels in *C. elegans*. Tissue-specific rescue experiments also show that active MTM-6 can revert the QL.d migration defect when overexpressed in the Wnt-producing cells. Concurrently, the expression pattern of the *mtm-9* gene shows its presence in various tissues including the Wnt-producing cells (Silhankova et al., 2010). These results support the previously reported MTM-6/9 functional interaction in *C. elegans* as well as MTMR6-MTMR9 interaction in mammalian cells *in vitro* (Dang et al., 2004; Zou et al., 2009). Results of Silhankova et al. research suggest that the MTM-6/9 complex regulates the Wnt signaling pathway via the control of MIG-14/Wls recycling. Comparable results of Wls regulation by MTMR6 in *D. melanogaster* indicate the evolutionary conservation of this process (Silhankova et al., 2010). The MTM-6/9 heterodimer was also shown to affect the number and positions of synapses in the DA9 motor neuron in *C. elegans*. Similarly to the QL.d migration, DA9 synapse formation is at least partially regulated by Wnt secretion (Ericson et al., 2014).

It is also possible for MTMRs to regulate Wnt signaling indirectly via crosstalk with other signaling pathways. The role of MTMR14 and other MTMRs in PI3K-mediated autophagocytosis was already described in previous chapters (Chua et al., 2022; Kovács et al., 2022; J. Liu et al., 2014; Vergne et al., 2009). It was also shown that autophagy leads to increased  $\beta$ -catenin interaction with N-cadherin in glioblastoma cells. N-cadherin-mediated sequestration of cytoplasmic  $\beta$ -catenin in turn leads to Wnt signaling impairment (Colella et al., 2019). This is, however, a highly speculative mode of possible MTMRs involvement in the Wnt pathway regulation. The current state of the research on the MTMRs intersection with the Wnt pathway is rather incomplete and more experimental work needs to be done to elucidate any possible relevance of this connection.

The genome-wide screen of mouse embryonic stem cells for the new phosphoregulating enzymes of the Wnt signaling pathway identified several candidate genes. One of the positive hits in this experiment was the AAK1 kinase. The knock-down of AAK1 via siRNA caused an upregulation of Wnt signaling (Groenendyk & Michalak, 2011). This was later confirmed by Agajanian et al. in their gain-of-function kinome screen (Agajanian et al., 2019). Agajanian et al. further showed that after the Wnt signaling activation, AAK1 progressively phosphorylates the AP2 $\mu$ 2 subunit which in turn leads to stimulation of the CME of the Wnt ligand coreceptor LRP5/6. AAK1 knock-down causes an increase in levels of LRP5/6 on the PM. Conversely, LRP5/6 levels on the PM decrease after AAK1 overexpression. The Wnt ligand-induced LRP5/6 endocytosis mediated by AAK1 phosphorylation activity thus seems to work as part of the negative feedback loop (Agajanian et al., 2019).

## 2. Publications

Doubravská, L., Dostál, V., Knop, F., Libusová, L., Macůrková, M. (2020). Human myotubularin-related protein 9 regulates ER-to-GA trafficking and modulates WNT3A secretion. *Experimental cell research* 386(1), 111709.

Knop, F., Zounarová, A., Macůrková, M. (2024). *Caenorhabditis elegans* SEL-5/AAK1 regulates cell migration and cell outgrowth independently of its kinase activity. *BioRxiv* preprint doi: <https://doi.org/10.1101/2023.03.29.534638>



# Human myotubularin-related protein 9 regulates ER-to-Golgi trafficking and modulates WNT3A secretion

Lenka Doubravská, Vojtěch Dostál, Filip Knop, Lenka Libusová, Marie Macůrková\*

Department of Cell Biology, Faculty of Science, Charles University, Viničná 7, 128 00, Prague 2, Czech Republic

## ARTICLE INFO

### Keywords:

Myotubularin-related protein 9  
Golgi apparatus  
Intermediate compartment  
WNT3A  
Secretion  
RAB1A

## ABSTRACT

Regulation of phosphatidylinositol phosphates plays a crucial role in signal transduction, membrane trafficking or autophagy. Members of the myotubularin family of lipid phosphatases contribute to phosphoinositide metabolism by counteracting the activity of phosphoinositide kinases. The mechanisms determining their sub-cellular localization and targeting to specific membrane compartments are still poorly understood.

We show here that the inactive phosphatase MTMR9 localizes to the intermediate compartment and to the Golgi apparatus and is able to recruit its active phosphatase partners MTMR6 and MTMR8 to these locations. Furthermore, MTMR8 and MTMR9 co-localize with the small GTPase RAB1A and regulate its localization. Loss of MTMR9 expression compromises the integrity of the Golgi apparatus and results in altered distribution of RAB1A and actin nucleation-promoting factor WHAMM. Loss or overexpression of MTMR9 leads to decreased rate of protein secretion. We demonstrate that secretion of physiologically relevant cargo exemplified by the WNT3A protein is affected after perturbation of MTMR9 levels.

## 1. Introduction

Myotubularin and myotubularin-related proteins (MTM1 and MTMR1-14, respectively) constitute a family of lipid phosphatases that utilize phosphatidylinositol (PtdIns) phosphates as their major substrate. For simplicity, members of the family will be collectively referred to as “myotubularins” hereafter. The biological significance of this protein family is highlighted by the fact that mutations in several myotubularin family genes are linked to severe human pathologies, including mutations in MTM1 (X-linked centronuclear myopathy) [1], MTMR2 (Charcot-Marie-Tooth neuropathy type 4B1) [2] and MTMR13/SBF2 (Charcot-Marie-Tooth neuropathy type 4B2) [3,4].

Myotubularin family consists of both phosphatase-active and phosphatase-dead members, which can form homo- or heterodimers. Heterodimers are most often composed of one active and one inactive phosphatase (reviewed in Ref. [5]). Their preferred substrates are PtdIns3P and PtdIns(3,5)P2 and these are dephosphorylated to PtdIns and PtdIns5P, respectively. PtdIns3P and PtdIns(3,5)P2 are significantly enriched in the endolysosomal system and several myotubularins indeed localize to endosomal membranes. MTM1 was found on membranes of early and late endosomes [6,7], while MTMR4 was detected in early, late and recycling endosomes [8–11]. Myotubularins were also found to localize to other membrane compartments in the cell,

including the endoplasmic reticulum (ER) in case of MTMR3, MTMR6 and MTMR9 [12,13] or the plasma membrane, to which MTM1 could be recruited by the GTPase Rac1 [14]. It is of note, though, that while localization of myotubularins to specific membrane compartments was documented, substantial pool of most myotubularins resides in the cytoplasm (reviewed in Ref. [15]). The mechanisms recruiting different myotubularins to specific membranes are still poorly understood.

Active myotubularins MTMR6, MTMR7 and MTMR8 together with the inactive member MTMR9 comprise a distinct subgroup within the myotubularin family. The active phosphatases of this group exclusively utilize MTMR9 as their inactive binding partner, while MTMR9 could possibly also homodimerize or interact with MTMR2 [8,16]. MTMR9 has been shown to modulate the substrate specificity of its active partners. While MTMR6/MTMR9 complex shows much higher activity towards PtdIns(3,5)P2, MTMR8/MTMR9 complex prefers PtdIns3P as its substrate [17]. Several cellular processes have been linked to the function of MTMR6/7/8/9 subgroup of myotubularin proteins. First, MTMR6 knock-down increased the activity of a calcium dependent potassium channel KCa3.1 in human CD4 T cells and stimulated their proliferation after reactivation [18]. In a different study, knock-down of MTMR9 led to enhanced differentiation of CD4 T cells into T-helper (Th)1 cells while knock-down of MTMR7 promoted Th2 and Th17 differentiation [19]. Knock-downs of MTMR6 [13,20] or MTMR9 [13]

\* Corresponding author.

E-mail address: [marie.macurkova@natur.cuni.cz](mailto:marie.macurkova@natur.cuni.cz) (M. Macůrková).

<https://doi.org/10.1016/j.yexcr.2019.111709>

Received 14 June 2019; Received in revised form 10 October 2019; Accepted 31 October 2019

Available online 06 November 2019

0014-4827/ © 2019 Elsevier Inc. All rights reserved.

were shown to promote apoptosis. Several reports also demonstrated that loss of either MTMR6 or the MTMR8/MTMR9 complex lead to increased autophagy [17,21]. A possible mechanism was suggested for the role of MTMR6 in autophagy. MTMR6 transiently interacts with RAB1 GTPase and is recruited to the intermediate compartment (IC) in between the ER and the Golgi apparatus [22]. There it could dephosphorylate PtdIns3P and thus regulate the recruitment of PtdIns3P-binding proteins like DFCP1 and affect autophagosome biogenesis [23]. However, direct impact of MTMR6 on any PtdIns3P-binding protein localization has not been demonstrated. Loss of MTMR6 in NRK cells resulted in accelerated secretion of VSVG protein, indicating that by localizing to the IC compartment, MTMR6 could also regulate the secretory pathway [22]. A role in macropinocytosis was also described for MTMR6 and MTMR9 [24].

In this study we focused on the functional consequences of either loss or overexpression of the inactive myotubularin MTMR9 and analysed its role in the secretory pathway. We show that MTMR9 localizes to the IC in concert with the RAB1 GTPase and drives the localization of its partners MTMR6 and MTMR8 to this compartment. MTMR9 regulates the passage of secretory cargo and thus can influence major cellular signalling pathways as we demonstrate on the example of WNT3A signalling.

## 2. Results

### 2.1. Cellular localization of MTMR9

Previous studies of MTMR9 described mostly cytoplasmic localization in the cell [8] or enrichment in the ER [13]. We decided to first analyse in detail the subcellular distribution of MTMR9. We tested commercially available antibodies against MTMR9 but unfortunately none of them was able to specifically detect endogenous MTMR9 protein (data not shown). In order to map MTMR9 intracellular localization we therefore transiently expressed MTMR9 tagged with mNeonGreen (NG) at its C-terminus in RPE-1 cells. Confocal microscopy on both living and fixed cells revealed MTMR9-NG localization to the cytoplasm and to a distinct pool of vesicular structures in the perinuclear area (Fig. 1A). MTMR9 could also be detected at or in the close proximity to the plasma membrane (Fig. 1A). Live-cell imaging further unveiled that the MTMR9-labelled vesicles form two populations differing in their mobility. A pool of fast moving MTMR9 vesicles travelled from peripheral locations towards a more static pool of MTMR9 vesicles located close to the nucleus (Video 1). To disclose the identity of these vesicles we performed co-localization experiments with a panel of markers for various intracellular compartments. We could not detect co-localization with markers for the early (EEA1) or late (RAB7) endosomes, lysosomes (LAMP1) or recycling endosomes (RAB11) (Fig. S1A). Partial overlap of MTMR9 signal was detected with markers of the *cis*- (GM130) and *trans*-Golgi apparatus (GOLGIN97) (Fig. 1A). MTMR6, one of the binding partners of MTMR9, was found to localize to the intermediate compartment (IC) [22]. This prompted us to test for co-localization between MTMR9 and RAB1, the hallmark of the IC [25]. Indeed, strong co-localization was observed when tagged MTMR9 and RAB1A were co-expressed in cells (Fig. 1B). Interestingly, the localization pattern of RAB1A changed when it was co-expressed with MTMR9 compared to the pattern observed when the protein was expressed alone (Fig. 1B). RAB1A alone was detected predominantly in the Golgi apparatus and weaker signal corresponded to the IC vesicles, the ER or the plasma membrane (Fig. 1B). When co-expressed with MTMR9, the signal of RAB1A in the Golgi area was less prominent and the vesicular pool could be clearly detected (Fig. 1B). The MTMR9 signal also appeared less cytoplasmic and more vesicular in the RAB1A and MTMR9 double transfected cells. This effect was dependent on the GTP/GDP status of RAB1A, as MTMR9 co-expression with the GDP-bound form RAB1AS25 N did not show such an effect and the localization of RAB1AS25 N remained cytoplasmic when expressed alone or

in combination with MTMR9 (Fig. 1B). RAB2A, another GTPase localizing to the IC [26], was also found in MTMR9-positive vesicles, however no striking localization interdependence was observed in this case (Fig. 1B). RAB6, a GTPase that regulates retrograde traffic from the Golgi to the endoplasmic reticulum independently of COPI vesicles [27], was not present in MTMR9-positive vesicles (Fig. S1B).

Supplementary data related to this article can be found online at

To further characterize the cellular pools of MTMR9 we treated cells with brefeldin A (BFA) and looked for any effect on MTMR9 localization. BFA treatment causes disappearance of clearly identifiable Golgi elements and redistribution of Golgi proteins into the ER [28–30]. We observed dispersion of the MTMR9 signal in the Golgi area very similar to that observed in cells expressing RAB1A or RAB2 (Fig. 2A) or in cells stained for the *cis*-Golgi marker GM130 (Fig. 2B). Similarly, when cells expressing both RAB1A and MTMR9 were treated with BFA, the perinuclear signal became dispersed indicating its affiliation with the Golgi (Fig. 2A). MTMR9-labelled vesicles were nevertheless found also outside of the juxtannuclear Golgi area and these were not grossly affected by BFA treatment, suggesting they could represent the IC pool (Fig. 2A and B). Taken together, our data indicate that apart from the cytoplasmic localization, MTMR9 could be found also at the plasma membrane, in the Golgi and in the IC.

### 2.2. MTMR9 drives vesicular localization of its active phosphatase partners

We next asked whether MTMR9 could drive vesicular localization of its active phosphatase binding partners MTMR6 and MTMR8. MTMR7, the last binding partner of MTMR9, is specifically expressed in the brain and in neuronal cells [31], therefore we omitted MTMR7 from our analyses. C-terminal tagged versions of MTMR6 and MTMR8 were expressed alone or together with MTMR9 in RPE-1 cells and their localization patterns were compared. Strikingly, when expressed alone, MTMR8 displayed predominantly cytoplasmic localization, but when it was co-expressed with MTMR9, vesicular pattern became apparent (Fig. 3A). This effect was also detected, albeit less prominently, with MTMR6, where cytoplasmic and weak Golgi localization was visible when MTMR6 was expressed alone, but MTMR9 co-expression enhanced the vesicular pattern (Fig. 3A).

Apart from influencing the localization pattern of its active binding partners MTMR6 and MTMR8, we have seen that MTMR9 also influenced RAB1A localization (Fig. 1B). RAB1 (both RAB1A and RAB1B) was previously shown to interact with MTMR6 [22]. We therefore tested whether either MTMR6 or MTMR8 could influence RAB1A localization when co-expressed together in RPE-1 cells. Surprisingly, MTMR6 expression had no effect on the localization of RAB1A while MTMR8 and RAB1A co-expression resulted in similar vesicular pattern as in case of MTMR9 and RAB1A (Fig. 3B, compare with Figs. 1A and 3A).

### 2.3. Loss of MTMR9 expression affects RAB1A localization and the integrity of the Golgi apparatus

In order to understand the role of MTMR9 in the Golgi and the IC compartment we targeted *MTMR9* gene using CRISPR/Cas9 in HeLa cells to generate *MTMR9* knock-out (*MTMR9* KO) cell line. Using a mix of three gRNAs we obtained two clones where changes in the genomic DNA of the targeted locus were introduced. Both clones contain a homozygous single base pair insertion in exon 2 resulting in a premature termination of the reading frame and also a deletion of variable length (approx. 120 base pair) in exon 4 (Fig. 4A). Using qRT-PCR we confirmed that in both clones the level of *MTMR9* mRNA was severely reduced (Fig. 4B). Nevertheless it was still possible to extract full length *MTMR9* cDNA from clone 1 and sequencing of the cDNA confirmed the nonsense mutation in exon 2 and missing exon 4 (Fig. 4A). Clone A1 was used in subsequent experiments.

We first tested whether the *MTMR9* KO cells display the previously described increase in autophagy [17]. We monitored the processing of



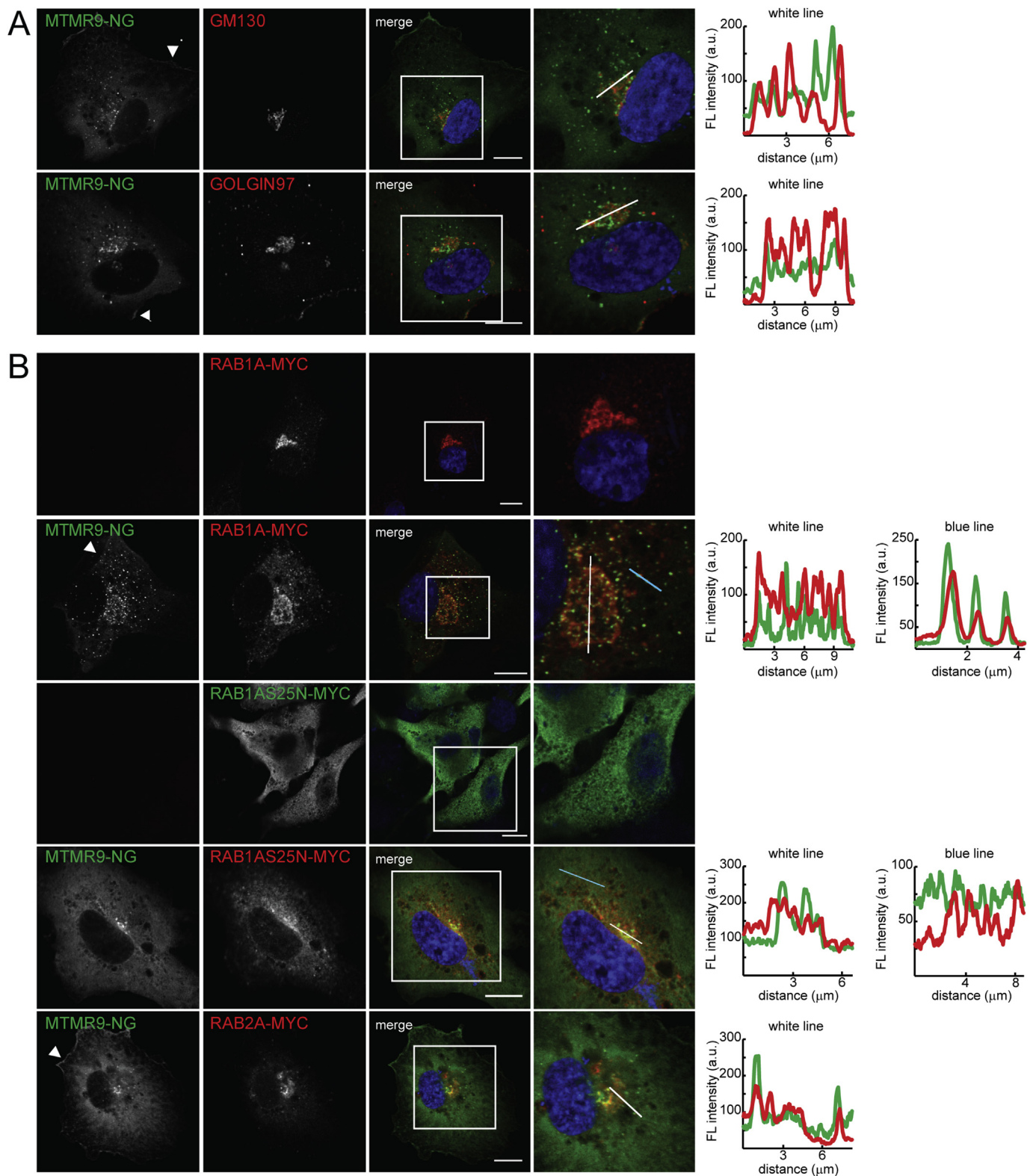


**Fig. 1.** MTMR9 localizes to the Golgi and the IC and co-localizes with RAB1A. A) To identify MTMR9 positive intracellular structures RPE-1 cells were transfected by C-terminally tagged MTMR9-NG and stained for endogenous Golgi markers GM130 (*cis*-Golgi) or GOLGIN97 (*trans*-Golgi). B) IC marker RAB1A-MYC shows different vesicular pattern when co-transfected with or without MTMR9-NG. The effect is dependent on RAB1A GTP/GDP status as RAB1A-S25N-MYC does not co-localize with MTMR9-NG. RAB2A-MYC co-localizes with MTMR9-NG in IC vesicles but compared to RAB1A, no apparent mutual dependence on localization is observed. Images are single confocal sections. Arrowheads in A and B point to the plasma membrane-associated MTMR9 signal. White square delineates the magnified area. White and blue lines indicate the selection analysed by RGB profiler. Scale bars correspond to 10 μm. FL – fluorescence, a.u. – arbitrary units.

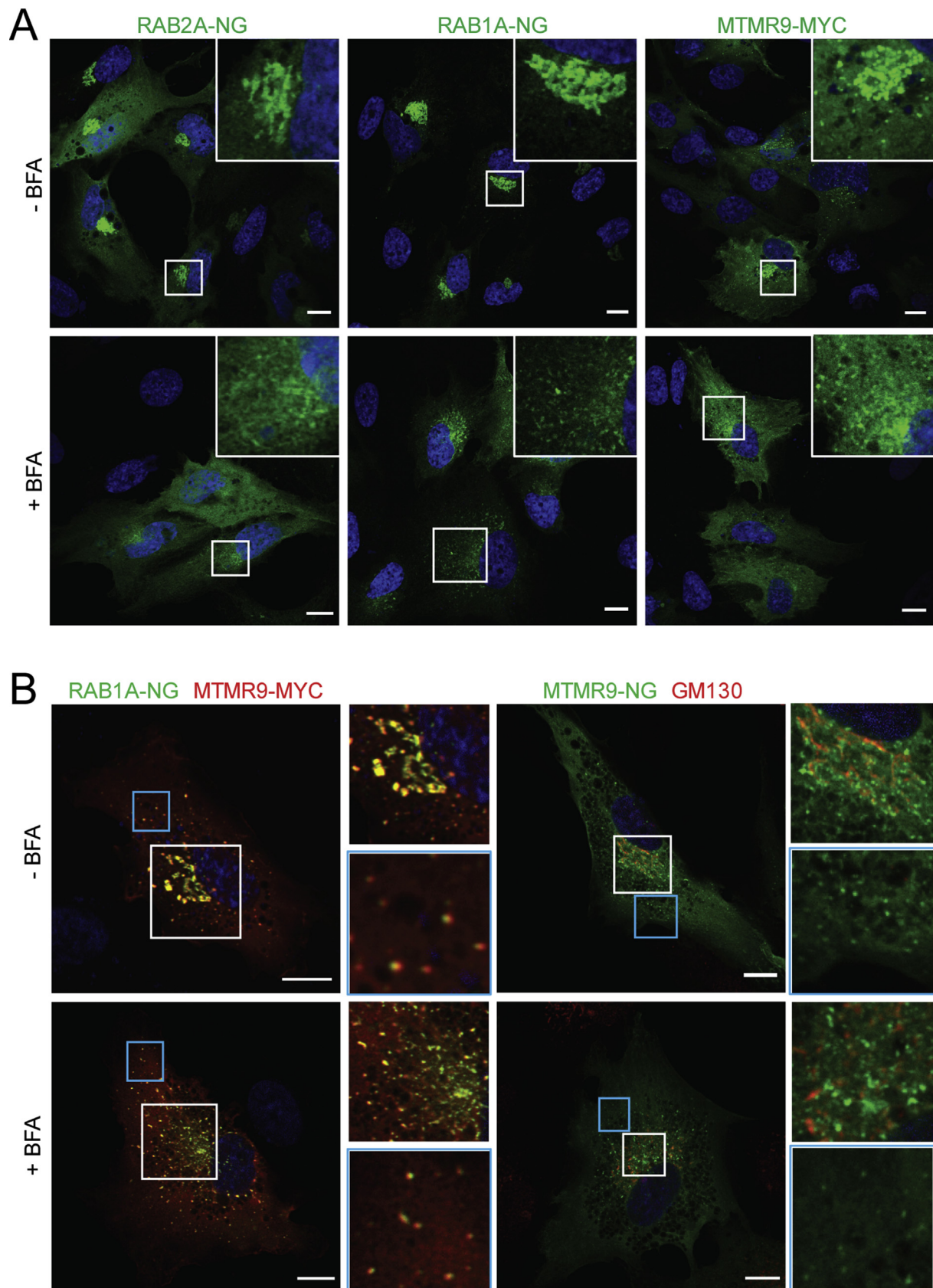


**Fig. 2.** BFA treatment results in dispersal of the Golgi associated MTMR9 pool. **A)** MTMR9-MYC signal in the Golgi area disperses in a similar manner as RAB1A-NG and RAB2A-MYC after 2 h BFA treatment. **B)** Similarly RAB1A-NG and MTMR9-MYC positive Golgi structures as well as *cis*-Golgi region marked by GM130 (white selection) are dispersed after BFA treatment. MTMR9 positive vesicles outside of the Golgi region (blue selection) are not visibly affected by BFA. Images are single confocal sections. White and blue squares delineate the magnified area. Scale bars correspond to 10  $\mu\text{m}$ .



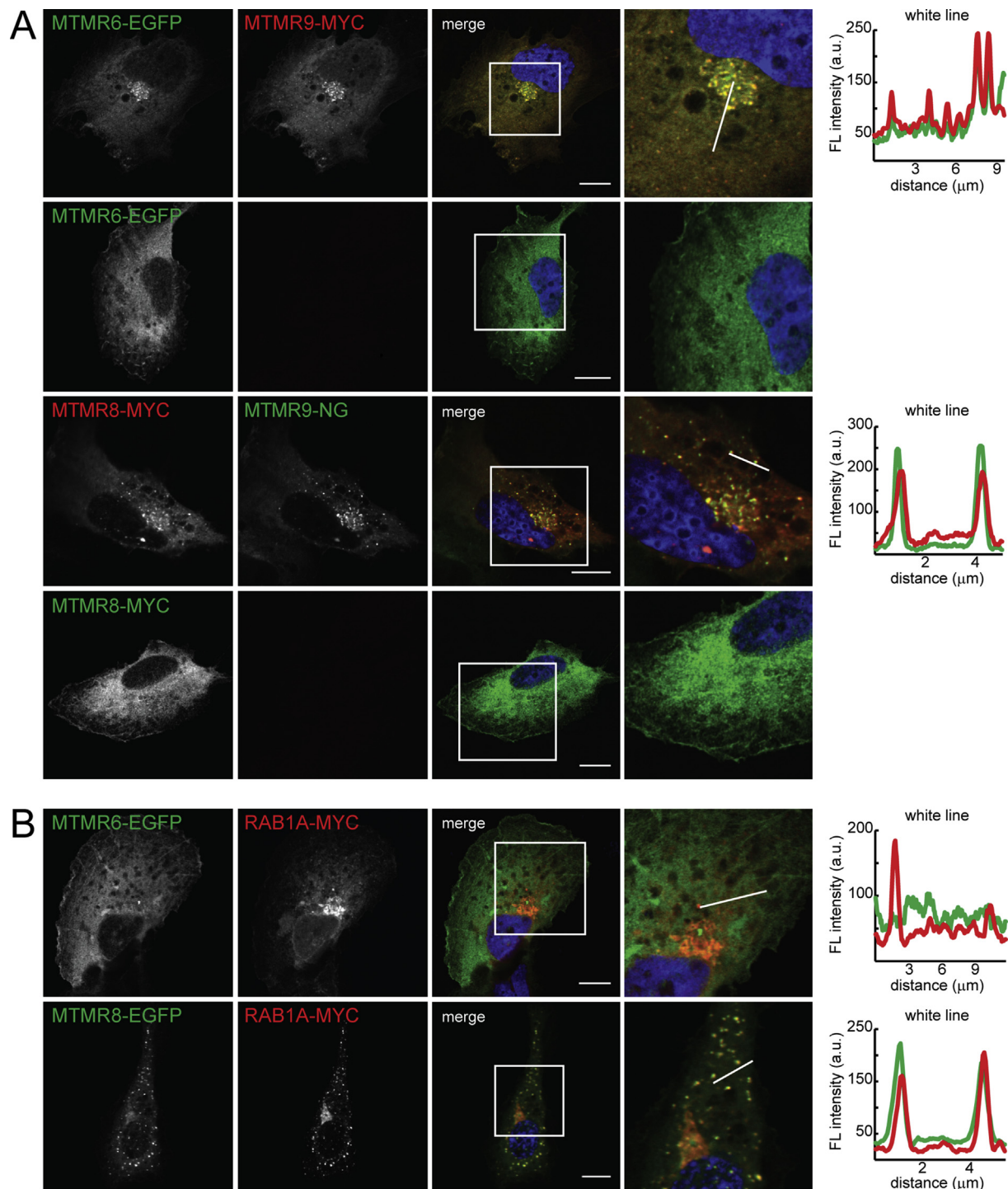


**Fig. 3.** Subcellular localization of active myotubularins MTMR6 and MTMR8 depends on MTMR9. A) When RPE-1 cells are transfected by MTMR6-EGFP or MTMR8-MYC alone, mostly cytoplasmic staining of MTMR6 and MTMR8 is observed. Upon MTMR9-MYC or MTMR9-NG co-transfection, MTMR6 and MTMR8 relocate into MTMR9-positive structures. B) MTMR8-EGFP but not MTMR6-EGFP co-localizes with RAB1A-MYC. RAB1A-MYC intracellular distribution changes from predominantly Golgi-associated into more vesicular when co-transfected with MTMR8-EGFP. Images are single confocal sections. White square delineates the magnified area. White line indicates the selection analysed by RGB profiler. Scale bars correspond to 10  $\mu\text{m}$ . FL – fluorescence, a.u. – arbitrary units.

LC3B by immunoblotting as a measure of autophagy level in parental and *MTMR9* KO cells and found out that the basal level of autophagy is increased in the *MTMR9* KO cells (Fig. S2A). We thus confirmed that the *MTMR9* KO cells phenocopy the results obtained using reduction-of-function approaches [17].

To test whether loss of *MTMR9* expression would influence RAB1A localization we expressed tagged RAB1A in the *MTMR9* KO cells and analysed its distribution. Indeed, RAB1A distribution changed in the

*MTMR9* KO cells compared to wild type controls. RAB1A vesicular pool increased in the *MTMR9* KO cells relative to the Golgi (Fig. 4C). Staining with antibody against the *cis*-Golgi marker GM130 also revealed less compact Golgi organisation in *MTMR9* KO cells compared to controls (Fig. 4D, S2B). To characterize the Golgi dispersion phenotype further we analysed the number and size of GM130 positive particles per cell in control and *MTMR9* KO cells. Loss of *MTMR9* expression resulted in more GM130 positive particles of smaller size compared to

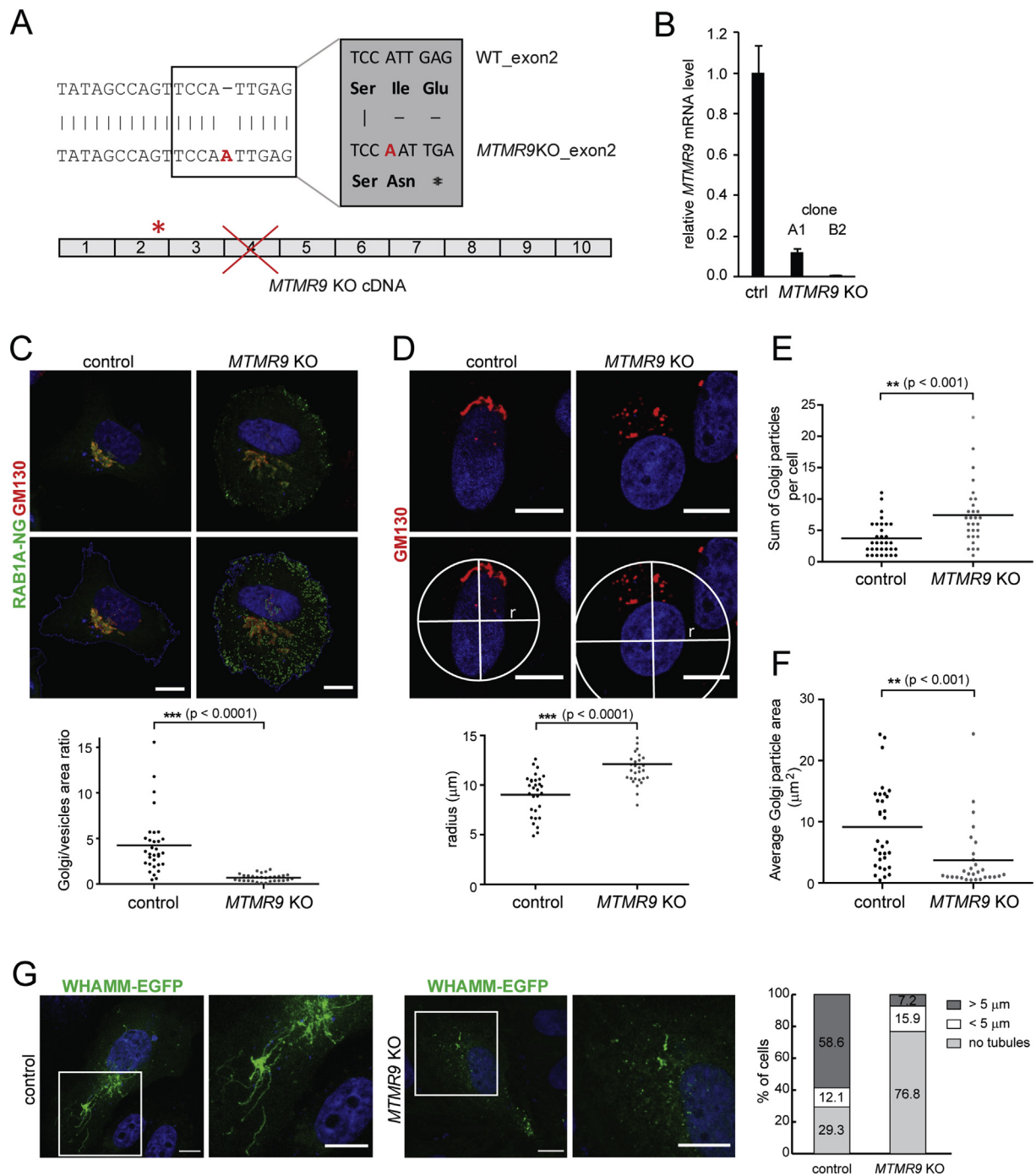


**Fig. 4.** Knocking out *MTMR9* changes RAB1A and WHAMM cellular distribution and results in Golgi dispersal. A) Mutations in genomic DNA of *MTMR9* KO clones were identified by sequencing. Clones A1 and B2 contain a single nucleotide insertion in exon 2 generating premature stop codon (marked by an asterisk) and large deletions in exon 4 leading to excision of the whole exon 4 after transcription into mRNA. B) Two *MTMR9* KO clones, A1 and B2, were analysed for *MTMR9* mRNA expression by qRT-PCR using primers amplifying region of exon 1. C) Parental and *MTMR9* KO HeLa (clone A1) cells were transfected by RAB1A-NG and after fixation and permeabilization stained for endogenous GM130 marker (upper panel). Distribution of RAB1A in the Golgi (area of RAB1A co-localization with GM130, red ROI in the lower panel) and in vesicles (green ROI in the lower panel) was determined as a sum of areas for individual cells (the boundary of the cell depicted as blue ROI in the lower panel). The ratio of these sums (Golgi/vesicles) for individual analysed cells is shown in the graph below the panel. 32 and 30 individual cells were analysed for control and *MTMR9* KO cells, respectively. D) GM130 staining in *MTMR9* KO (clone A1) compared to control cells shows dispersed Golgi apparatus (upper panel). White circle indicates Golgi dispersion whereas radius (r) reflects its magnitude in µm (lower panel and graph below). 30 cells for each condition were analysed. E) The same set of cells as in D) was analysed for the sum of GM130 positive structures per cell and in F) for average area (µm<sup>2</sup>) of such a structure in the cell. The dots represent individual cells with the line showing mean value. Data were analysed with unpaired Student's t-test and the significance (p value) is shown for each graph. G) Control and *MTMR9* KO cells were transfected with WHAMM-EGFP and the extent of tubulation was compared between the samples. Cells were scored as either having no, less than 5 µm or more than 5 µm long WHAMM decorated tubules. The percentage of cells in each category is shown in the graph. 58 and 69 cells were analysed for control and *MTMR9* KO cells, respectively. Images are single confocal sections. White square delineates the magnified area. Scale bars correspond to 10 µm.

control cells (Fig. 4E and F). This suggests that the Golgi structure is fragmented. Taken together, disruption of *MTMR9* expression in the cells confirmed that *MTMR9* is required for correct RAB1A localization and Golgi organization.

RAB1A was found to interact with WHAMM (WASP homolog associated with actin, membranes and microtubules) - an activator of Arp2/3 complex-mediated actin nucleation [32]. WHAMM localizes to the cis-Golgi and the IC compartment [33]. We investigated whether loss of *MTMR9* expression could affect WHAMM localization in cells. We therefore expressed WHAMM tagged with EGFP in control and *MTMR9* KO cells and compared its distribution. Expression of WHAMM in cells can lead to the appearance of tubular membranes [33] and we have observed this phenotype in the control cells, where almost 60% of cells contained WHAMM-decorated tubules longer than 5  $\mu\text{m}$  (Fig. 4G). Strikingly, only 7% of *MTMR9* KO cells displayed these longer tubules while more than 75% of KO cells contained no tubules and WHAMM signal was distributed in small patches (Fig. 4G).

WHAMM regulates membrane tubulation by interacting with both the actin and microtubule cytoskeleton [32,33]. Particular mutations in WHAMM resulted in alterations of actin cytoskeleton in fibroblast cells [34]. We therefore tested whether the change in WHAMM behaviour in *MTMR9* KO cells would have any impact on cytoskeletal organization. We visualized microtubules and actin in control and *MTMR9* KO cells but we could not detect any obvious difference in either actin or microtubule arrangement (Fig. S2C).

#### 2.4. *MTMR9* is required for efficient protein secretion

We set to analyse how *MTMR9* influences the function of the IC and Golgi compartments. Previous study of *MTMR6* described a possible role in protein secretion [22]. We therefore first employed the VENUS-tagged version of the temperature-sensitive vesicular stomatitis virus G protein (ts045VSVG-VENUS) as a model secretory cargo [35]. We expressed VSVG-VENUS either alone or together with *MTMR9*-MYC in RPE-1 cells, cultivated them at the restrictive temperature for 12 h and then shifted to 15  $^{\circ}\text{C}$  for 3 h. After that we scored number of cells where VSVG-VENUS was still in the ER, in transit between ER and the Golgi and completely in the Golgi (Fig. 5A). While in the control cells majority of VSVG already reached the Golgi, in cells overexpressing *MTMR9* only 30% of cells displayed this phenotype suggesting that *MTMR9* overexpression could slow down the speed of cargo transport through the secretory route. Nevertheless, in both control and *MTMR9* overexpressing cells VSVG-VENUS eventually reached the plasma membrane (data not shown) indicating that secretion is not fully inhibited. To verify that VSVG passed through *MTMR9*-associated vesicles on its way to the cell surface we expressed *MTMR9*-MYC together with VSVG and performed again temperature shift from 40  $^{\circ}\text{C}$ /12 h to 15  $^{\circ}\text{C}$ /3 h in RPE-1 cells to highlight the IC compartment. VSVG-VENUS co-localized to the same vesicles as *MTMR9*-MYC and the expression pattern highly resembled the one observed when *MTMR9* was expressed together with RAB1A (Fig. 5B).

#### 2.5. *MTMR9* is required for efficient WNT3A secretion

We next asked whether secretion of a more physiological cargo would also be affected by either loss or overexpression of *MTMR9*. It has been previously reported that the MTM-6/MTM-9 complex is involved in regulating Wnt secretion in *C. elegans* [36]. The proposed mechanism suggested that MTM-6/MTM-9 complex would regulate PI3P levels on endosomes and thus control the membrane association of the retromer complex. This in turn would influence the recycling of the Wnt cargo receptor MIG-14/Wntless (WLS). Based on the *MTMR9* localization described above and on published localization of *MTMR6* [22], such mechanism does not seem plausible in the mammalian system. However, Wnt proteins pass through the secretory route on the way out of the cell accompanied by WLS [37,38] and *MTMR9* thus

could affect Wnt secretion at the level of ER-to-Golgi transport. To explore this possibility we utilized the Retention Using Selective Hook (RUSH) system [39]. This system allows a synchronized release of a cargo from the ER and consists of two components - the protein of interest fused to a fluorescent tag and a streptavidin binding peptide (SBP), and the "hook", protein stably located in the ER fused to streptavidin. When these two components are expressed together in cells, the streptavidin moiety of the "hook" binds to the SBP tag of the protein of interest and thus effectively retains it in the ER. Once the cells are supplemented with biotin, the protein of interest is released from the "hook" and its passage through the secretory route can be followed. The RUSH system has already been successfully adapted to study Wnt protein trafficking [40]. We expressed the RUSH-EGFP-WNT3A construct in control and *MTMR9* KO cells, treated the cells with biotin for 10 min at 37  $^{\circ}\text{C}$  to initiate WNT3A release from the ER and then incubated the cells at 15  $^{\circ}\text{C}$  for 3 h to slow down the trafficking. WNT3A distribution was then analysed. While in the control samples WNT3A could be detected in transit between the ER and the Golgi or already in the Golgi in more than 70% of cells, in the *MTMR9* KO samples more than 65% of cells had no detectable WNT3A signal outside of the ER at the same time point (Fig. 6A). This suggests that similarly to *MTMR9* overexpression, loss of *MTMR9* results in deceleration of transport through the secretory route.

To further examine the possibility that WNT3A secretion is affected by change in *MTMR9* level, we employed HEK293STF cells (hereafter referred to as STF cells). STF cells stably express the SuperTOPFLASH reporter which responds to canonical Wnt signalling by expression of firefly luciferase. We transiently transfected STF cells with WNT3A and either *MTMR9*-NG or empty vector (EV) and 24 h later measured the luciferase activity. This autocrine activation assay revealed that overexpression of *MTMR9* diminished the Wnt reporter activity three times compared to the control (Fig. 6B). The autocrine assay however cannot discriminate between a block in Wnt secretion and Wnt signal transduction. We therefore expressed WNT3A with either *MTMR9* or EV in HEK293T cells, 24 h post transfection we co-cultured them with STF cells for another 24 h and subsequently we measured the luciferase activity. The luciferase activity was four times lower in STF cells co-cultured with cells expressing WNT3A together with *MTMR9* compared to STF cell co-cultured with cells expressing WNT3A and empty vector (Fig. 6C). This paracrine setup demonstrated that *MTMR9* affected Wnt secretion rather than Wnt signal transduction. To confirm this observation, we again transiently transfected HEK293T cells with WNT3A and either *MTMR9* or EV, cultivated them for three days, collected the conditioned media and then stimulated STF cells with either the conditioned media or by co-culturing them with the transfected cells. Surprisingly, quantification of the results uncovered that the conditioned media from both control and *MTMR9* overexpressing cells stimulated STF cells in a comparable manner, while control cells were significantly more efficient in stimulating STF cells than *MTMR9* overexpressing cells (Fig. 6D). This might suggest that the difference between control and *MTMR9* overexpressing cells lies in the WNT3A pool associated with the plasma membrane and not in the pool released into the media. At the same time the results indicate that WNT3A released into the media is properly modified en route to the cell surface and is fully functional.

### 3. Discussion

Based on the published interaction data active and inactive myotubularin phosphatases can potentially form at least 19 different homo- or heterodimeric complexes (summarized in Ref. [5]), representing a battery of units able to specifically modulate individual PtdIns3P and PtdIns(3,5)P<sub>2</sub> pools in the cell. Although the substrate specificity is common to all myotubularins, they seem to have non-overlapping functions. Despite more than 20 years of research and the medical significance of myotubularin protein family, the understanding of the



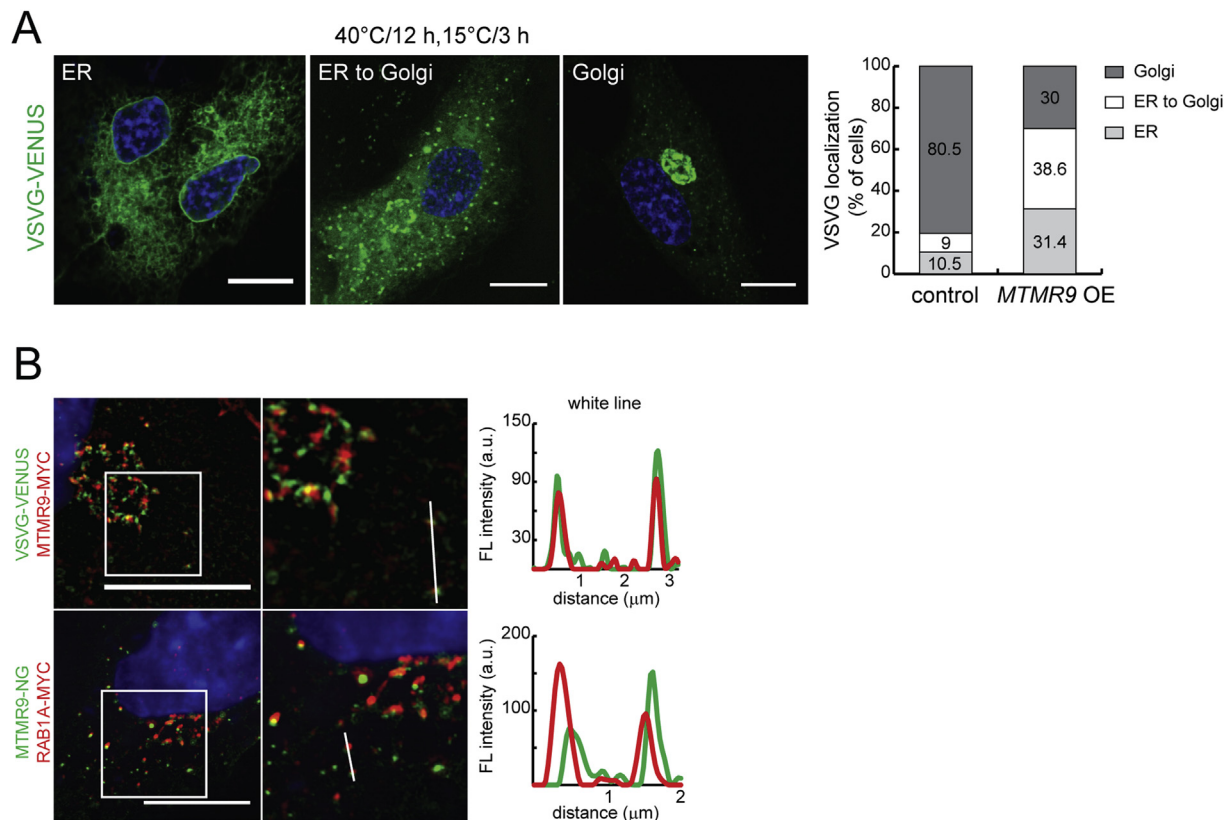


**Fig. 5.** Overexpression of MTMR9 results in delayed VSVG trafficking. A) RPE-1 cells overexpressing MTMR9 and control cells were transfected by VSVG-VENUS and left in 40 °C for 12 h before shifting to 15 °C for 3 h. VSVG-VENUS localization was categorized as either localizing to the ER, ER-to-Golgi or to the Golgi. The percentage of cells in each category is shown in the graph. 100 cells were analysed for each condition. B) Super-resolution microscopy images of RPE-1 cells transfected with VSVG-VENUS and MTMR9-MYC or MTMR9-NG and RAB1A-MYC. Cells were cultivated at 40 °C for 12 h and then shifted to 15 °C for 3 h. VSVG and RAB1A proteins are both found in MTMR9 positive vesicles. White square delineates the magnified area. White line indicates the selection analysed by RGB profiler. Scale bars correspond to 10  $\mu\text{m}$ . FL – fluorescence, OE - overexpression, a.u. – arbitrary units.

molecular mechanisms regulating the specificity of individual myotubularin complexes is still fragmented. In this study we characterized in detail the subcellular localization of MTMR9, the common inactive binding partner of active myotubularins MTMR6, MTMR7 and MTMR8. Using knock-out and overexpression approaches we have outlined MTMR9 role in the secretory pathway and demonstrated that important signalling molecules like the Wnt proteins can be perturbed by manipulating MTMR9 levels.

We have shown here that MTMR9 localizes to the Golgi and the IC compartment. Several observations supported this statement: i) MTMR9 co-localized with GTPases RAB1 and RAB2 ii) MTMR9 localization to the perinuclear area was sensitive to brefeldin A treatment and iii) MTMR9 and RAB1 co-expression potentiated vesicular localization of both proteins. RAB1 was previously shown to physically interact with MTMR6 albeit the interaction was weak or temporal [22]. We observed strong co-localization and accentuation of the vesicular pattern when MTMR9 and RAB1 were co-expressed in cells. Contrary to the published data [22] we did not observe this effect with MTMR6 and RAB1 co-expression, but instead we observed strong co-localization when MTMR8 and RAB1 were co-expressed. In *MTMR9* knock-out cells RAB1 localization also changed. RAB1 signal was more prominent in vesicles and these vesicles were found mostly at the cell periphery. This could be due to relocation of RAB1 from the Golgi to the IC pool in the absence of MTMR9. However, we have also demonstrated that in *MTMR9* KO cells the Golgi becomes fragmented. Similar phenotype can be induced by RAB1 knock-down [41]. It is possible that loss of MTMR9 induces RAB1 relocation towards the IC compartment and this shift is responsible for the Golgi fragmentation phenotype, or alternatively, loss of MTMR9 could induce Golgi fragmentation by RAB1 independent

mechanism and RAB1 relocation would be a consequence of the Golgi disorganization. At the moment we cannot discriminate between these possibilities. The change in RAB1 signal distribution could be either caused by direct protein-protein interaction between MTMR9 and RAB1 which has not been demonstrated yet, or alternatively could be caused by changes in PtdIns3P or PtdIns(3,5)P2 levels. Direct binding of RAB1 to PtdIns3P was recently demonstrated [34].

MTMR9 serves as a common binding partner for active myotubularins MTMR6, MTMR7 and MTMR8 [8]. Interaction with MTMR9 modulates the activity and substrate specificity of the catalytically active partner. For instance, while both MTMR6 and MTMR8 are able to dephosphorylate PtdIns3P and PtdIns(3,5)P2, MTMR6-MTMR9 complex shows higher activity towards PtdIns(3,5)P2 and MTMR8-MTMR9 complex preferentially dephosphorylates PtdIns3P [17]. Our data show that MTMR9 is able to recruit both MTMR6 and MTMR8 to the IC and Golgi locations. However, in our hands only MTMR8 and MTMR9 show strong co-localization with RAB1. This is in conflict with the published observation that RAB1B co-localizes with MTMR6 [22]. A possible explanation of this discrepancy is that in their co-localization studies, Mochizuki and colleagues used NRK cells that come from rat kidney. MTMR8 is not present in mice and rats [42]; it is thus plausible that the roles played by a single MTMR6-MTMR9 complex in rat are divided between two complexes in human cells, MTMR6-MTMR9 and MTMR8-MTMR9.

We speculate that the change in PtdIns levels could regulate transport of vesicles between the IC and the Golgi. The important function of PtdIns3P at the ER-Golgi interface has been documented in relation with autophagy induction [43]. Loss of MTMR6 or MTMR14/Jumpy increased autophagy initiation [21], similar observation was made after

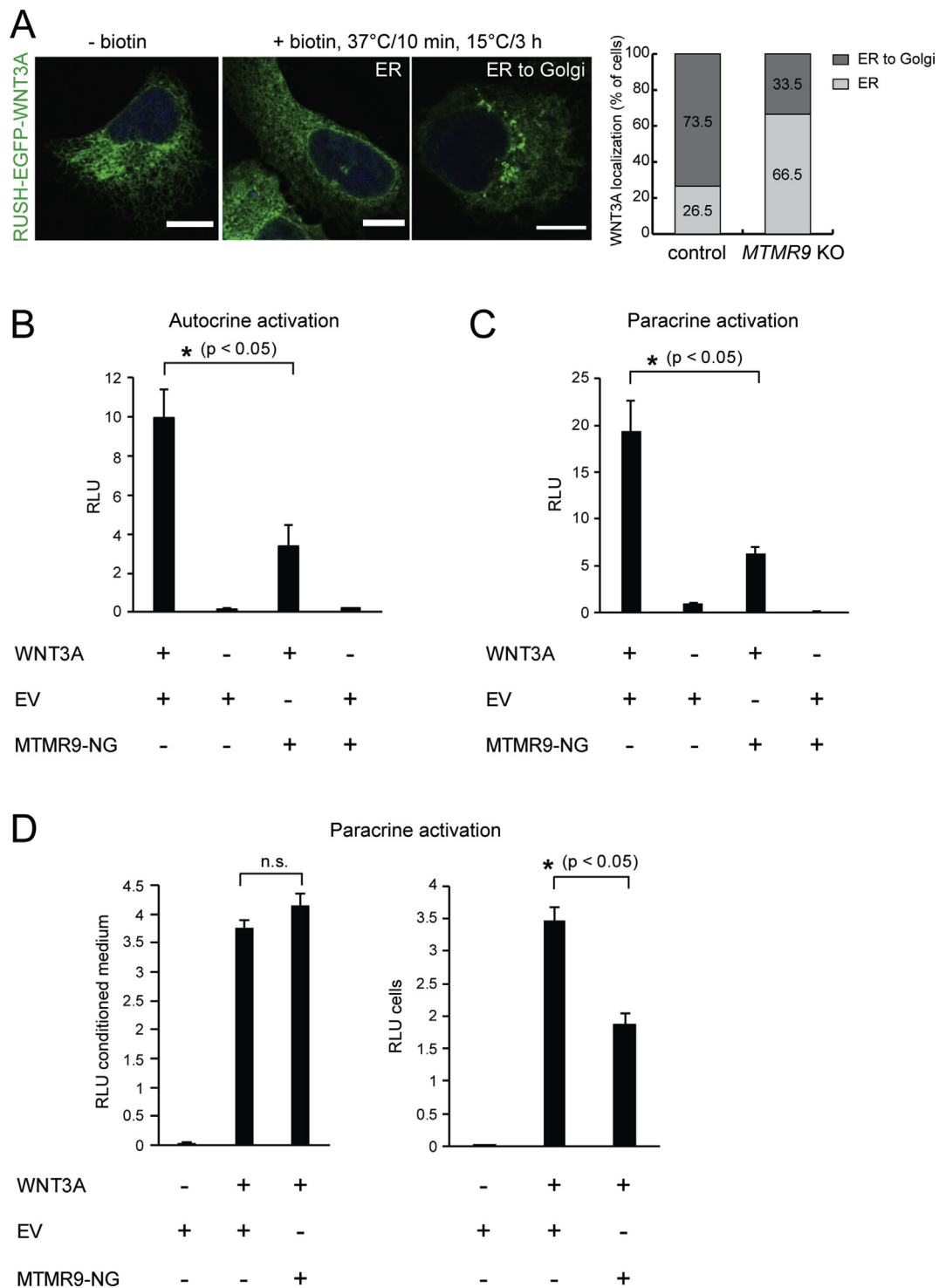


**Fig. 6.** MTMR9 deletion or overexpression interferes with efficient WNT3A secretion and signalling. A) RUSH-EGFP-WNT3A expressing control or *MTMR9* KO cells (clone A1) were treated with biotin for 10 min in 37 °C to release WNT3A from the ER and then shifted to 15 °C for 3 h to slow down the transport into the Golgi. After fixation cells were assigned to one of two categories: cells with WNT3A still trapped in the ER (ER) or cells with WNT3A on the way to the Golgi (ER to Golgi). The percentage of cells in each category is shown in the graph. More than 100 cells were analysed in both control and *MTMR9* KO samples. Images are single confocal sections. Scale bars correspond to 10 µm. B) Autocrine activation by WNT3A was assessed by transfecting Wnt reporter STF cell line with WNT3A and empty vector pNG (EV) or only empty vector as negative control and compared to STF cells transfected with WNT3A and MTMR9-NG or MTMR9-NG with empty vector to have the same DNA content in all the cases. Renilla luciferase construct was added to assess transfection rate. After 24 h firefly and Renilla luciferase activity was measured to obtain relative luciferase units (RLU). C) Paracrine activation by WNT3A was assessed by transfecting HEK293T cells as in Fig. 6B. 24 h later STF reporter cells were added for another 24 h and subsequently the firefly and Renilla luciferase activity was measured. D) To distinguish between the signalling activity of WNT3A secreted into the media and WNT3A associated with the plasma membrane of the producing cells, HEK293T cells were transfected as in Fig. 6B. 48 h later conditioned media were collected and added to STF cells for 24 h (left panel). Producing cells were co-cultured with STF cells for 24 h (right panel). Firefly luciferase values from STF cells cultivated in conditioned media were normalized to WNT3A protein levels in the media detected by immunoblotting (data not shown). n.s. – not significant.

loss of MTMR3 [12] or the MTMR8/MTMR9 complex [17]. We have confirmed that loss of MTMR9 resulted in increased basal level of autophagy. The role of MTMR proteins in autophagy is to control the level of PtdIns3P at the limiting membrane of the pre-autophagosome and thus regulate recruitment of autophagic PtdIns3P effectors DFCP1 or WIPI2 [23,44]. Our data show that MTMR9 as part of a PtdIns3P-metabolizing enzyme complex is important also for basal ER-to-Golgi transport and protein secretion. We demonstrated that two different secretory cargos are affected by loss or overexpression of MTMR9. First, manipulation of MTMR9 levels resulted in decelerated transport of the VSVG protein. Second, transport of the lipid-modified signalling molecule WNT3A was slowed down in *MTMR9* KO cells. Finally, surface presentation of WNT3A was reduced by MTMR9 overexpression as evidenced by the decrease in WNT3A signalling activity in a paracrine assay dependent on intercellular contacts. The common denominator for MTMR9 function in secretion and autophagy could be the RAB1 GTPase. It is required for autophagosome formation from the ER [45,46] and at the same time it plays a fundamental role in the ER-to-Golgi transport and as a result, in protein secretion [47]. Our data indicate strong correlation between MTMR9 and RAB1 localization. It is thus conceivable that the MTMR8-MTMR9 complex could influence RAB1 localization by regulating PtdIns3P levels along the ER-to-Golgi transport route and that the imbalance in PtdIns3P metabolism disrupts both autophagy and secretion by interfering with RAB1 function. It is worth mentioning that loss of MTMR9 expression resulted also in altered distribution of the actin nucleation-promoting factor WHAMM. WHAMM directly interacts with RAB1 [32] and both RAB1 and WHAMM have been shown to interact with PtdIns3P [34]. WHAMM has been implicated both in the regulation of autophagy and in the ER-to-Golgi transport [33,48]. An intriguing possibility is thus that MTMR9 could modulate the function of the RAB1-WHAMM complex.

When following WNT3A as a secretory cargo, we made an interesting observation that the overexpression of MTMR9 did not affect the pool of WNT3A that was released into the media but selectively affected only the pool that presumably remained in contact with the cell membrane. WNT proteins can be delivered to the membrane and into the extracellular space by several mechanisms. They could be delivered directly to the plasma membrane, released on exovesicles, lipoprotein particles or transported along filopodia [49,50]. The mechanisms directing WNT proteins to a particular release pathway are not well understood. MTMR9 could represent one of the factors that discriminate between the “free” and “membrane bound” route of WNT release. It has been shown recently that WNT3A loaded vesicles pause for up to several minutes immediately below the plasma membrane before disappearing, presumably by fusing with the plasma membrane [40]. We consistently detected MTMR9 localizing to the plasma membrane. It is thus conceivable that apart from its suggested role in the ER-to-Golgi transport, MTMR9 could also play a role in regulating the plasma membrane dynamics during vesicle release and thus interfere with WNT3A surface presentation.

Taken together our data consolidate the role of MTMR9 in the ER-to-Golgi trafficking and in the secretory pathway and strengthen the notion that PtdIns3P and PtdIns(3,5)P<sub>2</sub> play an important role along these routes. It would be interesting to further investigate the specific roles of the two complexes, MTMR6-MTMR9 and MTMR8-MTMR9 in human cells and to find the PtdIns3P and/or PtdIns(3,5)P<sub>2</sub> effectors along the ER-to-Golgi route.

## 4. Materials and methods

### 4.1. Plasmids

Human MTMR9-pcDNA4TOMycHis (accession BC112240) and MTMR6-pcDNA4TOMycHis (accession BC040012) were purchased from Abgent. Human *MTMR8* cDNA was obtained from ThermoFisher Scientific (accession BC012399.1) and was cloned into

pcDNA4TOMycHis vector (ThermoFisher Scientific). We also prepared EGFP or mNeonGreen [51] C-terminus tagged versions of MTMR9, MTMR6 and MTMR8. Empty vector pNG was kindly provided by H. Stenmark. PCMV-intron myc RAB1AWT and PCMV-intron myc RAB2WT were a gift from Terry Hébert (Addgene plasmid # 46776; <http://n2t.net/addgene:46776>; RRID:Addgene\_46776, Addgene plasmid # 46779; <http://n2t.net/addgene:46779>; RRID:Addgene\_46779) [52]. pVENUS-VSVG was a gift from Jennifer Lipincott-Schwartz (Addgene plasmid # 11914; <http://n2t.net/addgene:11914>; RRID:Addgene\_11914) [35]. Str-KDEL\_SBP-EGFP-WNT3A was a gift from David Virshup (Addgene plasmid # 108344; <http://n2t.net/addgene:108344>; RRID:Addgene\_108344). pEGFP-WHAMM [33] was a kind gift from K. Campellone. RAB1A-S25N-MYC was prepared by site-directed mutagenesis and RAB1A was cloned into pNG vector to be tagged on N-terminus. pEGFP-RAB6A was a kind gift from A. Akhmanova [53], pEGFP-RAB7 [54] was provided by J. Forstova and pEGFP-RAB11A [55] was a kind gift from H. Stenmark. The construct for Wnt signalling activation mWNT3ApCMV and vector for monitoring transfection rate in luciferase assays pRL-SV40 (Renilla) was obtained from V. Korinek. Details of plasmid constructs are available on request.

### 4.2. Cell culture, transfection and knock-out cell line

Human RPE-1, HeLa and human embryonic kidney (HEK) 293 were purchased from ATCC. SuperTOPFLASH HEK 293 T (STF) cells containing the genome-integrated Wnt/ $\beta$ -catenin-responsive firefly luciferase reporter [56], were kindly provided by V. Korinek. All cell lines were maintained in Dulbecco's modified Eagle's medium (DMEM + Glutamax, Gibco) supplemented with 10% fetal bovine serum (Gibco), penicillin and streptomycin (Biowest). Transient transfections were performed using X-tremeGENE™ HP DNA Transfection Reagent (Roche).

HeLa *MTMR9* knock-out line (*MTMR9* KO) was generated using MTMR8/9 CRISPR/Cas9 KO plasmid (sc-413097) and MTMR8/9 HDR plasmid (sc-413097-HDR), purchased from Santa Cruz Biotechnology. Emerging cell clones were selected on puromycin and tested for mutations in genomic DNA. The system contains three guide RNAs targeting exon 2, exon 3 and exon 4. Putatively mutated areas of genomic DNA from selected clones were amplified by PCR and cloned into pJet1.2 vector (CloneJET PCR Cloning Kit, Fermentas). Five individual colonies for each targeted region were analysed by sequencing and compared to sequences from parental HeLa cells.

### 4.3. Antibodies and chemicals

The following commercially available rabbit polyclonal and mouse and rabbit monoclonal antibodies were used: *anti*-GFP (11814460001, Roche), *anti*-WNT3A (ab28472, Abcam), *anti*-GM130 (ab52649, Abcam), *anti*-GOLGIN97 (A21270, Molecular Probes), *anti*-MYC (11-433-C100, Exbio).

Peroxidase-conjugated anti-mouse or anti-rabbit goat antibodies and fluorescently labelled anti-mouse or anti-rabbit donkey antibodies (DAM-CY5, DAR-CY5) were purchased from Jackson ImmunoResearch. Goat anti-mouse secondary antibody conjugated with Alexa 488 was purchased from Molecular Probes.

Brefeldin A (B7651, Sigma) was dissolved in DMSO and used at 5  $\mu$ g/ml final concentration in the culture media.

### 4.4. Immunofluorescence staining and microscopy

RPE-1 cells were grown on coverslips and transfected with the appropriate plasmid combination. 24 h post transfection the cells were fixed by 3% paraformaldehyde/MSB (20 mM MES, 2 mM EGTA, 2 mM MgCl<sub>2</sub>, 4% PEG6000, diluted in Hanks' Balanced Salt Solution) for 10 min, permeabilized in 0.1% TritonX-100 for 5 min and stained by



primary antibodies overnight. Next day, cells were washed three times by PBS and incubated for 1 h with an appropriate secondary antibody (DAM-CY5 or DAR-CY5), followed by three washes in PBS and mounting of the coverslips into Mowiol/DAPI solution. The samples were examined using Leica TCS SP2 AOBS confocal microscope (Leica Microsystems).

For live cell imaging, MTMR9-NG was transfected into RPE-1 cells. Time-lapse video was acquired with Hamamatsu camera on Olympus Cell'R microscope in 37 °C/5% CO<sub>2</sub> conditions. Image data were deconvolved by classical maximum likelihood estimation algorithm (CMLE) in Huygens software (SVI, Netherlands). For further processing the Fiji image processing package [57] was used.

#### 4.5. VSVG-*VENUS* secretion assay

The temperature sensitive viral protein VSVG (*VENUS*-tagged) was examined to follow secretion route. When transfected cells are grown at 40 °C, VSVG misfolds and is trapped in the ER. Upon a shift to lower temperature (33 °C or 15 °C in this work), VSVG folds properly and travels from the ER to the Golgi via IC and later to the plasma membrane. In 33 °C, RPE-1 cells allow VSVG to get to the plasma membrane in 60 min. For better focus on IC compartment, a shift to 15 °C is preferred [35]. Under such conditions, VSVG transports from the ER to the Golgi in 3 h.

MTMR9-MYC overexpressing RPE-1 and control cells were transfected by VSVG-*VENUS*. After cultivation in 40 °C for 12 h, cells were shifted to 15 °C for 3 h and then fixed, permeabilized and stained for the Golgi marker GM130. One hundred cells were analysed for VSVG progress from the ER to the Golgi and the VSVG pattern was divided into three categories – localizing mostly to the ER, in transit between the ER and the GA, localizing mostly to the GA. Similarly RPE-1 cells were transfected by VSVG-*VENUS*/MTMR9-MYC and MTMR9-NG/RAB1A-MYC and treated as previously (40 °C for 12 h followed by 15 °C for 3 h) before fixation, permeabilization and staining with *anti*-MYC antibody as described above. Super-resolution microscopy using technology SIM was performed on Zeiss Elyra SP.1 microscope.

#### 4.6. *RUSH* assay

Control HeLa and *MTMR9* KO cells were transfected by *RUSH*-EGFP-WNT3A construct. Twenty hours later 100 μM biotin (B4501, Sigma) in dimethyl sulfoxide (DMSO) or DMSO alone were added to the cells. Cells were incubated 10 min in 37 °C and then shifted to 15 °C for 3 h. After this treatment the cells were fixed and the phenotype was scored. Cells were assigned to one of two categories – WNT3A still trapped in the ER or WNT3A in transit between the ER and the Golgi. The second category also included occasional cells with clear Golgi signal. The samples were anonymized and scored independently by three individuals. More than 100 cells for each condition were scored.

#### 4.7. Autocrine and paracrine Wnt reporter gene assays

To assay autocrine Wnt signalling, STF cells were transfected by DNA mixtures containing mWNT3A construct with MTMR9-NG or empty vector (pNG) and Renilla pRL-SV40 plasmid as an internal control. Cells were harvested 24 h later. For paracrine signalling HEK293T cells were transfected as above using mWNT3A/EV/Renilla or mWNT3A/MTMR9-NG/Renilla DNA mixtures. One day post transfection HEK293T cells were co-cultivated with reporter STF cells. After 24 h of co-culture the cells were harvested and activities of firefly and Renilla luciferase in cell lysates were determined using the Dual-Glo Luciferase Assay System (Promega) and GloMax 20/20 Luminometer (Promega). Reporter gene activities were normalized against the activity of Renilla luciferase to get relative luciferase units (RLU). All reporter gene assays were performed in triplicate. The results of a representative experiment from three in total are presented.

To distinguish between signalling activity of the Wnt produced into the media and the Wnt attached to the producing cells (plasma membrane or extracellular matrix), conditioned media from mWNT3A transfected HEK293T cells were harvested after 48 h of cultivation, centrifuged to avoid cell contamination and cultivated with STF cells for 24 h. The transfected HEK293T cell were also co-cultured with STF cells for 24 h in new media. Firefly and Renilla luciferase activities were determined as above.

#### 4.8. Software and statistical analysis of data

Microscopic data were analysed using the Fiji image processing package [57]. RGB profiler plug-in (for Fiji) was used to create two colour fluorescence intensity profiles of line selections (white or blue lines). The x-axis shows the length of selection in micrometers, while the y-axis displays arbitrary units of fluorescence intensity. To compare the distribution of RAB1A-NG positive structures in control and *MTMR9* KO cells, two pools of RAB1A-NG signal were measured. The first pool corresponded to the Golgi area as defined by the GM130 marker and was marked as red ROI by “Moments” algorithm autothreshold. The second pool corresponded to the vesicles outside of the Golgi and was marked as green ROI by manually adjusted “Otsu dark” algorithm autothreshold. Only green particles bigger than 0.5 μm were taken into account. The ratio between the sum of Golgi areas and the sum of vesicle areas was taken as a measure of RAB1A distribution inside the cells (Golgi/vesicles). The outline of the cell was highlighted in blue and was defined by an automatic Huang algorithm threshold. 32 and 30 individual cells were analysed for control and *MTMR9* KO cells, respectively.

Golgi dispersion was analysed by manually setting a circle with its centre in the middle of the nucleus (Fiji centre of mass analysis) and its circumference encompassing the periphery of the GM130 positive structures. The circle radius (r) was taken as an approximation of Golgi dispersal. 30 cells for each condition were analysed. The same set of cells was analysed for sum of GM130 positive structures (under “Moments” algorithm autothreshold) per cell. The average area of such GM130 positive structure was calculated for each individual cell.

Data sets obtained in the luciferase assays and microscopic analyses were evaluated by Student's t-test.

#### 4.9. Quantitative RT-PCR

Total RNA was isolated from HeLa cells by the Qiagen RNeasy kit according to the manufacturer's instructions. First strand cDNA was synthesized from 1 μg RNA using the Superscript III reverse transcriptase (ThermoFisher Scientific), primed by oligo (dT) primer. qPCR was performed using the 5x HOT FIREPol EvaGreen qPCR Supermix (Solis Biodyne) according to the manufacturer's protocol. Relative mRNA quantities were calculated by the ΔΔCt method [58]. Actin served as an internal control. Results were obtained from at least two independent experiments performed in triplicates. Primer sequences for each gene are as follows: ACTB\_F: GCCCTGAGGCACTCTTCCA, ACTB\_R: CGGATGTCCACGTCACACTTC, MTMR9\_F: TCACCAATCCCCTCTTTGA, MTMR9\_R: CGTCCTGTGTTCCAGTTC.

#### Declarations of interest

None.

#### Acknowledgements

We thank V. Korinek, H. Stenmark, K. Campellone, A. Akhmanova and J. Forstova for providing plasmids and reagents and O. Šebesta for technical assistance with microscopy data acquisition and analyses. This work was funded by Czech Science Foundation grant 16-17966Y to M.M. and by Charles University programme SVV 260435. Microscopy

was performed in the Laboratory of Confocal and Fluorescence Microscopy co-financed by the European Regional Development Fund and the state budget of the Czech Republic, project no. CZ.1.05/4.1.00/16.0347 and CZ.2.16/3.1.00/21515, and supported by the Czech-BioImaging large RI project LM2015062.

## Appendix A. Supplementary data

Supplementary data to this article can be found online at <https://doi.org/10.1016/j.yexcr.2019.111709>.

## References

- [1] J. Laporte, L.J. Hu, C. Kretz, J.-L. Mandel, P. Kioschis, J.F. Coy, S.M. Klauk, A. Poustka, N. Dahl, A gene mutated in X-linked myotubular myopathy defines a new putative tyrosine phosphatase family conserved in yeast, *Nat. Genet.* 13 (1996) 175–182, <https://doi.org/10.1038/ng0696-175>.
- [2] A. Bolino, M. Muglia, F.L. Conforti, E. LeGuern, M.A.M. Salih, D.-M. Georgiou, K. Christodoulou, I. Hausmanowa-Petrusewicz, P. Mandich, A. Schenone, A. Gambardella, F. Bono, A. Quattrone, M. Devoto, A.P. Monaco, Charcot-Marie-Tooth type 4B is caused by mutations in the gene encoding myotubularin-related protein-2, *Nat. Genet.* 25 (2000) 17–19, <https://doi.org/10.1038/75542>.
- [3] H. Azzedine, A. Bolino, T. Taieb, N. Birouk, M. Di Duca, A. Bouhouche, S. Benamou, A. Mrabet, T. Hammadouche, T. Chkili, R. Gouider, R. Ravazzolo, A. Brice, J. Laporte, E. LeGuern, Mutations in MTMR13, a new pseudophosphatase homologue of MTMR2 and Sbf1, in two families with an autosomal recessive demyelinating form of Charcot-Marie-Tooth disease associated with early-onset glaucoma, *Am. J. Hum. Genet.* 72 (2003) 1141–1153, <https://doi.org/10.1086/375034>.
- [4] J. Senderek, Mutation of the SBF2 gene, encoding a novel member of the myotubularin family, in Charcot-Marie-Tooth neuropathy type 4B2/11p15, *Hum. Mol. Genet.* 12 (2003) 349–356, <https://doi.org/10.1093/hmg/ddg030>.
- [5] M.A. Raess, S. Friant, B.S. Cowling, J. Laporte, Wanted - dead or alive: myotubularins, a large disease-associated protein family, *Adv. Biol. Regul.* 63 (2017) 49–58, <https://doi.org/10.1016/j.jbior.2016.09.001>.
- [6] C. Cao, J. Laporte, J.M. Backer, A. Wandinger-Ness, M.-P. Stein, Myotubularin lipid phosphatase binds the hVPS15/hVPS34 lipid kinase complex on endosomes, *Traffic* 8 (2007) 1052–1067, <https://doi.org/10.1111/j.1600-0854.2007.00586.x>.
- [7] K. Ketel, M. Krauss, A.-S. Nicot, D. Puchkov, M. Wiewer, R. Müller, D. Subramanian, C. Schultz, J. Laporte, V. Haucke, A phosphoinositide conversion mechanism for exit from endosomes, *Nature* 529 (2016) 408–412, <https://doi.org/10.1038/nature16516>.
- [8] O. Lorenzo, S. Urbe, M.J. Clague, Systematic analysis of myotubularins: heteromeric interactions, subcellular localisation and endosomere-related functions, *J. Cell Sci.* 119 (2006) 2953–2959, <https://doi.org/10.1242/jcs.03040>.
- [9] M.J. Naughtin, D.A. Sheffield, P. Rahman, W.E. Hughes, R. Gurung, J.L. Stow, H.H. Nandurkar, J.M. Dyson, C.A. Mitchell, The myotubularin phosphatase MTMR4 regulates sorting from early endosomes, *J. Cell Sci.* 123 (2010) 3071–3083, <https://doi.org/10.1242/jcs.060103>.
- [10] J. Yu, L. Pan, X. Qin, H. Chen, Y. Xu, Y. Chen, H. Tang, MTMR4 attenuates transforming growth factor  $\beta$  (TGF $\beta$ ) signaling by dephosphorylating R-smads in endosomes, *J. Biol. Chem.* 285 (2010) 8454–8462, <https://doi.org/10.1074/jbc.M109.075036>.
- [11] H.Q. Pham, K. Yoshioka, H. Mohri, H. Nakata, S. Aki, K. Ishimaru, N. Takuwa, Y. Takuwa, MTMR4, a phosphoinositide-specific 3'-phosphatase, regulates TFEB activity and the endocytic and autophagic pathways, *Genes Cells* 23 (2018) 670–687, <https://doi.org/10.1111/gtc.12609>.
- [12] N. Taguchi-Atarashi, M. Hamasaki, K. Matsunaga, H. Omori, N.T. Ktistakis, T. Yoshimori, T. Noda, Modulation of local PtdIns3P levels by the PI phosphatase MTMR3 regulates constitutive autophagy, *Traffic* 11 (2010) 468–478, <https://doi.org/10.1111/j.1600-0854.2010.01034.x>.
- [13] J. Zou, S.-C. Chang, J. Marjanovic, P.W. Majerus, MTMR9 increases MTMR6 enzyme activity, stability, and role in apoptosis, *J. Biol. Chem.* 284 (2009) 2064–2071, <https://doi.org/10.1074/jbc.M804292200>.
- [14] J. Laporte, F. Blondeau, A. Gansmuller, Y. Lutz, J.-L. Vonesch, J.-L. Mandel, The PtdIns3P phosphatase myotubularin is a cytoplasmic protein that also localizes to Rac 1-inducible plasma membrane ruffles, *J. Cell Sci.* 115 (2002) 3105–3117, <http://www.ncbi.nlm.nih.gov/pubmed/12118066>, Accessed date: 26 April 2019.
- [15] F.L. Robinson, J.E. Dixon, Myotubularin phosphatases: policing 3-phosphoinositides, *Trends Cell Biol.* 16 (2006) 403–412, <https://doi.org/10.1016/j.tcb.2006.06.001>.
- [16] N. St-Denis, G.D. Gupta, Z.Y. Lin, B. Gonzalez-Badillo, L. Pelletier, A.-C. Gingras, Myotubularin-related proteins 3 and 4 interact with polo-like kinase 1 and centrosomal protein of 55 kDa to ensure proper abscission, *Mol. Cell. Proteom.* 14 (2015) 946–960, <https://doi.org/10.1074/mcp.M114.046086>.
- [17] J. Zou, C. Zhang, J. Marjanovic, M.V. Kisseleva, P.W. Majerus, M.P. Wilson, Myotubularin-related protein (MTMR) 9 determines the enzymatic activity, substrate specificity, and role in autophagy of MTMR8, *Proc. Natl. Acad. Sci.* 109 (2012) 9539–9544, <https://doi.org/10.1073/pnas.1207021109>.
- [18] S. Srivastava, K. Ko, P. Choudhury, Z. Li, A.K. Johnson, V. Nadkarni, D. Unutmaz, W.A. Coetzee, E.Y. Skolnik, Phosphatidylinositol-3 phosphatase myotubularin-related protein 6 negatively regulates CD4 T cells, *Mol. Cell. Biol.* 26 (2006) 5595–5602, <https://doi.org/10.1128/MCB.00352-06>.
- [19] L. Guo, C. Martens, D. Bruno, S.F. Porcella, H. Yamane, S.M. Caucheteux, J. Zhu, W.E. Paul, Lipid phosphatases identified by screening a mouse phosphatase shRNA library regulate T-cell differentiation and protein kinase B AKT signaling, *Proc. Natl. Acad. Sci. U. S. A.* 110 (2013) E1849–E1856, <https://doi.org/10.1073/pnas.1305070110>.
- [20] J.P. MacKeigan, L.O. Murphy, J. Blenis, Sensitized RNAi screen of human kinases and phosphatases identifies new regulators of apoptosis and chemoresistance, *Nat. Cell Biol.* 7 (2005) 591–600, <https://doi.org/10.1038/ncb1258>.
- [21] I. Vergne, E. Roberts, R.A. Elmaoued, V. Tosch, M.A. Delgado, T. Proikas-Cezanne, J. Laporte, V. Deretic, Control of autophagy initiation by phosphoinositide 3-phosphatase jumpy, *EMBO J.* 28 (2009) 2244–2258, <https://doi.org/10.1038/emboj.2009.159>.
- [22] Y. Mochizuki, R. Ohashi, T. Kawamura, H. Iwanari, T. Kodama, M. Naito, T. Hamakubo, Phosphatidylinositol 3-phosphatase myotubularin-related protein 6 (MTMR6) is regulated by small GTPase Rab1B in the early secretory and autophagic pathways, *J. Biol. Chem.* 288 (2013) 1009–1021, <https://doi.org/10.1074/jbc.M112.395087>.
- [23] E.L. Axe, S.A. Walker, M. Manifava, P. Chandra, H.L. Roderick, A. Habermann, G. Griffiths, N.T. Ktistakis, Autophagosome formation from membrane compartments enriched in phosphatidylinositol 3-phosphate and dynamically connected to the endoplasmic reticulum, *J. Cell Biol.* 182 (2008) 685–701, <https://doi.org/10.1083/jcb.200803137>.
- [24] M. Maekawa, S. Terasaka, Y. Mochizuki, K. Kawai, Y. Ikeda, N. Araki, E.Y. Skolnik, T. Taguchi, H. Arai, Sequential breakdown of 3-phosphorylated phosphoinositides is essential for the completion of macropinocytosis, *Proc. Natl. Acad. Sci.* 111 (2014) E978–E987, <https://doi.org/10.1073/pnas.1311029111>.
- [25] J. Saraste, M. Marie, Intermediate compartment (IC): from pre-Golgi vacuoles to a semi-autonomous membrane system, *Histochem. Cell Biol.* 150 (2018) 407–430, <https://doi.org/10.1007/s00418-018-1717-2>.
- [26] E.J. Tisdale, J.R. Bourne, R. Khosravi-Far, C.J. Der, W.E. Balch, GTP-binding mutants of rab1 and rab2 are potent inhibitors of vesicular transport from the endoplasmic reticulum to the Golgi complex, *J. Cell Biol.* 119 (1992) 749–761, <https://doi.org/10.1083/jcb.119.4.749>.
- [27] M. Matsuo, F. Kano, M. Murata, Reconstitution of the targeting of Rab6A to the Golgi apparatus in semi-intact HeLa cells: a role of BICD2 in stabilizing Rab6A on Golgi membranes and a concerted role of Rab6A/BICD2 interactions in Golgi-to-ER retrograde transport, *Biochim. Biophys. Acta Mol. Cell Res.* 1853 (2015) 2592–2609, <https://doi.org/10.1016/j.bbamcr.2015.05.005>.
- [28] R.W. Doms, G. Russ, J.W. Yewdell, Brefeldin A redistributes resident and itinerant Golgi proteins to the endoplasmic reticulum, *J. Cell Biol.* 109 (1989) 61–72, <https://doi.org/10.1083/jcb.109.1.61>.
- [29] J. Lippincott-Schwartz, L.C. Yuan, J.S. Bonifacino, R.D. Klausner, Rapid redistribution of Golgi proteins into the ER in cells treated with brefeldin A: evidence for membrane cycling from Golgi to ER, *Cell* 56 (1989) 801–813, [https://doi.org/10.1016/0092-8674\(89\)90685-5](https://doi.org/10.1016/0092-8674(89)90685-5).
- [30] J. Saraste, K. Svensson, Distribution of the intermediate elements operating in ER to Golgi transport, *J. Cell Sci.* 100 (Pt 3) (1991) 415–430, <http://www.ncbi.nlm.nih.gov/pubmed/1808196>, Accessed date: 8 October 2019.
- [31] Y. Mochizuki, P.W. Majerus, Characterization of myotubularin-related protein 7 and its binding partner, myotubularin-related protein 9, *Proc. Natl. Acad. Sci.* 100 (2003) 9768–9773, <https://doi.org/10.1073/pnas.1333958100>.
- [32] A.J. Russo, A.J. Mathiowetz, S. Hong, M.D. Welch, K.G. Campellone, Rab1 recruits WHAMM during membrane remodeling but limits actin nucleation, *Mol. Biol. Cell* 27 (2016) 967–978, <https://doi.org/10.1091/mbc.E15-07-0508>.
- [33] K.G. Campellone, N.J. Webb, E.A. Znameroski, M.D. Welch, WHAMM is an arp2/3 complex activator that binds microtubules and functions in ER to Golgi transport, *Cell* 134 (2008) 148–161, <https://doi.org/10.1016/j.cell.2008.05.032>.
- [34] A.J. Mathiowetz, E. Baple, A.J. Russo, A.M. Coulter, E. Carrano, J.D. Brown, R.N. Jinks, A.H. Crosby, K.G. Campellone, An Amish founder mutation disrupts a PI (3)P-WHAMM-Arp2/3 complex-driven autophagosomal remodeling pathway, *Mol. Biol. Cell* 28 (2017) 2492–2507, <https://doi.org/10.1091/mbc.E17-01-0022>.
- [35] J.F. Presley, N.B. Cole, T.A. Schroer, K. Hirschberg, K.J.M. Zaal, J. Lippincott-Schwartz, ER-to-Golgi transport visualized in living cells, *Nature* 389 (1997) 81–85, <https://doi.org/10.1038/38001>.
- [36] M. Silhankova, F. Port, M. Harterink, K. Basler, H.C. Korswagen, Wnt signalling requires MTM-6 and MTM-9 myotubularin lipid-phosphatase function in Wnt-producing cells, *EMBO J.* 29 (2010) 4094–4105, <https://doi.org/10.1038/emboj.2010.278>.
- [37] M.J. Lorenzowicz, H.C. Korswagen, Sailing with the Wnt: charting the Wnt processing and secretion route, *Exp. Cell Res.* 315 (2009) 2683–2689, <https://doi.org/10.1016/j.yexcr.2009.06.015>.
- [38] F. Port, K. Basler, Wnt trafficking: new insights into Wnt maturation, secretion and spreading, *Traffic* 11 (2010) 1265–1271, <https://doi.org/10.1111/j.1600-0854.2010.01076.x>.
- [39] G. Boncompain, F. Perez, Synchronizing protein transport in the secretory pathway, *Curr. Protoc. Cell Biol.* John Wiley & Sons, Inc., Hoboken, NJ, USA, 2012, <https://doi.org/10.1002/0471143030.cb1519s57> Unit 15.19.
- [40] N. Moti, J. Yu, G. Boncompain, F. Perez, D.M. Virshup, Wnt traffic from endoplasmic reticulum to filopodia, *PLoS One* 14 (2019) e0212711, <https://doi.org/10.1371/journal.pone.0212711>.
- [41] M. Aizawa, M. Fukuda, Small GTPase Rab2B and its specific binding protein golgi-associated Rab2B interactor-like 4 (GARIL4) regulate Golgi morphology, *J. Biol. Chem.* 290 (2015) 22250–22261, <https://doi.org/10.1074/jbc.M115.669242>.
- [42] O. Lecompte, O. Poch, J. Laporte, PtdIns5P regulation through evolution: roles in membrane trafficking? *Trends Biochem. Sci.* 33 (2008) 453–460, <https://doi.org/10.1016/j.tibs.2008.07.002>.

- [43] I. Vergne, V. Deretic, The role of PI3P phosphatases in the regulation of autophagy, *FEBS Lett.* 584 (2010) 1313–1318, <https://doi.org/10.1016/j.febslet.2010.02.054>.
- [44] H.C. Dooley, M.I. Wilson, S.A. Tooze, WIPI2B links PtdIns3P to LC3 lipidation through binding ATG16L1, *Autophagy* 11 (2015) 190–191, <https://doi.org/10.1080/15548627.2014.996029>.
- [45] F.C.M. Zoppino, R. Damián Militello, I. Slavin, C. Álvarez, M.I. Colombo, autophagosome formation depends on the small GTPase Rab1 and functional ER exit sites, *Traffic* 11 (2010) 1246–1261, <https://doi.org/10.1111/j.1600-0854.2010.01086.x>.
- [46] J. Huang, C.L. Birmingham, S. Shahnazari, J. Shiu, Y.T. Zheng, A.C. Smith, K.G. Campellone, W. Do Heo, S. Gruenheid, T. Meyer, M.D. Welch, N.T. Ktistakis, P.K. Kim, D.J. Klionsky, J.H. Brumell, Antibacterial autophagy occurs at PI(3)P-enriched domains of the endoplasmic reticulum and requires Rab1 GTPase, *Autophagy* 7 (2011) 17–26, <https://doi.org/10.4161/auto.7.1.13840>.
- [47] J. Saraste, Spatial and functional aspects of ER-golgi rabs and tethers, *Front. Cell Dev. Biol.* 4 (2016) 28, <https://doi.org/10.3389/fcell.2016.00028>.
- [48] D.J. Kast, A.L. Zajac, E.L.F. Holzbaur, E.M. Ostap, R. Dominguez, WHAMM directs the arp2/3 complex to the ER for autophagosome biogenesis through an actin comet tail mechanism, *Curr. Biol.* 25 (2015) 1791–1797, <https://doi.org/10.1016/j.cub.2015.05.042>.
- [49] J.C. Gross, M. Boutros, Secretion and extracellular space travel of Wnt proteins, *Curr. Opin. Genet. Dev.* 23 (2013) 385–390, <https://doi.org/10.1016/j.gde.2013.02.017>.
- [50] E. Stanganello, S. Scholpp, Role of cytonemes in Wnt transport, *J. Cell Sci.* 129 (2016) 665–672, <https://doi.org/10.1242/jcs.182469>.
- [51] N.C. Shaner, G.G. Lambert, A. Chammas, Y. Ni, P.J. Cranfill, M.A. Baird, B.R. Sell, J.R. Allen, R.N. Day, M. Israelsson, M.W. Davidson, J. Wang, A bright monomeric green fluorescent protein derived from Branchiostoma lanceolatum, *Nat. Methods* 10 (2013) 407–409, <https://doi.org/10.1038/nmeth.2413>.
- [52] D.J. Dupré, M. Robitaille, N. Éthier, L.R. Villeneuve, A.M. Mamarbachi, T.E. Hébert, Seven transmembrane receptor core signaling complexes are assembled prior to plasma membrane trafficking, *J. Biol. Chem.* 281 (2006) 34561–34573, <https://doi.org/10.1074/jbc.M605012200>.
- [53] T. Matanis, A. Akhmanova, P. Wulf, E. Del Nery, T. Weide, T. Stepanova, N. Galjart, F. Grosveld, B. Goud, C.I. De Zeeuw, A. Barnekow, C.C. Hoogenraad, Bicaudal-D regulates COPI-independent Golgi-ER transport by recruiting the dynein-dynactin motor complex, *Nat. Cell Biol.* 4 (2002) 986–992, <https://doi.org/10.1038/ncb891>.
- [54] C. Bucci, P. Thomsen, P. Nicoziani, J. McCarthy, B. van Deurs, Rab7: a key to lysosome biogenesis, *Mol. Biol. Cell* 11 (2000) 467–480, <https://doi.org/10.1091/mbc.11.2.467>.
- [55] W. Chen, Y. Feng, D. Chen, A. Wandinger-Ness, Rab11 is required for trans-golgi network-to-plasma membrane transport and a preferential target for GDP dissociation inhibitor, *Mol. Biol. Cell* 9 (1998) 3241–3257, <https://doi.org/10.1091/mbc.9.11.3241>.
- [56] Q. Xu, Y. Wang, A. Dabdoub, P.M. Smallwood, J. Williams, C. Woods, M.W. Kelley, L. Jiang, W. Tasman, K. Zhang, J. Nathans, Vascular development in the retina and inner ear: control by Norrin and Frizzled-4, a high-affinity ligand-receptor pair, *Cell* 116 (2004) 883–895, [https://doi.org/10.1016/S0092-8674\(04\)00216-8](https://doi.org/10.1016/S0092-8674(04)00216-8).
- [57] J. Schindelin, I. Arganda-Carreras, E. Frise, V. Kaynig, M. Longair, T. Pietzsch, S. Preibisch, C. Rueden, S. Saalfeld, B. Schmid, J.-Y. Tinevez, D.J. White, V. Hartenstein, K. Eliceiri, P. Tomancak, A. Cardona, Fiji: an open-source platform for biological-image analysis, *Nat. Methods* 9 (2012) 676–682, <https://doi.org/10.1038/nmeth.2019>.
- [58] T.D. Schmittgen, K.J. Livak, Analyzing real-time PCR data by the comparative C(T) method, *Nat. Protoc.* 3 (2008) 1101–1108, <https://doi.org/10.1038/nprot.2008.73>.



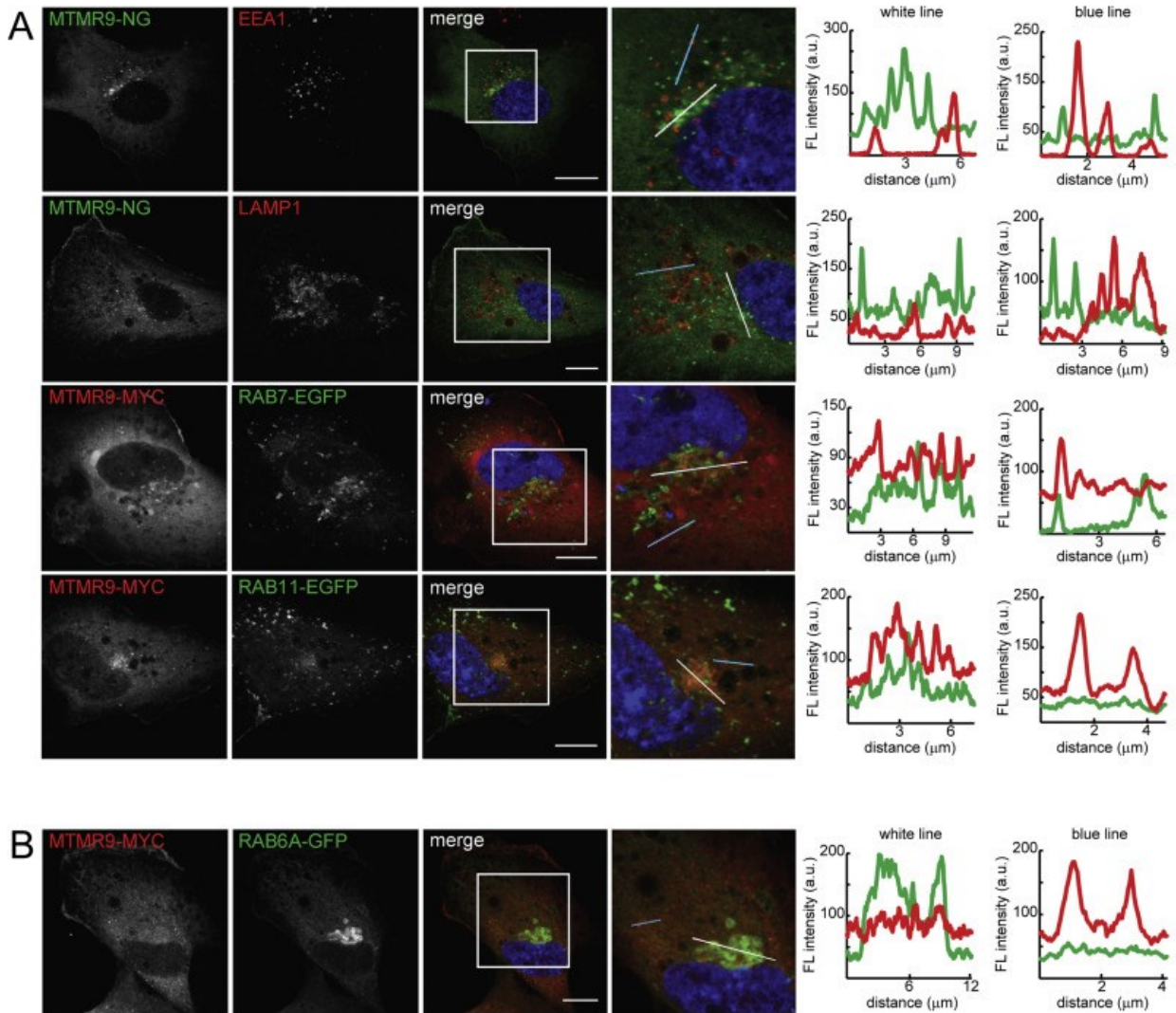


**Figure S1.** MTMR9 does not significantly co-localize with endosomal and lysosomal markers. A) To define MTMR9 positive vesicles identity RPE-1 cells were transfected by MTMR9-NG and after fixation and membrane permeabilization stained for early endosome marker EEA1 (red) or lysosome marker LAMP1 (red). To exclude that vesicles are late or recycling endosomes, MTMR9-MYC (red) was co-transfected with RAB7-EGFP or RAB11-EGFP, respectively. B) MTMR9-MYC was co-transfected with RAB6A-GFP as a marker of Golgi-to-ER retrograde transport vesicles. The cells were mounted into Mowiol/DAPI solution. White square delineates the magnified area. White and blue lines indicate the selection analysed by RGB profiler. Scale bars correspond to 10 μm. FL – fluorescence, a.u. – arbitrary units

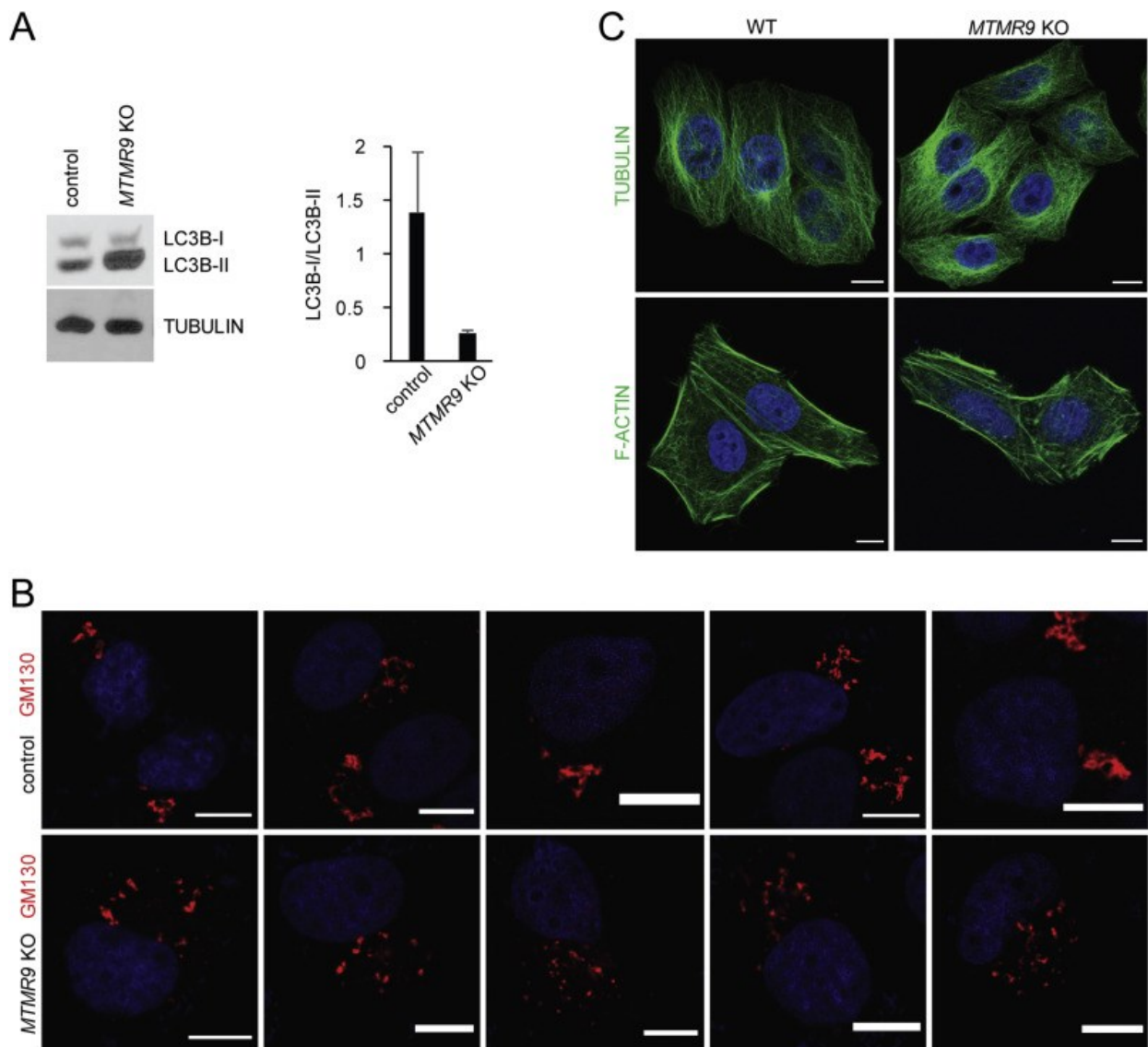


**Figure S2.** Characterization of *MTMR9* KO cells. A) Loss of *MTMR9* expression results in increase in the basal level of autophagy. Processing of the autophagy marker LC3B was analysed in parental HeLa and *MTMR9* KO cells by Western blot. Quantification of the ratio between the LC3B-I and LC3B-II forms from three independent experiments is shown in the graph. Data are presented as mean  $\pm$  SEM. Shift towards the LC3B-II form in *MTMR9* KO cells indicates higher rate of autophagy. B) Loss of *MTMR9* expression results in dispersal of the Golgi. Randomly selected examples of control and *MTMR9* KO cells stained with GM130 antibody show the Golgi dispersal in *MTMR9* KO cells. These cells belong to the set analysed in Fig. 4D-F. Images are single confocal sections. C) Loss of *MTMR9* expression does not affect the integrity of cytoskeleton. Control and *MTMR9* KO cells were fixed, permeabilized and stained for tubulin (upper panel) or F-actin (lower panel). No obvious differences in cytoskeleton organization were detected. Images are maximum projections of 8-10 confocal z-sections taken at 0.3  $\mu$ m steps. Scale bars correspond to 10  $\mu$ m

***Caenorhabditis elegans* SEL-5/AAK1 regulates cell migration and cell outgrowth independently of its kinase activity**

Filip Knop<sup>1</sup>, Apolena Zounarová<sup>1</sup>, Marie Macůrková<sup>1,\*</sup>

<sup>1</sup> Department of Cell Biology, Faculty of Science, Charles University, Vinicna 7, 128 00  
Prague 2, Czech Republic

\* Corresponding author

Keywords: SEL-5/AAK1, Wnt signalling, DPY-23/AP2M1, excretory cell, retromer

## Abstract

During *Caenorhabditis elegans* development multiple cells migrate long distances or extend processes to reach their final position and/or attain proper shape. Wnt signalling pathway stands out as one of the major coordinators of cell migration or cell outgrowth along the anterior-posterior body axis. Wnt signalling outcome is fine-tuned by various mechanisms including endocytosis. In this study we show that SEL-5, the *C. elegans* orthologue of mammalian AP2-associated kinase AAK1, acts together with the retromer complex as a positive regulator of EGL-20/Wnt signalling during the migration of QL neuroblast daughter cells. At the same time, SEL-5 in cooperation with the retromer complex is also required during excretory canal cell outgrowth in a Wnt-independent manner. Importantly, SEL-5 kinase activity is not required for its role in either neuronal migration or excretory cell outgrowth and neither of these processes is dependent on DPY-23/AP2M1 phosphorylation. While Wnt proteins do not significantly contribute to the excretory canal guidance, LIN-44/Wnt and LIN-17/Frizzled together generate a stop signal inhibiting further canal outgrowth.

## Introduction

During the development of *Caenorhabditis elegans* several cells, both neuronal and non-neuronal, migrate in a well-defined and invariant manner along the anterior-posterior (A-P) body axis. Other cells do not migrate but rather extend their processes along the same axis. In both instances the directionality of migration and growth is controlled by a set of guidance cues provided by the surrounding tissue and received by the corresponding signalling apparatus in the migrating or growing cell (Silhankova and Korswagen, 2007; Sundaram and Buechner, 2016; Sherwood and Plastino, 2018; Hutter, 2019). Gradients of Wnt proteins and panel of their receptors are the key determinants of the A-P guidance in *C.elegans*. Wnts can

act either as attractants, repellents or as permissive cues for given cell and the cell response depends on a given combination of Wnts, Frizzleds and other components of the Wnt pathway expressed in and around that particular cell (Silhankova and Korswagen, 2007; Ackley, 2014; Middelkoop and Korswagen, 2014; Rella et al., 2016).

Endocytosis is an important regulatory mechanism of Wnt signalling applied in both Wnt producing and Wnt receiving cells. On the way out of the producing cell Wnts are accompanied by a Wnt sorting receptor Wntless (WLS) (Banziger et al., 2006; Bartscherer et al., 2006; Goodman et al., 2006). Once WLS is relieved of its cargo at the plasma membrane, it is internalized by clathrin- and adaptor protein complex 2 (AP2)-dependent endocytosis (Pan et al., 2008; Port et al., 2008; Yang et al., 2008). Internalized WLS is subsequently recycled by a multisubunit retromer complex to the Golgi apparatus (Belenkaya et al., 2008; Franch-Marro et al., 2008; Pan et al., 2008; Port et al., 2008; Yang et al., 2008) and further to the endoplasmic reticulum (Yu et al., 2014). Disruption of AP2 or clathrin function results in decreased Wnt secretion due to improper WLS recycling (Pan et al., 2008; Port et al., 2008; Yang et al., 2008). In Wnt receiving cells, the activity of the Wnt-receptor complex, the signalosome, can be promoted by endocytosis, while at the same time endocytosis can also attenuate Wnt signalling by regulating the membrane availability of Wnt receptors (Albrecht et al., 2021; Colozza and Koo, 2021; Wu et al., 2021).

AP2-associated kinase 1 (AAK1) belongs to the Ark/Prk or Numb-associated (NAK) family of serine/threonine protein kinases (Smythe and Ayskough, 2003; Sorrell et al., 2016). Members of this family play an important role in regulating endocytosis in yeast, *Drosophila* or mammals (Smythe and Ayskough, 2003; Peng et al., 2009). Human AAK1 has been shown to phosphorylate AP2M1, the  $\mu$ 2 subunit of the AP2 adaptor complex (Conner and Schmid, 2002). Phosphorylation of  $\mu$ 2 at Thr156 by AAK1 enhances the binding affinity of AP2 to sorting signals of endocytosed proteins (Ricotta et al., 2002). AAK1 has also been shown to



phosphorylate the endocytic adaptor and negative regulator of Notch signalling Numb and affect its subcellular localization (Sorensen and Conner, 2008). Interestingly, AAK1 can also interact with membrane-tethered activated form of Notch receptor and promote its internalization (Gupta-Rossi et al., 2011).

AAK1 knock-down upregulated Wnt signalling in a mouse embryonic stem cell-based kinase and phosphatase siRNA screen (Groenendyk and Michalak, 2011). Recent study in human cells confirmed this observation and offered a mechanism. By phosphorylating AP2 AAK1 promotes endocytosis of LRP6 and thus shuts down the signalling (Agajanian et al., 2018). In *C. elegans*, AAK1 orthologue SEL-5 has been genetically implicated in Notch signalling as mutation in *sel-5* can suppress the constitutively active *lin-12*/Notch mutants. Suppression is however observed only in *lin-12* allele activating the membrane-anchored Notch and not when the pathway is activated by expression of the intracellular domain (Fares and Greenwald, 1999). This hints that SEL-5 could regulate endocytosis in a similar manner as its mammalian counterpart. So far, no link has been made between SEL-5 and *C. elegans* Wnt signalling regulation.

In this study we set to analyse the potential role of the SEL-5 kinase in Wnt signalling regulation and its contribution to DPY-23/AP2M1 phosphorylation in *C. elegans*. We show that SEL-5 acts in collaboration with the retromer complex as a positive regulator of EGL-20/Wnt signalling during the migration of QL neuroblast descendants. We further demonstrate that although SEL-5 participates on DPY-23 phosphorylation, the observed role of SEL-5 in neuroblast migration is independent of its kinase activity and the phosphorylation of DPY-23 is dispensable for Wnt-dependent migration of QL neuroblast descendants. SEL-5 together with the retromer is further required during the active phase of excretory cell canal extension, again independently of its kinase activity. Finally we show that Wnt proteins do

not serve as major guidance cues for excretory canal outgrowth but LIN-44/Wnt and LIN-17/Frizzled together define the stopping point for canal extension.

## Results

### Loss of SEL-5 affects migration of QL neuroblast descendants

Q cell descendant (Q.d) migration is dependent on EGL-20/Wnt signalling. While on the right side of the L1 larva QR divides and QR.d migrate in the default anterior direction, on the left side QL.d respond to the EGL-20 signal produced in several cells around the rectum by expressing homeotic gene *mab-5* and migrate to the posterior. In the absence of active EGL-20 signalling *mab-5* is not expressed and QL.d migrate to the anterior (Salser and Kenyon, 1992) (Fig. 1A). In order to visualize Q.d migration we utilized *Pmec-7::gfp* expressing transgene *muIs32* that is, apart from other cells, active in AVM and PVM touch neurons, which are QR and QL descendants, respectively (Ch'ng et al., 2003). We performed RNA interference (RNAi) against *sel-5* in wild type background and observed no effect on QL.d migration (Fig. 1B). To increase the sensitivity of the RNAi approach, we repeated the RNAi experiment using *vps-29(tm1320)* mutant strain. This strain harbours a null mutation in the VPS-29 retromer subunit, displays only weakly penetrant QL.d migration defect (Coudreuse et al., 2006) and has been used previously as a sensitized background to uncover genes required for the Q.d migration (Harterink et al., 2011; Lorenowicz et al., 2014). RNAi against *sel-5* significantly increased the QL.d migration defect of *vps-29(tm1320)* (Fig. 1B). To verify the results obtained with RNAi we assessed the QL.d migration in *sel-5(ok363)* and *sel-5(ok149)* mutants. Similarly to RNAi results, single *sel-5* mutation had no effect on QL.d migration while *sel-5 vps-29* double mutants displayed almost fully penetrant defect (Fig. 1C, D).

Loss of *vps-29* affects EGL-20/Wnt signalling at the level of Wnt production (Yang et al., 2008). We further tested whether loss of *sel-5* could enhance partially penetrant defects in QL.d migration in mutants acting at different level of the EGL-20/Wnt pathway. Loss of *sel-5* strongly increased the weak QL.d migration defect of the *lin-17*/Frizzled mutants but had no effect on the already more penetrant QL.d defect of *mig-1*/Frizzled mutant animals (Fig. 1D). We next asked whether loss of *sel-5* in the *vps-29* background affects other Wnt-dependent processes such as the polarization of the ALM and PLM neurons, CAN neuron migration or T cell polarity. Polarization of ALM and PLM is regulated by several Wnt proteins (Pan et al., 2006; Prasad and Clark, 2006; Hilliard and Bargmann, 2006), CAN neuron migration is governed predominantly by CWN-2 with minor contribution from CWN-1 and EGL-20 (Zinovyeva and Forrester, 2005; Zinovyeva et al., 2008) and T cell polarity depends on the LIN-44/Wnt signal (Herman et al., 1995). We observed weakly penetrant ALM polarization defects in both *sel-5(ok363) vps-29* and *sel-5(ok149) vps-29* double mutants, a very mild PLM polarization defect was detected in a strain carrying the *ok149* allele (Table 1). Mildly penetrant anterior displacement of the CAN neuron was observed in the double mutants, while about 17% of double mutant animals carrying the *ok149* allele did not correctly form the phasmid sensillum which indicates defects in T cell polarization (Table 1). Apart from these Wnt dependent phenotypes, we also observed reduced brood size in the double mutants compared to controls (Table 1) and defective tail formation (Fig. 1E).

The penetrance of the observed phenotypes was not the same in the two *sel-5* alleles. This was striking as both alleles carry deletions hitting the kinase domain of SEL-5 protein. We were able to amplify shorter than wild type transcripts from both *sel-5(ok363)* and *sel-5(ok149)* animals using primers in exon 1 and exon 17 (Fig. 1F). Sequencing of the *ok363* transcript revealed that amino acids 1 to 243 of the wild type protein followed by extra 32 amino acids would be translated due to a frameshift and a premature stop codon. Such protein

encompasses larger part of the SEL-5 kinase domain including the active site. In agreement with data published by Fares and Greenwald (Fares and Greenwald, 1999), sequencing of *okl49* transcript revealed that it can give rise to a protein containing the first 153 amino acids of SEL-5 followed by 21 extra amino acids and is thus devoid of the active site (Fig. 1F). If such truncated proteins are present in the mutants, it is possible that either one or both possess some residual activity that is responsible for the observed phenotypic differences.

### **SEL-5 is required in EGL-20/Wnt producing cells to direct QL.d migration**

The asymmetric migration of the Q neuroblast is regulated both cell-autonomously and non-autonomously. To analyse the tissue-specific requirement of SEL-5 in QL.d migration we expressed full-length SEL-5 tagged with GFP at its N-terminus under the control of different tissue-specific promoters in *sel-5 vps-29* background and assayed the QL.d migration. Expression of SEL-5 from *egl-20* promoter (Coudreuse et al., 2006) resulted in a significant rescue of the QL.d migration defect of *sel-5 vps-29* double mutants albeit not to the level of *vps-29* single mutant (Fig. 2A). No rescue was obtained when SEL-5 was expressed from the *wrt-2* promoter that is active in the seam cells and in the Q cell (Aspöck et al., 1999; Middelkoop et al., 2012). These data suggest that *sel-5* is required in the EGL-20/Wnt producing cells to control QL.d migration. However, similar level of rescue as with *egl-20* promoter was obtained also when SEL-5 was expressed from *hlh-1* promoter specific for the body wall muscle cells (Krause et al., 1990, Harfe et al., 1998). When SEL-5 was expressed from *egl-20* and *hlh-1* at the same time, the rescue almost reached the background frequency of the QL.d defect, caused by *vps-29* alone (Fig. 1D, 2A). Apart from the rectal epithelial cells, *egl-20* expression was also detected in posterior ventral body wall muscle quadrants VL23 and VR24 (Harterink et al., 2011), it is thus possible that *hlh-1* promoter-driven expression of SEL-5 in these muscle quadrants is responsible for the observed rescue and only

the combined expression from all EGL-20 producing cells is sufficient to drive a full rescue. Alternatively, the observed rescue pattern could indicate that SEL-5 is required both in the Wnt-producing and in the muscle cells which could for example participate in shaping the Wnt gradient.

To confirm that the tissues identified above in the rescue experiments are tissues with genuine *sel-5* expression we set to determine the endogenous *sel-5* expression pattern which has not been previously analysed. The only published expression data (Fares and Greenwald, 1999) were based on expression from *sel-12* instead of *sel-5* promoter. We generated GFP knock-in strains by inserting GFP into the *sel-5* genomic sequence using the SEC cassette approach (Dickinson et al., 2015). We obtained two strains, one expressing a transcriptional *Psel-5::gfp* reporter and one, after excision of the SEC cassette, an N-terminally tagged GFP::SEL-5 under the control of its own promoter (*Psel-5::gfp::sel-5*). Microscopic analyses of both strains revealed that *sel-5* is expressed broadly, but at low level judged by the GFP signal intensity. The most prominent expression was observed in the gonad from the beginning of its development (Fig. 2B). Expression was further observed in the developing oocytes, in the vulva, in epidermal cells and most notably, in the rectal epithelial cells that are known to produce EGL-20/Wnt (Whangbo and Kenyon, 1999) (Fig. 2B, C). These observations further support our finding that SEL-5 is required in EGL-20/Wnt producing cells to regulate QL.d migration. We could not detect *sel-5* expression in the muscles, although we cannot exclude that low level of expression, below the detection limit using the endogenous locus-tagging approach, is present. Interestingly oocytes and epidermal seam cells expressing the GFP::SEL-5 fusion protein revealed its distinct subcellular localization. Protein localized to punctate structures located close to the cell surface (Fig. 2C). This pattern resembles the subcellular distribution of human AAK1 (Conner and Schmid, 2002) hinting that SEL-5 could be involved in regulating intracellular transport similar to AAK1.

## **SEL-5-associated phenotypes are independent of DPY-23 phosphorylation**

SEL-5 orthologue AAK1 has been implicated in endocytosis regulation (Conner and Schmid, 2002; Ricotta et al., 2002). The obvious candidate that could be affected by SEL-5-dependent endocytosis in Wnt producing cells is the Wnt cargo receptor MIG-14/Wls. Human AAK1 can phosphorylate AP2 subunit  $\mu$ 2 (AP2M1) (Conner and Schmid, 2002; Ricotta et al., 2002) and thus increase AP2 affinity to cargo molecules (Ricotta et al., 2002). It is conceivable that SEL-5 could regulate MIG-14/Wls trafficking at the level of AP2-dependent endocytosis. We first tested whether loss of *sel-5* expression has any effect on the level of phosphorylation of DPY-23 (also known as APM-2), the *C. elegans*  $\mu$ 2 subunit of AP2 complex. A phospho-specific antibody recognizing the phosphorylated threonine T160 (T156 in mammalian AP2M1) of DPY-23 (Hollopeter et al., 2014) revealed a decrease in the level of phosphorylated endogenous DPY-23 in *sel-5* mutants compared to wild type animals (Fig. 3A). Similarly, T160 phosphorylation was reduced on overexpressed GFP-tagged DPY-23 (Fig. 3B). Next we assessed MIG-14 levels and localization in *sel-5 vps-29* mutants. However, as shown in Fig. 3C and D, neither levels nor subcellular distribution of a functional MIG-14::GFP protein changed significantly in *sel-5 vps-29* compared to *vps-29* single mutant. Levels of MIG-14::GFP in *sel-5* single mutants were variable yet on average comparable to wild type. We therefore concluded that the significant increase in QL.d migration defect in *sel-5 vps-29* compared to *vps-29* cannot be attributed to changes in MIG-14/Wls trafficking.

Although it is possible that endocytic cargo other than MIG-14 is affected in *sel-5 vps-29* mutants, we could not exclude the possibility that the observed phenotypes are a consequence of defects in other mechanisms unrelated to DPY-23 phosphorylation. To test this hypothesis we repeated the rescue experiment presented in Fig. 2A now with SEL-5 carrying a point mutation in the kinase active site, D178A. When expressed under the control of *egl-20*

promoter, the mutant SEL-5 protein could still rescue the QL migration phenotype to a similar extent as the wild type version (Fig. 3E). Similar results were obtained when a point mutation was introduced to the ATP binding site, K75A. This indicates that SEL-5 kinase activity is not responsible for the phenotypes observed in *sel-5 vps-29* mutants. We next asked whether the absence of DPY-23 phosphorylation at T160 position leads to defects in QL.d migration. To this end we utilized *dpy-23(mew25)* mutant allele harbouring T160A point mutation (G. Hollopeter and G. Beacham, unpublished). Animals carrying *dpy-23(mew25)* alone or in combination with *sel-5(ok149)* did not show any defects in QL.d migration (Fig. 3F). Variable increase in QL.d migration defects were observed in *vps-29;dpy-23(mew25)* animals, but the penetrance of the defect never reached levels comparable to those in *sel-5 vps-29* mutants (Fig. 1D, 3F). Together these observations strongly suggest that the role of SEL-5 in regulation of QL.d migration is not dependent on its kinase activity and moreover, that DPY-23 phosphorylation at T160 is not a major regulatory event in this process.

### **The outgrowth of excretory cell canals is impaired in *sel-5 vps-29* mutants**

We did not observe any gross morphological defects in the *sel-5 vps-29* double mutant strain. However, in some animals we unexpectedly noticed a severe shortening of the posterior canals of the excretory cell that prompted us to analyse this phenotype in more detail. Excretory cell (also called excretory canal cell) is a large H-shaped cell required for osmoregulation (Buechner et al., 1999; Liegeois et al., 2007). Excretory canal cell body is located near the posterior bulb of the pharynx and four excretory canals emanate from the cell body – two short ones directed to the anterior and two posterior canals extending to the rectum (Fig. 4A). To assess the morphology of the excretory cell we expressed GFP under the control of *p<sub>gpg-12</sub>* promoter which is active exclusively in the excretory cell (Zhao et al., 2004) and analysed the length of the canals in late L4 or early adult animals. While the

posterior canal length in *sel-5* or *vps-29* single mutants was indistinguishable from the wild type controls, in more than 60 % of *sel-5 vps-29* mutants the posterior canals stopped at various positions anterior to the rectum (Fig. 4A,B). Similar effect, albeit with lower penetrance, was observed when assessing the anterior canal length (Fig. 4C). Interestingly, the posterior canal on the right side of the animal was significantly more affected than its counterpart on the left side in *sel-5 vps-29* double mutants carrying the *ok149* allele (Fig. 4D). Similar trend was observed in *sel-5(ok363) vps-29* animals, although the difference observed there did not reach statistical significance (Fig. 4D).

The active growth of the canals starts during embryogenesis and continues during L1, after that the canals passively grow with the growing animal (Fujita et al., 2003). Comparison of canal lengths at several time points within a 24-hour interval after hatching revealed that in *sel-5 vps-29* double mutants the posterior canals of the excretory cell are shorter already at the time of hatching and the growth defect prevails into the larval development (Fig. 4E).

Excretory canal shortening has not previously been reported for any of the retromer components. We therefore tested whether this phenotype is specific for the *vps-29* retromer subunit or whether the whole retromer complex is required together with *sel-5* for proper excretory canal extension. We performed RNAi against *vps-35*, *vps-26*, *snx-1* and *snx-3* in *sel-5(ok149)* background and assessed the posterior canal length. Except for *snx-1* RNAi, significant shortening was observed with RNAi against all other retromer subunits, with *vps-35* showing the strongest phenotype (Fig. 4F). These data confirm that the whole retromer complex acts together with *sel-5* to control excretory canal outgrowth.

We next tested in which tissue SEL-5 activity is required for excretory cell outgrowth. We expressed SEL-5 from either *pgp-12* (excretory cell), *hlh-1* (body wall muscle cells) or *col-10* (hypodermis) promoters in *sel-5 vps-29* double mutants and checked for any rescue. As shown in Fig. 4G, expression of SEL-5 from *pgp-12* promoter almost fully rescued the



excretory cell shortening while SEL-5 expression from the muscle specific *hlh-1* promoter had no effect on the excretory cell phenotype of the *sel-5 vps-29* double mutants. As in the case of QL.d migration defect, the excretory canal length was efficiently rescued also by the SEL-5D178A variant expressed from *pdp-12* promoter arguing that SEL-5 kinase activity is not required for canal extension (Fig. 4G). Expression of VPS-29 in the excretory cell partially rescued the canal shortening suggesting that SEL-5 and the retromer complex act together within the same cell to regulate canal length. Interestingly, expression of SEL-5 from *col-10* promoter which is active in hypodermis (Spencer et al., 2001) also resulted in a significant rescue of the excretory canal shortening. This suggests that SEL-5 activity in both the excretory cell and in the hypodermis contribute to the regulation of the canal outgrowth. To support our finding that SEL-5 role in excretory canal outgrowth is independent of its kinase activity, we analysed posterior canal length in *dpy-23(mew25)* mutant animals. No canal shortening was observed in animals carrying *dpy-23(mew25)* alone (Fig. 4H), while very mild shortening was occasionally observed in either *sel-5; dpy-23(mew25)* or *vps-29; dpy-23(mew25)*. These observations are consistent with a role of SEL-5 other than DPY-23 phosphorylation at T160.

### **LIN-44/Wnt-dependent signalling is required to terminate excretory cell canal outgrowth**

We were interested whether the observed shortening of the excretory canals in *sel-5 vps-29* mutants could be a consequence of a crosstalk with the Wnt signalling as in the case of QL.d migration. There is some evidence that Wnt pathway components are involved in canal extension regulation. Firstly, *lin-17/Frizzled* mutants have been reported to show an overgrowth of the posterior excretory cell canals past the rectum into the tip of the tail (Hedgecock et al., 1987). Secondly, loss of *axl-1*, one of the two *C. elegans* Axin orthologues,

resulted in ectopic branching of the posterior excretory canal but no effect on the canal length was observed. The ectopic branching in *axl-1* mutants could be rescued by simultaneous loss of *bar-1*/ $\beta$ -catenin or *pop-1*/Tcf expression (Oosterveen et al., 2007). Wnt signalling thus seems to play a role in excretory canal growth, but so far, the other Wnt pathway components and their mechanism of action remained unknown. We therefore decided to test whether mutations in other Wnt pathway components could affect excretory cell growth. Among the four Wnts tested (EGL-20, LIN-44, CWN-1, CWN-2), only mutants in *lin-44*/Wnt exhibited almost fully penetrant posterior excretory canal overgrowth phenotype, as observed in *lin-17*/Frizzled mutants (Fig. 5A, B). Mild canal shortening was observed in *cwn-2*/Wnt and *cfz-2*/Frizzled mutants, while very weak overgrowth phenotype could be detected in *egl-20*/Wnt mutants (Fig. 5B). No change in excretory canal length was displayed by *cwn-1*/Wnt or *mig-1*/Frizzled mutants. Interestingly, highly penetrant canal overgrowth was also observed in *mig-14*/Wls mutants, while loss of *mig-5*/Dishevelled or *dsh-1*/Dishevelled resulted in partially penetrant overgrowth phenotype (Fig. 5B). We next tested various combinations of Wnt and Frizzled mutants and found out that simultaneous loss of *lin-44* and *cwn-1* or *lin-44* and *cwn-2* expression resulted in partial rescue of the canal overgrowth, same effect was observed after simultaneous loss of *lin-17* and *cfz-2*. These data suggest that there are at least two Wnt-dependent pathways acting during the extension of the excretory canal; one involving *lin-44*, *lin-17*, *dsh-1* and *mig-5* that is responsible for determining the stopping point for the growing canal, and one involving *cwn-1*, *cwn-2* and *cfz-2* that contributes to the canal growth.

The most striking phenotype is the overgrowth of the posterior excretory canal in *lin-17*, *lin-44* and *mig-14* mutants. Interestingly when we measured the length of the excretory canal within the 24-hour interval after hatching, no difference in canal length was detected between wild type controls and *lin-17*, *lin-44* and *mig-14* mutants (Fig. 5C). This suggests that the

initial growth is not affected in the mutants but rather that these mutants miss a signal determining the final position of the canal in later larval stages. Simultaneous loss of *lin-17* and *sel-5* led to a partial rescue of the *lin-17* phenotype (Fig. 5B). Similar effect was observed in *lin-44; sel-5* double mutants (Fig. 5B). Analysis of a *lin-17; sel-5 vps-29* triple mutant was not possible as such combination was lethal. These data indicate that *sel-5* is required for the initial growth of the excretory canals and the LIN-44/Wnt signal acting through LIN-17/Frizzled receptor is required at a later stage to terminate excretory canal extension.

### **SEL-5 and VPS-29 genetically interact with MIG-10/Lamellipodin to control excretory canal outgrowth**

So far, the most studied pathway regulating excretory canal outgrowth is the one involving UNC-53, the orthologue of mammalian Neuron Navigator 2 (Nav2), ABI-1 (Abelson-interactor protein-1) (Hedgecock et al., 1987; Stringham et al., 2002; Schmidt et al., 2009) and the Lamellipodin orthologue MIG-10 (Manser and Wood, 1990; Manser et al., 1997). All three proteins act in the same pathway for excretory canal outgrowth, possibly by affecting the cytoskeleton (McShea et al., 2013). However, it is not yet known from which membrane receptor and outside cue these proteins receive the guidance signal (Marcus-Gueret et al., 2012). To understand the relationship between *sel-5* and *vps-29* and the UNC-53/ABI-1/MIG-10 pathway we decided to analyse their genetic interaction. We chose *mig-10(ct41)* allele for testing as it displays the strongest excretory canal shortening phenotype and is predicted to act early in the pathway (McShea et al., 2013). In *sel-5 mig-10* and *mig-10 vps-29* animals we did not observe any enhancement of the posterior canal shortening compared to *mig-10* single mutants (Fig. 6A). Triple *sel-5 mig-10 vps-29* mutants were not viable. To overcome this obstacle, we performed RNAi against *vps-29* or *vps-35* in *sel-5 mig-10* double mutants. Both RNAi treatments resulted in more severe truncation of the posterior canals compared to the

controls. In *vps-35* RNAi treated animals 76% of the posterior canals did not initiate their extension at all (Fig. 6A,B). These findings suggest that SEL-5 and the retromer could act in parallel with MIG-10 to control excretory canal extension.

Taken together, our findings demonstrate that the length of the excretory cell canals is coordinated by several mechanisms, summarized in a model in Fig. 6C. First, the active outgrowth of the posterior canals is simultaneously controlled by *sel-5*, retromer and the *mig-10* pathway, possibly with a minor contribution from *cwn-1*, *cwn-2* and *cfz-2*. After reaching the proper length, further canal extension is inhibited by signalling through *lin-44* and *lin-17*. The exact wiring and crosstalk among these players in defining excretory canal length will require further investigation.

## Discussion

The NAK family kinase AAK1 has recently been added to the long list of Wnt signalling regulators (Agajanian et al., 2019), acting at the level of LRP6 endocytosis. In the present study we probed the role of *C. elegans* AAK1 orthologue SEL-5 in Wnt signalling and we uncovered its requirement for Wnt dependent QL neuroblast daughter cell migration. Furthermore, we also unveiled that SEL-5 is required during the outgrowth of the excretory canal cell prior to a Wnt dependent stop signal. Importantly, in both instances the role of SEL-5 is independent of its kinase activity, defining an alternative mode of action for this kinase.

The role of SEL-5 has not been extensively studied in *C. elegans*, the only available reports uncovered the role of *sel-5* as a genetic suppressor of a constitutively active *lin-12*/Notch mutation (Tax et al., 1997; Fares and Greenwald, 1999). Information about the protein function was missing. SEL-5 shows the highest similarity to the mammalian Numb-associated kinase family members AAK1 and BMP2K (Shaye and Greenwald 2011; Sorrell et al., 2016; Kim et al., 2018). Both AAK1 and BMP2K were shown to phosphorylate the  $\mu 2$  subunit of

the AP2 adaptor at position T156 and thus regulate the clathrin-mediated endocytosis (Conner and Schmid, 2002; Ricotta et al., 2002; Ramesh et al., 2021). Our findings uncovered some similarities between SEL-5 and AAK1 or BMP2K. Firstly, we show that the level of DPY-23/AP2M1 phosphorylation in *sel-5* mutants is decreased compared to controls. Secondly, the subcellular localization of SEL-5 to punctate structures proximal to the plasma membrane in oocytes and in epidermal seam cells resembles the subcellular distribution of human AAK1 (Conner and Schmid, 2002). These data support the notion that SEL-5 has a function analogous to its mammalian counterparts.

Given the established role of AAK1 in mammalian endocytosis regulation (Kadlecova et al., 2017; Agajanian et al., 2019; Wrobel et al., 2019), it was striking to see that loss of *sel-5* expression alone had no obvious developmental consequences. However, even in mammalian cells complete loss of AP2M1 T156 phosphorylation does not result in endocytosis block but only in a reduction of its efficiency (Motley et al., 2006; Wrobel et al., 2019). In cells expressing only an AP2M1T156A mutant protein the endocytosis of transferrin receptor was reduced by only 30% (Wrobel et al., 2019). We did not observe complete loss but only a partial reduction of DPY-23 phosphorylation in *sel-5* mutants. This implies that SEL-5 is not the only kinase responsible for DPY-23 phosphorylation. It also suggests that endocytosis is not inhibited but could be only partially compromised. In such case the level of ongoing endocytosis might be sufficient to support proper developmental decisions such as the direction of Q neuroblast migration. We argued that in combination with an additional insult to the intracellular trafficking machinery, in this case the retromer complex, the suboptimal function of endocytosis would manifest itself. Indeed, *sel-5 vps-29* double mutants display two highly penetrant phenotypes – the QL.d migration defect and the shortening of the excretory cell canals. Strikingly, neither of these phenotypes can be attributed to a decrease in endocytic efficiency due to lack of DPY-23 phosphorylation. Firstly, both phenotypes can be

rescued by a tissue-specific expression of a kinase-inactive SEL-5 mutant protein. Secondly, *vps-29*; *dpy-23(mew25)* mutants expressing only non-phosphorylatable DPY-23 do not phenocopy *sel-5 vps-29* mutants. The independence of the SEL-5 function on its kinase activity is the most striking finding of this work and to our knowledge there is no precedence for that in the mammalian AAK1 literature. Alternative mechanisms of SEL-5 function thus have to be considered. It is possible that either SEL-5 affects endocytosis by a mechanism not dependent on DPY-23 phosphorylation or that SEL-5 regulates QL.d migration and excretory cell canal extension by endocytosis-independent mechanisms. In favour of the second possibility is our finding that localization or degradation of MIG-14/Wls, the most obvious endocytic cargo candidate for QL.d migration, does not change when comparison is made between *vps-29* and *sel-5 vps-29* mutants. However, the effect of SEL-5 on a different endocytic cargo cannot be excluded. For example, EGL-20/Wnt itself could be endocytosed and SEL-5 thus could be one of the factors shaping Wnt gradient. This notion is supported by our finding that expression in both EGL-20-producing cells and in the surrounding muscle cells is necessary to fully rescue the QL migration phenotype, although so far little is known about possible EGL-20 endocytic recycling by the producing cells. In case of excretory canal extension, the putative endocytic cargo is less evident. SEL-5 could possibly regulate the turnover of guidance receptors at the plasma membrane of the growing tip of the canal. In *Drosophila*, loss of Numb-associated kinase (Nak) results in the absence or shortening of higher order dendrites and Nak has been shown to promote endocytosis of Neuroglian/L1-CAM during dendrite extension and branching (Yang et al., 2011). In *C. elegans* excretory cell, PAT-3/ $\beta$ 1-integrin is required for canal outgrowth (Hedgecock et al., 1987). Integrins constantly cycle between the plasma membrane and intracellular compartments using various trafficking routes (Moreno-Layseca et al., 2019). Interestingly, a retromer-dependent retrograde trafficking route of unliganded  $\beta$ 1-integrin has been described in persistently

migrating mammalian cells (Shafaq-Zadah et al., 2015). This pathway may serve to replenish the integrin pool at the leading edge of the migrating cell. Same study also pointed out the similarity in gonad migration defects caused by depletion of *vps-35*, *ina-1/α-integrin* and *pat-3* in *C. elegans* (Lee et al., 2001; Shafaq-Zadah et al., 2015), suggesting that such retrograde integrin trafficking pathway may not be restricted to mammalian cells. The canal shortening phenotype is only observed after simultaneous loss of both *sel-5* and *vps-29*, which suggests that SEL-5 and the retromer act in parallel. For example, SEL-5 could stimulate integrin endocytosis at the tip of the growing canal while retromer could secure the delivery of new integrin molecules to the growing tip.

Possible mechanism how SEL-5 could affect endocytosis independently of DPY-23 phosphorylation follows from the finding, that SEL-5 physically interacted with REPS-1 protein in a yeast-two-hybrid assay (Tsushima et al., 2013). REPS-1 is an orthologue of mammalian REPS1 (RALBP1-associated Eps Domain-containing 1), an Eps homology containing protein known to interact with RALBP1 (RalA-binding protein 1) (Yamaguchi et al., 1997). RALBP1 is an effector of Ral GTPase that can interact with the  $\mu$ 2 subunit of AP2 and regulate endocytosis (Jullien-Flores et al., 2000). Importantly, human AAK1 interacted with both RALBP1 and REPS1 in several high-throughput mass spectrometry analyses (Huttlin et al., 2017; Huttlin et al., 2021; Cho et al., 2022; Golkowski et al., 2023). SEL-5 thus could possibly regulate AP2 complex indirectly via interaction with the REPS1-RALBP1 complex.

Searching for possible endocytosis-independent mechanism of SEL-5 activity is complicated by the fact that while in the case of QL.d migration SEL-5 function is cell-nonautonomous, cell-autonomous expression of SEL-5 is sufficient to rescue the *sel-5 vps-29* excretory canal extension defect. This suggests that more than one mechanism might exist. One possibility common for both phenotypes comes from recent studies in mammalian cells. BMP2K has

been shown to localize to the early secretory compartment and to regulate COPII coat assemblies (Cendrowski et al., 2020). SEL-5 thus could possibly affect Wnt secretion in case of QL.d migration or new guidance receptor delivery to the plasma membrane in case of the excretory canals. Interestingly, REPS1 and RALBP1 were recently implicated also in regulation of exocytosis and knock-down of either of them reduced neurite outgrowth in cultured neuronal cells (Wang et al., 2023). SEL-5 interaction with REPS-1 thus could be the key to the mechanism of SEL-5 action. Our data so far cannot discriminate among the above outlined possibilities and more experiments will be required to establish how SEL-5 exerts its function. The biggest question to answer will be how it does so independently of its kinase activity.

Apart from the role of SEL-5 and the retromer complex in excretory cell canal extension, we have also uncovered a significant contribution of Wnt pathway components in defining excretory canal length. The role of Wnt signalling in the outgrowth of the excretory canals has been suggested (Sundaram and Buechner, 2016), however the only evidence came from the early observation that canals overgrow in *lin-17* mutants (Hedgecock et al., 1987) and that erroneous canal branching is observed in *axl-1*/Axin-like mutants (Oosterveen et al., 2007). More recently, it has been shown that loss of PLR-1, a transmembrane E3 ubiquitin ligase, results in excretory canal shortening (Bhatt et al., 2015). PLR-1 is responsible for internalization of Frizzled receptors from the cell surface (Moffat et al., 2014). However, direct link between PLR-1 function in the excretory cell and Wnt signalling has not been established. Our analysis of single and double Wnt mutants revealed that no single or double combination tested results in pronounced shortening of the excretory canals. This suggests that Wnts do not act as major attractive cues for excretory cell outgrowth. However, it cannot be excluded that several Wnts act redundantly and only simultaneous loss of more than two Wnts would be necessary to observe canal shortening. Interestingly, excretory canals in *lin-44*



mutants grew past the normal stopping point at the level of the rectum, similar to the canals in *lin-17* mutants. LIN-44 together with its receptor LIN-17 thus seems to act as a repulsive or stop signal defining the final position of the tip of the canal. Similar role of LIN-44/LIN-17 complex has been described in case of a posterior axon of *C. elegans* GABAergic DD6 motor neuron (Maro et al., 2009). In this instance EGL-20 acts also as a repellent as simultaneous loss of *lin-44* and *egl-20* expression results in more severe posterior overgrowth of the axon. In case of the excretory canal LIN-44 is the sole repelling cue. LIN-44 has also been suggested to act as a repellent in case of several tail neurons including the PLM touch receptor neuron, ALN and PLN neurons (Zheng et al., 2015). Loss of *lin-44* or *lin-17* expression promoted outgrowth of the posterior neurites of these bipolar neurons implicating that in wild type animals LIN-44 serves as a repulsive cue.

Taken together, we have uncovered cooperation between *C. elegans* orthologue of AAK1 kinase, SEL-5, and the retromer complex in regulating cell migration and cell outgrowth, and we have also outlined the engagement of Wnt pathway components in defining the length of the excretory cell canals. The surprising independence of SEL-5 function on its kinase activity opens a new path for investigation with high relevance also for mammalian biology. AAK1 has been proposed as a potential drug target for treating various neurological disorders and preventing viral entry, where the kinase activity is the target for inhibition (Martinez-Gualda et al., 2021; Xin et al., 2023). In light of our findings, the non-enzymatic activities of AAK1 should also be taken into account.

## Materials and methods

### *Caenorhabditis elegans* strains and culture

Standard methods of cultivation, manipulation and genetics of *C. elegans* were used as described previously (Brenner 1974). Bristol N2 strain was used as wild type. Other strains, extrachromosomal and integrated arrays used in this study:

LGI: *pry-1(mu38)* (Malooof et al, 1999), *lin-17(n671)* (Brenner 1974), *lin-44(n1792)* (Herman and Horvitz, 1994), *mig-1(e1787)* (Brenner 1974)

LGII: *cwn-1(ok546)*, *dsh-1(ok1445)*, *mig-14(mu71)* (Harris et al., 1996), *muIs32* [*Pmec-7::gfp*; *lin-15(+)*] (Ch'ng et al, 2003), *huSi2* [*Pmig-14::mig-14::gfp*], *mig-5(cp385[mNG-GLO^AID::mig-5])* (Heppert et al., 2018)

LGIII: *sel-5(ok363)*, *sel-5(ok149)*, *vps-29(tm1320)*, *sIs10089* (McKay et al., 2003)

LGIV: *egl-20(n585)* (Harris et al., 1996), *cwn-2(ok895)*

LGV: *muIs35* [*Pmec-7::gfp*; *lin-15(+)*] (Ch'ng et al, 2003), *cfz-2(ok1201)*

LGX: *dpy-23(mew25)*(G. Hollopeter and G. Beacham, unpublished), *kyIs4* [*Pceh-23::unc-76::gfp* + *lin-15(+)*] (Zallen et al., 1999)

### Molecular biology, germline transformation and RNA interference

Total RNA was isolated using the TRIzol<sup>TM</sup> reagent (cat.# 15596026, ThermoFisher Scientific) from a mixed stage population of *C. elegans* N2 strain collected from a single 9 cm NGM plate. cDNA was transcribed from total RNA using SuperScript<sup>TM</sup> III Reverse Transcriptase (cat.# 18080093, ThermoFisher Scientific) and an oligo(dT) primer. Full-length *sel-5* (isoform a), *vps-29* (isoform a) or *dpy-23* (isoform b) cDNA was PCR-amplified using gene-specific primers. PCR products were cloned into pJet1.2/blunt vector (cat.# K1232, ThermoFisher Scientific) and sequenced. Same procedure was applied to clone truncated *sel-5* cDNA from *sel-5(ok363)* and *sel-5(ok149)* mutant animals. Two- or three-fragment Gibson

assembly (Gibson et al., 2009) was employed to construct tissue-specific gene expression vectors. For that, 524 bp of *col-10* promoter sequence, 600 bp of *eft-3* promoter sequence, 4419 bp of *egl-20* promoter sequence, 2896 bp of *hlh-1* promoter sequence, 3410 bp of *pgp-12* promoter sequence and 1629 bp of *wrt-2* promoter sequence were PCR-amplified from N2 genomic DNA, cDNAs were amplified from the corresponding pJet1.2 vectors and pPD95.81 (a gift from Andrew Fire (Addgene plasmid # 1497 ; <http://n2t.net/addgene:1497> ; RRID:Addgene\_1497)) was a source of backbone and GFP sequences. Fragments were assembled in the desired combinations and correct assembly was verified by sequencing. SEL-5 was tagged with GFP at its N-terminus, VPS-29 and DPY-23 were tagged at their C-termini. Point mutations were introduced into *sel-5* and *dpy-23* sequences using the QuikChange Site-directed Mutagenesis kit (Agilent). Transcriptional reporter *Ppgp-12::gfp* was created by inserting 3410 bp of *pgp-12* promoter upstream of GFP in pPD95.81. To create extrachromosomal arrays constructs were microinjected into distal gonads of young adults using inverted microscope Leica DMI8 equipped with DIC filters and microinjection system InjectMan® 4 and FemtoJet® 4i (Eppendorf). Microinjection mixtures contained 10 ng/μL of the plasmid of interest, 5 ng/μL *Pmyo-2::tdTomato* as a co-injection marker and 135 ng/μL pBluescript as a carrier DNA.

CRISPR/Cas9 SEC knock-in method (Dickinson et al., 2015) was used to generate GFP tagged endogenous *sel-5* locus and performed virtually as described (Dickinson et al., 2015 and <http://wormcas9hr.weebly.com/protocols.html>). 647 bp upstream of *sel-5* ATG (5' homology arm) and 558 bp *sel-5* genomic sequence starting from ATG (3' homology arm) were PCR-amplified from N2 genomic DNA with primers harbouring overhangs for Gibson assembly with the pDD282 vector (Dickinson et al., 2013) (a gift from Bob Goldstein (Addgene plasmid # 66823; <http://n2t.net/addgene:66823>; RRID:Addgene\_66823)) and assembled with pDD282 digested with ClaI and SpeI. Sequence

GCTGAAAAGCCCTAGAGGCA was inserted into pDD162 vector for sgRNA expression (Dickonson et al., 2013) (pDD162 was a gift from Bob Goldstein (Addgene plasmid # 47549; <http://n2t.net/addgene:47549> ; RRID:Addgene\_47549)). Injection was performed as described above, injection mix contained 10 ng/μl pDD282 with homology arms, 50 ng/μl pDD162 with corresponding sgRNA sequence, 5 ng/μl *Pmyo-2::tdTomato*. Line expressing *Psel-5::gfp* was first established, several L1 animals were then exposed to a heat shock for 4 hours at 34°C to excise the selection SEC cassette and create a *Psel-5::gfp::sel-5* knock-in line.

RNA interference experiments were conducted by feeding using bacterial strains from the Ahringer library (Kamath et al. 2003). L4 larvae were transferred to RNAi plates with the desired bacterial clones and the effect of RNAi was assessed in the next generation after 3-4 days at 20°C.

### **Protein isolation and Western blotting**

For MIG-14::GFP detection, gravid hermaphrodites were subjected to hypochlorite treatment and released embryos were left to hatch overnight in M9 buffer. Larvae were collected and washed twice in M9 buffer. Pelleted larvae were then resuspended in TX-114 buffer (25 mM Tris-HCl pH 7.5, 150 mM NaCl, 0.5 mM CaCl<sub>2</sub>, 1% TX-114 and cOmplete® protease inhibitors (Roche)), snap frozen and then ground in liquid nitrogen. Thawed lysates were centrifuged at 20,800 g for 30 minutes at 4°C, mixed with Laemmli sample buffer, separated on 8% SDS-PAGE and transferred onto Amersham™ Protran® Premium Western blotting nitrocellulose membrane. GFP was detected with monoclonal anti-GFP antibody (cat.# 11814460001, Roche) and equal loading was assessed by staining with monoclonal anti  $\alpha$ -tubulin antibody (cat. # T9026, Sigma Aldrich). Secondary goat anti-mouse HRP-conjugated antibody (cat.# 115-035-146, Jackson Immuno-Research Laboratories) and WesternBright ECL HRP substrate (Advansta) were used to visualize the signal. Images of membranes were

taken on ImageQuant (LAS4000) and Fiji Gels plug-in was used for subsequent densitometric analysis. For endogenous phosphorylated DPY-23 and DPY-23::GFP detection, 200 L4 larvae or young adults positive for DPY-23::GFP were collected into M9 buffer for each analysed strain. Animals were washed once with M9 buffer and two times with M9 buffer with 0,001% Triton X-100. 33  $\mu$ L of animal pellet in M9/0.001% Triton X-100 was mixed with 33  $\mu$ L of 4X Laemmli buffer, 4  $\mu$ L of 20x PhosStop® phosphatase inhibitors (Roche), 4  $\mu$ L of 20x cOmplete® protease inhibitors (Roche) and 1,6  $\mu$ L of 1 M DTT. Samples were snap frozen in liquid nitrogen, thawed on ice, and sonicated with 2x 10 pulses at 0.8 amplitude, 0.85 duty cycle with UP50H ultrasound processor (Hielscher). Samples were heated to 99 °C for 5 minutes and centrifuged at 20,000 g for 10 minutes. 20  $\mu$ L of each sample were loaded on 9% SDS-PAGE, separated and further processed as above using anti-GFP and anti-phosphoAP2M1 (cat. # ab109397, Abcam) antibodies.

### ***Caenorhabditis elegans* phenotypes, microscopy and statistical analyses**

Final position of QL.paa (PVM – QL.d phenotype), polarity of ALM and PLM neurons was assessed in L4 larvae carrying transgene *muIs32* or *muIs35*. PVM migration was scored as defective when PVM was located anteriorly to the posterior edge of the vulva. ALM polarity was scored as defective when bipolar or reversed neurites were observed. CAN neurons were visualized with *kyIs4* transgene and their position relative to V3 seam cell was scored. CAN positioned anterior to V3 was scored as displaced. For DiI staining, L3-L4 well-fed animals were washed from a plate with M9 buffer and incubated for three hours in 10  $\mu$ g/ml DiI solution (D282, ThermoFisher Scientific, dissolved to 2 mg/ml stock solution in dimethylformamide). Animals were then washed three times in M9 buffer and directly observed. Excretory cell canals lengths were scored in L4 or young adult animals carrying integrated *Ppgp-12::gfp* transgene (*sIs10089*) or *Ppgp-12::gfp* expressed from an

extrachromosomal array (*mamEx11* or *mamEx29*). Posterior canals were scored as wild type when they reached region between the inner edge of posterior gonadal turn and the rectum. Shortened canal phenotype was graded according to the region within worm body the canal reached and following landmarks were used for each category: 0 – excretory canal missing entirely or reaching the inner edge of anterior gonadal turn, 1 – canal reaching anterior spermatheca, 2 – canal reaching vulva, 3 – canal reaching posterior spermatheca, 4 – canal reaching inner edge of posterior gonadal turn, 5 – canal reaching rectum (wild type). Canals which overgrew the rectum and reached the tail tip were scored as 6. Anterior excretory cell canals were measured and their length normalized to measured distance between the posterior edge of the pharynx and the nose tip. Larval excretory cell posterior canals were measured at four developmental stages (hatch, 4, 8 and 24 h after hatching) and normalized to animal body length. For microscopy imaging worms were anaesthetised either with 10 mM sodium azide or 1 mM levamisole and mounted on 3% agarose pads. Images were taken on inverted microscope Leica DM6. For confocal imaging Zeiss LSM880 confocal microscope was used. Images were processed with Fiji image processing package (Schindelin et al., 2012). Statistical analyses were performed either in GraphPad Prism or in Excel equipped with the Real Statistics Resource Pack software (Release 7.6). Copyright (2013 – 2021) Charles Zaiontz, [www.real-statistics.com](http://www.real-statistics.com).

### **Acknowledgements**

We thank Gunther Hollopeter and Gwendolyn Beacham (Cornell University, USA) for sharing the *apm-2(mew25)* allele. We thank Jan Mašek and Teije C. Middelkoop for critically reading the manuscript. Some strains were provided by the Caenorhabditis Genetics Center (CGC) which is supported by the National Institutes of Health - Office of Research Infrastructure Programs (P40 OD010440). This work was funded by Charles University Grant



Agency grant 1446218/2018 to F.K. and by Charles University programme SVV 260559. Microscopy was performed in the Vinicna Microscopy Core Facility co-financed by the Czech-BioImaging large RI project LM2023050. Computational resources were supplied by the project "e-Infrastruktura CZ" (e-INFRA LM2018140) provided within the program Projects of Large Research, Development and Innovations Infrastructures

## References

- Ackley, B. D. (2014). Wnt-signaling and planar cell polarity genes regulate axon guidance along the anteroposterior axis in *C. elegans*. *Developmental Neurobiology*, *74*(8), 781–796. <https://doi.org/10.1002/dneu.22146>
- Agajanian, M. J., Walker, M. P., Axtman, A. D., Ruela-de-Sousa, R. R., Serafin, D. S., Rabinowitz, A. D., Graham, D. M., Ryan, M. B., Tamir, T., Nakamichi, Y., Zuercher, W. J., & Major, M. B. (2019). WNT Activates the AAK1 Kinase to Promote Clathrin-Mediated Endocytosis of LRP6 and Establish a Negative Feedback Loop. *Cell Reports*, *26*(1), 79-93.e8. <https://doi.org/10.1016/j.celrep.2018.12.023>
- Albrecht, L. V., Tejada-Muñoz, N., & de Robertis, E. M. (2021). Cell Biology of Canonical Wnt Signaling. In *Annual Review of Cell and Developmental Biology* (Vol. 37). <https://doi.org/10.1146/annurev-cellbio-120319-023657>
- Aspöck, G., Kagoshima, H., Niklaus, G., & Bürglin, T. R. (1999). *Caenorhabditis elegans* has scores of hedgehog-related genes: Sequence and expression analysis. *Genome Research*, *9*(10), 909–923. <https://doi.org/10.1101/gr.9.10.909>
- Bänziger, C., Soldini, D., Schütt, C., Zipperlen, P., Hausmann, G., & Basler, K. (2006). Wntless, a Conserved Membrane Protein Dedicated to the Secretion of Wnt Proteins from Signaling Cells. *Cell*, *125*(3), 509–522. <https://doi.org/10.1016/j.cell.2006.02.049>
- Bartscherer, K., Pelte, N., Ingelfinger, D., & Boutros, M. (2006). Secretion of Wnt Ligands Requires Evi, a Conserved Transmembrane Protein. *Cell*, *125*(3), 523–533. <https://doi.org/10.1016/j.cell.2006.04.009>
- Belenkaya, T. Y., Wu, Y., Tang, X., Zhou, B., Cheng, L., Sharma, Y. V., Yan, D., Selva, E. M., & Lin, X. (2008). The Retromer Complex Influences Wnt Secretion by Recycling Wntless from Endosomes to the Trans-Golgi Network. *Developmental Cell*, *14*(1), 120–131. <https://doi.org/10.1016/j.devcel.2007.12.003>
- Bhat, J. M., Pan, J., & Hutter, H. (2015). PLR-1, a putative E3 ubiquitin ligase, controls cell polarity and axonal extensions in *C. elegans*. *Developmental Biology*, *398*(1), 44–56. <https://doi.org/10.1016/j.ydbio.2014.11.008>
- Brenner, S. (1974). The genetics of *Caenorhabditis elegans*. *Genetics*, *77*(1), 71-94. <https://doi.org/10.1093/genetics/77.1.71>

- Buechner, M., Hall, D. H., Bhatt, H., & Hedgecock, E. M. (1999). Cystic canal mutants in *Caenorhabditis elegans* are defective in the apical membrane domain of the renal (excretory) cell. *Developmental Biology*, *214*(1), 227–241. <https://doi.org/10.1006/dbio.1999.9398>
- Cendrowski, J., Kaczmarek, M., Mazur, M., Kuzmicz-Kowalska, K., Jastrzebski, K., Brewinska-Olchowik, M., Kominek, A., Piwocka, K., & Miaczynska, M. (2020). Splicing variation of *bmp2k* balances abundance of *copii* assemblies and autophagic degradation in erythroid cells. *ELife*, *9*, 1–26. <https://doi.org/10.7554/ELIFE.58504>
- Ch'ng, Q., Williams, L., Lie, Y. S., Sym, M., Whangbo, J., & Kenyon, C. (2003). Identification of genes that regulate a left-right asymmetric neuronal migration in *Caenorhabditis elegans*. *Genetics*, *164*(4), 1355–1367. <https://doi.org/10.1093/genetics/164.4.1355>
- Cho, N. H., Cheveralls, K. C., Brunner, A. D., Kim, K., Michaelis, A. C., Raghavan, P., Kobayashi, H., Savy, L., Li, J. Y., Canaj, H., Kim, J.Y.S., Stewart, E. M., Gnann, C., McCarthy, F., Cabrera, J. P., Brunetti, R. M., Chhun, B. B., Dingle, G., Hein, M.Y., Huang, B., Mehta, S. B., Weissman, J. S., Gómez-Sjöberg, R., Itzha, D. N., Royer, L. A., Mann, M., & Leonetti, M. D. (2022). OpenCell: Endogenous tagging for the cartography of human cellular organization. *Science*, *375*(6585):eabi6983. <https://doi.org/10.1126/science.abi6983>
- Colozza, G., & Koo, B.-K. (2021). Ub and Dub of RNF43/ZNRF3 in the WNT signalling pathway. *EMBO Reports*, *22*(5). <https://doi.org/10.15252/embr.202152970>
- Conner, S. D., & Schmid, S. L. (2002). Identification of an adaptor-associated kinase, AAK1, as a regulator of clathrin-mediated endocytosis. *Journal of Cell Biology*, *156*(5), 921–929. <https://doi.org/10.1083/jcb.200108123>
- Coudreuse, D. Y. M., Roël, G., Betist, M. C., Destrée, O., & Korswagen, H. C. (2006). Wnt gradient formation requires retromer function in Wnt-producing cells. *Science*, *312*(5775), 921–924. <https://doi.org/10.1126/science.1124856>
- Dickinson, D. J., Ward, J. D., Reiner, D. J., & Goldstein, B. (2013). Engineering the *Caenorhabditis elegans* genome using Cas9-triggered homologous recombination. *Nature Methods*, *10*(10), 1028–1034. <https://doi.org/10.1038/nmeth.2641>
- Dickinson, D. J., Pani, A. M., Heppert, J. K., Higgins, C. D., & Goldstein, B. (2015). Streamlined genome engineering with a self-excising drug selection cassette. *Genetics*, *200*(4), 1035–1049. <https://doi.org/10.1534/genetics.115.178335>
- Fares, H., & Greenwald, I. (1999). SEL-5, a serine/threonine kinase that facilitates *lin-12* activity in *Caenorhabditis elegans*. *Genetics*, *153*(4), 1641–1654. <https://doi.org/10.1093/genetics/153.4.1641>
- Franch-Marro, X., Wendler, F., Guidato, S., Griffith, J., Baena-Lopez, A., Itasaki, N., Maurice, M. M., & Vincent, J.-P. (2008). Wingless secretion requires endosome-to-Golgi retrieval of Wntless/Evi/ Sprinter by the retromer complex. *Nature Cell Biology*, *10*(2), 170–177. <https://doi.org/10.1038/ncb1678>
- Fujita, M., Hawkinson, D., King, K. V., Hall, D. H., Sakamoto, H., & Buechner, M. (2003). The role of the ELAV homologue EXC-7 in the development of the *Caenorhabditis elegans* excretory canals. *Developmental Biology*, *256*(2), 290–301. [https://doi.org/10.1016/S0012-1606\(03\)00040-X](https://doi.org/10.1016/S0012-1606(03)00040-X)
- Gibson, D. G., Young, L., Chuang, R.-Y., Venter, J. C., Hutchison, C. A., & Smith, H. O. (2009). Enzymatic assembly of DNA molecules up to several hundred kilobases. *Nature Methods*, *6*(5), 343–345. <https://doi.org/10.1038/nmeth.1318>

- Golkowski, M., Lius, A., Sapre, T., Lau, H. T., Moreno, T., Maly, D.J., & Ong, S. E. (2023). Multiplexed kinase interactome profiling quantifies cellular network activity and plasticity. *Molecular Cell*, 83(5), 803–818.e8. <https://doi.org/10.1016/j.molcel.2023.01.015>
- Goodman, R. M., Thombre, S., Firtina, Z., Gray, D., Betts, D., Roebuck, J., Spana, E. P., & Selva, E. M. (2006). Sprinter: A novel transmembrane protein required for Wg secretion and signaling. *Development*, 133(24), 4901–4911. <https://doi.org/10.1242/dev.02674>
- Groenendyk, J., & Michalak, M. (2011). A Genome-Wide siRNA Screen Identifies Novel Phosphoenzymes Affecting Wnt/ $\beta$ -Catenin Signaling in Mouse Embryonic Stem Cells. *Stem Cell Reviews and Reports*, 7(4), 910–926. <https://doi.org/10.1007/s12015-011-9265-3>
- Gupta-Rossi, N., Ortica, S., Meas-Yedid, V., Heuss, S., Moretti, J., Olivo-Marin, J.-C., & Israël, A. (2011). The adaptor-associated kinase 1, AAK1, is a positive regulator of the notch pathway. *Journal of Biological Chemistry*, 286(21), 18720–18730. <https://doi.org/10.1074/jbc.M110.190769>
- Harfe, B. D., Branda, C. S., Krause, M., Stern, M. J., & Fire, A. (1998). MyoD and the specification of muscle and non-muscle fates during postembryonic development of the *C. elegans* mesoderm. *Development*, 125(13), 2479–2488. <https://doi.org/10.1242/dev.125.13.2479>
- Harris, J., Honigberg, L., Robinson, N., & Kenyon, C. (1996). Neuronal cell migration in *C. elegans*: Regulation of Hox gene expression and cell position. *Development*, 122(10), 3117–3131. <https://doi.org/10.1242/dev.122.10.3117>
- Harterink, M., Kim, D. H., Middelkoop, T. C., Doan, T. D., van Oudenaarden, A., & Korswagen, H. C. (2011). Neuroblast migration along the anteroposterior axis of *C. elegans* is controlled by opposing gradients of Wnts and a secreted Frizzled-related protein. *Development*, 138(14), 2915–2924. <https://doi.org/10.1242/dev.064733>
- Hedgecock, E. M., Culotti, J. G., Hall, D. H., & Stern, B. D. (1987). Genetics of cell and axon migrations in *Caenorhabditis elegans*. *Development*, 100(3), 365–382. <https://doi.org/10.1242/dev.100.3.365>
- Heppert, J. K., Pani, A. M., Roberts, A. M., Dickinson, D. J., & Goldstein, B. (2018). A CRISPR tagging-based screen reveals localized players in wnt-directed asymmetric cell division. *Genetics*, 208(3), 1147–1164. <https://doi.org/10.1534/genetics.117.300487>
- Herman, M. A., & Robert Horvitz, H. (1994). The *Caenorhabditis elegans* gene *lin-44* controls the polarity of asymmetric cell divisions. *Development*, 120(5), 1035–1047. <https://doi.org/10.1242/dev.120.5.1035>
- Herman, M. A., Vassilieva, L. L., Horvitz, H. R., Shaw, J. E., & Herman, R. K. (1995). The *C. elegans* gene *lin-44*, which controls the polarity of certain asymmetric cell divisions, encodes a Wnt protein and acts cell nonautonomously. *Cell*, 83(1), 101–110. [https://doi.org/10.1016/0092-8674\(95\)90238-4](https://doi.org/10.1016/0092-8674(95)90238-4)
- Hilliard, M. A., & Bargmann, C. I. (2006). Wnt signals and Frizzled activity orient anterior-posterior axon outgrowth in *C. elegans*. *Developmental Cell*, 10(3), 379–390. <https://doi.org/10.1016/j.devcel.2006.01.013>
- Hollopeter, G., Lange, J. J., Zhang, Y., Vu, T. N., Gu, M., Ailion, M., Lambie, E. J., Slaughter, B. D., Unruh, J. R., Florens, L., Florens, L., & Jorgensen, E. M. (2014). The membrane-associated proteins FCHO and SGIP are allosteric activators of the AP2 clathrin adaptor complex. *ELife*, 3. <https://doi.org/10.7554/eLife.03648>

- Hutter, H. (2019). Formation of longitudinal axon pathways in *Caenorhabditis elegans*. *Seminars in Cell and Developmental Biology*, 85, 60–70. <https://doi.org/10.1016/j.semcdb.2017.11.015>
- Huttlin, E. L., Bruckner, R. J., Navarrete-Perea, J., Cannon, J. R., Baltier, K., Gebreab, F., Gygi, M. P., Thornock, A., Zarraga, G., Tam, S., Harper, J. W., & Gygi, S. P. (2021). Dual proteome-scale networks reveal cell-specific remodeling of the human interactome. *Cell*, 184(11), 3022–3040.e28. <https://doi.org/10.1016/j.cell.2021.04.011>
- Huttlin, E. L., Bruckner, R. J., Paulo, J. A., Cannon, J. R., Ting, L., Baltier, K., Colby, G., Gebreab, F., Gygi, M. P., Parzen, H., Gygi, S. P., & Wade Harper, J. (2017). Architecture of the human interactome defines protein communities and disease networks. *Nature*, 545(7655), 505–509. <https://doi.org/10.1038/nature22366>
- Jullien-Flores, V., Mahe, Y., Mirey, G., Leprince, C., Meunier-Bisceuil, B., Sorkin, A., & Camonis, J. H. (2000). RLIP76, an effector of the GTPase Ral, interactas with the AP2 complex: Involvement of the Ral pathway in receptor endocytosis. *Journal of Cell Science*, 113(16), 2837–2844. <https://doi.org/10.1242/jcs.113.16.2837>
- Kadlecova, Z., Spielman, S. J., Loerke, D., Mohanakrishnan, A., Reed, D. K., & Schmid, S. L. (2017). Regulation of clathrin-mediated endocytosis by hierarchical allosteric activation of AP2. *Journal of Cell Biology*, 216(1), 167–179. <https://doi.org/10.1083/jcb.201608071>
- Kamath, R. S., & Ahringer, J. (2003). Genome-wide RNAi screening in *Caenorhabditis elegans*. *Methods*, 30(4), 313–321. [https://doi.org/10.1016/S1046-2023\(03\)00050-1](https://doi.org/10.1016/S1046-2023(03)00050-1)
- Kim, H., & Ronai, Z. A. (2018). Rewired Notch/p53 by Numb'ing Mdm2. *Journal of Cell Biology*, 217(2), 445–446. <https://doi.org/10.1083/jcb.201712007>
- Krause, M., Fire, A., Harrison, S. W., Priess, J., & Weintraub, H. (1990). CeMyoD accumulation defines the body wall muscle cell fate during *C. elegans* embryogenesis. *Cell*, 63(5), 907–919. [https://doi.org/10.1016/0092-8674\(90\)90494-Y](https://doi.org/10.1016/0092-8674(90)90494-Y)
- Lee, M., Cram, E. J., Shen, B., & Schwarzbauer, J. E. (2001). Roles for  $\beta$ pat-3 Integrins in Development and Function of *Caenorhabditis elegans* Muscles and Gonads. *Journal of Biological Chemistry*, 276(39), 36404–36410. <https://doi.org/10.1074/jbc.M105795200>
- Liégeois, S., Benedetto, A., Michaux, G., Belliard, G., & Labouesse, M. (2007). Genes required for osmoregulation and apical secretion in *Caenorhabditis elegans*. *Genetics*, 175(2), 709–724. <https://doi.org/10.1534/genetics.106.066035>
- Lorenowicz, M. J., Macurkova, M., Harterink, M., Middelkoop, T. C., de Groot, R., Betist, M. C., & Korswagen, H. C. (2014). Inhibition of late endosomal maturation restores Wnt secretion in *Caenorhabditis elegans* vps-29 retromer mutants. *Cellular Signalling*, 26(1), 19–31. <https://doi.org/10.1016/j.cellsig.2013.09.013>
- Maloof, J. N., Whangbo, J., Harris, J. M., Jongeward, G. D., & Kenyon, C. (1999). A Wnt signaling pathway controls Hox gene expression and neuroblast migration in *C. elegans*. *Development*, 126(1), 37–49. <https://doi.org/10.1242/dev.126.1.37>
- Manser, J., Roonprapunt, C., & Margolis, B. (1997). *C. elegans* cell migration gene mig-10 shares similarities with a family of SH2 domain proteins and acts cell nonautonomously in excretory canal development. *Developmental Biology*, 184(1), 150–164. <https://doi.org/10.1006/dbio.1997.8516>
- Manser, J., & Wood, W. B. (1990). Mutations affecting embryonic cell migrations in *Caenorhabditis elegans*. *Developmental Genetics*, 11(1), 49–64. <https://doi.org/10.1002/dvg.1020110107>

- Marcus-Gueret, N., Schmidt, K. L., & Stringham, E. G. (2012). Distinct cell guidance pathways controlled by the Rac and Rho GEF domains of UNC-73/TRIO in *Caenorhabditis elegans*. *Genetics*, *190*(1), 129–142. <https://doi.org/10.1534/genetics.111.134429>
- Maro, G. S., Klassen, M. P., & Shen, K. (2009). A  $\beta$ -catenin-dependent Wnt pathway mediates anteroposterior axon guidance in *C. elegans* motor neurons. *PLoS ONE*, *4*(3). <https://doi.org/10.1371/journal.pone.0004690>
- Martinez-Gualda, B., Graus, M., Camps, A., Vanhulle, E., Saul, S., Azari, S., Nhu Tran, D. H., Vangeel, L., Chiu, W., Neyts, J., Vermeire, K., & de Jonghe, S. (2022). Synthesis and evaluation of 3-alkynyl-5-aryl-7-aza-indoles as broad-spectrum antiviral agents. *Frontiers in Chemistry*, *10*. <https://doi.org/10.3389/fchem.2022.1058229>
- McKay, S. J., Johnsen, R., Khattra, J., Asano, J., Baillie, D. L., Chan, S., Dube, N., Fang, L., Goszczynski, B., Ha, E., Zhao, Z., & Moerman, D. G. (2003). Gene expression profiling of cells, tissues, and developmental stages of the nematode *C. elegans*. In *Cold Spring Harbor Symposia on Quantitative Biology* (Vol. 68). <https://doi.org/10.1101/sqb.2003.68.159>
- McShea, M. A., Schmidt, K. L., Dubuke, M. L., Baldiga, C. E., Sullender, M. E., Reis, A. L., Zhang, S., O'Toole, S. M., Jeffers, M. C., Warden, R. M., Stringham, E. G., & Ryder, E. F. (2013). Abelson interactor-1 (ABI-1) interacts with MRL adaptor protein MIG-10 and is required in guided cell migrations and process outgrowth in *C. elegans*. *Developmental Biology*, *373*(1), 1–13. <https://doi.org/10.1016/j.ydbio.2012.09.017>
- Middelkoop, T. C., & Korswagen, H. C. (2014). Development and migration of the *C. elegans* Q neuroblasts and their descendants. *WormBook: The Online Review of C. Elegans Biology*, 1–23. <https://doi.org/10.1895/wormbook.1.173.1>
- Middelkoop, T. C., Williams, L., Yang, P.-T., Luchtenberg, J., Betist, M. C., Ji, N., van Oudenaarden, A., Kenyon, C., & Korswagen, H. C. (2012). The thrombospondin repeat containing protein MIG-21 controls a left-right asymmetric Wnt signaling response in migrating *C. elegans* neuroblasts. *Developmental Biology*, *361*(2), 338–348. <https://doi.org/10.1016/j.ydbio.2011.10.029>
- Moffat, L. L., Robinson, R. E., Bakoulis, A., & Clark, S. G. (2014). The conserved transmembrane RING finger protein PLR-1 downregulates Wnt signaling by reducing Frizzled, Ror and Ryk cell-surface levels in *C. elegans*. *Development (Cambridge)*, *141*(3), 617–628. <https://doi.org/10.1242/dev.101600>
- Moreno-Layseca, P., Icha, J., Hamidi, H., & Ivaska, J. (2019). Integrin trafficking in cells and tissues. *Nature Cell Biology*, *21*(2), 122–132. <https://doi.org/10.1038/s41556-018-0223-z>
- Motley, A. M., Berg, N., Taylor, M. J., Sahlender, D. A., Hirst, J., Owen, D. J., & Robinson, M. S. (2006). Functional analysis of AP-2  $\alpha$  and  $\mu$ 2 subunits. *Molecular Biology of the Cell*, *17*(12), 5298–5308. <https://doi.org/10.1091/mbc.E06-05-0452>
- Oosterveen, T., Coudreuse, D. Y. M., Yang, P.-T., Fraser, E., Bergsma, J., Dale, T. C., & Korswagen, H. C. (2007). Two functionally distinct Axin-like proteins regulate canonical Wnt signaling in *C. elegans*. *Developmental Biology*, *308*(2), 438–448. <https://doi.org/10.1016/j.ydbio.2007.05.043>
- Pan, C.-L., Baum, P. D., Gu, M., Jorgensen, E. M., Clark, S. G., & Garriga, G. (2008). *C. elegans* AP-2 and Retromer Control Wnt Signaling by Regulating MIG-14/Wntless. *Developmental Cell*, *14*(1), 132–139. <https://doi.org/10.1016/j.devcel.2007.12.001>
- Pan, C.-L., Howell, J. E., Clark, S. G., Hilliard, M., Cordes, S., Bargmann, C. I., & Garriga, G. (2006). Multiple Wnts and Frizzled receptors regulate anteriorly directed cell and growth cone



- migrations in *Caenorhabditis elegans*. *Developmental Cell*, 10(3), 367–377. <https://doi.org/10.1016/j.devcel.2006.02.010>
- Peng, Y.-H., Yang, W.-K., Lin, W.-H., Lai, T.-T., & Chien, C.-T. (2009). Nak regulates Dlg basal localization in *Drosophila* salivary gland cells. *Biochemical and Biophysical Research Communications*, 382(1), 108–113. <https://doi.org/10.1016/j.bbrc.2009.02.139>
- Port, F., Kuster, M., Herr, P., Furger, E., Bänziger, C., Hausmann, G., & Basler, K. (2008). Wingless secretion promotes and requires retromer-dependent cycling of Wntless. *Nature Cell Biology*, 10(2), 178–185. <https://doi.org/10.1038/ncb1687>
- Prasad, B. C., & Clark, S. G. (2006). Wnt signaling establishes anteroposterior neuronal polarity and requires retromer in *C. elegans*. *Development*, 133(9), 1757–1766. <https://doi.org/10.1242/dev.02357>
- Ramesh, S. T., Navyasree, K. V., Sah, S., Ashok, A. B., Qathoon, N., Mohanty, S., Swain, R. K., & Umasankar, P. K. (2021). BMP2K phosphorylates AP-2 and regulates clathrin-mediated endocytosis. *Traffic*, 22(11), 377–396. <https://doi.org/10.1111/tra.12814>
- Rella, L., Fernandes Póvoa, E. E., & Korswagen, H. C. (2016). The *Caenorhabditis elegans* Q neuroblasts: A powerful system to study cell migration at single-cell resolution in vivo. *Genesis*, 54(4), 198–211. <https://doi.org/10.1002/dvg.22931>
- Ricotta, D., Conner, S. D., Schmid, S. L., von Figura, K., & Höning, S. (2002). Phosphorylation of the AP2  $\mu$  subunit by AAK1 mediates high affinity binding to membrane protein sorting signals. *Journal of Cell Biology*, 156(5), 791–795. <https://doi.org/10.1083/jcb.200111068>
- Salser, S. J., & Kenyon, C. (1992). Activation of a *C. elegans* Antennapedia homologue in migrating cells controls their direction of migration. *Nature*, 355(6357), 255–258. <https://doi.org/10.1038/355255a0>
- Schindelin, J., Arganda-Carreras, I., Frise, E., Kaynig, V., Longair, M., Pietzsch, T., Preibisch, S., Rueden, C., Saalfeld, S., Schmid, B., Tomancak, P., & Cardona, A. (2012). Fiji: An open-source platform for biological-image analysis. *Nature Methods*, 9(7), 676–682. <https://doi.org/10.1038/nmeth.2019>
- Schmidt, K. L., Marcus-Gueret, N., Adeleye, A., Webber, J., Baillie, D., & Stringham, E. G. (2009). The cell migration molecule UNC-53/NAV2 is linked to the ARP2/3 complex by ABI-1. *Development*, 136(4), 563–574. <https://doi.org/10.1242/dev.016816>
- Shafaq-Zadah, M., Gomes-Santos, C. S., Bardin, S., Maiuri, P., Maurin, M., Iranzo, J., Gautreau, A., Lamaze, C., Caswell, P., Goud, B., Goud, B., & Johannes, L. (2016). Persistent cell migration and adhesion rely on retrograde transport of  $\beta$  1 integrin. *Nature Cell Biology*, 18(1), 54–64. <https://doi.org/10.1038/ncb3287>
- Shaye, D. D., & Greenwald, I. (2011). Ortholist: A compendium of *C. elegans* genes with human orthologs. *PLoS ONE*, 6(5). <https://doi.org/10.1371/journal.pone.0020085>
- Sherwood, D. R., & Plastino, J. (2018). Invading, leading and navigating cells in *caenorhabditis elegans*: Insights into cell movement in vivo. *Genetics*, 208(1), 53–78. <https://doi.org/10.1534/genetics.117.300082>
- Silhankova, M., & Korswagen, H. C. (2007). Migration of neuronal cells along the anterior-posterior body axis of *C. elegans*: Wnts are in control. *Current Opinion in Genetics and Development*, 17(4), 320–325. <https://doi.org/10.1016/j.gde.2007.05.007>



- Smythe, E., & Ayscough, K. R. (2003). The Ark1/Prk1 family of protein kinases. Regulators of endocytosis and the actin cytoskeleton. *EMBO Reports*, 4(3), 246–251. <https://doi.org/10.1038/sj.embor.embor776>
- Sorensen, E. B., & Conner, S. D. (2008). AAK1 regulates Numb function at an early step in clathrin-mediated endocytosis. *Traffic*, 9(10), 1791–1800. <https://doi.org/10.1111/j.1600-0854.2008.00790.x>
- Sorrell, F. J., Szklarz, M., Abdul Azeez, K. R., Elkins, J. M., & Knapp, S. (2016). Family-wide Structural Analysis of Human Numb-Associated Protein Kinases. *Structure*, 24(3), 401–411. <https://doi.org/10.1016/j.str.2015.12.015>
- Spencer, A. G., Orita, S., Malone, C. J., & Han, M. (2001). A RHO GTPase-mediated pathway is required during P cell migration in *Caenorhabditis elegans*. *Proceedings of the National Academy of Sciences of the United States of America*, 98(23), 13132–13137. <https://doi.org/10.1073/pnas.241504098>
- Stringham, E., Pujol, N., Vandekerckhove, J., & Bogaert, T. (2002). Unc-53 controls longitudinal migration in *C. elegans*. *Development*, 129(14), 3367–3379. <https://doi.org/10.1242/dev.129.14.3367>
- Sundaram, M. V., & Buechner, M. (2016). The *caenorhabditis elegans* excretory system: A model for tubulogenesis, cell fate specification, and plasticity. *Genetics*, 203(1), 35–63. <https://doi.org/10.1534/genetics.116.189357>
- Tax, F. E., Thomas, J. H., Ferguson, E. L., & Horvitz, H. R. (1997). Identification and characterization of genes that interact with lin-12 in *Caenorhabditis elegans*. *Genetics*, 147(4), 1675–1695. <https://doi.org/10.1093/genetics/147.4.1675>
- Tsushima, H., Malabarba, M. G., Confalonieri, S., Senic-Matuglia, F., Verhoef, L. G. G. C., Bartocci, C., D’Ario, G., Cocito, A., di Fiore, P. P., & Salcini, A. E. (2013). A Snapshot of the Physical and Functional Wiring of the Eps15 Homology Domain Network in the Nematode. *PLoS ONE*, 8(2). <https://doi.org/10.1371/journal.pone.0056383>
- Wang, S., Chen, X., Crisman, L., Dou, X., Winborn, C. S., Wan, C., Puscher, H., Yin, Q., Kennedy, M. J., & Shen, J. (2023). Regulation of cargo exocytosis by a Repl1-Ralbp1-RalA module. *Science Advances*, 9(8), eade2540. <https://doi.org/10.1126/sciadv.ade2540>
- Whangbo, J., & Kenyon, C. (1999). A Wnt signaling system that specifies two patterns of cell migration in *C. elegans*. *Molecular Cell*, 4(5), 851–858. [https://doi.org/10.1016/S1097-2765\(00\)80394-9](https://doi.org/10.1016/S1097-2765(00)80394-9)
- Wrobel, A. G., Kadlecova, Z., Kamenicky, J., Yang, J.-C., Herrmann, T., Kelly, B. T., McCoy, A. J., Evans, P. R., Martin, S., Müller, S., Honing, S., & Owen, D. J. (2019). Temporal Ordering in Endocytic Clathrin-Coated Vesicle Formation via AP2 Phosphorylation. *Developmental Cell*, 50(4), 494–508.e11. <https://doi.org/10.1016/j.devcel.2019.07.017>
- Wu, Y. C., Chiang, Y. C., Chou, S. H., & Pan, C. L. (2021). Wnt signalling and endocytosis: Mechanisms, controversies and implications for stress responses. *Biology of the Cell*, 113(2), 95–106. <https://doi.org/10.1111/boc.202000099>
- Xin, X., Wang, Y., Zhang, L., Zhang, D., Sha, L., Zhu, Z., Huang, X., Mao, W., & Zhang, J. (2023). Development and therapeutic potential of adaptor-associated kinase 1 inhibitors in human multifaceted diseases. *European Journal of Medicinal Chemistry*, 248:115102. <https://doi.org/10.1016/j.ejmech.2023.115102>

- Yamaguchi, A., Urano, T., Goi, T., & Feig, L. A. (1997). An Eps homology (EH) domain protein that binds to the Ral-GTPase target, RalBP1. *Journal of Biological Chemistry*, 272(50), 31230–31234. <https://doi.org/10.1074/JBC.272.50.31230>
- Yang, P.-T., Lorenowicz, M. J., Silhankova, M., Coudreuse, D. Y. M., Betist, M. C., & Korswagen, H. C. (2008). Wnt Signaling Requires Retromer-Dependent Recycling of MIG-14/Wntless in Wnt-Producing Cells. *Developmental Cell*, 14(1), 140–147. <https://doi.org/10.1016/j.devcel.2007.12.004>
- Yang, W.-K., Peng, Y.-H., Li, H., Lin, H.-C., Lin, Y.-C., Lai, T.-T., Suo, H., Wang, C.-H., Lin, W.-H., Ou, C.-Y., Chang, H., & Chien, C.-T. (2011). Nak regulates localization of clathrin sites in higher-order dendrites to promote local dendrite growth. *Neuron*, 72(2), 285–299. <https://doi.org/10.1016/j.neuron.2011.08.028>
- Yu, J., Chia, J., Canning, C. A., Jones, C. M., Bard, F. A., & Virshup, D. M. (2014). WLS Retrograde transport to the endoplasmic reticulum during Wnt secretion. *Developmental Cell*, 29(3), 277–291. <https://doi.org/10.1016/j.devcel.2014.03.016>
- Zallen, J. A., Kirch, S. A., & Bargmann, C. I. (1999). Genes required for axon pathfinding and extension in the *C. elegans* nerve ring. *Development*, 126(16), 3679–3692. <https://doi.org/10.1242/dev.126.16.3679>
- Zhao, Z., Sheps, J. A., Ling, V., Fang, L. L., & Baillie, D. L. (2004). Expression analysis of ABC transporters reveals differential functions of tandemly duplicated genes in *Caenorhabditis elegans*. *Journal of Molecular Biology*, 344(2), 409–417. <https://doi.org/10.1016/j.jmb.2004.09.052>
- Zheng, C., Diaz-Cuadros, M., & Chalfie, M. (2015). Dishevelled attenuates the repelling activity of Wnt signaling during neurite outgrowth in *Caenorhabditis elegans*. *Proceedings of the National Academy of Sciences of the United States of America*, 112(43), 13243–13248. <https://doi.org/10.1073/pnas.1518686112>
- Zinovyeva, A. Y., & Forrester, W. C. (2005). The *C. elegans* Frizzled CFZ-2 is required for cell migration and interacts with multiple Wnt signaling pathways. *Developmental Biology*, 285(2), 447–461. <https://doi.org/10.1016/j.ydbio.2005.07.014>
- Zinovyeva, A. Y., Yamamoto, Y., Sawa, H., & Forrester, W. C. (2008). Complex network of Wnt signaling regulates neuronal migrations during *Caenorhabditis elegans* development. *Genetics*, 179(3), 1357–1371. <https://doi.org/10.1534/genetics.108.090290>

**Table 1.** Phenotypes of *sel-5* and *vps-29* single and double mutants

Genotype	ALM (%) <sup>a</sup>	PLM (%) <sup>b</sup>	CAN (%) <sup>c</sup>	Dye filling (%) <sup>d</sup>	Fecundity (n) <sup>e</sup>
Wild type	0.0	0.0	0.6	0.5	280 ± 41
<i>sel-5(ok149)</i>	0.0	0.0	8.9	4.7	236 ± 24
<i>sel-5(ok363)</i>	0.0	0.0	10.9	1.0	249 ± 37
<i>vps-29(tm1320)</i>	0.0	0.0	2.9	4.3	221 ± 28
<i>sel-5(ok149) vps-29</i>	29.9	9.1	17.7	17.4	132 ± 40
<i>sel-5(ok363) vps-29</i>	7.2	2.8	16.3	7.1	159 ± 23

<sup>a</sup>% of animals with axons of one or both ALM reversed/bipolar, n > 60

<sup>b</sup>% of animals with axons of one or both PLM neurons reversed, n > 60

<sup>c</sup>% of CAN neurons located anteriorly of V3 seam cell, n > 40

<sup>d</sup>% of animals with one or both phasmid sensilla not dyed with DiI, n > 40

<sup>e</sup> average number of progeny from 5 hermaphrodites, ± s.d.

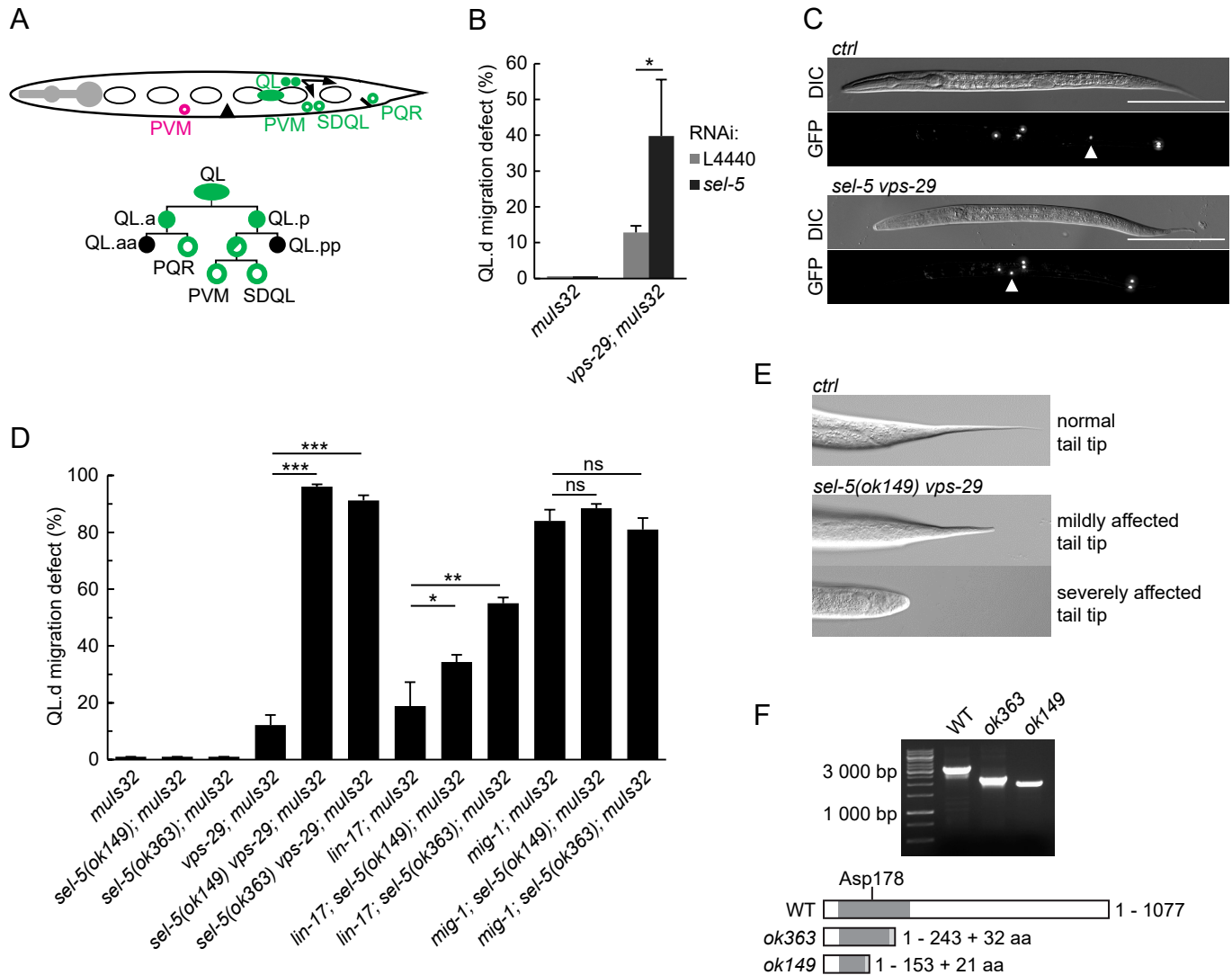


**Figure 1. Loss of *sel-5* potentiates QL migration defect in retromer and Wnt pathway mutants.** A) QL neuroblast lineage and a cartoon indicating the position of terminally differentiated neurons (depicted with empty circles) (adapted from Rella et al., 2016). Aberrant position of PVM neuron, as observed in QL.d migration defect, is highlighted in magenta. B) RNAi against *sel-5* increases the penetrance of *vps-29* QL.d migration defect when compared to the control (L4440) RNAi. No defect is observed in wild type background. C) PVM position in L2 larvae of control (transgene only) and *sel-5 vps-29* double mutant animals. PVM position indicated with white arrowhead, neurons visualized by expression of *Pmec-7::gfp* transgene *muls32*, scale bar represents 100  $\mu$ m. D) Mutation in *sel-5* results in increased penetrance of QL.d migration defect of *vps-29* and *lin-17*, but not *mig-1* mutants. E) Examples of mild and severe alteration of tail tip morphology in *sel-5 vps-29* double mutants. F) Shortened transcripts are produced from the *sel-5* locus in both *ok363* and *ok149* alleles. Potential protein products resulting from these transcripts are depicted showing the impact of the truncation on the kinase domain (dark grey box). Extra amino acids resulting from a frameshift and thus not present in the wild type protein are also depicted (light grey box). Position of the active site is indicated. For B) and D) results are shown as mean + s.d. of at least three independent experiments,  $n > 150$  animals in total for each strain, unpaired two-tailed Student's t-test was performed to assess the difference between the samples, \* p-value < 0.05, \*\* p-value < 0.01, \*\*\* p-value < 0.001, ns – not significant.

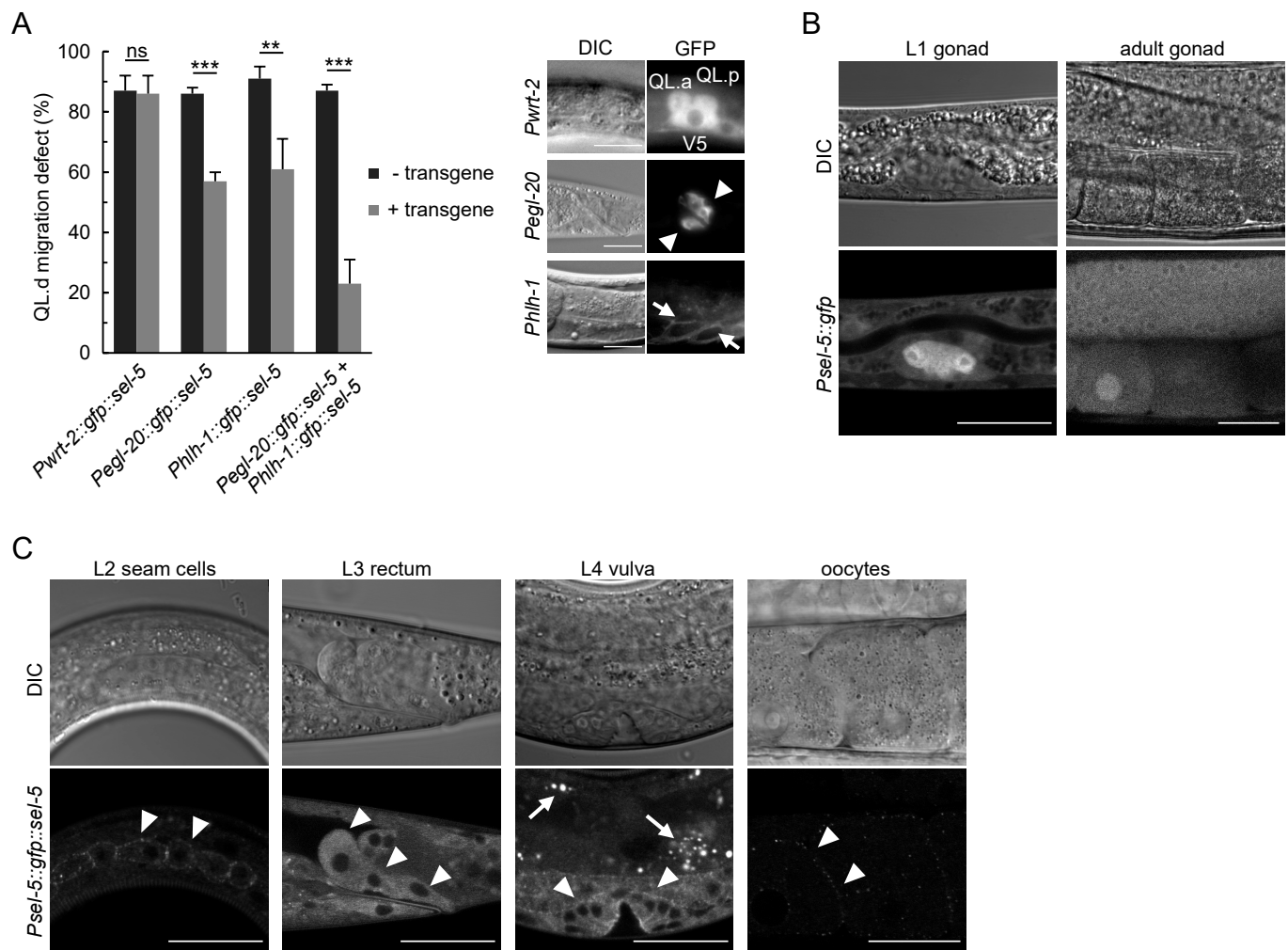


**Figure 2. SEL-5 is expressed in multiple tissues and is required cell-nonautonomously for QL.d migration.** A) Transgenic rescue of the QL.d migration defect. *sel-5* was expressed under the control of various promoters from an extrachromosomal array in *sel-5 vps-29; mulS32* background and the effect of such expression on QL.d migration was quantified. Comparison was made between animals carrying the transgene and their siblings which have lost the transgenic array. Expression of each transgene in the expected tissue is shown on the right. Results are shown as mean + s.d. of at least three independent experiments,  $n > 100$  animals in total for each condition. Unpaired two-tailed Student's t-test was performed to assess the difference between the samples, \*\* p-value  $< 0.01$ , \*\*\* p-value  $< 0.001$ , ns – not significant. B) GFP expression driven by an endogenous *sel-5* promoter in the gonad of L1 and adult animals. C) Expression of GFP::SEL-5 fusion protein driven by endogenous *sel-5* promoter in various larval and adult tissues. Localized GFP::SEL-5 expression is indicated by white arrowheads, white arrows point to autofluorescent signal from gut granules. Scale bar represents 20  $\mu\text{m}$  in A) – C).

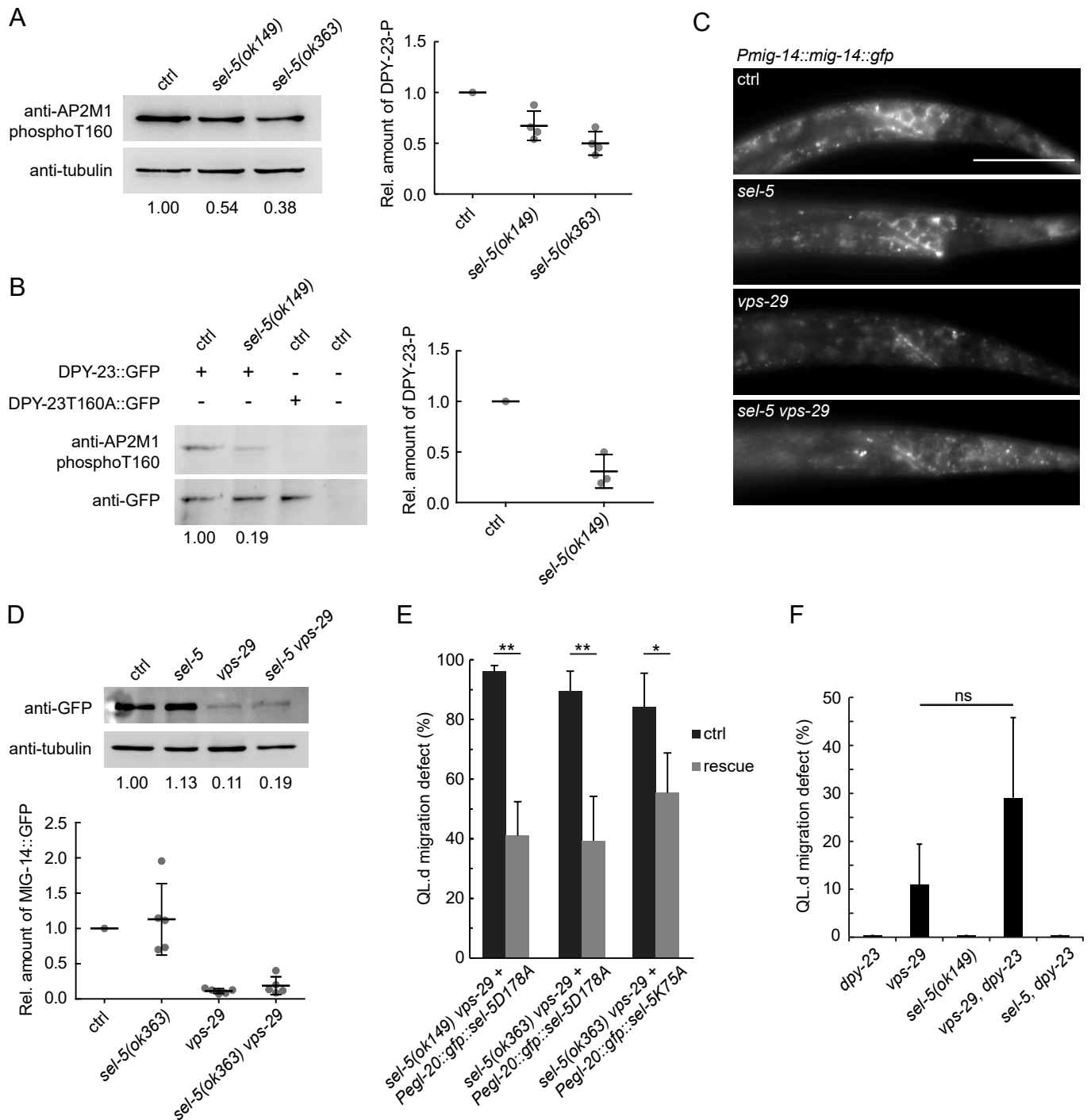


**Figure 3. SEL-5 alters the phosphorylation status of DPY-23 but its kinase activity is not required for QL.d migration.** A) Level of DPY-23 phosphorylation at position T160 is reduced in *sel-5* mutant animals. Phosphorylation was detected by Western blot analysis in lysates from a population of L4/young adults of indicated strains using phospho-specific antibody against human AP2M1. Band intensities were normalized to an alpha tubulin loading control and compared to the control sample (sample/control ratio indicated below each lane). Representative Western blot example is shown on the left, relative quantification of four independent experiments is shown on the right. B) Level of DPY-23::GFP phosphorylation is reduced in *sel-5* mutants. Phosphorylation at T160 of GFP tagged DPY-23 was detected by Western blot analysis in lysates from a population of L4/young adults using phospho-specific antibody against human AP2M1. Strains expressing either no GFP fusion protein or a GFP tagged DPY-23T160A mutant protein



(continued) were included as controls. Band intensities were normalized to a GFP signal intensity and compared to the control sample (DPY-23::GFP in wild type background), sample/control ratio is indicated below each lane. Representative Western blot example is shown on the left, relative quantification of three independent experiments is shown on the right. C) L2 animals expressing MIG-14::GFP from the *huSi2* transgene were imaged using confocal microscope. Posterior part of the body with Wnt expressing cells is shown. Anterior to the left, dorsal up, scale bar represents 20  $\mu\text{m}$ . D) Western blot analysis of MIG-14::GFP levels expressed from a *huSi2* transgene in various mutant backgrounds. MIG-14::GFP was detected in lysates from synchronized populations of L1 larvae of the indicated strains. Band intensities were normalized to an alpha tubulin loading control and compared to the control sample (sample/control ratio indicated below each lane). Representative Western blot example is shown on the top, relative quantification of five independent experiments is shown below. E) Transgenic rescue of the QL.d migration defect with kinase-inactive SEL-5. D178A or K75A SEL-5 mutant protein was expressed from *egl-20* promoter in *sel-5 vps-29; muls32* mutant background from an extrachromosomal array and the QL.d migration defect was quantified in animals carrying the transgene and their siblings which have lost the transgenic array. F) The absence of DPY-23 T160 phosphorylation does not result in QL.d migration defect. The presence of *dpy-23(mew25)* allele carrying T160A substitution either alone or in combination with *sel-5* or *vps-29* does not significantly contribute to the QL.d migration defect. For E) and F) results are shown as mean + s.d. of at least three independent experiments,  $n > 100$ . Unpaired two-tailed Student's t-test was performed to assess the difference between the samples, \* p-value < 0.05, \*\* p-value < 0.01, ns – not significant.

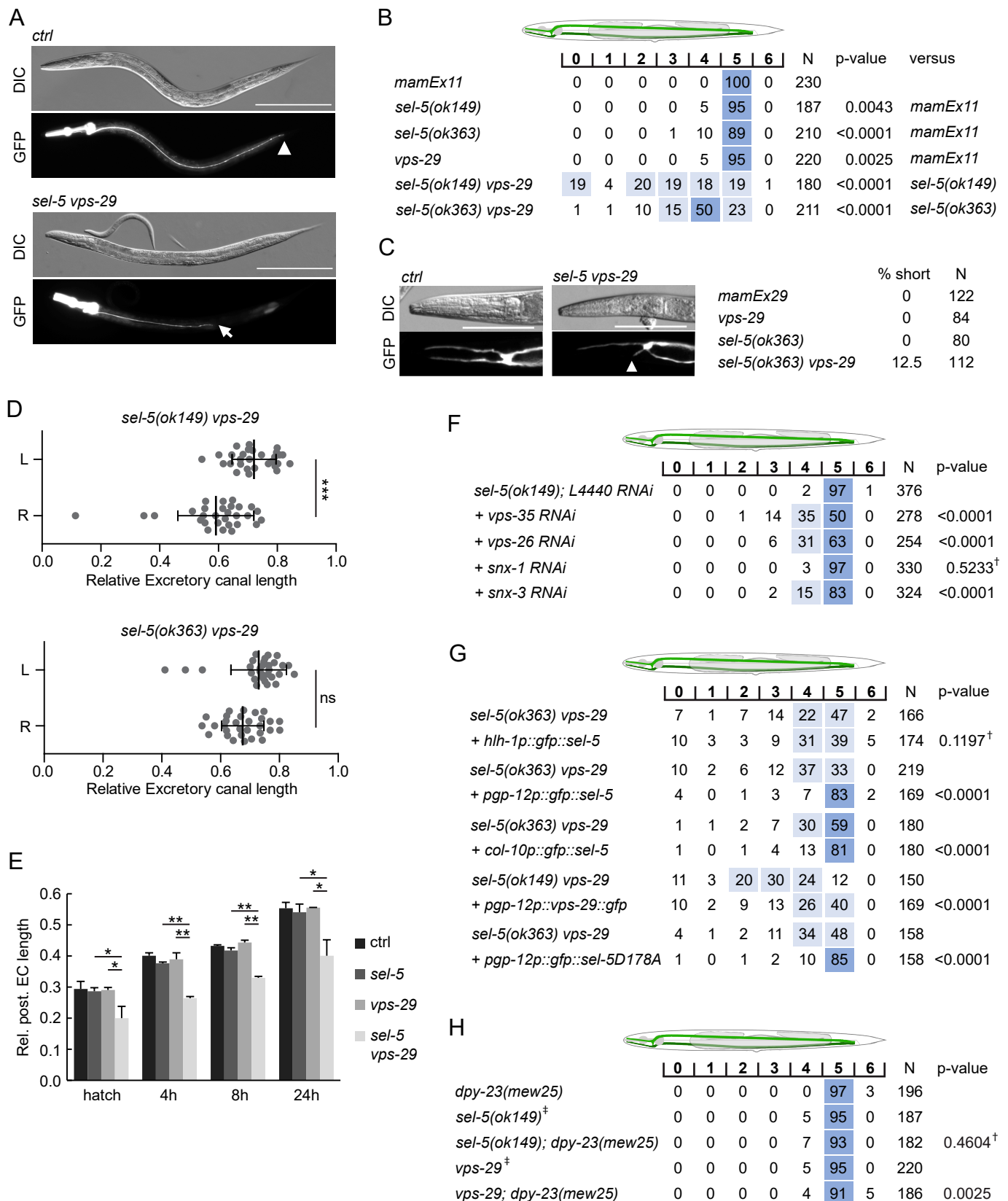


**Figure 4. *sel-5* cooperates with the retromer complex to regulate the length of excretory cell canals.**

A) Posterior canals of the excretory cell are significantly shortened in *sel-5 vps-29* mutants. Excretory cell was visualized by *Ppqp-12::gfp* expression from a *mamEx11* transgene. Scale bar represents 200  $\mu$ m. B) Quantification of posterior canal outgrowth defects. The outgrowth of the posterior canal of the

(continued) excretory cell was quantified by dividing the region between the posterior bulb of the pharynx to the tip of the tail into seven segments. Percentage of canal arms terminating in each segment is indicated. Segment scoring 50% or higher was highlighted in dark blue, segment scoring 15 – 49% was highlighted light blue for easier orientation. All strains contained the *mamEx11* transgene to visualize the excretory cell. Statistical significance of differences between the strains was analysed using Fisher's exact test for 2x3 table. For the test, data from segments 0 – 4 were pooled into one category ("shorter"), data from segments 5 and 6 were used as the two other categories ("normal" and "longer", respectively). Comparison was made either to the control strain or to the more severe single mutant in the case of double mutant strains. Bonferroni correction for multiple testing was applied. C) Anterior canals of the excretory cell are shortened in *sel-5 vps-29* double mutants. Excretory cell was visualized by *Ppgp-12::gfp* expression from a *mamEx29* transgene. Scale bar represents 100  $\mu$ m. D) Posterior canals on the right side of the animals are more severely affected compared to their left counterparts. The length of the posterior canal on each side of the animal was measured and normalized to the length of the whole body of the animal. Paired t-test was used to assess the significance of the difference between the two sides, \*\*\* p-value < 0.001, ns – not significant. E) Posterior excretory canals are shorter already at the time of hatching in *sel-5 vps-29* mutants. The dynamics of posterior canal outgrowth was assessed by measuring the canal length and normalizing it to the total body length at hatching and at three time points during early larval development. Results are presented as mean + s.d. of at least 30 canals for each condition. Unpaired two-tailed Student's t-test was performed to assess the difference between the samples, \* p-value < 0.05, \*\* p-value < 0.01. F) Loss of either *vps-35*, *vps-26* or *snx-3* retromer component expression induces posterior canal shortening in *sel-5* mutants. Canal outgrowth was scored as in 4B. G) Both cell-autonomous and non-autonomous expression of *sel-5* rescues excretory canal shortening in *sel-5 vps-29* mutants. SEL-5 was expressed from an extrachromosomal array under the control of *pgp-12*, *hlh-1* or *col-10* promoters. Canal outgrowth was scored as in 4B and comparison was made between animals carrying the array and their siblings which have lost the transgenic array. All strains contained also the *mamEx29* extrachromosomal array to visualize the excretory canal. H) T160 phosphorylation of DPY-23 is not required for posterior excretory canal outgrowth. Canal outgrowth was scored as in 4B in strains containing *dpy-23(mew25)* allele carrying T160A substitution. Comparison was made between the double mutants and either *sel-5* or *vps-29* single mutant. For F) – H) † – differences not significant, ‡ – same data as in B).

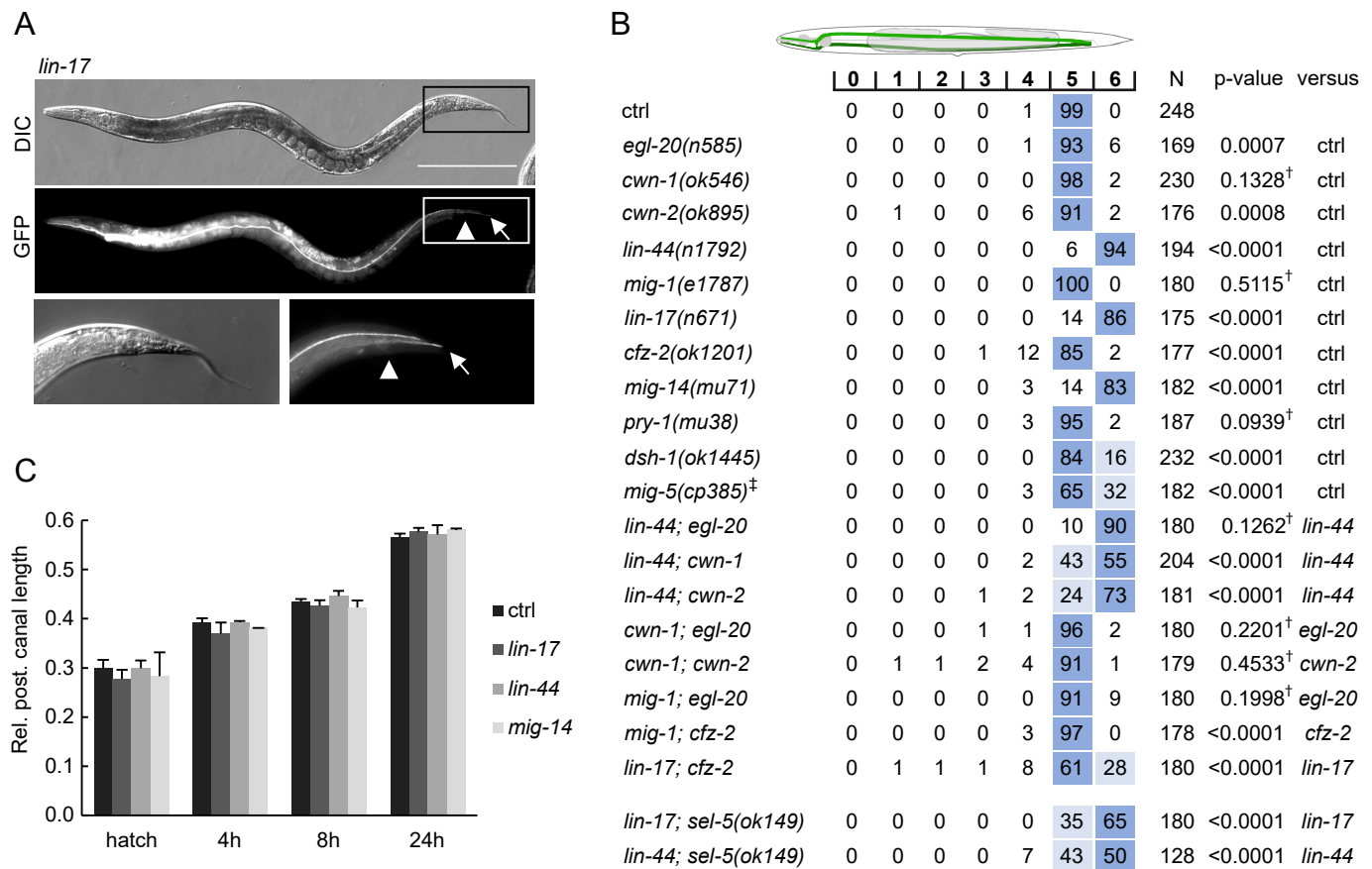


**Figure 5. Wnt pathway components LIN-44/Wnt and LIN-17/Frizzled determine the stopping point for excretory canal outgrowth.** A) Posterior canals of the excretory cell overgrow into the tip of the tail in *lin-17* mutants. Excretory cell was visualized by *Ppgp-12::gfp* expression from the *sIs10089* transgene. Boxed areas are magnified in the bottom row, scale bar represents 200  $\mu$ m. B) Quantification of posterior canal outgrowth in Wnt pathway mutants. Canal outgrowth was scored as in Fig. 4B and comparison was made either to the control strain (*sIs10089*) only or to the more severe single mutant in the case of double mutant strains. All strains contained the *sIs10089* transgene to visualize excretory canals except for *lin-17; sel-5* and *lin-44; sel-5* which contained *mamEx11*, and *mig-5*, which contained *mamEx29*. <sup>†</sup> – differences not significant. <sup>‡</sup> Full genotype was *mig-5(cp385[mNG-GLO<sup>^</sup>AID::mig-5]); mamEx29; mamEx34[eft-3p::TIR::mRuby; myo2p::tdTomato]* and animals were grown on NGM plates with 1 mM auxin from L1 till L4/young adult stage. Only animals containing the *mamEx34* array were used for analysis. C) Posterior excretory canals display normal length during early larval development. The dynamics of posterior canal outgrowth in *lin-44*, *lin-17* and *mig-14* mutants was assessed by measuring the canal length and normalizing it to the total body length at hatching and at three time points during early larval development. Results are presented as mean + s.d. of at least 30 measured canals. Comparison between samples assessed by unpaired two-tailed Student's t-test did not reveal any significant differences.

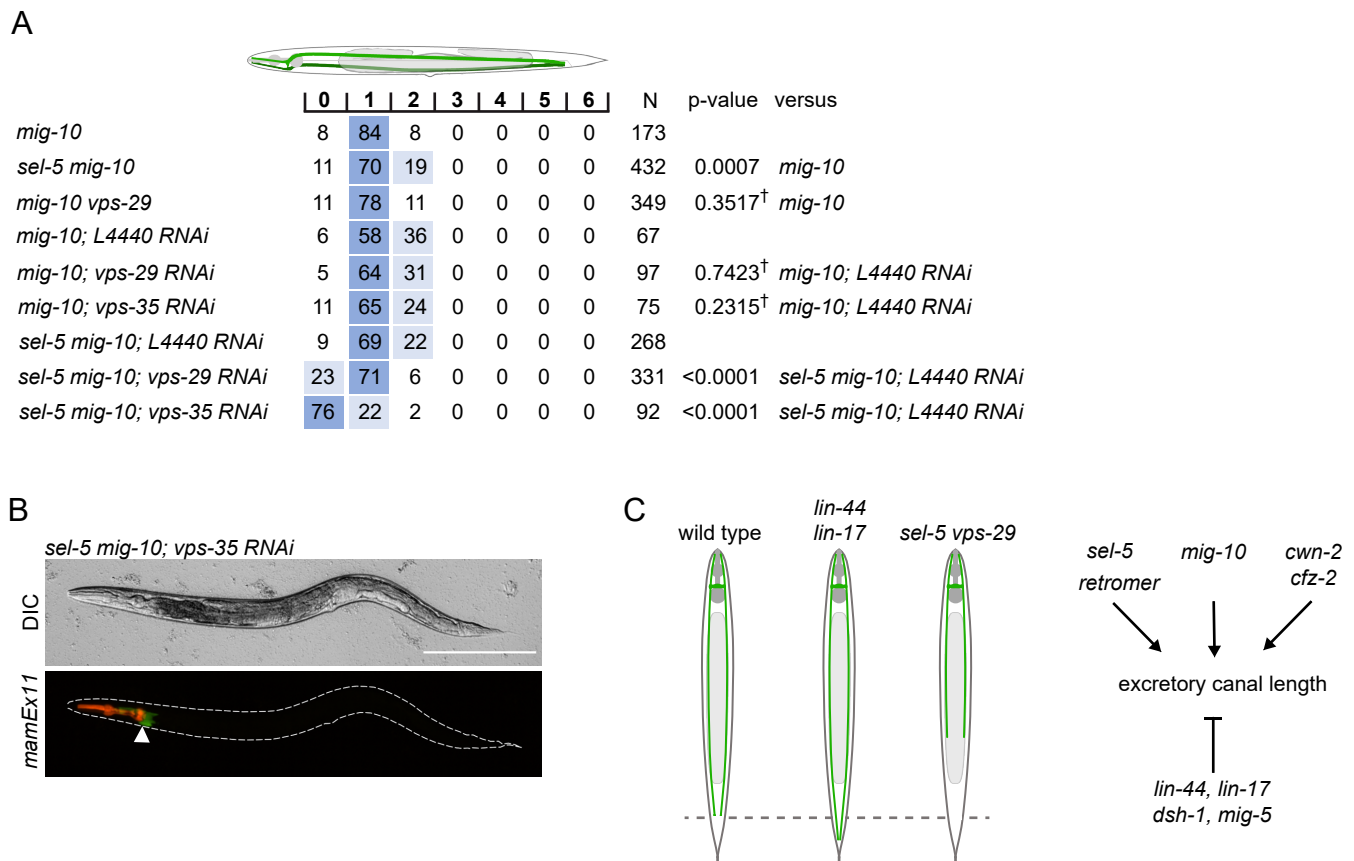


**Figure 6. SEL-5 and retromer genetically interact with MIG-10/Lamellipodin in excretory cell outgrowth.** A) The length of the excretory cell posterior canals was assessed in *mig-10* mutants and after simultaneous loss of *mig-10* and *sel-5* or the retromer or both. Canal shortening was determined as in Fig. 4B, statistical comparison was made to the appropriate control condition. For the Fisher's exact test data from segments 0, 1 and 2 were used as the three tested categories. All strains contained the *mamEx11* transgene. B) Complete lack of posterior canal outgrowth in *sel-5 mig-10* animals treated with *vps-35* RNAi. Co-injection marker *Pmyo-2::tdTomato* expression labels the pharynx of the animal, white arrowhead points to the excretory cell body. C) Model summarizing the effect of various mutants on the outgrowth of the excretory cell posterior canals. On the left, the three possible outcomes of canal outgrowth are outlined. In wild type animals posterior canals reach to the level of rectum (dashed line). In *lin-44* or *lin-17* mutants, a putative stop signal is missing and the canals grow past the rectum into the tip of the tail. On the other hand, simultaneous loss of *sel-5* and the retromer complex components prevents the canals to reach the wild type position. Several inputs are integrated to define the proper length of posterior excretory canals; those discussed in this work are summarized on the right.

### 3. Unpublished results

#### 3.1. Effects of *sel-5* on touch receptor neurons (TRNs) migration, position, and polarity

Our RNAi screen for new regulators of Wnt signaling revealed *sel-5* gene as a potential modulator of this pathway. RNAi knock-down of *sel-5* in *vps-29* sensitized background caused a marked increase in QL.d migration defect (Figure 1 in article 2). Effect of *sel-5* mutation manifests itself as several observable phenotypes in the group of touch receptor neurons (TRNs). Among these neurons are two ALMs in the middle section of *C. elegans*, two PLMs in its tail, and descendants of QL and QR neuroblasts including PVM and AVM, respectively. These touch-sensitive cells enable *C. elegans* to navigate through their environment. QL.d migration defect and ALMs and PLMs polarity reversal phenotypes are discussed in article 2 of this work. Here we will expand on results not included in the article mentioned above.

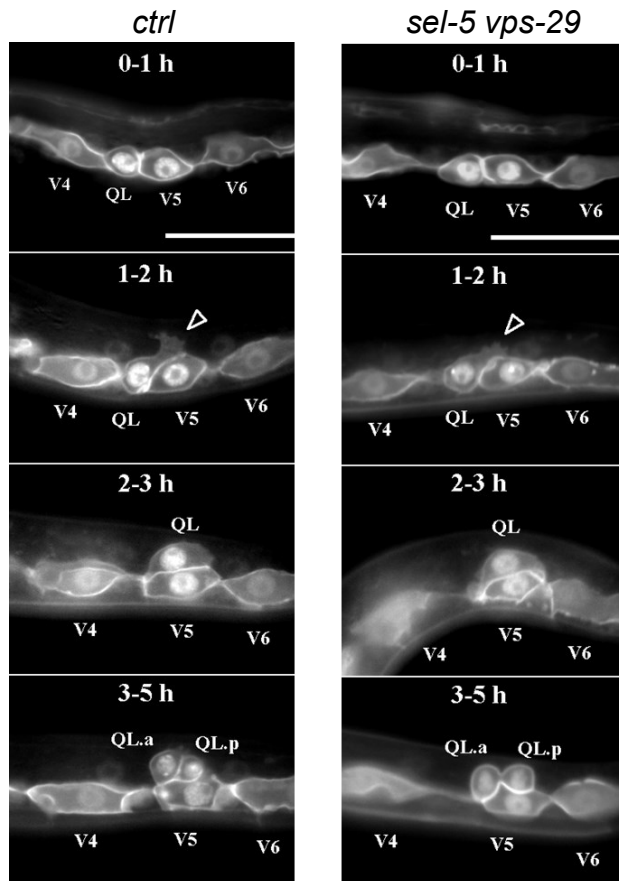


**Figure S1. Initial polarization and migration of QL neuroblast in *sel-5 vps-29* mutant animals.** Polarization and initial Wnt-independent migration of QL neuroblast was not different in controls and *sel-5 vps-29* double mutants. In both cases QL was observed anteriorly to its sister seam cell V5. At the two-hour time point a cellular protrusion was visible growing posteriorly over the V5 seam cell (arrowheads). This protrusion formation was followed by posterior migration of QL cell over the V5 seam cell. Once at the top of V5 seam cell QL neuroblast divided giving rise to first QL.d cells, QL.a and QL.p. These two QL daughter cells were fully divided five hours after L1 larvae hatching. Anterior is to the left side. A *C. elegans* strain carrying *hIs63* transgene was used to visualize the nucleus and the PM of seam cells (V1-V6) and QL neuroblast. Scale bar represents 20  $\mu$ m.

Migration of QL.d can be divided into two phases. First is a Wnt-independent initial polarization and short posterior migration of the QL neuroblast over the V5 seam cell. Second phase is a Wnt-dependent posterior migration of QL.d (Rella et al., 2016). Although our tissue-specific rescue experiments pointed to a Wnt-dependent function of *sel-5*, we could not exclude the possibility that the initial phase is affected as well. We therefore mapped the first



five hours of QL neuroblast development. We did not observe any difference in initial polarization or migration of QL neuroblast in *sel-5 vps-29* double mutants compared with control animals (Figure S1). This further supports the scenario in which SEL-5 kinase participates on the second phase of QL.d migration regulated by Wnt signaling.

Final position of ALML and ALMR neurons and the length of posterior neurites of PLML and PLMR were previously described to be at least partially regulated by the Wnt pathway (Zheng et al., 2015; Zinovyeva & Forrester, 2005). Both ALM neurons are born in the anterior of the worm and migrate posteriorly during development to their final position between V2 and V3 seam cells. *cwn-1/Wnt* and *cwn-2/Wnt* double mutant worms showed pronounced undermigration of ALM neurons (Zinovyeva & Forrester, 2005). To determine whether *sel-5* mutation by itself or in combination with *vps-29* effects ALM migration we measured distances of final ALMs positions from the posterior pharynx and compared them to the distance between posterior pharynx and the vulva. Relative positions of ALMs did not seem to change in any single or double mutant worms in our experiment (Figure S2). PLML and PLMR are bipolar neurons with a long anterior and shorter posterior neurite. The polarity and the length of PLMs neurites were shown to be regulated by several proteins from the Wnt pathway. Underextended PLM posterior neurites were observed in animals with overexpressed *lin-44/Wnt* or mutated *dsh-1/Dvl* (Zheng et al., 2015). We tested *sel-5* and *vps-29* single and double mutants for PLM posterior neurite shortening, however, we did not observe any change in relative length of these cellular processes (Figure S2).

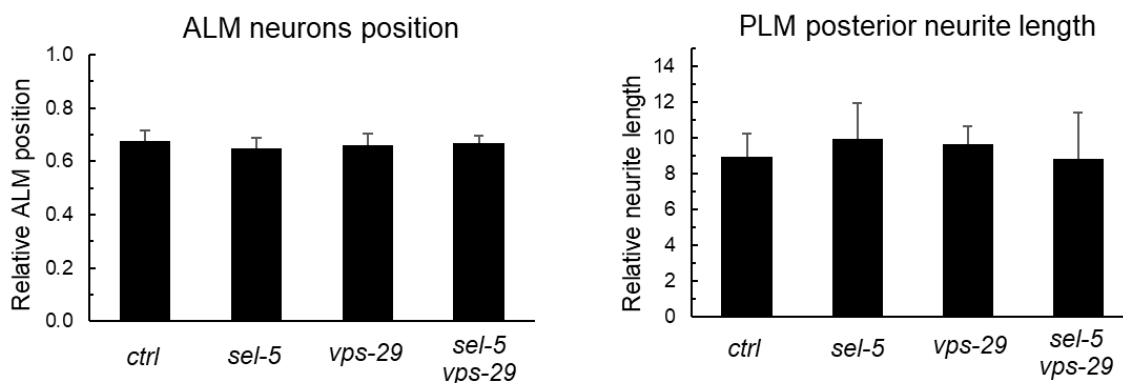


**Figure S2. Measurement of the relative final positions of ALMs and lengths of PLMs posterior neurites.** Single and double *sel-5* and *vps-29* mutants were tested for changes in the positions of ALM neurons compared to a distance between posterior pharynx and vulva. Same mutant strains were also measured for the PLMs posterior neurite length relative to PLM cell body length. Neither experiment showed any difference between control and mutated animals. For ALM experiment the final positions of 20 ALM neurons were measured for each strain and shown in graph as averages with error bars as SD. For PLM experiment lengths of 10 PLM neurites were measured for each strain and depicted as averages with error bars as SD.

A series of tissue-specific rescue experiments was conducted in *sel-5 vps-29* double mutants to locate the site of SEL-5 action. While there was no rescue of QL.d migration defect when *sel-5* expression was regulated by tissue-specific promoters for intestine, hypodermis or LIN-44/Wnt producing cells (data not shown), we observed a significant QL.d migration phenotype attenuation when *sel-5* was expressed under the control of EGL-20/Wnt producing cells- or body wall muscle cells-specific promoters (Figure 2 in article 2). So far, the N-terminal kinase domain of SEL-5 is the only known functional domain of this enzyme. The rest of the protein consists of a 700 AA long unstructured C-terminus. To test whether the C-terminal part of SEL-5 is necessary for its function we created two truncated forms of the *sel-5* rescue constructs; *sel-5R2* with 350 AA eliminated from the C-terminus and *sel-5R3* with the unstructured C-terminus completely missing and leaving only the kinase domain intact. Interestingly, when expressed under the control of EGL-20/Wnt producing cell-specific promoter both of these constructs exhibited lower ability to rescue the QL.d migration defect compared to the full-length construct (Figure 2 in article 2, Figure S3). This suggests that the C-terminus of the SEL-5 kinase is necessary to recapitulate *sel-5* construct full rescue ability.

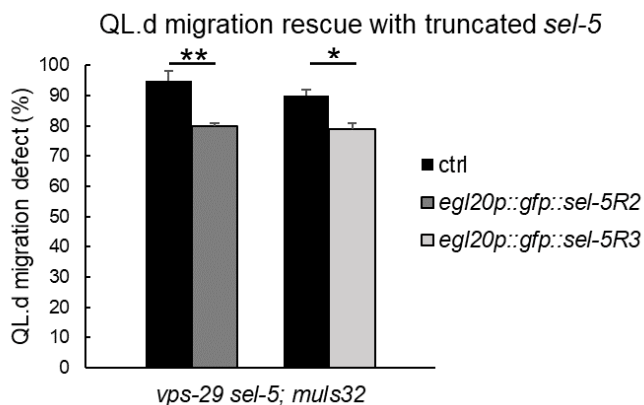


**Figure S3. QL.d migration defect rescue by truncated versions of *sel-5*.**

Two versions of shortened *sel-5* construct expressed under the control of *egl-20/Wnt* producing cell-specific promoter are still able to partially reduce QL.d migration defect phenotype of *sel-5 vps-29* mutants. *sel-5R2* is missing 350 AA from its C-terminus while *sel-5R3* is missing C-terminus entirely leaving only the

kinase domain intact. Results are shown as averages of three experiments (with at least 60 animals counted in each experiment) and error bars as SD. \*  $p = 0.0021$ , \*\*  $p = 0.0009$

Our experiments suggested that enzymatic function of SEL-5 kinase may not be necessary for QL.d migration regulation (Figure 3 in article 2). There is a *sel-5* paralogue *gakh-1* in *C. elegans*. To exclude the possibility that kinase-dead SEL-5 functionally interacts with GAKH-1 endogenous kinase we conducted a RNAi knock-down experiments of *gakh-1*. We did not see any change in QL.d migration phenotype in *sel-5* and *vps-29* single mutants or *sel-5 vps-29* double mutants after *gakh-1* RNAi (data not shown).

Wnt signal for regulation of QL neuroblast posterior migration is transduced mainly via LIN-17 and MIG-1, two homologs of Wnt receptor Frizzled (Harris et al., 1996). Given the putative role of SEL-5 in regulating endocytosis, we argued that altered levels of LIN-17 at the plasma membrane could account for the observed phenotype. We therefore employed transgenic worms carrying *lin-17::gfp* to determine whether overexpression of Wnt receptor gene *lin-17* would be able to rescue QL.d migration defect in *sel-5 vps-29* double mutants. Firstly, we tested the ability of *lin-17::gfp* to rescue QL.d migration defect induced by *lin-17* mutation. While *lin-17* single mutation caused a mild QL.d migration defect, this phenotype

could indeed be rescued by overexpression of *lin-17::gfp* transgene (Figure S4). Double mutants in *sel-5* and *vps-29* showed almost fully penetrant QL.d migration defect when QL neuroblast and its descendants were visualized with *mulS32* transgene (Figure 1 article 2). Here for convenience, we used *mulS35* instead of *mulS32* transgene because it is located on a different chromosome and thus facilitates construction of the compound strains. The same *sel-5 vps-29* double mutant showed slightly lower QL.d migration defect when *mulS35* instead of *mulS32* was used (Figure S4). Interestingly, upon overexpression of *lin-17::gfp* we observed a small but significant increase in QL.d penetrance (Figure S4). This suggests that *sel-5 vps-29* double mutant defect in QL migration is not a consequence of a low level of LIN-17 Wnt receptor. A more detailed discussion will be provided in later chapters.

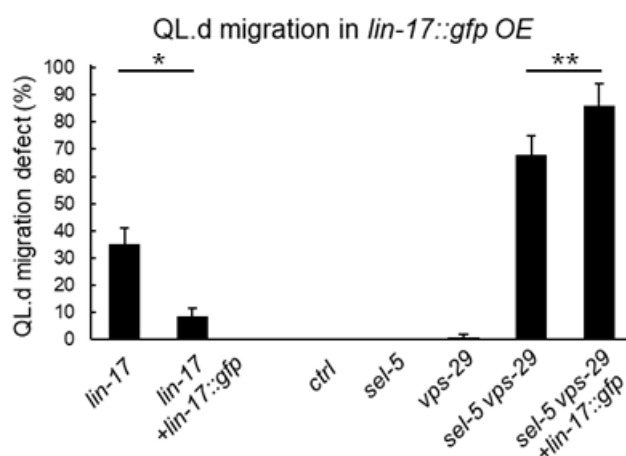


**Figure S4. Effects of *lin-17::gfp* transgene overexpression (OE) on QL.d migration defect.** Roughly one third of animals with *lin-17* mutation have their QL.d migration reversed. This phenotype could be rescued by overexpression of extrachromosomal ectopic *lin-17::gfp*. The same OE construct caused a small albeit significant increase in QL.d migration defect in *sel-5 vps-29* double mutants. Results are shown as averages of three experiments (minimum of a hundred animals counted in each) with error bars as SD. \*  $p = 0.0420$ , \*\*  $p = 0.0020$

In parallel we also visually monitored the level of *lin-17::gfp* in control and *sel-5 vps-29* double mutants. Apart from other tissues we observed *lin-17* expression in a group of *egl-20/Wnt* producing rectal epithelial cells, which we have identified as a probable site of *sel-5* action. However, we did not observe any difference in amount or distribution of LIN-17::GFP in *sel-5 vps-29* compared to control animals (Figure S5).

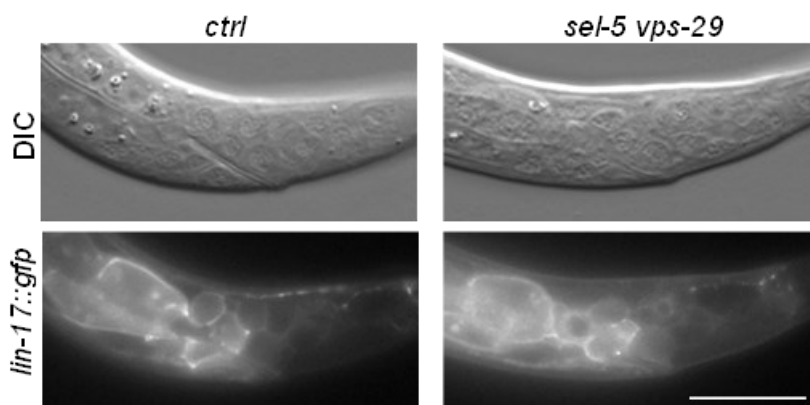


**Figure S5. Expression and distribution of *lin-17::gfp* in *egl-20/Wnt* producing cells.** A group of epithelial cells around the rectum producing EGL-20 that regulates QL.d migration strongly express *lin-17::gfp*. Double mutants *sel-5 vps-29* did not show any difference in the level or distribution of

LIN-17::GFP compared to control animals. Details of the posterior part of L2 larvae around the rectum are depicted. Scale bar represents 20  $\mu\text{m}$ .

We also observed a strong *lin-17::gfp* expression in the excretory cell and body wall muscle cells (Figure S6). Our observation of LIN-17::GFP in the long canals that grow from the excretory cell also supports previously suggested *lin-17* role in regulation of the excretory canals' length (Hedgecock et al., 1987). Taking advantage of *lin-17::gfp* expression in excretory cell we also noticed the effect of *sel-5 vps-29* double mutation on the length of posterior excretory canals. The *sel-5* role in the regulation of excretory cell canals length will be described in the next chapter.

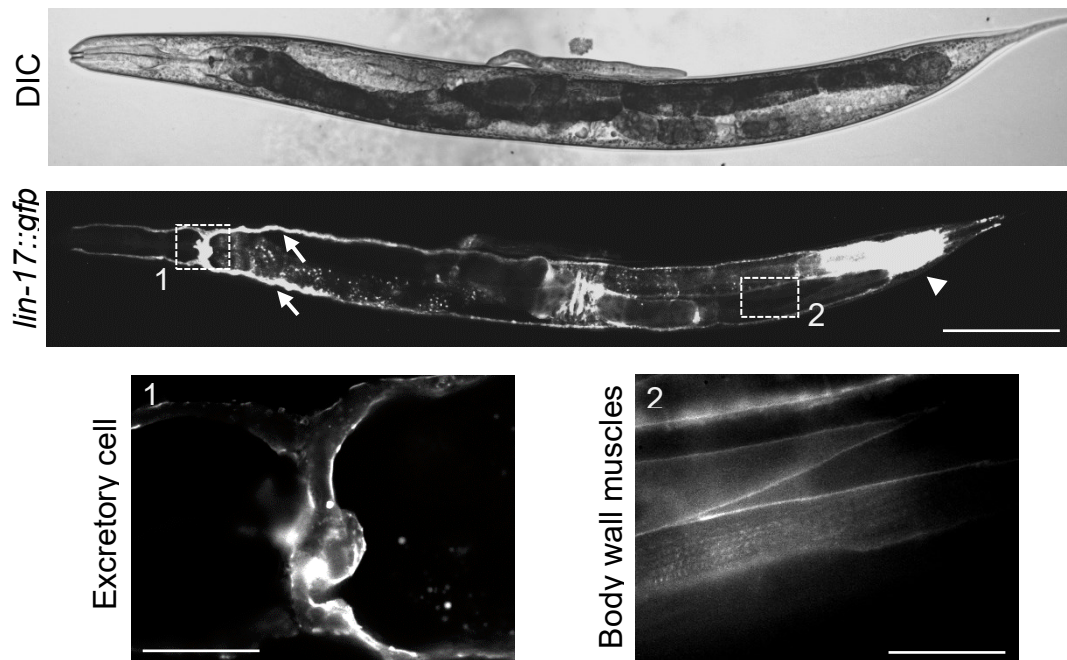


**Figure S6. Ectopic *lin-17::gfp* overexpression in adult *C. elegans*.** LIN-17::GFP signal was most prominently visible in the body of the excretory cell (expanded selection 1) and its long posterior canals (white arrows). Expanded selection 2 clearly depicts a presence of LIN-17::GFP in the body wall muscle tissue. The strong signal in the posterior region of the worm (white arrowhead) is located in gut cells which is an artefact of transgenic *gfp* expression which is often present in these overexpression experiments. The anterior of the worm is to the left, posterior to the right. Scale bar represents 100 $\mu$ m in a whole worm picture and 20 $\mu$ m in selections.

### 3.2. Effects of *sel-5* on excretory cell canals morphology

The excretory system in *Caenorhabditis elegans* consists of only three cells: a pore cell, a duct cell, and an excretory cell. The unilateral pore and duct cells interact together and connect the bilateral H-shaped lumen of the excretory cell with the surrounding environment. The lumen of the excretory system forms a continuous compartment throughout the whole length of each worm (Nelson et al., 1983). The exact function of the excretory system in *C. elegans* is still not known. It was suggested that its main task is an adjustment of the worm's inner osmolarity in

accordance with that of its surroundings. A complete loss of the excretory system in larval stages leads to developmental arrest and death (Nelson & Riddle, 1984).

In our experiments with *lin-17::gfp* overexpression we observed a strong signal present in excretory cell and its long posterior canals (Figure S6). Moreover, we also observed that the length and morphology of excretory cell canals in L1 larvae differed in *sel-5 vps-29* compared to control animals (Figure S7). While at the end of L1 larval stage excretory canals normally extend well beyond the midpoint of a larval length, *sel-5 vps-29* double mutants showed visibly shortened and sometimes malformed canals (Figure S7).

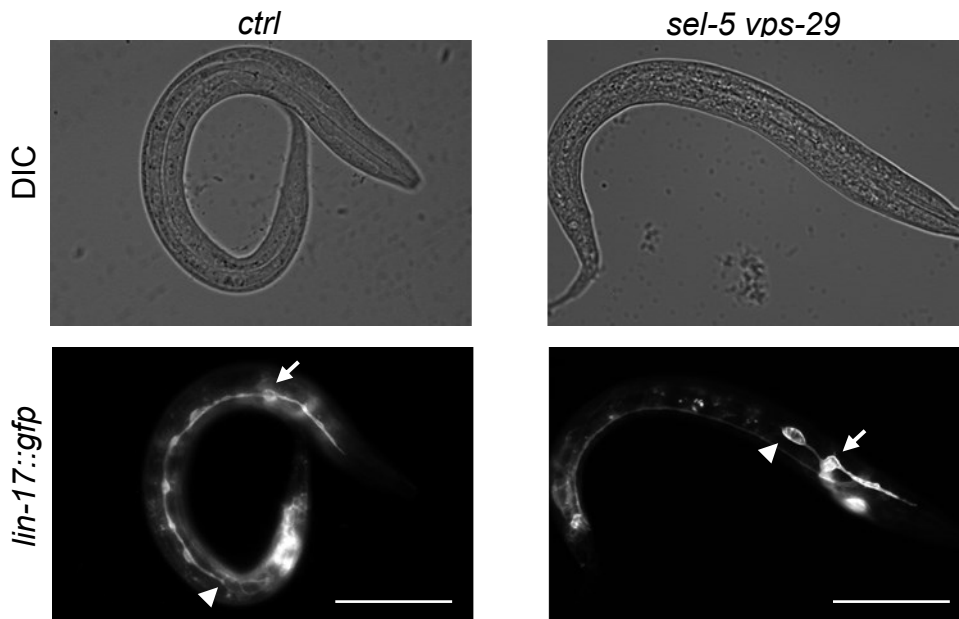



**Figure S7. Length of L1 larvae posterior excretory canals in control and *sel-5 vps-29* double mutant.** During the larval development of *C. elegans* excretory cell (white arrows) extends a pair of posterior excretory canals. These are normally already reaching almost to the rectum of animals at the end of L1 stage (white arrowhead in ctrl worm). However, in *sel-5 vps-29* double mutants posterior canals extension tend to be visibly shorter (white arrowhead in *sel-5 vps-29*). The head is to the right of the picture. Scale bar represents 20 $\mu$ m.

Similarly to our experiments with tissue-specific rescue of QL.d migration defect, we tested ability to rescue *sel-5 vps-29* excretory canals shortening for *sel-5* under the control of variable tissue-specific promoters. These experiments showed that *sel-5* combines a cell-autonomous function in the excretory cell itself with a cell non-autonomous function in the hypodermis (Figure 4 in article 2). The excretory cell canals outgrowth was previously shown to depend on the PAT-3/integrin (Hedgecock et al., 1987). We argued that PAT-3 plasma membrane levels or intracellular trafficking could be compromised in *sel-5 vps-29* background. We therefore tested whether overexpression of *pat-3* could rescue the shortened excretory canals of *sel-5 vps-29* double mutants. To this end *pat-3* rescue construct was expressed under the control of excretory cell-specific promoter. We did not observe any difference in the excretory canal shortening phenotype (data not shown). We also did not see any change of *pat-3::gfp* distribution in *sel-5 vps-29* when compared to control animals (Figure S8).

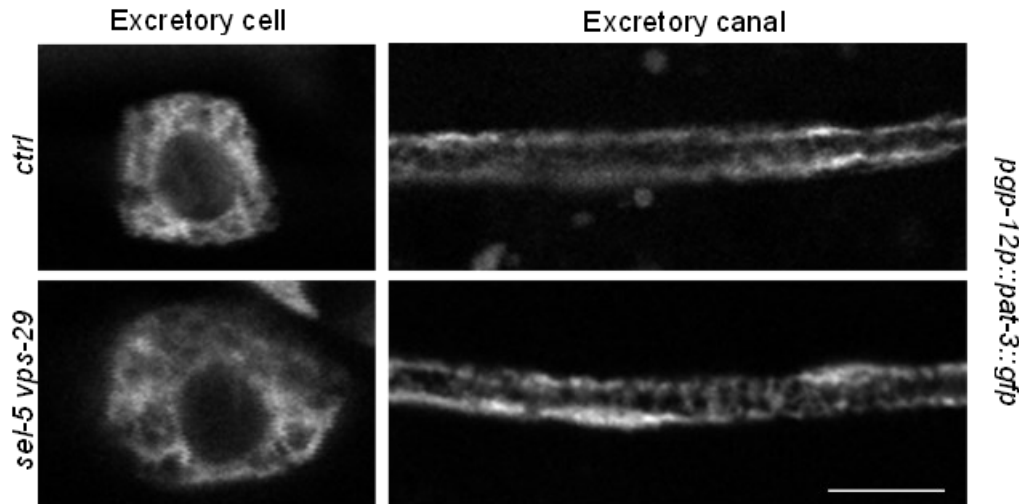


**Figure S8. Distribution of *C. elegans* integrin homolog *pat-3::gfp* in control animals and *sel-5 vps-29* mutants.** No change in level or localization of PAT-3::GFP was observed in *sel-5 vps-29* double mutant animals. Excretory cells are on the left and the section of excretory canals on the right. Scale bar corresponds to 10  $\mu$ m.

The mammalian SEL-5 homolog AAK1 was described as a regulator in the process of AP2-mediated endocytosis (Conner & Schmid, 2002; Ricotta et al., 2002). In *C. elegans* it was shown that endocytosis defects caused by mutation in *fcho-1/FCho* can be rescued by mutation in the AP2M1 subunit DPY-23 which eliminates the T160 phosphorylation site (Hollopeter et al., 2014). This site might be phosphorylated by SEL-5. We reasoned that if the role of SEL-5 is to phosphorylate T160, then loss of *sel-5* should rescue *fcho-1* phenotypes in a similar manner as nonphosphorylatable *dpy-23*. We first tested whether mutation *fcho-1* has an effect on the excretory cell canal outgrowth. Posterior excretory cell canals tended to overgrow their normal stop position around the rectal region in *fcho-1* mutants compared to controls and *sel-5* mutants (Figure S9). When *sel-5* and *fcho-1* mutations were combined we did not observe any change in the excretory canals' length compared to the control (Figure S9). This suggests that SEL-5 does not affect the excretory canal length by DPY-23 phosphorylation. We further uncovered that DPY-23 phosphorylation at T160 is not necessary for proper excretory canal extension (Figure 4 in article 2).



	0	1	2	3	4	5	6	N
<i>ctrl</i>	0	0	0	0	0	100	0	230
<i>sel-5</i>	0	0	0	0	5	95	0	187
<i>fcho-1</i>	0	0	1	1	3	83	12	184
<i>fcho-1; sel-5</i>	0	0	0	1	1	83	15	198

**Figure S9. Effect of *fcho-1* on the length of excretory cell canals.** Mutation in *fcho-1* caused a mild overgrowing phenotype in posterior excretory canal. The penetrance of this phenotype was same in single *fcho-1* mutation compared to *fcho-1; sel-5* double mutants. Transgenic *mamEx11* strain was used to visualize the excretory cell and its canals. Animals were divided into seven regions along their antero-posterior axis and posterior canals were scored accordingly.



To test whether the excretory cell canals shortening that we observed in *sel-5 vps-29* double mutants has any physiological consequences, we challenged these worms with hyperosmotic stress. Compared to wild-type animals, *sel-5 vps-29* mutants tended to have a longer recovery time after a 10-minute hyperosmotic shock. However, this extension of the recovery time did not show statistical significance and times measured in each worm fluctuated between experiments (Figure S10). We also tested these strains for their ability to survive a long-term hyperosmotic shock. As expected, we observed a smaller percentage of surviving worms with a longer exposure to high NaCl concentrations (Figure S10). However, as was the case with a short hyperosmotic shock, the results of long-term hyperosmotic experiments fluctuated wildly between measurements. Thus, we were unable to discern any consistent trends in survival among tested strains.

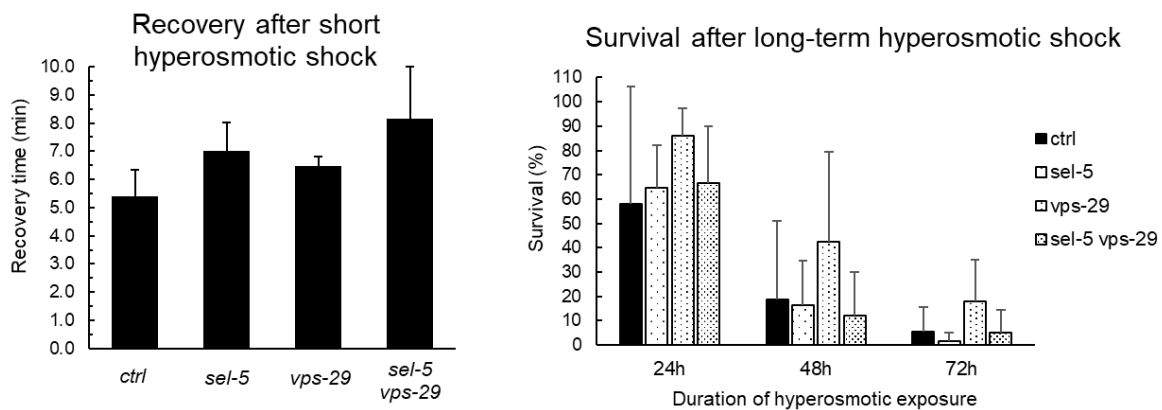


**Figure S10. Short- and long-term hyperosmotic shock effects on *C. elegans*.** A recovery after a short 10-minute hyperosmotic shock tends to be longer for double mutant *sel-5 vps-29* compared to a control and single mutant worms. However, these results are not statistically significant. Similarly, a long-term hyperosmotic shock lasting 24, 48 or 72 hours does not seem to differently affect the survival of control, single, or double mutant worms. Results in both graphs are shown as averages of three independent experiments. Individual experiments gave results with a conspicuous variability and no statistical significance was observed.

The excretory system also consists of a dispensable binucleate gland cell with unknown function, and a laterally symmetrical pair of CAN neurons. CAN neurons are born in the anterior of *C. elegans* and during development migrate posteriorly to their final position in the middle section of the worm body. Both CANL and CANR have two long axons running along the posterior canals of the excretory cell. Absence of functional CAN neurons blocks a proper morphogenesis of excretory canals and is typically lethal (unpublished data Buechner et al., 1992). We utilized *kyIs4* transgenic worms to visualize the position of CAN neurons and observed their undermigration in a subset of double mutants *sel-5 vps-29* (Table 1 in article 2). However, the morphology of CAN neurons seems to be intact suggesting that they developed properly. It was previously shown that even in the case of undermigrated CAN neurons, the excretory canals reached their usual length as long as CAN development is not impaired (Manser & Wood, 1990). Therefore, it seems unlikely that a slight difference in CAN neurons positions could be the cause of the excretory cell canals shortening.

## 4. Discussion

In this work the data from two attached publications as well as our unpublished results are compiled to discuss the non-enzymatic roles of phosphatases and kinases. Two proteins, MTMR9 and SEL-5/AAK1, were central in our research. While the MTMR9 was previously described as a putative pseudophosphatase without any known enzymatic activity, this was not the case of SEL-5/AAK1 kinase. Earlier studies of SEL-5/AAK1 always presumed a necessity of kinase activity for its respective functions. Contrary to this belief our work suggests that while kinase activity is indeed present and relevant, there is, however, a subset of regulatory roles of SEL-5/AAK1 that seems independent of this enzymatic activity. We studied both proteins predominantly in their relationship to Wnt signaling pathway. Nevertheless, especially in the case of SEL-5/AAK1 our results pointed to both Wnt pathway related and unrelated regulatory activities. Wnt thus mostly, but not exclusively, serves as a connection between the roles of the proteins studied in this work.

### 4.1. MTMR9 regulation of autophagy and early secretory pathway

Based on the previous research of MTM-6/MTM-9 complex in *C. elegans* and *D. melanogaster*, it is presumed to play a role in the transport and secretion of Wnt ligand from the Wnt producing cells (Silhankova et al., 2010). We studied the potential role of MTM-9 human homolog MTMR9 in regulation of protein secretion generally, and its specific regulation of Wnt ligand secretion. Firstly, we checked for the distribution of fluorescently tagged MTMR9 within RPE-1 cells. As previously described in the work of others MTMR9 showed nonspecific cytosolic distribution as well as distribution on vesicular structures in perinuclear area (Lorenzo et al., 2006). Further colocalization experiments identified these structures as both *cis*- and *trans*-GA. The MTMR9 positive structures in proximity of the nucleus showed only a limited mobility while the more dynamic pool on vesicles dispersed throughout the cytoplasm moved quickly towards the static pool around the nucleus. Movement of these vesicles resembles the flow of vesicular transport from the ER to the more centralized GA. Relatively stable points of exit from the ER, so called ER exit sites (ERES), were suggested as sites of cargo packaging before it begins its anterograde transport to its final locations. These ERES sites localize to the ER branches that are continuously dispersed throughout the cytoplasm of cells (Hammond & Glick, 2000). While in simplified models of anterograde cargo movement direct transport from the ER to the GA is often depicted, it seems to be likely that at least a subset of cargo additionally transfers through an intermediate compartment (IC) on its way to the GA. This compartment occurs in literature under a variety of names, ER-GA intermediate compartment (ERGIC) or vesicular-tubular cluster. One of the markers of early secretory pathway is small GTPase Rab1 which is consistently found in the pre-Golgi compartments including the ERGIC (Saraste & Marie, 2018). We observed a colocalization of MTMR9 and Rab1 fluorescent signal. Interestingly, Rab1 localization shifted upon coexpression with MTMR9 compared to its localization when expressed alone. Rab1 expressed by itself localized centrally next to a nucleus to what seemed to be late pre-GA. Once MTMR9 was coexpressed with Rab1 its central localization weakened and appeared to be dispersed on vesicles throughout the cytoplasm. This dispersed vesicular localization of Rab1 was also

observed after *MTMR9* knock-out. It thus seems that disruption of normal level of *MTMR9* either by knock-out or by expression of exogenous *MTMR9* leads to a similar phenotype regarding the localization of GTPase Rab1. The mechanism of this disruption is, however, not known. Rab1 localization could be possibly affected by the PIP composition in the prospective target membrane. PI3P was shown to be able to interact with Rab1 in-vitro (Mathiowetz et al., 2017). While *MTMR9* itself is enzymatically inactive pseudophosphatase it, nevertheless, belongs to a group of phosphatases using various PIPs as substrates. It was previously shown to directly interact with catalytically active members of *MTMRs* subgroup including *MTMR6*, *7* and *8* (Lorenzo et al., 2006; Mochizuki & Majerus, 2003; Zou et al., 2009). Previous research suggests that activity and/or PIP substrate specificity of *MTMR6* and *MTMR8* are affected by *MTMR9* while their localization was unchanged (Zou et al., 2009, 2012). In *C. elegans* a predominant localization of *MTM-6* and *MTM-9* is also in the cytoplasm and to a lesser degree in the regions adjacent to the PM (Dang et al., 2004). As is the case of the *MTMR6*-*MTMR9* complex in HeLa cells, *in vivo* *MTM-6* localization was not affected by *mtm-9* mutation (Dang et al., 2004; Zou et al., 2009). This suggests that similarly to cultured human cells, worm *MTM-6* activity rather than localization is regulated by dimerization with *MTM-9*. Contrary to this, we observed a significant relocation of both *MTMR6* and *MTMR8* upon coexpression with exogeneous *MTMR9*. Their mostly cytoplasmic staining shifted towards vesicular clusters in the proximity of nucleus. One obvious explanation for this discrepancy would be the usage of different cell lines. While we used RPE1 cells Zou et al. used HeLa cells. Supporting our findings, active *MTMR2* localization was also shown to be affected by pairing with its inactive partner *MTMR5* in COS-1 cells (Kim et al., 2003). Similarly, Kim et al. reported that loss of coiled-coil (CC) domain in *MTM1* led to a diffusion of *MTM1* staining pattern. The CC domains are the main way of forming various *MTMRs* heterodimers (Mochizuki & Majerus, 2003). It is thus possible that heterodimerization of *MTMR9* regulates activity of its partner *MTMRs* through both substrate selection (shown in the work of others) and localization (shown in this work). Given that *MTMR9* regulates the activity of three different *MTMRs* it is currently unknown which of these heterodimers influences proper localization of Rab1. As previously mentioned Rab1 interacts with PI3P, at least in-vitro (Mathiowetz et al., 2017). PI3P in turn is a preferred substrate of *MTMR8*-*MTMR9* heterodimer whose activity reduces the cellular PI3P content (Zou et al., 2012). Accordingly, in our work we were able to detect not only colocalization of Rab1 with *MTMR9* but additionally with *MTMR8*. At the same time, we did not observe colocalization of Rab1 with *MTMR6*. Contrary to our findings Rab1 was previously described to colocalize with *MTMR6* (Mochizuki et al., 2013). This discrepancy could be explained either by the difference in used cell lines, as mentioned in our published paper, or by the difference between *RAB1A* and *RAB1B*. While we used *RAB1A* Mochizuki et al. used *RAB1B* in most of their work. They found that *MTMR6* was preferentially bound to GDP-restricted *RAB1B* mutants, however, they were also able to detect a weak interaction with both *RAB1A* and *RAB1B*. While both proteins are very similar, their expression differs in various cell lines and their function is not necessarily redundant (Yang et al., 2016). Variable research groups identified *RAB1A*, *RAB1B* or both as early regulators of autophagy. In their recent paper Gyurkovska et al. claim that while *RAB1A* plays a regulatory role in both early secretory pathway and autophagy, *RAB1B* is only involved in secretion (Gyurkovska et al., 2023).

The exact role of the three interacting partners, *RAB1*, *PI3P*, and *MTMR9* in the stability of the ER-to-GA transport is currently missing. There are some data available on the role of the

three similar partners, RAB21, PI3P, and MTMR13 in the regulation of endosomal cargo flow in *D. melanogaster* (Jean et al., 2012). This situation is, however, somewhat unique as Sbf/MTMR13 contains DENN domain which can work as a guanine nucleotide exchange factor (GEF) for various RABs (Yoshimura et al., 2010). Sbf/MTMR13 thus serves two concurrent functions in *D. melanogaster*. First, it switches RAB21 on by GEF activity of its DENN domain, and second, it regulates PI3P turnover by interacting with its active Mtm partner (Jean et al., 2012). Unlike Sbf/MTMR13 or MTMR5, MTMR9 does not contain DENN domain. Contrary to DENN, all mammalian MTMRs, both active and inactive, have PH-GRAM domain in their N-terminal region (Raess et al., 2017). PH-GRAM is thought to be primarily responsible for MTMRs interaction with PIPs (Berger et al., 2003; Lorenzo et al., 2005). However, MTMR6 interaction with RAB1B was abolished upon deletion of PH-GRAM suggesting the role of this domain in binding multiple partners including RABs (Mochizuki et al., 2013). Given that the PH-GRAM domain is also present at the N-terminal region of MTMR9, this could possibly explain the mode of its interaction with RAB1A in the absence of DENN domain. MTMR-mediated regulation of PI3P at the ER and GA is also important for the process of autophagy in cells. Overexpression of inactivated version of MTMR3 as well as knock-down of MTMR3 in A549 cells led to an increased autophagosomal formation (Taguchi-Atarashi et al., 2010). This elevated autophagosomal formation was preceded by an increase in PI3P. The importance of PtdIns kinases PI3K for local increase in PI3P and its role in autophagosomal regulation was described previously (Blommaert et al., 1997). Increase in PI3P subsequently leads to an increase in the presence of its binding partner RAB1 at the nascent autophagosomes. Overexpression of Rab1 leads to an increase in the number of autophagosomes, and conversely, Rab1 knock-down decreases autophagosomal formation (Zoppino et al., 2010). This supports the data of Taguchi-Atarashi et al. where elimination of MTMR3 phosphatase function also leads to increase in autophagy (Taguchi-Atarashi et al., 2010). Presumably this increase is facilitated by accumulation of PI3P which in turn leads to an increased recruitment of RAB1 and other autophagosome-stimulating proteins. Similarly, MTMR6 and MTMR14 were shown to negatively regulate autophagosomal formation via PI3P in various cell lines (Vergne et al., 2009). Interestingly, MTMR14 protein level was also shown to correlate with the age of the human brain. The MTMR14 accumulation inhibits the ability of aged neurons to undergo autophagy and subsequently causes accumulation of damaged cells in neural tissue (Kovács et al., 2022). In addition, and perhaps more relevant to our data, MTMR8-MTMR9 complex was also identified in autophagosomal regulation (Zou et al., 2012). MTMR8-MTMR9 overexpression caused accumulation of p62, a protein targeted for autophagosomal degradation, and RNAi of these two MTMRs led to p62 decrease (Zou et al., 2012). Based on these data it seems that multiple MTMRs could be involved in negative regulation of autophagy via PI3P level. While Zou et al. reported no change in the level of autophagosomal activity upon RNAi of MTMR9 only, we observed a significant autophagy increase in MTMR9 knock-out in HeLa cells. This could be explained by a higher effectivity of knock-out compared to RNAi knock-down method.

Both ER-to-GA transport and autophagy initiation are located at the beginning of the secretory pathway. We and others detected RAB1, MTMR8, and MTMR9 on the *cis*-GA as well as on the vesicles dispersed throughout the cytoplasm. The dispersed vesicular pools of these colocalizing proteins would presumably represent the ERGIC mediating the ER-to-GA transport and should be immune to Brefeldin A-mediated GA disassembly (Ward et al., 2001). We indeed observed a dispersal of the GA upon Brefeldin A treatment and no significant effect

on vesicular localization of RAB1 or MTMR9. Similarly, there should not be a gross disruption of autophagy which arises from organelles spatially preceding the GA. While we did not test for changes in autophagosomal process, previous research suggests that this process is indeed intact in cells after Brefeldin A exposure (Zoppino et al., 2010). Brefeldin A blocks transport from ER and ERGIC to GA which leads to its destabilization. In the case of MTMR9 role in the early secretory pathway an effect similar to that of Brefeldin A on GA stability would be expected. We indeed observed a fracturing of a relatively compact *cis*-GA in MTMR9 knock-out cells. The number of GA particles increased and at the same time the average area of individual particles got smaller compared to control cells. This GA fragmentation phenotype is not as severe as the Brefeldin A treatment. GA fragmentation of the similar extend as we observed in MTMR9 knock-out cells was also observed in RAB1A or RAB1B knock-out cells (Gyurkovska et al., 2023). Another identified protein regulator of both autophagy and secretory is WASP homolog associated with actin, membranes, and microtubules (WHAMM) (Campellone et al., 2008; Kast et al., 2015). WHAMM is an activator of Arp2/3 which in turn stimulates actin nucleation and polymerization. Similarly to MTMR9, RAB1A, and RAB1B knock-outs, and Brefeldin A treatment, depletion of WHAMM leads to the GA dispersal (Campellone et al., 2008). Overexpression of WHAMM can cause excessive tubulation of ERGIC vesicles. We observed WHAMM-EGFP decorated tubular structures in the subset of cells. The formation of these tubulations seemed to be largely abolished in MTMR9 knock-out cells. Anterograde transport of temperature-sensitive viral protein VSV-G was shown to be disrupted by both overexpression and deletion of WHAMM (Campellone et al., 2008). As our results and results of others suggest the role of MTMR9 and associated proteins in early secretory pathway we decided to focus more specifically on MTMR9 role in this process.

## 4.2. MTMR9 regulation of secretory pathway

Knock-down of MTMR6, a binding partner of MTMR9, was shown to increase the rate of the ER-to-GA transport of VSV-G (Mochizuki et al., 2013). In our MTMR9 overexpression experiments we observed an opposite effect on the efficacy of VSV-G transport from the ER to the GA and the PM. At the restrictive temperature VSV-G accumulates in the ER until the shift to secretion-permissive temperature when VSV-G is exported from the ER and gradually accumulates in the GA before its transport to the PM. While after 3 hours in the permissive temperature most of the control cells have majority of VSV-G in the GA, in MTMR9 overexpressing cells this was not the case. Only a third of these cells have the majority of VSV-G in the GA. The rest presented VSV-G either still in the ER or at the intersection of ER and GA, presumably in the ERGIC. This would suggest that as was the case of MTMR regulation of autophagy, the secretory pathway is also regulated by MTMRs. While VSV-G is widely used for transport assay experiments, it is a viral origin protein and thus not a natural cargo of cellular secretion. We used WNT3A as a more biological cargo of secretory pathway in cells. WNT3A is a ligand in the Wnt signaling pathway that is translated in the ER and subsequently transported to the GA and the PM (Tanaka et al., 2000). Proper posttranslational modifications and assistance of transmembrane Wntless protein are necessary for efficient secretion of WNT3A (Bänziger et al., 2006; Bartscherer et al., 2006; Coombs et al., 2010; Goodman et al., 2006). We utilized the retention using selective hook (RUSH) system that was previously used to visualize the transport route and dynamic of WNT3A secretion (Moti et al., 2019). Our comparison of MTMR9 knock-out and control cells revealed a decrease in WNT3A

secretion efficiency. Similarly to the VSV-G experiment in MTMR9 overexpressing cells, we were unable to detect WNT3A downstream of the ER in most MTMR9 knock-out cells. At the same time, WNT3A was detectable in the GA and at the ER-to-GA intersection in the majority of control cells. In our hands both overexpression and knock-out of MTMR9 led to the same outcome in the effects on VSV-G and WNT3A secretion, respectively. Secretion efficiency at the level of the ER-to-GA seemed to be hindered in both cases. Contrary to our findings for WNT3A in MTMR9 knock-out cells, knock-down of MTMR6 was previously shown to increase the ratio of VSV-G secretion (Mochizuki et al., 2013). Similarly, knock-out of two active MTMRs, MTMR3 and MTMR4 in macrophage cells led to ER-to-GA transport acceleration of a specific immune response regulator protein STING (Putri et al., 2019). Given that MTMR9 is known to stimulate activity of MTMR6, we would expect the similar effects of MTMR9 on secretion that were observed in MTMR6 knock-down and MTMR3-MTMR4 knock-out. It is possible that knock-down of active MTMR6 only in Mochizuki et al. positively affects VSV-G secretion, while our MTMR9 knock-out has a wider effect on multiple active MTMRs binding partners. This plus other hitherto unknown MTMR9 roles could represent a more complex mode of secretory regulation with seemingly opposite effect on secretion compared to that of MTMR6 alone or MTMR3 and MTMR4 combination.

To evaluate the effect of a retarded WNT3A transport in the context of the Wnt signaling pathway we utilized super TOPFlesh reporter cell line (STF) measuring Wnt signaling activity. The disruption of WNT3A early-stage transport indeed translated into the limited Wnt pathway activity. STF cells that were transfected with WNT3A along with MTMR9 showed limited activity of Wnt reporter compared to STF cells transfected with WNT3A alone. However, in this case the autocrine Wnt signaling context of our experiment did not allow to distinguish between the possible effect of MTMR9 on the WNT3A secretion versus its effect on WNT3A transduction. We overcame this limitation by separating WNT3A producing cells from STF cells carrying Wnt activity reporter. In this adjusted experimental setup, we were able to replicate the previous result of diminished Wnt activity upon coexpression of WNT3A and MTMR9 in producing cells. A discussion of different capacities of the PM-bound and extracellular Wnt to stimulate Wnt signal transduction is still ongoing. To distinguish these two possibilities, we tweaked the previous experimental setup slightly. We used conditioned media from producing cells transfected with either WNT3A alone or cotransfected with WNT3A and MTMR9. Surprisingly, there did not seem to be any significant difference in the ability of these two conditioned media to activate Wnt response as measured by STF reporter cells. Conversely, the ability of the PM-associated pool of Wnt ligand on producing cells to activate Wnt signaling was diminished upon overexpression of MTMR9. This and the previous experiment suggest that, at least in our experimental conditions, there could be two pools of Wnt ligand that exist concurrently. As mentioned in the introductory chapter, every Wnt ligand must be modified by a lipid to become relevant for the Wnt pathway signaling (Kurayoshi et al., 2007). Hydrophobic properties of Wnt ligands thus make them dependent on other molecules for their ability to spread through the tissues and work as a *bona fide* morphogens. One solution to this problem would be a permanent association of Wnt ligands with the PM. While this could limit its ability for a long distance signaling there are ways to surpass this problem. Long filopodia were previously shown to stretch the PM to form extensive protrusions with Wnt associated to the PM of such protrusions (Stanganello et al., 2015). Moreover, these Wnt signaling filopodia were shown to have the ability to activate the Wnt signaling pathway in cells which were contacted by these filopodia (Brunt et al., 2021). Our results support the ability of the



PM-associated Wnt pool to activate Wnt pathway and additionally shown that this Wnt is dependent on MTMR9 in its transport to the PM. Contrary to this, the extracellular Wnt pool did not seem to be affected by changes in MTMR9 level. There could be an alternative, MTMR9-independent, way for Wnt to be secreted into the extracellular space. As we observed the effect of MTMR9 on Wnt transport early in the secretory route it seems possible that bifurcation of the PM-associated Wnt and extracellular Wnt secretory pathways occurs already at the level of the ER or the ERGIC. Wntless, a protein necessary for Wnt transport towards the PM, was originally thought to only bind Wnt in the GA (Belenkaya et al., 2008b). However, it was later shown that Wntless is recycled from the PM all the way to the ER (Yu et al., 2014). Complex of Wntless and Wnt in the ER recruits Sar1-specific GEF, SEC12, which activates Sar1 and initiates formation of COPII vesicle at the ERES (Sun et al., 2017). HEK293T cells transiently overexpressing SEC12 had higher levels of secreted WNT3A in the medium while SEC12 knock-down had an opposite effect (Sun et al., 2017). Another important regulator of Wnt secretion is transmembrane protein TMEM132A which was shown to colocalize and directly interact with Wntless (Li & Niswander, 2020). Interestingly, mouse embryonic fibroblasts (MEFs) with *Tmem132a* deletion allele showed a lower level of WNT3A and WNT5A in their cell culture medium. However, Li and Niswander also measured lower cytoplasmic level of both Wnts, which could be the reason for their subsequent lower level in cell culture medium (Li & Niswander, 2020). Overall, our results suggesting two separate ways of Wnt transport giving rise to two separate, concurrent Wnt ligand pools are so far not supported by conclusive evidence in literature.

### 4.3. SEL-5/AAK1 regulation of QL.d migration in *C. elegans*

We analyzed the effect of SEL-5 kinase in the series of Wnt-dependent and Wnt-independent developmental processes in *C. elegans*. For most of these processes we did not observe any difference between control animals and either *sel-5(ok149)* or *sel-5(ok363)* mutant alleles. Both mutants tend to have slightly lower number of progeny (lowered fecundity) and very low penetrance of CAN neuron undermigration phenotype. We therefore used *yps-29* mutation to sensitize *C. elegans* to the effects of *sel-5* gene disruption. We were able to observe a multitude of phenotypes in *sel-5 yps-29* double mutants that were not present in single mutants. One of the most prominent phenotypes was a reversed migration of QL neuroblast and its descendants (QL.d migration defect). QL.d migration is known to be regulated by the Wnt signaling pathway and this phenotype has been previously used in assays evaluating the Wnt pathway in *C. elegans* (Korswagen et al., 2000; Maloof et al., 1999; Whangbo & Kenyon, 1999). To determine the genetic interaction between *sel-5* and other members of the Wnt signaling pathway we generated double mutants of *sel-5* with either *lin-17* or *mig-1*, two homologs of the Wnt receptors Frizzled that were previously shown to be involved in QL migration (Harris et al., 1996). While we did not observe any change in QL.d migration defect penetrance in *mig-1; sel-5* compared to *mig-1* single mutant, there was a significant increase of this phenotype in *lin-17; sel-5* compared to *lin-17* single mutant. The reason for this discrepancy could be the already high penetrance of QL.d migration defect in *mig-1* single mutant reaching roughly 80%. Posterior QL.d migration depends on cell autonomous expression of Wnt signaling target gene *mab-5* (Salser & Kenyon, 1992). Of the five Wnt ligand homologs identified in *C. elegans* it is EGL-20 that is mainly responsible for activation of Wnt signaling and *mab-5* transcription in

QL migration (Zinovyeva & Forrester, 2005). Interestingly, while Wnt is necessary for posterior migration of QL descendant cells, the initial polarization and short posterior migration of QL neuroblast are Wnt-independent processes (Honigberg & Kenyon, 2000). A group of proteins interacting with Netrin receptor UNC-40 establish this initial short migration and its disruption leads to a random initial QL polarity. Regardless of the Wnt signaling state, QL.d subsequently migrate in the direction of initial polarization (Sundararajan & Lundquist, 2012). We tracked the initial polarization and migration of QL neuroblast in *sel-5 vps-29* double mutants to determine whether *sel-5* plays a role in this initial polarization rather than the subsequent Wnt signaling. We did not observe any changes in the initial QL neuroblast polarization, suggesting the *sel-5* role in Wnt signaling as more likely. We looked whether other developmental processes known to be regulated by the Wnt signaling were also affected in *sel-5 vps-29* mutants. We observed an increased penetrance of reversed polarity in ALMs and PLMs neurons compared to control animals or any single mutants. Contrary to this, there was no change in migration of ALM neurons from their initial position in the anterior or in the length of PLMs posterior neurites. We also observed a mild increase in undermigrated CAN neurons in *sel-5 vps-29* compared to single mutants. With the exception of QL.d migration defect, other phenotypes showed only low or mild penetrance. This could be explained by a very strong effect of the single EGL-20/Wnt on the QL.d migration compared to weak effects of single Wnt mutations in other phenotypes. ALM posterior migration did not seem to be affected by single mutations in genes coding for *C. elegans* Wnts *cwn-1*, *cwn-2*, or *egl-20*, and only mildly affected by a mutation in the Wnt receptor gene *cfz-2* (Zinovyeva & Forrester, 2005). The stronger penetration of ALMs undermigration phenotype was observable only after combining those mutations. Similarly to a strong effect of EGL-20/Wnt mutation on QL.d migration, there was previously observed a strong effect of the single LIN-44/Wnt mutation on PLMs polarity (Hilliard & Bargmann, 2006; Prasad & Clark, 2006). Our *sel-5 vps-29* mutants only show very low PLM polarity reversal. This suggests that unlike in EGL-20 dependent QL.d migration, SEL-5 role is either dispensable or redundant in polarity regulation of PLM by LIN-44.

A series of tissue-specific rescue experiments in *sel-5 vps-29* mutants suggested the role of SEL-5 kinase in the Wnt producing cells rather than receiving cells. We detected a significant rescue of QL.d migration defect upon reintroduction of *sel-5* in either rectal epithelial cells or posterior body wall muscles. While the rescue of QL.d migration defect was significant in both cases, it did not reach the basal level of *vps-29* mutants. Only after expressing *sel-5* in both tissues concurrently did we see the low penetrance of QL.d migration defect at the levels seen in background *vps-29* mutant. This is not entirely surprising as it was previously shown that rectal epithelial cells as well as ventral posterior body wall muscle quadrants produce EGL-20 in L1 larvae (Harterink et al., 2011; Whangbo & Kenyon, 1999). Alternatively, SEL-5 in body wall muscles could help to form a proper EGL-20 gradient originating from rectal epithelial cells. Our CRISPR-generated GFP-tagged endogenous SEL-5 seemed to be expressed ubiquitously. There was a strong expression in the gonad from a very early developmental stage that persisted into adulthood and was also present in maturing oocytes. Apart from other tissues with SEL-5 expression, we also detected GFP signal in rectal epithelial cells which are primary source of EGL-20 (Whangbo & Kenyon, 1999). This endogenous pattern of *sel-5* expression is in agreement with our previous experiments suggesting a role of SEL-5 in Wnt producing cells. In some, but not all tissues, SEL-5 subcellular localization resembled the localization of SEL-5 mammalian homolog AAK1 in rat neurons and HeLa cells (Conner & Schmid, 2002). This punctual localization of SEL-5 at the PM or in its proximity was mainly visible in maturing

oocytes and the seam cells. AAK1 was previously shown to regulate clathrin-mediated endocytosis via the phosphorylation of its substrate  $\mu 2$ , a subunit of AP2 complex (Pauloin & Thuriereau, 1993). Our experiments confirmed the ability of SEL-5 to regulate phosphorylation of both endogenous and overexpressed GFP-tagged DPY-23, a *C. elegans* homolog of  $\mu 2$  subunit. However, to our surprise we saw the same rescue of QL.d migration defect when we used an inactive version of SEL-5 with the mutated catalytic site or ATP binding pocket. Mutation of *dpy-23* was previously shown to cause a penetrance of QL.d migration defect similar to that caused by mutation in *egl-20* (Pan et al., 2008). Interestingly, null allele *dpy-23(e840)* led to a same degree of QL.d migration defect phenotype as *dpy-23(gm17)*, a mutation that is predicted to cause truncation of DPY-23 leaving the phosphorylation site targeted by SEL-5 intact. One of several possible explanations could be that while DPY-23 regulates migration of QL.d, this regulation may be independent of DPY-23 phosphorylation. We tested this possibility by measuring the QL.d migration defect in *dpy-23(mew25)* which carries a point mutation eliminating threonine 160 (Thr160) which is normally a target of SEL-5 phosphorylation. We did not observe any QL.d migration defect in *dpy-23(mew25)* single or *sel-5; dpy-23* double mutants. We noted a tendency in increase of QL.d migration defect in *vps-29; dpy-23* compared to *vps-29* single mutants. The penetrance of this phenotype was, however, highly variable, and much lower compared to the penetrance seen in *sel-5 vps-29* double mutants. This supports our previous data pointing towards the dispensability of SEL-5 kinase activity in regulation of QL.d migration.

#### 4.4. SEL-5/AAK1 regulation of *C. elegans* excretory system

Apart from defects in neuronal migrations and polarity we also noticed a shortening of excretory canals in *sel-5 vps-29* mutants. Long bilateral canals growing from the single excretory cell together with few other cells form an excretory system presumed to be important for osmoregulation (Kenneth Nelson et al., 1983; Nelson & Riddle, 1984). Similarly to the QL.d migration, effects of *sel-5* mutation were only obvious in *vps-29* mutated background. Posterior canals shortening was also seen in *sel-5* mutation combined with RNAi knock-down of other members of the retromer complex suggesting a cooperative regulation of canals length by SEL-5 and the retromer. While our data suggest a role of SEL-5 in the Wnt-regulated QL.d migration along with the retromer complex, it does not seem to be the case that the excretory canals growth is regulated via Wnt signaling. We measured the lengths of excretory canals in various mutants of the Wnt signaling pathway and did not observe any canal shortening comparable to that detected in *sel-5 vps-29* double mutants. Contrary to this, we observed a significant overgrowing of the normal canal length in mutants for *lin-44/Wnt*, *lin-17/Frizzled* and *mig-14/Wntless*. This supports a previous report of LIN-17/Frizzled effect on the excretory canals overgrowing (Hedgecock et al., 1987). LIN-44/Wnt, expressed in the tail hypodermis region of *C. elegans*, seems to function with its receptor LIN-17 as a stop signal in the late stage of excretory cell outgrowth. SEL-5 on the other hand affects the initial active outgrowth of excretory canals. To confirm this, we measured changes in the length of excretory cell canals after hatching and during L1 larval stage. While we did not observe any effect of *lin-44*, *lin-17*, or *mig-14* on the length of canals during the L1 development, we saw shortened canals in *sel-5 vps-29* mutants. This shortening was apparent already at the hatching and persisted throughout the L1 larval stage until 24 hours after hatching when experiment was ended. Additionally,

combination of *sel-5* with *lin-44* or *lin-17* mutation caused lower penetrance of overgrown canals compared to *lin-44* or *lin-17* single mutations, further validating the idea of Wnt-independent role of SEL-5 in active phase of the excretory canals' outgrowth.

We again performed a series of tissue-specific rescue experiments to determine the location of SEL-5 action in the excretory cell posterior canal length regulation. We observed rescue of canals shortening phenotype after reintroduction of *sel-5* to the excretory cell itself or to the hypodermis and no rescue after reintroduction of *sel-5* to body wall muscle cells. As was the case in the QL.d migration, the excretory canals outgrowth was rescued upon expression of kinase dead version of *sel-5*. We also tested the effect of *dpy-23(mew25)* on excretory cell canals. Similarly to the case of QL.d migration, DPY-23 with mutated phosphorylation site Thr160 did not have any effect on the length of excretory canals. The excretory cell canals outgrowth is thus a second developmental process regulated by SEL-5 kinase for which the kinase activity itself seems to be dispensable.

Knowledge of the SEL-5 kinase role or its potential substrates in *C. elegans* is currently limited. The suggestion of DPY-23 as a target of SEL-5 mediated phosphorylation is based on the functional interaction of mammalian homologs of these two proteins, AAK1 and AP2 $\mu$ 2, respectively (Pauloin & Thuriereau, 1993). While results of our experiments hint to a similar interaction in *C. elegans* a conclusive proof is still missing. Mutations in *sel-5* were previously described as suppressors of activation mutation in Notch receptor LIN-12 (Tax et al., 1997). Interestingly, only *lin-12* activation mutations that leave LIN-12 attached to the PM could be suppressed by elimination of *sel-5*. No suppression was observed for *lin-12* mutations that leave active intracellular fragment of LIN-12 dissociated from the PM (Fares & Greenwald, 1999). Fares and Greenwald identified two splice variants of *sel-5* gene coding for SEL-5A and a shorter version SEL-5B, which both contained identical kinase domain in their N-terminal end. At least for cell fate determination studied in Fares and Greenwald both SEL-5 versions had identical role in LIN-12/Notch signaling. Our experiments showed expression of endogenous *sel-5* in multiple tissues including gonads, vulva, hypodermis, and rectal epithelium. Fares and Greenwald similarly detected SEL-5 in gonads and developing vulva and contrary to our observation in multiple neurons and ventral nerve cord. The differences are likely caused by different experimental settings. While we used GFP knock-in by CRISPR method, Fares and Greenwald used overexpression of *sel-5* controlled by ectopic *sel-12* promoter (Fares & Greenwald, 1999). AAK1/SEL-5 role in Notch signaling seems to be conserved in mammals as different localization of activated, membrane-tethered Notch receptor was observed based on the status of AAK1. Depletion of AAK1 caused a decrease in activated Notch receptor localization to Rab5-positive endocytic vesicles while AAK1 overexpression had an opposite effect in HeLa cells (Gupta-Rossi et al., 2011). Moreover, a direct interaction between AAK1 and activated membrane-tethered Notch receptor was detected. At the same time AAK1 seemed to be unable to interact with either transmembrane full length inactive Notch receptor or its detached cytosolic fragment. This is in agreement with SEL-5 role in the *C. elegans* Notch signaling where *sel-5* mutation only suppresses membrane bound LIN-12/NOTCH activity (Fares & Greenwald, 1999). Notch signaling was previously shown to be involved in left-right cellular migrations of P11/12 cells in *C. elegans* (Delattre & Félix, 2001). However, this migration is very short and dependent on the cell-cell contacts which is in accordance with the nature of Notch signaling. No member of the Notch signaling cascade has been indicted in migration defects of QL neuroblast or QL.d so far. There is some evidence of the Notch pathway involvement in the excretory system establishment (Lambie & Kimble, 1991). Mutations in

Notch receptors *lin-12* and *glp-1* or Notch signaling regulators *lag-1* and *lag-2* led to a missing excretory cell and subsequent lethality. These mutations disrupt the lineage development of the excretory cell predecessors and do not seem to have effect on excretory canals outgrowth in later developmental stages (Moskowitz & Rothman, 1996). Currently there is no evidence suggesting that SEL-5 regulation of either excretory canals outgrowth or QL.d migration is mediated via Notch signaling. Moreover, while Notch receptor is itself not a substrate of AAK1, it seems that kinase activity of AAK1 is necessary for a full activation of Notch pathway (Gupta-Rossi et al., 2011).

Kinase activity of AAK1 was also invoked in regulation of the clathrin-mediated endocytosis (CME) of several endocytic cargo proteins (Conner & Schmid, 2002). AAK1 phosphorylation of AP2 subunit  $\mu 2$  leads to a stimulation of the CME and simultaneously, assembled clathrin stimulates AAK1 activity (Conner et al., 2003). The most obvious target of the CME in the context of our *C. elegans* experiments would be MIG-14/Wntless. Upon knock-down of several AP2 complex subunits, accumulation of MIG-14 was observed on the PM (Pan et al., 2008; Yang et al., 2008). Disruption of retromer-mediated recycling of MIG-14, which occurs downstream of the CME, led to the MIG-14 accumulation in lysosomes and subsequent degradation (Belenkaya et al., 2008b; Franch-Marro et al., 2008; Pan et al., 2008; P.-T. Yang et al., 2008). In our experiments we did not recapitulate either MIG-14 accumulation nor degradation in *sel-5* single mutants. Double mutants *sel-5 vps-29* showed a reduction of MIG-14 levels comparable to that in *vps-29* mutation alone. These results suggest that SEL-5 does not play a role in the regulation of the CME-mediated MIG-14 recycling. We also did not see any change in the amount or distribution of integrin PAT-3 which regulates excretory canal extension (Hedgecock et al., 1987). Integrins are involved in many vital cellular functions, and they are constantly trafficked between the PM and cellular interior via the CME and other endocytic routes (reviewed in Paul et al., 2015). While the role of AAK1 in endocytic trafficking regulation is mediated by phosphorylation of its substrate AP2 $\mu 2$ , we did not observe changes in QL.d migration or excretory canal length in DPY-23/AP2 $\mu 2$  mutants with missing phosphorylation site. This could either mean that endocytosis in our case is regulated independently of DPY-23 or that SEL-5 regulation is not involved in endocytosis at all. Given that the effects of AAK1/SEL-5 on the CME and other processes observed in various experimental settings required its kinase activity, it rises a question how does kinase-inactive SEL-5 in our experiments regulate excretory canals outgrowth and QL.d migration. One possibility is that SEL-5 acts as a protein adaptor connecting other players involved in the processes described above. Both SEL-5 and AAK1 were shown to interact with Eps15 homology domain containing protein REPS-1/REPS1 (Huttlin et al., 2017; Tsushima et al., 2013). REPS1 in turn interacts with RALBP1 that is able to bind AP2 $\mu 2$  and is itself an effector of small GTPase RalB which was shown to regulate transferrin receptor (TfnR) endocytosis (Jullien-Flores et al., 2000). While the region of AP2 $\mu 2$  around threonine 156 (Thr156), a target of AAK1-mediated phosphorylation, is necessary for the interaction with RALBP1, the role of Thr156 phosphorylation status in this interaction was not studied (Jullien-Flores et al., 2000). AAK1 was also detected as an important regulator of Wnt signaling in cultured human cells (Agajanian et al., 2019). Contrary to our findings for SEL-5 in *C. elegans*, AAK1 was shown to play a role in regulating levels of Wnt coreceptor LRP6 on the PM of Wnt-receiving cells. It is possible that while SEL-5 and AAK1 regulation of Wnt pathway is conserved, the mechanism differs in *C. elegans* and mammals. Once more, however, the AAK1 ability to regulate LRP6 levels was dependent on its intact kinase domain which is contradictory to our findings. AAK1

was also shown to regulate intracellular trafficking downstream of the CME (Henderson & Conner, 2007). The C-terminal region of AAK1 was necessary for TfnR recycling from endosomal compartments of HeLa cells. We tested truncated versions of SEL-5 for their ability to rescue QL.d migration defect in *C. elegans*. SEL-5 with its C-terminal half completely missing rescued this migration very poorly compared to that of the full length SEL-5. It thus seems likely that while kinase activity itself may not be necessary, both the N-terminal and C-terminal regions are still important for SEL-5 function. Another possibility is that SEL-5 forms a heterodimer with another kinase and together they phosphorylate substrates other than DPY-23. The ability to dimerize has been proposed for the mammalian GAK kinase, however, in this particular case dimerization seems to inactivate the GAK kinase and a physiological relevance of such a dimer is questionable (Chaikuad et al., 2014).



## 5. Conclusions

- Using fluorescently tagged proteins we detected enzymatically inactive myotubularin MTMR9 localization to the compartments of the early secretory pathway, the IC and the GA. Furthermore, overexpression of MTMR9 led to a redistribution of MTMR9 binding partners, two active myotubularins MTMR6 and MTMR8, from their predominantly cytoplasmic to vesicular localization. Additionally, we observed a similar pattern of MTMR9 and small GTPase RAB1 colocalization upon their simultaneous overexpression.
- Relocalization of MTMR9 upon its coexpression with RAB1 depended on the GTPase activity as the dominant-negative mutant RAB1S25N did not elicit a similar effect on MTMR9 localization change. Unlike RAB1, the MTMR9 coexpression with either RAB2 or RAB6 did not cause comparable relocalization of MTMR9 and these GTPases to vesicular structures.
- We created a MTMR9 knock-out cell line and observed a shift of fluorescently tagged RAB1 distribution from predominantly GA pool towards a vesicular pool. We also quantified a significant fragmentation and dispersal of the GA in the same MTMR9 knock-out cell line.
- MTMR9 overexpression led to a reduction in effective secretion of viral protein VSVG. Similarly, we detected a reduced effectivity of WNT3A trafficking from the ER to the GA in MTMR9 knock-out cell line. Supporting the latter observation we also measured reduction of Wnt pathway activation upon transient overexpression of MTMR9.
  
- In *Caenorhabditis elegans* we identified novel roles of protein kinase SEL-5 in two independent developmental processes; migration of QL neuroblast descendant cells (QL.d), and outgrowth of long canals from the excretory cell. While QL.d migration seems to be regulated by SEL-5 via the Wnt signaling, the regulation of the posterior excretory canals' growth, at least in its initial stages, appears to be independent of this pathway.
- A proper posterior QL.d migration in L1 larval stage requires SEL-5 regulatory role in EGL-20/Wnt producing rectal epithelial cell and posterior body wall muscle cells. Interestingly, rescue experiments showed that kinase activity of SEL-5 may be dispensable for its regulatory role. We also found that a phosphorylation status of DPY-23, a supposed target of SEL-5 kinase, does not affect QL.d migration.
- Regulation of excretory canals outgrowth, unlike that of QL.d migration, requires a cell-autonomous expression of *sel-5*. However, similarly to the QL.d migration, the kinase activity of SEL-5 does not seem to be necessary for excretory cell canals outgrowth regulation.
- While we identified the role of LIN-44/Wnt and LIN-17/Frizzled as a stop signal for excretory canals outgrowth, this final stage regulation of excretory system development appears to be SEL-5 independent. This suggests a role of SEL-5 in *C. elegans* development that is not limited to the Wnt signaling pathway and exhibits a broader regulatory scope.

## 6. Publications and author contributions

Doubravská, L., Dostál, V., Knop, F., Libusová, L., Macůrková, M. (2020). Human myotubularin-related protein 9 regulates ER-to-GA trafficking and modulates WNT3A secretion. *Experimental cell research* 386(1), 111709.

- MTMRs colocalization experiments and imaging, participation in manuscript preparation.

Knop, F., Zounarová, A., Macůrková, M. (2024). *Caenorhabditis elegans* SEL-5/AAK1 regulates cell migration and cell outgrowth independently of its kinase activity. *BioRxiv* preprint doi: <https://doi.org/10.1101/2023.03.29.534638>

- Most of the experimental work, imaging and raw data processing was done by the first author as well as participation in the manuscript preparation.

Panská, L., Nedvěďová, Š., Vacek, V., Křivská, D., Konečný, L., Knop, F., Kutil, Z., Škultétyová, L., Leontovyč, A., Ulrichová, L., Sakanari, Asahino, M., Bařinka, C., Macůrková, M., Dvořák, J. (2024). Uncovering the essential roles of glutamate carboxypeptidase 2 orthologs in *Caenorhabditis elegans*. *Bioscience reports* 44(1), BSR20230502. (Not part of the dissertation)

- Preparation of the transgenic *C. elegans* strain by microinjection.

## 7. References

- Aberle, H., Bauer, A., Stappert, J., Kispert, A., & Kemler, R. (1997).  $\beta$ -catenin is a target for the ubiquitin-proteasome pathway. *EMBO Journal*, *16*(13), 3797–3804. <https://doi.org/10.1093/emboj/16.13.3797>
- Agajanian, M. J., Walker, M. P., Axtman, A. D., Ruela-de-Sousa, R. R., Serafin, D. S., Rabinowitz, A. D., Graham, D. M., Ryan, M. B., Tamir, T., Nakamichi, Y., Zuercher, W. J., & Major, M. B. (2019). WNT Activates the AAK1 Kinase to Promote Clathrin-Mediated Endocytosis of LRP6 and Establish a Negative Feedback Loop. *Cell Reports*, *26*(1), 79–93.e8. <https://doi.org/10.1016/j.celrep.2018.12.023>
- Alonso, A., Burkhalter, S., Sasini, J., Tautz, L., Bogetz, J., Huynh, H., Bremer, M. C. D., Holsinger, L. J., Godzik, A., & Mustelin, T. (2004). The minimal essential core of a cysteine-based protein-tyrosine phosphatase revealed by a novel 16-kDa VH1-like phosphatase, VHZ. *Journal of Biological Chemistry*, *279*(34), 35768–35774. <https://doi.org/10.1074/jbc.M403412200>
- Alonso, A., Sasin, J., Bottini, N., Friedberg, I., Friedberg, I., Osterman, A., Godzik, A., Hunter, T., Dixon, J., & Mustelin, T. (2004). Protein tyrosine phosphatases in the human genome. *Cell*, *117*(6), 699–711. <https://doi.org/10.1016/j.cell.2004.05.018>
- Ardito, F., Giuliani, M., Perrone, D., Troiano, G., & Muzio, L. L. (2017). The crucial role of protein phosphorylation in cell signaling and its use as targeted therapy (Review). *International Journal of Molecular Medicine*, *40*(2), 271–280. <https://doi.org/10.3892/ijmm.2017.3036>
- Baeg, G.-H., Lin, X., Khare, N., Baumgartner, S., & Perrimon, N. (2001). Heparan sulfate proteoglycans are critical for the organization of the extracellular distribution of Wntless. *Development*, *128*(1), 87–94.
- Bänziger, C., Soldini, D., Schütt, C., Zipperlen, P., Hausmann, G., & Basler, K. (2006). Wntless, a Conserved Membrane Protein Dedicated to the Secretion of Wnt Proteins from Signaling Cells. *Cell*, *125*(3), 509–522. <https://doi.org/10.1016/j.cell.2006.02.049>
- Bardwell, L., & Thorner, J. (1996). A conserved motif at the amino termini of MEKs might mediate high-affinity interaction with the cognate MAPKs. *Trends in Biochemical Sciences*, *21*(10), 373–374. [https://doi.org/10.1016/0968-0004\(96\)30032-7](https://doi.org/10.1016/0968-0004(96)30032-7)
- Bartscherer, K., Pelte, N., Ingelfinger, D., & Boutros, M. (2006). Secretion of Wnt Ligands Requires Evi, a Conserved Transmembrane Protein. *Cell*, *125*(3), 523–533. <https://doi.org/10.1016/j.cell.2006.04.009>
- Baulac, S., Gourfinkel-An, I., Couarch, P., Depienne, C., Kaminska, A., Dulac, O., Baulac, M., LeGuern, E., & Nabbout, R. (2008). A novel locus for generalized epilepsy with

- febrile seizures plus in French families. *Archives of Neurology*, 65(7), 943–951.  
<https://doi.org/10.1001/archneur.65.7.943>
- Beacham, G. M., Partlow, E. A., Lange, J. J., & Hollopeter, G. (2018). NECAPs are negative regulators of the AP2 clathrin adaptor complex. *ELife*, 7.  
<https://doi.org/10.7554/eLife.32242>
- Belenkaya, T. Y., Wu, Y., Tang, X., Zhou, B., Cheng, L., Sharma, Y. V., Yan, D., Selva, E. M., & Lin, X. (2008a). The Retromer Complex Influences Wnt Secretion by Recycling Wntless from Endosomes to the Trans-Golgi Network. *Developmental Cell*, 14(1), 120–131. <https://doi.org/10.1016/j.devcel.2007.12.003>
- Belenkaya, T. Y., Wu, Y., Tang, X., Zhou, B., Cheng, L., Sharma, Y. V., Yan, D., Selva, E. M., & Lin, X. (2008b). The Retromer Complex Influences Wnt Secretion by Recycling Wntless from Endosomes to the Trans-Golgi Network. *Developmental Cell*, 14(1), 120–131. <https://doi.org/10.1016/j.devcel.2007.12.003>
- Berger, P., Schaffitzel, C., Berger, I., Ban, N., & Suter, U. (2003). Membrane association of myotubularin-related protein 2 is mediated by a pleckstrin homology-GRAM domain and a coiled-coil dimerization module. *Proceedings of the National Academy of Sciences of the United States of America*, 100(21), 12177–12182.  
<https://doi.org/10.1073/pnas.2132732100>
- Bhanot, P., Brink, M., Samos, C. H., Hsieh, J.-C., Wang, Y., Macke, J. P., Andrew, D., Nathans, J., & Nusse, R. (1996). A new member of the frizzled family from *Drosophila* functions as a wingless receptor. *Nature*, 382(6588), 225–231.  
<https://doi.org/10.1038/382225a0>
- Bhave, M., Mino, R. E., Wang, X., Lee, J., Grossman, H. M., Lakoduk, A. M., Danuser, G., Schmid, S. L., & Mettlen, M. (2020). Functional characterization of 67 endocytic accessory proteins using multiparametric quantitative analysis of CCP dynamics. *Proceedings of the National Academy of Sciences of the United States of America*, 117(50), 31591–31602. <https://doi.org/10.1073/pnas.2020346117>
- Bilić, J., Huang, Y.-L., Davidson, G., Zimmermann, T., Cruciat, C.-M., Bienz, M., & Niehrs, C. (2007). Wnt induces LRP6 signalosomes and promotes dishevelled-dependent LRP6 phosphorylation. *Science*, 316(5831), 1619–1622.  
<https://doi.org/10.1126/science.1137065>
- Blommaart, E. F. C., Krause, U., Schellens, J. P. M., Vreeling-Sindelárová, H., & Meijer, A. J. (1997). The phosphatidylinositol 3-kinase inhibitors wortmannin and LY294002 inhibit in isolated rat hepatocytes. *European Journal of Biochemistry*, 243(1–2), 240–246.  
<https://doi.org/10.1111/j.1432-1033.1997.0240a.x>
- Blondeau, F., Laporte, J., Bodin, S., Superti-Furga, G., Payrastre, B., & Mandel, J.-L. (2000). Myotubularin, a phosphatase deficient in myotubular myopathy, acts on phosphatidylinositol 3-kinase and phosphatidylinositol 3-phosphate pathway. *Human*

*Molecular Genetics*, 9(15), 2223–2229.  
<https://doi.org/10.1093/oxfordjournals.hmg.a018913>

- Boll, W., Rapoport, I., Brunner, C., Modis, Y., Prehn, S., & Kirchhausen, T. (2002). The  $\mu 2$  subunit of the clathrin adaptor AP-2 binds to FDNPVY and YppØ sorting signals at distinct sites. *Traffic*, 3(8), 590–600. <https://doi.org/10.1034/j.1600-0854.2002.30808.x>
- Boudeau, J., Miranda-Saavedra, D., Barton, G. J., & Alessi, D. R. (2006). Emerging roles of pseudokinases. *Trends in Cell Biology*, 16(9), 443–452.  
<https://doi.org/10.1016/j.tcb.2006.07.003>
- Brunt, L., Greicius, G., Rogers, S., Evans, B. D., Virshup, D. M., Wedgwood, K. C. A., & Scholpp, S. (2021). Vangl2 promotes the formation of long cytonemes to enable distant Wnt/ $\beta$ -catenin signaling. *Nature Communications*, 12(1). <https://doi.org/10.1038/s41467-021-22393-9>
- Campellone, K. G., Webb, N. J., Znameroski, E. A., & Welch, M. D. (2008). WHAMM Is an Arp2/3 Complex Activator That Binds Microtubules and Functions in ER to Golgi Transport. *Cell*, 134(1), 148–161. <https://doi.org/10.1016/j.cell.2008.05.032>
- Chaikuad, A., Keates, T., Vincke, C., Kaufholz, M., Zenn, M., Zimmermann, B., Gutiérrez, C., Zhang, R.-G., Hatzos-Skintges, C., Joachimiak, A., Knapp, S., & Müller, S. (2014). Structure of cyclin G-associated kinase (GAK) trapped in different conformations using nanobodies. *Biochemical Journal*, 459(1), 59–69. <https://doi.org/10.1042/BJ20131399>
- Chen, M. J., Dixon, J. E., & Manning, G. (2017). Genomics and evolution of protein phosphatases. *Science Signaling*, 10(474). <https://doi.org/10.1126/scisignal.aag1796>
- Chen, W.-J., Goldstein, J. L., & Brown, M. S. (1990). NPXY, a sequence often found in cytoplasmic tails, is required for coated pit-mediated internalization of the low density lipoprotein receptor. *Journal of Biological Chemistry*, 265(6), 3116–3123.
- Chua, J. P., Bedi, K., Paulsen, M. T., Ljungman, M., Tank, E. M. H., Kim, E. S., McBride, J. P., Colón-Mercado, J. M., Ward, M. E., Weisman, L. S., Weisman, L. S., & Barmada, S. J. (2022). Myotubularin-related phosphatase 5 is a critical determinant of autophagy in neurons. *Current Biology*, 32(12), 2581-2595.e6.  
<https://doi.org/10.1016/j.cub.2022.04.053>
- Cohen, P. T. W. (2002). Protein phosphatase 1 - Targeted in many directions. *Journal of Cell Science*, 115(2), 241–256.
- Colella, B., Faienza, F., Carinci, M., D’Alessandro, G., Catalano, M., Santoro, A., Cecconi, F., Limatola, C., & di Bartolomeo, S. (2019). Autophagy induction impairs Wnt/ $\beta$ -catenin signalling through  $\beta$ -catenin localisation in glioblastoma cells. *Cellular Signalling*, 53, 357–364. <https://doi.org/10.1016/j.cellsig.2018.10.017>

- Conner, S. D., & Schmid, S. L. (2002). Identification of an adaptor-associated kinase, AAK1, as a regulator of clathrin-mediated endocytosis. *Journal of Cell Biology*, *156*(5), 921–929. <https://doi.org/10.1083/jcb.200108123>
- Conner, S. D., & Schmid, S. L. (2003). Differential requirements for AP-2 in clathrin-mediated endocytosis. *Journal of Cell Biology*, *162*(5), 773–779. <https://doi.org/10.1083/jcb.200304069>
- Conner, S. D., Schröter, T., & Schmid, S. L. (2003). AAK1-mediated  $\mu$ 2 phosphorylation is stimulated by assembled clathrin. *Traffic*, *4*(12), 885–890. <https://doi.org/10.1046/j.1398-9219.2003.0142.x>
- Coombs, G. S., Yu, J., Canning, C. A., Veltri, C. A., Covey, T. M., Cheong, J. K., Utomo, V., Banerjee, N., Zhang, Z. H., Jadulco, R. C., Ireland, C. M., & Virshup, D. M. (2010). WLS-dependent secretion of WNT3A requires Ser209 acylation and vacuolar acidification. *Journal of Cell Science*, *123*(19), 3357–3367. <https://doi.org/10.1242/jcs.072132>
- Cotter, D., Kerwin, R., Al-Sarraj, S., Brion, J. P., Chadwich, A., Lovestone, S., Anderton, B., & Everall, I. (1998). Abnormalities of Wnt signalling in schizophrenia - Evidence for neurodevelopmental abnormality. *NeuroReport*, *9*(7), 1379–1383. <https://doi.org/10.1097/00001756-199805110-00024>
- Cremona, O., Di Paolo, G., Wenk, M. R., Lüthi, A., Kim, W. T., Takei, K., Daniell, L., Nemoto, Y., Shears, S. B., Flavell, R. A., McCormick, D. A., & De Camilli, P. (1999). Essential role of phosphoinositide metabolism in synaptic vesicle recycling. *Cell*, *99*(2), 179–188. [https://doi.org/10.1016/S0092-8674\(00\)81649-9](https://doi.org/10.1016/S0092-8674(00)81649-9)
- Cui, J., Zhou, X., Liu, Y., Tang, Z., & Romeih, M. (2003). Wnt signaling in hepatocellular carcinoma: Analysis of mutation and expression of beta-catenin, T-cell factor-4 and glycogen synthase kinase 3-beta genes. *Journal of Gastroenterology and Hepatology (Australia)*, *18*(3), 280–287. <https://doi.org/10.1046/j.1440-1746.2003.02973.x>
- Dang, H., Li, Z., Skolnik, E. Y., & Fares, H. (2004). Disease-related Myotubularins Function in Endocytic Traffic in *Caenorhabditis elegans*. *Molecular Biology of the Cell*, *15*(1), 189–196. <https://doi.org/10.1091/mbc.E03-08-0605>
- Delattre, M., & Félix, M.-A. (2001). Development and evolution of a variable left-right asymmetry in nematodes: The handedness of P11/P12 migration. *Developmental Biology*, *232*(2), 362–371. <https://doi.org/10.1006/dbio.2001.0175>
- Ericson, V. R., Spilker, K. A., Tugizova, M. S., & Shen, K. (2014). MTM-6, a phosphoinositide phosphatase, is required to promote synapse formation in *Caenorhabditis elegans*. *PLoS ONE*, *9*(12). <https://doi.org/10.1371/journal.pone.0114501>



- Eyers, P. A., & Murphy, J. M. (2013). Exploring Kinomes: Pseudokinases and beyond: Dawn of the dead: Protein pseudokinases signal new adventures in cell biology. *Biochemical Society Transactions*, *41*(4), 969–974. <https://doi.org/10.1042/BST20130115>
- Fares, H., & Greenwald, I. (1999). SEL-5, a serine/threonine kinase that facilitates lin-12 activity in *Caenorhabditis elegans*. *Genetics*, *153*(4), 1641–1654.
- Franch-Marro, X., Wendler, F., Guidato, S., Griffith, J., Baena-Lopez, A., Itasaki, N., Maurice, M. M., & Vincent, J.-P. (2008). Wingless secretion requires endosome-to-Golgi retrieval of Wntless/Evi/ Sprinter by the retromer complex. *Nature Cell Biology*, *10*(2), 170–177. <https://doi.org/10.1038/ncb1678>
- Goh, X. Y., Rees, J. R. E., Paterson, A. L., Chin, S. F., Marioni, J. C., Save, V., O'Donovan, M., Eijk, P. P., Alderson, D., Ylstra, B., Caldas, C., & Fitzgerald, R. C. (2011). Integrative analysis of array-comparative genomic hybridisation and matched gene expression profiling data reveals novel genes with prognostic significance in oesophageal adenocarcinoma. *Gut*, *60*(10), 1317–1326. <https://doi.org/10.1136/gut.2010.234179>
- Goode, B. L., Eskin, J. A., & Wendland, B. (2014). Actin and endocytosis in budding yeast. *Genetics*, *199*(2), 315–358. <https://doi.org/10.1534/genetics.112.145540>
- Goodman, R. M., Thombre, S., Firtina, Z., Gray, D., Betts, D., Roebuck, J., Spana, E. P., & Selva, E. M. (2006). Sprinter: A novel transmembrane protein required for Wg secretion and signaling. *Development*, *133*(24), 4901–4911. <https://doi.org/10.1242/dev.02674>
- Greener, T., Zhao, X., Nojima, H., Eisenberg, E., & Greene, L. E. (2000). Role of cyclin G-associated kinase in uncoating clathrin-coated vesicles from non-neuronal cells. *Journal of Biological Chemistry*, *275*(2), 1365–1370. <https://doi.org/10.1074/jbc.275.2.1365>
- Groenen, L. C., Walker, F., Burgess, A. W., & Treutlein, H. R. (1997). A model for the activation of the epidermal growth factor receptor kinase: Involvement of an asymmetric dimer. *Biochemistry*, *36*(13), 3826–3836. <https://doi.org/10.1021/BI9614141>
- Groenendyk, J., & Michalak, M. (2011). A Genome-Wide siRNA Screen Identifies Novel Phospho-enzymes Affecting Wnt/ $\beta$ -Catenin Signaling in Mouse Embryonic Stem Cells. *Stem Cell Reviews and Reports*, *7*(4), 910–926. <https://doi.org/10.1007/s12015-011-9265-3>
- Gross, J. C., Chaudhary, V., Bartscherer, K., & Boutros, M. (2012). Active Wnt proteins are secreted on exosomes. *Nature Cell Biology*, *14*(10), 1036–1045. <https://doi.org/10.1038/ncb2574>
- Guo, L., Martens, C., Bruno, D., Porcella, S. F., Yamane, H., Caucheteux, S. M., Zhu, J., & Paul, W. E. (2013). Lipid phosphatases identified by screening a mouse phosphatase shRNA library regulate T-cell differentiation and Protein kinase B AKT signaling.

*Proceedings of the National Academy of Sciences of the United States of America*, 110(20). <https://doi.org/10.1073/pnas.1305070110>

- Gupta-Rossi, N., Ortica, S., Meas-Yedid, V., Heuss, S., Moretti, J., Olivo-Marin, J.-C., & Israël, A. (2011). The adaptor-associated kinase 1, AAK1, is a positive regulator of the notch pathway. *Journal of Biological Chemistry*, 286(21), 18720–18730. <https://doi.org/10.1074/jbc.M110.190769>
- Gyurkovska, V., Murtazina, R., Zhao, S. F., Shikano, S., Okamoto, Y., & Segev, N. (2023). Dual function of Rab1A in secretion and autophagy: hypervariable domain dependence. *Life Science Alliance*, 6(5). <https://doi.org/10.26508/lsa.202201810>
- Hammond, A. T., & Glick, B. S. (2000). Dynamics of transitional Endoplasmic Reticulum sites in vertebrate cells. *Molecular Biology of the Cell*, 11(9), 3013–3030. <https://doi.org/10.1091/mbc.11.9.3013>
- Hanks, S. K., & Hunter, T. (1995). The eukaryotic protein kinase superfamily: Kinase (catalytic) domain structure and classification. *FASEB Journal*, 9(8), 576–596. <https://doi.org/10.1096/fasebj.9.8.7768349>
- Hanks, S. K., Quinn, A. M., & Hunter, T. (1988). The protein kinase family: Conserved features and deduced phylogeny of the catalytic domains. *Science*, 241(4861), 42–52. <https://doi.org/10.1126/SCIENCE.3291115>
- Harris, J., Honigberg, L., Robinson, N., & Kenyon, C. (1996). Neuronal cell migration in *C. elegans*: Regulation of Hox gene expression and cell position. *Development*, 122(10), 3117–3131.
- Harterink, M., Kim, D. H., Middelkoop, T. C., Doan, T. D., van Oudenaarden, A., & Korswagen, H. C. (2011). Neuroblast migration along the anteroposterior axis of *C. elegans* is controlled by opposing gradients of Wnts and a secreted Frizzled-related protein. *Development*, 138(14), 2915–2924. <https://doi.org/10.1242/dev.064733>
- Hedgecock, E. M., Culotti, J. G., Hall, D. H., & Stern, B. D. (1987). Genetics of cell and axon migrations in *Caenorhabditis elegans*. *Development*, 100(3), 365–382.
- Henderson, D. M., & Conner, S. D. (2007). A novel AAK1 splice variant functions at multiple steps of the endocytic pathway. *Molecular Biology of the Cell*, 18(7), 2698–2706. <https://doi.org/10.1091/mbc.E06-09-0831>
- Henne, W. M., Boucrot, E., Meinecke, M., Evergren, E., Vallis, Y., Mittal, R., & McMahon, H. T. (2010). FCHo proteins are nucleators of Clathrin-Mediated endocytosis. *Science*, 328(5983), 1281–1284. <https://doi.org/10.1126/science.1188462>
- Henne, W. M., Kent, H. M., Ford, M. G. J., Hegde, B. G., Daumke, O., Butler, P. J. G., Mittal, R., Langen, R., Evans, P. R., & McMahon, H. T. (2007). Structure and Analysis of FCHo2 F-BAR Domain: A Dimerizing and Membrane Recruitment Module that Effects

- Membrane Curvature. *Structure*, 15(7), 839–852.  
<https://doi.org/10.1016/j.str.2007.05.002>
- Hilliard, M. A., & Bargmann, C. I. (2006). Wnt signals and Frizzled activity orient anterior-posterior axon outgrowth in *C. elegans*. *Developmental Cell*, 10(3), 379–390.  
<https://doi.org/10.1016/j.devcel.2006.01.013>
- Hinshaw, J. E., & Schmid, S. L. (1995). Dynamin self-assembles into rings suggesting a mechanism for coated vesicle budding. *Nature*, 374(6518), 190–192.  
<https://doi.org/10.1038/374190a0>
- Hnia, K., Vaccari, I., Bolino, A., & Laporte, J. (2012). Myotubularin phosphoinositide phosphatases: Cellular functions and disease pathophysiology. *Trends in Molecular Medicine*, 18(6), 317–327. <https://doi.org/10.1016/j.molmed.2012.04.004>
- Hobmayer, B., Rentzsch, F., Kuhn, K., Happel, C. M., von Laue, C. C., Snyder, P., Rothbacher, U., & Holstein, T. W. (2000). WNT signalling molecules act in axis formation in the diploblastic metazoan Hydra. *Nature*, 407(6801), 186–189.  
<https://doi.org/10.1038/35025063>
- Hollopeter, G., Lange, J. J., Zhang, Y., Vu, T. N., Gu, M., Ailion, M., Lambie, E. J., Slaughter, B. D., Unruh, J. R., Florens, L., Florens, L., & Jorgensen, E. M. (2014). The membrane-associated proteins FCHO and SGIP are allosteric activators of the AP2 clathrin adaptor complex. *ELife*, 3. <https://doi.org/10.7554/eLife.03648>
- Holstein, S. E. H., Ungewickell, H., & Ungewickell, E. (1996). Mechanism of clathrin basket dissociation: Separate functions of protein domains of the DnaJ homologue auxilin. *Journal of Cell Biology*, 135(4), 925–937. <https://doi.org/10.1083/jcb.135.4.925>
- Holstein, T. W. (2012). The evolution of the wnt pathway. *Cold Spring Harbor Perspectives in Biology*, 4(7), 1–17. <https://doi.org/10.1101/cshperspect.a007922>
- Honigberg, L., & Kenyon, C. (2000). Establishment of left/right asymmetry in neuroblast migration by UNC-40/DCC, UNC-73/Trio and DPY-19 proteins in *C. elegans*. *Development*, 127(21), 4655–4668.
- Höning, S., Ricotta, D., Krauss, M., Späte, K., Spolaore, B., Motley, A., Robinson, M., Robinson, C., Haucke, V., & Owen, D. J. (2005). Phosphatidylinositol-(4,5)-bisphosphate regulates sorting signal recognition by the clathrin-associated adaptor complex AP2. *Molecular Cell*, 18(5), 519–531.  
<https://doi.org/10.1016/j.molcel.2005.04.019>
- Hotta, K., Kitamoto, T., Kitamoto, A., Mizusawa, S., Matsuo, T., Nakata, Y., Kamohara, S., Miyatake, N., Kotani, K., Komatsu, R., Nakao, K., & Sekine, A. (2011). Association of variations in the FTO, SCG3 and MTMR9 genes with metabolic syndrome in a Japanese population. *Journal of Human Genetics*, 56(9), 647–651.  
<https://doi.org/10.1038/jhg.2011.74>

- Hughes, W. E., Woscholski, R., Cooke, F. T., Patrick, R. S., Dove, S. K., McDonald, N. Q., & Parker, P. J. (2000). SAC1 encodes a regulated lipid phosphoinositide phosphatase, defects in which can be suppressed by the homologous Inp52p and Inp53p phosphatases. *Journal of Biological Chemistry*, 275(2), 801–808. <https://doi.org/10.1074/jbc.275.2.801>
- Huttlin, E. L., Bruckner, R. J., Paulo, J. A., Cannon, J. R., Ting, L., Baltier, K., Colby, G., Gebreab, F., Gygi, M. P., Parzen, H., Gygi, S. P., & Wade Harper, J. (2017). Architecture of the human interactome defines protein communities and disease networks. *Nature*, 545(7655), 505–509. <https://doi.org/10.1038/nature22366>
- Itoh, K., Antipova, A., Ratcliffe, M. J., & Sokol, S. (2000). Interaction of Dishevelled and Xenopus Axin-related protein is required for Wnt signal transduction. *Molecular and Cellular Biology*, 20(6), 2228–2238. <https://doi.org/10.1128/MCB.20.6.2228-2238.2000>
- Jackson, A. P., Flett, A., Smythe, C., Hufton, L., Wetley, F. R., & Smythe, E. (2003). Clathrin promotes incorporation of cargo into coated pits by activation of the AP2 adaptor  $\mu$ 2 kinase. *Journal of Cell Biology*, 163(2), 231–236. <https://doi.org/10.1083/jcb.200304079>
- Jackson, L. P., Kelly, B. T., McCoy, A. J., Gaffry, T., James, L. C., Collins, B. M., Höning, S., Evans, P. R., & Owen, D. J. (2010). A large-scale conformational change couples membrane recruitment to cargo binding in the AP2 clathrin adaptor complex. *Cell*, 141(7), 1220–1229. <https://doi.org/10.1016/j.cell.2010.05.006>
- Jean, S., Cox, S., Schmidt, E. J., Robinson, F. L., & Kiger, A. (2012). Sbf/MTMR13 coordinates PI(3)P and Rab21 regulation in endocytic control of cellular remodeling. *Molecular Biology of the Cell*, 23(14), 2723–2740. <https://doi.org/10.1091/mbc.E12-05-0375>
- Jha, A., Agostinelli, N. R., Mishra, S. K., Keyel, P. A., Hawryluk, M. J., & Traub, L. M. (2004). A Novel AP-2 Adaptor Interaction Motif Initially Identified in the Long-splice Isoform of Synaptojanin 1, SJ170. *Journal of Biological Chemistry*, 279(3), 2281–2290. <https://doi.org/10.1074/jbc.M305644200>
- Jing, S., Spencer, T., Miller, K., Hopkins, C., & Trowbridge, I. S. (1990). Role of the human transferrin receptor cytoplasmic domain in endocytosis: localization of a specific signal sequence for internalization. *The Journal of Cell Biology*, 110(2), 283–294. <https://doi.org/10.1083/JCB.110.2.283>
- Jullien-Flores, V., Mahe, Y., Mirey, G., Leprince, C., Meunier-Bisceuil, B., Sorkin, A., & Camonis, J. H. (2000). RLIP76, an effector of the GTPase Ral, interacts with the AP2 complex: Involvement of the Ral pathway in receptor endocytosis. *Journal of Cell Science*, 113(16), 2837–2844.
- Kadlecova, Z., Spielman, S. J., Loerke, D., Mohanakrishnan, A., Reed, D. K., & Schmid, S. L. (2017). Regulation of clathrin-mediated endocytosis by hierarchical allosteric activation of AP2. *Journal of Cell Biology*, 216(1), 167–179. <https://doi.org/10.1083/jcb.201608071>

- Kakugawa, S., Langton, P. F., Zebisch, M., Howell, S. A., Chang, T. H., Liu, Y., Feizi, T., Bineva, G., O'Reilly, N., Snijders, A. P., Jones, E. Y., & Vincent, J. P. (2015). Notum deacylates Wnt proteins to suppress signalling activity. *Nature*, *519*(7542). <https://doi.org/10.1038/nature14259>
- Kanaoka, Y., Kimura, S. H., Okazaki, I., Ikeda, M., & Nojima, H. (1997). GAK: A cyclin G associated kinase contains a tensin/auxilin-like domain. *FEBS Letters*, *402*(1), 73–80. [https://doi.org/10.1016/S0014-5793\(96\)01484-6](https://doi.org/10.1016/S0014-5793(96)01484-6)
- Karim, M., Saul, S., Ghita, L., Sahoo, M. K., Ye, C., Bhalla, N., Lo, C.-W., Jin, J., Park, J.-G., Martinez-Gualda, B., de Jonghe, S., & Einav, S. (2022). Numb-associated kinases are required for SARS-CoV-2 infection and are cellular targets for antiviral strategies. *Antiviral Research*, *204*. <https://doi.org/10.1016/j.antiviral.2022.105367>
- Kast, D. J., Zajac, A. L., Holzbaur, E. L. F., Ostap, E. M., & Dominguez, R. (2015). WHAMM Directs the Arp2/3 Complex to the ER for Autophagosome Biogenesis through an Actin Comet Tail Mechanism. *Current Biology*, *25*(13), 1791–1797. <https://doi.org/10.1016/j.cub.2015.05.042>
- Kenneth Nelson, F., Albert, P. S., & Riddle, D. L. (1983). Fine structure of the *Caenorhabditis elegans* secretory-excretory system. *Journal of Ultrastructure Research*, *82*(2), 156–171. [https://doi.org/10.1016/S0022-5320\(83\)90050-3](https://doi.org/10.1016/S0022-5320(83)90050-3)
- Kim, S.-A., Vacratsis, P. O., Firesteint, R., Clearyt, M. L., & Dixon, J. E. (2003). Regulation of myotubularin-related (MTMR)2 phosphatidylinositol phosphatase by MTMR5, a catalytically inactive phosphatase. *Proceedings of the National Academy of Sciences of the United States of America*, *100*(8), 4492–4497. <https://doi.org/10.1073/pnas.0431052100>
- Kinzler, K. W., & Vogelstein, B. (1996). Lessons from hereditary colorectal cancer. *Cell*, *87*(2), 159–170. [https://doi.org/10.1016/S0092-8674\(00\)81333-1](https://doi.org/10.1016/S0092-8674(00)81333-1)
- Kirchhausen, T. (1999). Adaptors for clathrin-mediated traffic. In *Annual Review of Cell and Developmental Biology* (Vol. 15). <https://doi.org/10.1146/annurev.cellbio.15.1.705>
- Kitagawa, M., Hatakeyama, S., Shirane, M., Matsumoto, M., Ishida, N., Hattori, K., Nakamichi, I., Kikuchi, A., Nakayama, K.-I., & Nakayama, K. (1999). An F-box protein, FWD1, mediates ubiquitin-dependent proteolysis of  $\beta$ -catenin. *EMBO Journal*, *18*(9), 2401–2410. <https://doi.org/10.1093/emboj/18.9.2401>
- Klingensmith, J., Nusse, R., & Perrimon, N. (1994). The *Drosophila* segment polarity gene dishevelled encodes a novel protein required for response to the wingless signal. *Genes and Development*, *8*(1), 118–130. <https://doi.org/10.1101/gad.8.1.118>
- Knighton, D. R., Zheng, J., ten Eyck, L. F., Ashford, V. A., Xuong, N. H., Taylor, S. S., & Sowadski, J. M. (1991). Crystal structure of the catalytic subunit of cyclic adenosine

- monophosphate-dependent protein kinase. *Science*, 253(5018), 407–414.  
<https://doi.org/10.1126/SCIENCE.1862342>
- Korswagen, H. C., Herman, M. A., & Clevers, H. C. (2000). Distinct  $\beta$ -catenins mediate adhesion and signalling functions in *C. elegans*. *Nature*, 406(6795), 527–532.  
<https://doi.org/10.1038/35020099>
- Kovács, T., Szinyákovics, J., Billes, V., Murányi, G., Varga, V. B., Bjelik, A., Légrádi, Á., Szabó, M., Sándor, S., Kubinyi, E., Maglóczky, Z., & Vellai, T. (2022). A conserved MTMR lipid phosphatase increasingly suppresses autophagy in brain neurons during aging. *Scientific Reports*, 12(1). <https://doi.org/10.1038/s41598-022-24843-w>
- Kroppen, B., Teske, N., Yambire, K. F., Denkert, N., Mukherjee, I., Tarasenko, D., Jaipuria, G., Zweckstetter, M., Milosevic, I., Steinem, C., Steinem, C., & Meinecke, M. (2021). Cooperativity of membrane-protein and protein–protein interactions control membrane remodeling by epsin 1 and affects clathrin-mediated endocytosis. *Cellular and Molecular Life Sciences*, 78(5), 2355–2370. <https://doi.org/10.1007/s00018-020-03647-z>
- Kurayoshi, M., Yamamoto, H., Izumi, S., & Kikuchi, A. (2007). Post-translational palmitoylation and glycosylation of Wnt-5a are necessary for its signalling. *Biochemical Journal*, 402(3), 515–523. <https://doi.org/10.1042/BJ20061476>
- Lahiry, P., Torkamani, A., Schork, N. J., & Hegele, R. A. (2010). Kinase mutations in human disease: Interpreting genotype-phenotype relationships. *Nature Reviews Genetics*, 11(1), 60–74. <https://doi.org/10.1038/nrg2707>
- Lamaze, C., Fujimoto, L. M., Yin, H. L., & Schmid, S. L. (1997). The actin cytoskeleton is required for receptor-mediated endocytosis in mammalian cells. *Journal of Biological Chemistry*, 272(33), 20332–20335. <https://doi.org/10.1074/jbc.272.33.20332>
- Lambie, E. J., & Kimble, J. (1991). Two homologous regulatory genes, *lin-12* and *glp-1*, have overlapping functions. *Development*, 112(1), 231–240.
- Laporte, J., Bedez, F., Bolino, A., & Mandel, J.-L. (2003). Myotubularins, a large disease-associated family of cooperating catalytically active and inactive phosphoinositides phosphatases. *Human Molecular Genetics*, 12(REV. ISS.).  
<https://doi.org/10.1093/hmg/ddg273>
- Laporte, J., Guiraud-Chaumeil, C., Vincent, M.-C., Mandel, J.-L., Tanner, S. M., Liechti-Gallati, S., Wallgren-Pettersson, C., Dahl, N., Kress, W., Bolhuis, P. A., Samson, F., & Bertini, E. (1997). Mutations in the *MTM1* gene implicated in X-linked myotubular myopathy. *Human Molecular Genetics*, 6(9), 1505–1511.  
<https://doi.org/10.1093/hmg/6.9.1505>
- Lee, P. N., Kumburegama, S., Marlow, H. Q., Martindale, M. Q., & Wikramanayake, A. H. (2007). Asymmetric developmental potential along the animal-vegetal axis in the



- anthozoan cnidarian, *Nematostella vectensis*, is mediated by Dishevelled. *Developmental Biology*, 310(1), 169–186. <https://doi.org/10.1016/j.ydbio.2007.05.040>
- Lee, S. H., Demeterco, C., Geron, I., Abrahamsson, A., Levine, F., & Itkin-Ansari, P. (2008). Islet specific Wnt activation in human type II diabetes. *Experimental Diabetes Research*, 2008, 728763. <https://doi.org/10.1155/2008/728763>
- Letourneur, F., & Klausner, R. D. (1992). A novel di-leucine motif and a tyrosine-based motif independently mediate lysosomal targeting and endocytosis of CD3 chains. *Cell*, 69(7), 1143–1157. [https://doi.org/10.1016/0092-8674\(92\)90636-Q](https://doi.org/10.1016/0092-8674(92)90636-Q)
- Levin, L. R., & Zoller, M. J. (1990). Association of catalytic and regulatory subunits of cyclic AMP-dependent protein kinase requires a negatively charged side group at a conserved threonine. *Molecular and Cellular Biology*, 10(3), 1066–1075. <https://doi.org/10.1128/MCB.10.3.1066>
- Levine, B., & Deretic, V. (2007). Unveiling the roles of autophagy in innate and adaptive immunity. *Nature Reviews Immunology*, 7(10), 767–777. <https://doi.org/10.1038/nri2161>
- Li, B., & Niswander, L. A. (2020). TMEM132A, a Novel Wnt Signaling Pathway Regulator Through Wntless (WLS) Interaction. *Frontiers in Cell and Developmental Biology*, 8. <https://doi.org/10.3389/fcell.2020.599890>
- Liu, C., Li, Y., Semenov, M., Han, C., Baeg, G.-H., Tan, Y., Zhang, Z., Lin, X., & He, X. (2002). Control of  $\beta$ -catenin phosphorylation/degradation by a dual-kinase mechanism. *Cell*, 108(6), 837–847. [https://doi.org/10.1016/S0092-8674\(02\)00685-2](https://doi.org/10.1016/S0092-8674(02)00685-2)
- Liu, J., Lv, Y., Liu, Q.-H., Qu, C.-K., & Shen, J. (2014). Deficiency of MTMR14 promotes autophagy and proliferation of mouse embryonic fibroblasts. *Molecular and Cellular Biochemistry*, 392(1–2), 31–37. <https://doi.org/10.1007/s11010-014-2015-5>
- Liu, Y., Qi, X., Donnelly, L., Elghobashi-Meinhardt, N., Long, T., Zhou, R. W., Sun, Y., Wang, B., & Li, X. (2022). Mechanisms and inhibition of Porcupine-mediated Wnt acylation. *Nature 2022 607:7920*, 607(7920), 816–822. <https://doi.org/10.1038/s41586-022-04952-2>
- Liu, Z., & West, A. B. (2017). The dual enzyme LRRK2 hydrolyzes GTP in both its GTPase and kinase domains in vitro. *Biochimica et Biophysica Acta - Proteins and Proteomics*, 1865(3), 274–280. <https://doi.org/10.1016/j.bbapap.2016.12.001>
- Lo, M.-T., Hinds, D. A., Tung, J. Y., Franz, C., Fan, C.-C., Wang, Y., Smeland, O. B., Schork, A., Holland, D., Kauppi, K., Andreassen, O. A., & Chen, C.-H. (2017). Genome-wide analyses for personality traits identify six genomic loci and show correlations with psychiatric disorders. *Nature Genetics*, 49(1), 152–156. <https://doi.org/10.1038/ng.3736>
- Lo, W.-T., Vujičić Žagar, A., Gerth, F., Lehmann, M., Puchkov, D., Krylova, O., Freund, C., Scapozza, L., Vadas, O., & Haucke, V. (2017). A Coincidence Detection Mechanism Controls PX-BAR Domain-Mediated Endocytic Membrane Remodeling via an Allosteric

- Structural Switch. *Developmental Cell*, 43(4), 522-529.e4.  
<https://doi.org/10.1016/j.devcel.2017.10.019>
- Lorenzo, Ó., Urbé, S., & Clague, M. J. (2005). Analysis of phosphoinositide binding domain properties within the myotubularin-related protein MTMR3. *Journal of Cell Science*, 118(9), 2005–2012. <https://doi.org/10.1242/jcs.02325>
- Lorenzo, Ó., Urbé, S., & Clague, M. J. (2006). Systematic analysis of myotubularins: Heteromeric interactions, subcellular localisation and endosome-related functions. *Journal of Cell Science*, 119(14), 2953–2959. <https://doi.org/10.1242/jcs.03040>
- Ma, L., Umasankar, P. K., Wrobel, A. G., Lyman, A., McCoy, A. J., Holkar, S. S., Jha, A., Pradhan-Sundd, T., Watkins, S. C., Owen, D. J., Owen, D. J., & Traub, L. M. (2015). Transient Fcho1/2·Eps15/R·AP-2 Nanoclusters Prime the AP-2 Clathrin Adaptor for Cargo Binding. *Developmental Cell*, 37(5), 428–443.  
<https://doi.org/10.1016/j.devcel.2016.05.003>
- Maehama, T., & Dixon, J. E. (1998). The tumor suppressor, PTEN/MMAC1, dephosphorylates the lipid second messenger, phosphatidylinositol 3,4,5-trisphosphate. *Journal of Biological Chemistry*, 273(22), 13375–13378.  
<https://doi.org/10.1074/jbc.273.22.13375>
- Maekawa, M., Terasaka, S., Mochizuki, Y., Kawai, K., Ikeda, Y., Araki, N., Skolnik, E. Y., Taguchi, T., & Arai, H. (2014). Sequential breakdown of 3-phosphorylated phosphoinositides is essential for the completion of macropinocytosis. *Proceedings of the National Academy of Sciences of the United States of America*, 111(11).  
<https://doi.org/10.1073/pnas.1311029111>
- Maloof, J. N., Whangbo, J., Harris, J. M., Jongeward, G. D., & Kenyon, C. (1999). A Wnt signaling pathway controls Hox gene expression and neuroblast migration in *C. elegans*. *Development*, 126(1), 37–49.
- Mammel, A. E., Delgado, K. C., Chin, A. L., Condon, A. F., Hill, J. Q., Aicher, S. A., Wang, Y., Fedorov, L. M., & Robinson, F. L. (2022). Distinct roles for the Charcot-Marie-Tooth disease-causing endosomal regulators Mtmr5 and Mtmr13 in axon radial sorting and Schwann cell myelination. *Human Molecular Genetics*, 31(8), 1216–1229.  
<https://doi.org/10.1093/hmg/ddab311>
- Manning, G., Whyte, D. B., Martinez, R., Hunter, T., & Sudarsanam, S. (2002). The protein kinase complement of the human genome. *Science*, 298(5600), 1912–1934.  
<https://doi.org/10.1126/science.1075762>
- Manser, J., & Wood, W. B. (1990). Mutations affecting embryonic cell migrations in *Caenorhabditis elegans*. *Developmental Genetics*, 11(1), 49–64.  
<https://doi.org/10.1002/dvg.1020110107>

- Mathiowetz, A. J., Baple, E., Russo, A. J., Coulter, A. M., Carrano, E., Brown, J. D., Jinks, R. N., Crosby, A. H., & Campellone, K. G. (2017). An Amish founder mutation disrupts a PI(3)P-WHAMM-Arp2/3 complex-driven autophagosomal remodeling pathway. *Molecular Biology of the Cell*, 28(19), 2492–2507. <https://doi.org/10.1091/mbc.E17-01-0022>
- Mattei, A. M., Smailys, J. D., Hepworth, E. M. W., & Hinton, S. D. (2021). The roles of pseudophosphatases in disease. *International Journal of Molecular Sciences*, 22(13). <https://doi.org/10.3390/ijms22136924>
- Meinecke, M., Boucrot, E., Camdere, G., Hon, W.-C., Mittal, R., & McMahon, H. T. (2013). Cooperative recruitment of dynamin and BIN/Amphiphysin/Rvs (BAR) domain-containing proteins leads to GTP-dependent membrane scission. *Journal of Biological Chemistry*, 288(9), 6651–6661. <https://doi.org/10.1074/jbc.M112.444869>
- Merrifield, C. J., Feldman, M. E., Wan, L., & Almers, W. (2002). Imaging actin and dynamin recruitment during invagination of single clathrin-coated pits. *Nature Cell Biology*, 4(9), 691–698. <https://doi.org/10.1038/ncb837>
- Merrifield, C. J., Qualmann, B., Kessels, M. M., & Almers, W. (2004). Neural Wiskott Aldrich Syndrome Protein (N-WASP) and the Arp 2/3 complex are recruited to sites of clathrin-mediated endocytosis in cultured fibroblasts. *European Journal of Cell Biology*, 83(1), 13–18. <https://doi.org/10.1078/0171-9335-00356>
- Mochizuki, Y., & Majerus, P. W. (2003). Characterization of myotubularin-related protein 7 and its binding partner, myotubularin-related protein 9. *Proceedings of the National Academy of Sciences of the United States of America*, 100(17), 9768–9773. <https://doi.org/10.1073/pnas.1333958100>
- Mochizuki, Y., Ohashi, R., Kawamura, T., Iwanari, H., Kodama, T., Naito, M., & Hamakubo, T. (2013). Phosphatidylinositol 3-phosphatase myotubularin-related protein 6 (MTMR6) is regulated by small GTPase Rab1B in the early secretory and autophagic pathways. *Journal of Biological Chemistry*, 288(2), 1009–1021. <https://doi.org/10.1074/jbc.M112.395087>
- Modi, V., & Dunbrack, R. L. (2019a). A Structurally-Validated Multiple Sequence Alignment of 497 Human Protein Kinase Domains. *Scientific Reports*, 9(1). <https://doi.org/10.1038/s41598-019-56499-4>
- Modi, V., & Dunbrack, R. L. (2019b). Defining a new nomenclature for the structures of active and inactive kinases. *Proceedings of the National Academy of Sciences of the United States of America*, 116(14), 6818–6827. <https://doi.org/10.1073/pnas.1814279116>
- Molenaar, M., Van De Wetering, M., Oosterwegel, M., Peterson-Maduro, J., Godsave, S., Korinek, V., Roose, J., Destree, O., & Clevers, H. (1996). XTcf-3 transcription factor mediates  $\beta$ -catenin-induced axis formation in xenopus embryos. *Cell*, 86(3), 391–399. [https://doi.org/10.1016/S0092-8674\(00\)80112-9](https://doi.org/10.1016/S0092-8674(00)80112-9)

- Morgan, J. R., Prasad, K., Hao, W., Augustine, G. J., & Lafer, E. M. (2000). A conserved clathrin assembly motif essential for synaptic vesicle endocytosis. *Journal of Neuroscience*, *20*(23), 8667–8676. <https://doi.org/10.1523/jneurosci.20-23-08667.2000>
- Moskowitz, I. P. G., & Rothman, J. H. (1996). *lin-12* and *glp-1* are required zygotically for early embryonic cellular interactions and are regulated by maternal GLP-1 signaling in *Caenorhabditis elegans*. *Development*, *122*(12), 4105–4117.
- Moti, N., Yu, J., Boncompain, G., Perez, F., & Virshup, D. M. (2019). Wnt traffic from endoplasmic reticulum to filopodia. *PLoS ONE*, *14*(2). <https://doi.org/10.1371/journal.pone.0212711>
- Mulligan, K. A., Fuerer, C., Ching, W., Fish, M., Willert, K., & Nusse, R. (2012). Secreted Wingless-interacting molecule (Swim) promotes long-range signaling by maintaining Wingless solubility. *Proceedings of the National Academy of Sciences of the United States of America*, *109*(2), 370–377. <https://doi.org/10.1073/pnas.1119197109>
- Murphy, J. M., Zhang, Q., Young, S. N., Reese, M. L., Bailey, F. P., Eyers, P. A., Ungureanu, D., Hammaren, H., Silvennoinen, O., Varghese, L. N., Babon, J. J., & Lucet, I. S. (2014). A robust methodology to subclassify pseudokinases based on their nucleotide-binding properties. *Biochemical Journal*, *457*(2), 323–334. <https://doi.org/10.1042/BJ20131174>
- Nelson, F. K., & Riddle, D. L. (1984). Functional study of the *Caenorhabditis elegans* secretory-excretory system using laser microsurgery. *Journal of Experimental Zoology*, *231*(1), 45–56. <https://doi.org/10.1002/jez.1402310107>
- Neumann, S., Coudreuse, D. Y. M., van der Westhuyzen, D. R., Eckhardt, E. R. M., Korswagen, H. C., Schmitz, G., & Sprong, H. (2009). Mammalian Wnt3a is released on lipoprotein particles. *Traffic*, *10*(3), 334–343. <https://doi.org/10.1111/j.1600-0854.2008.00872.x>
- Neveu, G., Ziv-Av, A., Barouch-Bentov, R., Berkerman, E., Mulholland, J., & Einav, S. (2015). AP-2-associated protein kinase 1 and cyclin G-associated kinase regulate hepatitis C virus entry and are potential drug targets. *Journal of Virology*, *89*(8), 4387–4404. <https://doi.org/10.1128/JVI.02705-14>
- Ohno, H., Stewart, J., Fournier, M.-C., Bosshart, H., Rhee, I., Miyatake, S., Saito, T., Gallusser, A., Kirchhausen, T., & Bonifacino, J. S. (1995). Interaction of tyrosine-based sorting signals with clathrin-associated proteins. *Science*, *269*(5232), 1872–1875. <https://doi.org/10.1126/science.7569928>
- Olah, G. A., Mitchell, R. D., Sosnick, T. R., Walsh, D. A., & Trewella, J. (1993). Solution Structure of the cAMP-Dependent Protein Kinase Catalytic Subunit and Its Contraction upon Binding the Protein Kinase Inhibitor Peptide. *Biochemistry*, *32*(14), 3649–3657. <https://doi.org/10.1021/bi00065a018>

- Olsen, J. V., Blagoev, B., Gnad, F., Macek, B., Kumar, C., Mortensen, P., & Mann, M. (2006). Global, In Vivo, and Site-Specific Phosphorylation Dynamics in Signaling Networks. *Cell*, *127*(3), 635–648. <https://doi.org/10.1016/j.cell.2006.09.026>
- Olusanya, O., Andrews, P. D., Swedlow, J. R., & Smythe, E. (2001). Phosphorylation of threonine 156 of the  $\mu$ 2 subunit of the AP2 complex is essential for endocytosis in vitro and in vivo. *Current Biology*, *11*(11), 896–900. [https://doi.org/10.1016/S0960-9822\(01\)00240-8](https://doi.org/10.1016/S0960-9822(01)00240-8)
- Pan, C.-L., Baum, P. D., Gu, M., Jorgensen, E. M., Clark, S. G., & Garriga, G. (2008). *C. elegans* AP-2 and Retromer Control Wnt Signaling by Regulating MIG-14/Wntless. *Developmental Cell*, *14*(1), 132–139. <https://doi.org/10.1016/j.devcel.2007.12.001>
- Panáková, D., Sprong, H., Marois, E., Thiele, C., & Eaton, S. (2005). Lipoprotein particles are required for Hedgehog and Wingless signalling. *Nature*, *435*(7038), 58–65. <https://doi.org/10.1038/nature03504>
- Pang, K., Ryan, J. F., Mullikin, J. C., Baxeavanis, A. D., & Martindale, M. Q. (2010). Genomic insights into Wnt signaling in an early diverging metazoan, the ctenophore *Mnemiopsis leidyi*. *EvoDevo*, *1*(1). <https://doi.org/10.1186/2041-9139-1-10>
- Papkoff, J., Rubinfeld, B., Schryver, B., & Polakis, P. (1996). Wnt-1 regulates free pools of catenins and stabilizes APC-catenin complexes. *Molecular and Cellular Biology*, *16*(5), 2128–2134. <https://doi.org/10.1128/MCB.16.5.2128>
- Paul, N. R., Jacquemet, G., & Caswell, P. T. (2015). Endocytic Trafficking of Integrins in Cell Migration. *Current Biology*, *25*(22), R1092–R1105. <https://doi.org/10.1016/j.cub.2015.09.049>
- Pauloin, A., Bernier, I., & Jollès, P. (1982). Presence of cyclic nucleotide- $\text{Ca}^{2+}$  independent protein kinase in bovine brain coated vesicles. *Nature*, *298*(5874), 574–576. <https://doi.org/10.1038/298574a0>
- Pauloin, A., & Thuriéau, C. (1993). The 50 kDa protein subunit of assembly polypeptide (AP) AP-2 adaptor from clathrin-coated vesicles is phosphorylated on threonine-156 by AP-1 and a soluble AP50 kinase which co-purifies with the assembly polypeptides. *Biochemical Journal*, *296*(2), 409–415. <https://doi.org/10.1042/bj2960409>
- Pearson, R. B., & Kemp, B. E. (1991). Protein Kinase Phosphorylation Site Sequences and Consensus Specificity Motifs: Tabulations. *Methods in Enzymology*, *200*(C), 62–81. [https://doi.org/10.1016/0076-6879\(91\)00127-I](https://doi.org/10.1016/0076-6879(91)00127-I)
- Petersen, C. P., & Reddien, P. W. (2011). Polarized notum activation at wounds inhibits Wnt function to promote planarian head regeneration. *Science*, *332*(6031), 852–855. <https://doi.org/10.1126/science.1202143>

- Port, F., Kuster, M., Herr, P., Furger, E., Bänziger, C., Hausmann, G., & Basler, K. (2008). Wingless secretion promotes and requires retromer-dependent cycling of Wntless. *Nature Cell Biology*, *10*(2), 178–185. <https://doi.org/10.1038/ncb1687>
- Posor, Y., Eichhorn-Grünig, M., & Haucke, V. (2015). Phosphoinositides in endocytosis. *Biochimica et Biophysica Acta - Molecular and Cell Biology of Lipids*, *1851*(6), 794–804. <https://doi.org/10.1016/j.bbaliip.2014.09.014>
- Prasad, B. C., & Clark, S. G. (2006). Wnt signaling establishes anteroposterior neuronal polarity and requires retromer in *C. elegans*. *Development*, *133*(9), 1757–1766. <https://doi.org/10.1242/dev.02357>
- Putri, D. D. P., Kawasaki, T., Murase, M., Sueyoshi, T., Deguchi, T., Ori, D., Suetsugu, S., & Kawai, T. (2019). PtdIns3P phosphatases MTMR3 and MTMR4 negatively regulate innate immune responses to DNA through modulating STING trafficking. *Journal of Biological Chemistry*, *294*(21), 8412–8423. <https://doi.org/10.1074/jbc.RA118.005731>
- Raess, M. A., Friant, S., Cowling, B. S., & Laporte, J. (2017). WANTED – Dead or alive: Myotubularins, a large disease-associated protein family. *Advances in Biological Regulation*, *63*, 49–58. <https://doi.org/10.1016/j.jbior.2016.09.001>
- Ramesh, S. T., Navyasree, K. V., Sah, S., Ashok, A. B., Qathoon, N., Mohanty, S., Swain, R. K., & Umasankar, P. K. (2021). BMP2K phosphorylates AP-2 and regulates clathrin-mediated endocytosis. *Traffic*, *22*(11), 377–396. <https://doi.org/10.1111/tra.12814>
- Reichsman, F., Smith, L., & Cumberledge, S. (1996). Glycosaminoglycans can modulate extracellular localization of the wingless protein and promote signal transduction. *Journal of Cell Biology*, *135*(3), 819–827. <https://doi.org/10.1083/jcb.135.3.819>
- Reiterer, V., Pawłowski, K., Desrochers, G., Pause, A., Sharpe, H. J., & Farhan, H. (2020). The dead phosphatases society: a review of the emerging roles of pseudophosphatases. *FEBS Journal*, *287*(19), 4198–4220. <https://doi.org/10.1111/febs.15431>
- Rella, L., Fernandes Póvoa, E. E., & Korswagen, H. C. (2016). The *Caenorhabditis elegans* Q neuroblasts: A powerful system to study cell migration at single-cell resolution in vivo. *Genesis*, *54*(4), 198–211. <https://doi.org/10.1002/dvg.22931>
- Reya, T., & Clevers, H. (2005). Wnt signalling in stem cells and cancer. *Nature*, *434*(7035), 843–850. <https://doi.org/10.1038/nature03319>
- Ricotta, D., Conner, S. D., Schmid, S. L., Von Figura, K., & Höning, S. (2002). Phosphorylation of the AP2  $\mu$  subunit by AAK1 mediates high affinity binding to membrane protein sorting signals. *Journal of Cell Biology*, *156*(5), 791–795. <https://doi.org/10.1083/jcb.200111068>
- Ricotta, D., Conner, S. D., Schmid, S. L., Von Figura, K., & Höning, S. (2002). Phosphorylation of the AP2  $\mu$  subunit by AAK1 mediates high affinity binding to

- membrane protein sorting signals. *Journal of Cell Biology*, 156(5), 791–795.  
<https://doi.org/10.1083/jcb.200111068>
- Rohatgi, R., Ma, L., Miki, H., Lopez, M., Kirchhausen, T., Takenawa, T., & Kirschner, M. W. (1999). The interaction between N-WASP and the Arp2/3 complex links Cdc42-dependent signals to actin assembly. *Cell*, 97(2), 221–231.  
[https://doi.org/10.1016/S0092-8674\(00\)80732-1](https://doi.org/10.1016/S0092-8674(00)80732-1)
- Rothnie, A., Clarke, A. R., Kuzmic, P., Cameron, A., & Smith, C. J. (2011). A sequential mechanism for clathrin cage disassembly by 70-kDa heat-shock cognate protein (Hsc70) and auxilin. *Proceedings of the National Academy of Sciences of the United States of America*, 108(17), 6927–6932. <https://doi.org/10.1073/pnas.1018845108>
- Salic, A., Lee, E., Mayer, L., & Kirschner, M. W. (2000). Control of  $\beta$ -catenin stability: Reconstitution of the cytoplasmic steps of the Wnt pathway in *Xenopus* egg extracts. *Molecular Cell*, 5(3), 523–532. [https://doi.org/10.1016/S1097-2765\(00\)80446-3](https://doi.org/10.1016/S1097-2765(00)80446-3)
- Salser, S. J., & Kenyon, C. (1992). Activation of a *C. elegans* Antennapedia homologue in migrating cells controls their direction of migration. *Nature*, 355(6357), 255–258.  
<https://doi.org/10.1038/355255a0>
- Saraon, P., Pathmanathan, S., Snider, J., Lyakisheva, A., Wong, V., & Stagljar, I. (2021). Receptor tyrosine kinases and cancer: oncogenic mechanisms and therapeutic approaches. *Oncogene*, 40(24), 4079–4093. <https://doi.org/10.1038/s41388-021-01841-2>
- Saraste, J., & Marie, M. (2018). Intermediate compartment (IC): from pre-Golgi vacuoles to a semi-autonomous membrane system. *Histochemistry and Cell Biology*, 150(5), 407–430.  
<https://doi.org/10.1007/s00418-018-1717-2>
- Sasaki, T., Takasuga, S., Sasaki, J., Kofuji, S., Eguchi, S., Yamazaki, M., & Suzuki, A. (2009). Mammalian phosphoinositide kinases and phosphatases. *Progress in Lipid Research*, 48(6), 307–343. <https://doi.org/10.1016/j.plipres.2009.06.001>
- Schlessinger, J. (2000). Cell signaling by receptor tyrosine kinases. *Cell*, 103(2), 211–225.  
[https://doi.org/10.1016/S0092-8674\(00\)00114-8](https://doi.org/10.1016/S0092-8674(00)00114-8)
- Schlossman, D. M., Schmid, S. L., Braell, W. A., & Rothman, J. E. (1984). An enzyme that removes clathrin coats: Purification of an uncoating ATPase. *Journal of Cell Biology*, 99(2), 723–733. <https://doi.org/10.1083/jcb.99.2.723>
- Schmid, S. L. (1997). Clathrin-coated vesicle formation and protein sorting: An integrated process. In *Annual Review of Biochemistry* (Vol. 66).  
<https://doi.org/10.1146/annurev.biochem.66.1.511>
- Schöneberg, J., Lehmann, M., Ullrich, A., Posor, Y., Lo, W.-T., Lichtner, G., Schmoranzer, J., Haucke, V., & Noé, F. (2017). Lipid-mediated PX-BAR domain recruitment couples local membrane constriction to endocytic vesicle fission. *Nature Communications*, 8.  
<https://doi.org/10.1038/ncomms15873>



- Shi, B., Conner, S. D., & Liu, J. (2014). Dysfunction of endocytic kinase AAK1 in ALS. *International Journal of Molecular Sciences*, *15*(12), 22918–22932. <https://doi.org/10.3390/ijms151222918>
- Shi, F., Telesco, S. E., Liu, Y., Radhakrishnan, R., & Lemmona, M. A. (2010). ErbB3/HER3 intracellular domain is competent to bind ATP and catalyze autophosphorylation. *Proceedings of the National Academy of Sciences of the United States of America*, *107*(17), 7692–7697. <https://doi.org/10.1073/PNAS.1002753107>
- Shi, Y. (2009). Serine/Threonine Phosphatases: Mechanism through Structure. *Cell*, *139*(3), 468–484. <https://doi.org/10.1016/j.cell.2009.10.006>
- Shi, Z., Jia, X., Tian, Y., Liu, X., Bai, J., Liu, Y., Zhang, F., Li, J., Gao, X., & Zhang, K. (2020). Genetic variants of the mtmr9 gene are associated with nonspecific intellectual disability: A family-based association study. *Genetic Testing and Molecular Biomarkers*, *24*(10), 625–631. <https://doi.org/10.1089/gtmb.2020.0145>
- Siegfried, E., Chou, T.-B., & Perrimon, N. (1992). wingless signaling acts through zeste-white 3, the drosophila homolog of glycogen synthase kinase-3, to regulate engrailed and establish cell fate. *Cell*, *71*(7), 1167–1179. [https://doi.org/10.1016/S0092-8674\(05\)80065-0](https://doi.org/10.1016/S0092-8674(05)80065-0)
- Silhankova, M., Port, F., Harterink, M., Basler, K., & Korswagen, H. C. (2010). Wnt signalling requires MTM-6 and MTM-9 myotubularin lipid-phosphatase function in Wnt-producing cells. *EMBO Journal*, *29*(24), 4094–4105. <https://doi.org/10.1038/emboj.2010.278>
- Smolich, B. D., McMahon, J. A., McMahon, A. P., & Papkoff, J. (1993). Wnt family proteins are secreted and associated with the cell surface. *Molecular Biology of the Cell*, *4*(12), 1267–1275. <https://doi.org/10.1091/mbc.4.12.1267>
- Sorensen, E. B., & Conner, S. D. (2008). AAK1 regulates Numb function at an early step in clathrin-mediated endocytosis. *Traffic*, *9*(10), 1791–1800. <https://doi.org/10.1111/j.1600-0854.2008.00790.x>
- Sorrell, F. J., Szklarz, M., Abdul Azeez, K. R., Elkins, J. M., & Knapp, S. (2016). Family-wide Structural Analysis of Human Numb-Associated Protein Kinases. *Structure*, *24*(3), 401–411. <https://doi.org/10.1016/j.str.2015.12.015>
- Stanganello, E., Hagemann, A. I. H., Mattes, B., Sinner, C., Meyen, D., Weber, S., Schug, A., Raz, E., & Scholpp, S. (2015). Filopodia-based Wnt transport during vertebrate tissue patterning. *Nature Communications*, *6*. <https://doi.org/10.1038/ncomms6846>
- Sun, J., Yu, S., Zhang, X., Capac, C., Aligbe, O., Daudelin, T., Bonder, E. M., & Gao, N. (2017). A Wntless-SEC12 complex on the ER membrane regulates early Wnt secretory vesicle assembly and mature ligand export. *Journal of Cell Science*, *130*(13), 2159–2171. <https://doi.org/10.1242/jcs.200634>

- Sundararajan, L., & Lundquist, E. A. (2012). Transmembrane proteins UNC-40/DCC, PTP-3/LAR, and MIG-21 control anterior-posterior neuroblast migration with left-right functional asymmetry in *Caenorhabditis elegans*. *Genetics*, *192*(4), 1373–1388. <https://doi.org/10.1534/genetics.112.145706>
- Taguchi-Atarashi, N., Hamasaki, M., Matsunaga, K., Omori, H., Ktistakis, N. T., Yoshimori, T., & Noda, T. (2010). Modulation of local Ptdins3P levels by the PI phosphatase MTMR3 regulates constitutive autophagy. *Traffic*, *11*(4), 468–478. <https://doi.org/10.1111/j.1600-0854.2010.01034.x>
- Tamai, K., Semenov, M., Kato, Y., Spokony, R., Liu, C., Katsuyama, Y., Hess, F., Saint-Jeannet, J.-P., & He, X. (2000). LDL-receptor-related proteins in Wnt signal transduction. *Nature*, *407*(6803), 530–535. <https://doi.org/10.1038/35035117>
- Tanaka, K., Okabayashi, K., Asashima, M., Perrimon, N., & Kadowaki, T. (2000). The evolutionarily conserved porcupine family is involved in the processing of the Wnt family. *European Journal of Biochemistry*, *267*(13), 4300–4311. <https://doi.org/10.1046/j.1432-1033.2000.01478.x>
- Tax, F. E., Thomas, J. H., Ferguson, E. L., & Horvitz, H. R. (1997). Identification and characterization of genes that interact with *lin-12* in *Caenorhabditis elegans*. *Genetics*, *147*(4), 1675–1695.
- Taylor, G. S., Maehama, T., & Dixon, J. E. (2000). Myotubularin, a protein tyrosine phosphatase mutated in myotubular myopathy, dephosphorylates the lipid second messenger, phosphatidylinositol 3-phosphate. *Proceedings of the National Academy of Sciences of the United States of America*, *97*(16), 8910–8915. <https://doi.org/10.1073/pnas.160255697>
- Tsushima, H., Malabarba, M. G., Confalonieri, S., Senic-Matuglia, F., Verhoef, L. G. G. C., Bartocci, C., D'Ario, G., Cocito, A., Di Fiore, P. P., & Salcini, A. E. (2013). A Snapshot of the Physical and Functional Wiring of the Eps15 Homology Domain Network in the Nematode. *PLoS ONE*, *8*(2). <https://doi.org/10.1371/journal.pone.0056383>
- Ultanir, S., Hertz, N., Li, G., Ge, W.-P., Burlingame, A., Pleasure, S., Shokat, K., Jan, L., & Jan, Y.-N. (2012). Chemical Genetic Identification of NDR1/2 Kinase Substrates AAK1 and Rabin8 Uncovers Their Roles in Dendrite Arborization and Spine Development. *Neuron*, *73*(6), 1127–1142. <https://doi.org/10.1016/j.neuron.2012.01.019>
- Umeda, A., Meyerholz, A., & Ungewickell, E. (2000). Identification of the universal cofactor (auxilin 2) in clathrin coat dissociation. *European Journal of Cell Biology*, *79*(5), 336–342. [https://doi.org/10.1078/S0171-9335\(04\)70037-0](https://doi.org/10.1078/S0171-9335(04)70037-0)
- Ungewickell, E., Ungewickell, H., Holstein, S. E. H., Lindner, R., Prasad, K., Barouch, W., Martini, B., Greene, L. E., & Eisenberg, E. (1995). Role of auxilin in uncoating clathrin-coated vesicles. *Nature*, *378*(6557), 632–635. <https://doi.org/10.1038/378632a0>

- Ungureanu, D., Wu, J., Pekkala, T., Niranjana, Y., Young, C., Jensen, O. N., Xu, C. F., Neubert, T. A., Skoda, R. C., Hubbard, S. R., & Silvennoinen, O. (2011). The pseudokinase domain of JAK2 is a dual-specificity protein kinase that negatively regulates cytokine signaling. *Nature Structural and Molecular Biology*, *18*(9), 971–976. <https://doi.org/10.1038/NSMB.2099>
- Vergne, I., Roberts, E., Elmaoued, R. A., Tosch, V., Delgado, M. A., Proikas-Cezanne, T., Laporte, J., & Deretic, V. (2009). Control of autophagy initiation by phosphoinositide 3-phosphatase jumpy. *EMBO Journal*, *28*(15), 2244–2258. <https://doi.org/10.1038/emboj.2009.159>
- Vicinanza, M., D'Angelo, G., di Campli, A., & de Matteis, M. A. (2008). Function and dysfunction of the PI system in membrane trafficking. *EMBO Journal*, *27*(19), 2457–2470. <https://doi.org/10.1038/emboj.2008.169>
- Walker, D. M., Urbé, S., Dove, S. K., Tenza, D., Raposo, G., & Clague, M. J. (2001). Characterization of MTMR3: An inositol lipid 3-phosphatase with novel substrate specificity. *Current Biology*, *11*(20), 1600–1605. [https://doi.org/10.1016/S0960-9822\(01\)00501-2](https://doi.org/10.1016/S0960-9822(01)00501-2)
- Wang, J., Sinha, T., & Wynshaw-Boris, A. (2012). Wnt signaling in mammalian development: Lessons from mouse genetics. *Cold Spring Harbor Perspectives in Biology*, *4*(5), 6. <https://doi.org/10.1101/cshperspect.a007963>
- Wang, Y., & Pallen, C. J. (1991). The receptor-like protein tyrosine phosphatase HPTP $\alpha$  has two active catalytic domains with distinct substrate specificities. *EMBO Journal*, *10*(11), 3231–3237. <https://doi.org/10.1002/j.1460-2075.1991.tb04886.x>
- Ward, T. H., Polishchuk, R. S., Caplan, S., Hirschberg, K., & Lippincott-Schwartz, J. (2001). Maintenance of Golgi structure and function depends on the integrity of ER export. *Journal of Cell Biology*, *155*(3), 557–570. <https://doi.org/10.1083/jcb.200107045>
- Whangbo, J., & Kenyon, C. (1999). A Wnt signaling system that specifies two patterns of cell migration in *C. elegans*. *Molecular Cell*, *4*(5), 851–858. [https://doi.org/10.1016/S1097-2765\(00\)80394-9](https://doi.org/10.1016/S1097-2765(00)80394-9)
- Wilde, A., & Brodsky, F. M. (1996). In vivo phosphorylation of adaptors regulates their interaction with clathrin. *Journal of Cell Biology*, *135*(3), 635–645. <https://doi.org/10.1083/jcb.135.3.635>
- Wrobel, A. G., Kadlecova, Z., Kamenicky, J., Yang, J.-C., Herrmann, T., Kelly, B. T., McCoy, A. J., Evans, P. R., Martin, S., Müller, S., Honing, S., & Owen, D. J. (2019). Temporal Ordering in Endocytic Clathrin-Coated Vesicle Formation via AP2 Phosphorylation. *Developmental Cell*, *50*(4), 494–508.e11. <https://doi.org/10.1016/j.devcel.2019.07.017>
- Wu, L., Buist, A., Den Hertog, J., & Zhang, Z.-Y. (1997). Comparative kinetic analysis and substrate specificity of the tandem catalytic domains of the receptor-like protein-tyrosine

- phosphatase  $\alpha$ . *Journal of Biological Chemistry*, 272(11), 6994–7002.  
<https://doi.org/10.1074/jbc.272.11.6994>
- Yanagiya, T., Tanabe, A., Iida, A., Saito, S., Sekine, A., Takahashi, A., Tsunoda, T., Kamohara, S., Nakata, Y., Kotani, K., Nakamura, Y., & Hotta, K. (2007). Association of single-nucleotide polymorphisms in MTMR9 gene with obesity. *Human Molecular Genetics*, 16(24), 3017–3026. <https://doi.org/10.1093/hmg/ddm260>
- Yang, P.-T., Lorenowicz, M. J., Silhankova, M., Coudreuse, D. Y. M., Betist, M. C., & Korswagen, H. C. (2008). Wnt Signaling Requires Retromer-Dependent Recycling of MIG-14/Wntless in Wnt-Producing Cells. *Developmental Cell*, 14(1), 140–147.  
<https://doi.org/10.1016/j.devcel.2007.12.004>
- Yang, W.-K., Peng, Y.-H., Li, H., Lin, H.-C., Lin, Y.-C., Lai, T.-T., Suo, H., Wang, C.-H., Lin, W.-H., Ou, C.-Y., Chang, H., & Chien, C.-T. (2011). Nak regulates localization of clathrin sites in higher-order dendrites to promote local dendrite growth. *Neuron*, 72(2), 285–299. <https://doi.org/10.1016/j.neuron.2011.08.028>
- Yang, X.-Z., Li, X.-X., Zhang, Y.-J., Rodriguez-Rodriguez, L., Xiang, M.-Q., Wang, H.-Y., & Zheng, X. F. S. (2016). Rab1 in cell signaling, cancer and other diseases. *Oncogene*, 35(44), 5699–5704. <https://doi.org/10.1038/onc.2016.81>
- Yoshimura, S.-I., Gerondopoulos, A., Linford, A., Rigden, D. J., & Barr, F. A. (2010). Family-wide characterization of the DENN domain Rab GDP-GTP exchange factors. *Journal of Cell Biology*, 191(2), 367–381. <https://doi.org/10.1083/jcb.201008051>
- Yu, J., Chia, J., Canning, C. A., Jones, C. M., Bard, F. A., & Virshup, D. M. (2014). WLS Retrograde transport to the endoplasmic reticulum during Wnt secretion. *Developmental Cell*, 29(3), 277–291. <https://doi.org/10.1016/j.devcel.2014.03.016>
- Zaccai, N. R., Kadlecova, Z., Dickson, V. K., Korobchevskaya, K., Kamenicky, J., Kovtun, O., Umasankar, P. K., Wrobel, A. G., Kaufman, J. G. G., Gray, S. R., Owen, D. J., & Traub, L. M. (2022). FCHO controls AP2's initiating role in endocytosis through a PtdIns(4,5)P<sub>2</sub>-dependent switch. *Science Advances*, 8(17).  
<https://doi.org/10.1126/sciadv.abn2018>
- Zheng, C., Diaz-Cuadros, M., & Chalfie, M. (2015). Dishevelled attenuates the repelling activity of Wnt signaling during neurite outgrowth in *Caenorhabditis elegans*. *Proceedings of the National Academy of Sciences of the United States of America*, 112(43), 13243–13248. <https://doi.org/10.1073/pnas.1518686112>
- Zinovyeva, A. Y., & Forrester, W. C. (2005). The *C. elegans* Frizzled CFZ-2 is required for cell migration and interacts with multiple Wnt signaling pathways. *Developmental Biology*, 285(2), 447–461. <https://doi.org/10.1016/j.ydbio.2005.07.014>
- Zoncu, R., Perera, R. M., Sebastian, R., Nakatsu, F., Chen, H., Balla, T., Ayala, G., Toomre, D., & de Camilli, P. V. (2007). Loss of endocytic clathrin-coated pits upon acute

depletion of phosphatidylinositol 4,5-bisphosphate. *Proceedings of the National Academy of Sciences of the United States of America*, 104(10), 3793–3798.  
<https://doi.org/10.1073/pnas.0611733104>

Zoppino, F. C. M., Militello, R. D., Slavin, I., Álvarez, C., & Colombo, M. I. (2010). Autophagosome formation depends on the small GTPase rab1 and functional ER exit sites. *Traffic*, 11(9), 1246–1261. <https://doi.org/10.1111/j.1600-0854.2010.01086.x>

Zou, J., Chang, S.-C., Marjanovic, J., & Majerus, P. W. (2009). MTMR9 increases MTMR6 enzyme activity, stability, and role in apoptosis. *Journal of Biological Chemistry*, 284(4), 2064–2071. <https://doi.org/10.1074/jbc.M804292200>

Zou, J., Zhang, C., Marjanovic, J., Kisseleva, M. V., Majerus, P. W., & Wilson, M. P. (2012). Myotubularin-related protein (MTMR) 9 determines the enzymatic activity, substrate specificity, and role in autophagy of MTMR8. *Proceedings of the National Academy of Sciences of the United States of America*, 109(24), 9539–9544.  
<https://doi.org/10.1073/pnas.1207021109>